Volume 16, Issue 2, June 2026
pISSN 2158-0510 eISSN - 2158-0529

IJBM

International Journal of BIOMEDICINE

www.ijbm.org

IJBM

INTERNATIONAL JOURNAL OF BIOMEDICINE

International Journal of Biomedicine (print ISSN - 2158-0510 and online ISSN - 2158-0529) is published four times a year by International Medical Research and Development Corp. (IMRDC). International Journal of Biomedicine (IJBM) is an international, peer-reviewed, open access journal. IJBM publishes scientific articles related to basic, applied, and translational research in biology and medicine. The main purpose of IJBM is to promote new scientific ideas and biomedical technologies. The distribution of freely accessible, high-quality content is a central mission of IJBM, aimed at increasing research visibility and accelerating scientific discovery. IJBM articles are published under a Creative Commons Attribution–NonCommercial–NoDerivatives 4.0 International (CC BY-NC ND 4.0) license.

International Journal of Biomedicine endorses and behaves in accordance with the codes of conduct and international standards established by the Committee on Publication Ethics (COPE).

Manuscript Submission: Original works will be accepted with the understanding that they are contributed solely to the Journal, are not under review by another publication, and have not previously been published except in abstract form.

IJBM

INTERNATIONAL JOURNAL OF BIOMEDICINE

IJBM
INTERNATIONAL JOURNAL OF BIOMEDICINE
www.ijbm.org
Volume 16 Issue 2 June 2026

CONTENTS

CONTENTS

International Journal of Biomedicine 16(2) (2026) 130-144
http://dx.doi.org/10.21103/Article16(2)_PV

POINT OF VIEW

INTERNATIONAL JOURNAL OF BIOMEDICINE

Metabolic Diseases: Cellular and Molecular Mechanisms: A Point of View

Gundu H. R. Rao*

Laboratory Medicine and Pathology, Director, Thrombosis Research, Lillehei Heart Institute, University of Minnesota, Minneapolis, Minnesota, USA

Abstract

The Developmental Origins of Health and Disease (DOHaD) framework highlights that unfavorable conditions during fetal development can trigger persistent biological changes, increasing the risk of metabolic disorders in adulthood. While clinical manifestations often appear only later in life, fetal programming produces subtle but permanent structural, functional, and epigenetic modifications in key metabolic organs—including the pancreas, liver, and skeletal muscle. These early alterations weaken physiological resilience and predispose tissues to dysfunction when exposed to postnatal challenges such as poor diet, sedentary behavior, chronic stress, or environmental toxins. Initially, compensatory mechanisms may mask these vulnerabilities, but with aging and cumulative metabolic stress, these reserves decline, culminating in overt conditions such as hypertension, obesity, type 2 diabetes, and vascular disease. Cellular and molecular mechanisms—including epigenetic remodeling, disrupted signaling pathways, mitochondrial impairment, and chronic low-grade inflammation—serve as mediators linking early-life insults to long-term metabolic dysregulation. Because individuals with normal birth weight also develop these disorders with advancing age, it is plausible that such disease clusters have an age-related component. Downstream consequences of metabolic dysfunction—such as oxidative stress, impaired vascular tone, endothelial dysfunction, dysregulated glucose and lipid metabolism, arterial narrowing, and activation of platelet and coagulation pathways—further drive the progression of metabolic risk. By dissecting these mechanisms, it becomes possible to identify early biomarkers and design targeted interventions that halt disease progression before irreversible damage sets in. Thus, integrating developmental biology with molecular medicine offers a powerful opportunity to prevent and treat metabolic disorders rooted in early life. However, contemporary medical practice remains largely disease-focused, emphasizing management of established risk factors. A more forward-looking approach must prioritize early detection, preventive strategies, and lifestyle modification, guided by a deep understanding of the cellular and molecular foundations of metabolic vulnerability.(**International Journal of Biomedicine. 2026;16(2):130-144.**)

Keywords: oxidative stress • inflammation • vascular dysfunction • hypertension • obesity • diabetes • vascular disease

For citation: Rao GHR. Metabolic Diseases: Cellular and Molecular Mechanisms: A Point of View. International Journal of Biomedicine. 2026;16(2):130-144. doi:10.21103/Article16(2)_PV

Abbreviations

CVD, cardiovascular disease; **DOHaD**, developmental origins of health and disease; **FOAD**, fetal origins of adult disease; **LDL**, low-density lipoprotein; **RAAS**, renin–angiotensin–aldosterone system; **T2D**, type 2 diabetes.

Introduction

British Epidemiologist David Barker's hypothesis focused on the "Fetal Origins of Adult Disease" (FOAD), often referred to as the Barker hypothesis, which proposed that adverse influences during critical periods of fetal development, particularly related to nutrition and the intrauterine environment, could "program" the fetus for increased susceptibility to a range of chronic diseases later in life.[1-19] These diseases, termed metabolic diseases, include hypertension, obesity, type 2 diabetes (T2D), vascular diseases, neurodegenerative diseases, and, to some extent, even cancer.[20-22] Low birth weight, a marker of poor fetal growth, has been linked to a higher risk of coronary artery disease, hypertension, and stroke in adulthood. Studies have shown associations between fetal undernutrition and increased risk of obesity, insulin resistance, and T2D.[2-5]

***Correspondence:** Emeritus Professor, Gundu H. R. Rao, PhD. Laboratory Medicine and Pathology, Director, Thrombosis Research, Lillehei Heart Institute, University of Minnesota, Minneapolis, Minnesota, USA. E-mail: gundurao9@gmail.com*

Research also suggests a link between fetal programming and the development of certain neurological conditions, including Parkinson's and Alzheimer's disease.[20] The FOAD hypothesis has also been explored in relation to cancer development and progression. Barker's hypothesis highlights the crucial role of early developmental influences, especially during the fetal period, in shaping long-term health outcomes and disease susceptibility.[1-5]

Metabolic disturbances during fetal development can trigger adult-onset metabolic diseases through several interconnected mechanisms, primarily linked to fetal programming and epigenetic modifications.[23,24] The fetal pancreas produces hormones like insulin and glucagon during key developmental periods. Maternal malnutrition or metabolic disorders can disrupt pancreatic development by altering transcription factors and signaling pathways, thereby reducing β-cell mass and function.[25,26] This deficiency can reduce insulin production and impair glucose sensing, thereby increasing the offspring's risk of T2D. The fetal liver is also a major target of programming, with its size and later function being shaped by the intrauterine environment.[27,28] Suboptimal nutrition during gestation can alter the expression of genes involved in hepatic energy production, leading to increased hepatic gluconeogenesis and insulin resistance in adulthood. This can contribute to hyperglycemia and the development of T2D. The fetal liver is also a major target of programming, with its size and later function being shaped by the intrauterine environment. Suboptimal nutrition during gestation can alter the expression of genes involved in hepatic energy production, leading to increased hepatic gluconeogenesis and insulin resistance in adulthood. This can contribute to hyperglycemia and the development of T2D. Maternal obesity or a high-fat diet during pregnancy can induce epigenetic changes in fetal adipose tissue, leading to increased adipogenesis and a predisposition to obesity in adulthood.[29,30]

Epigenetic changes are alterations in gene expression that do not involve changes in the DNA sequence itself but can be transmitted to subsequent cell divisions and even generations. [31] *DNA Methylation:* This involves adding methyl groups to CpG islands in DNA, often silencing gene expression. For example, studies have shown altered DNA methylation patterns in the insulin-like growth factor 2 (IGF2) gene in individuals exposed to prenatal famine, which is linked to increased risk of metabolic diseases.[32] *Histone Modifications:* These include modifications like acetylation and methylation of histone proteins, which can affect chromatin structure and gene accessibility. These modifications can alter the expression of genes involved in key metabolic pathways.[33] *MicroRNAs (miRNAs):* These small non-coding RNAs regulate gene expression by binding to target mRNAs, thereby affecting protein synthesis. Adverse intrauterine environments can alter miRNA expression profiles, thereby influencing metabolic pathways such as insulin signaling, lipid metabolism, and food intake.[34]

Fetal exposure to abnormal levels of hormones, such as insulin, glucocorticoids, and insulin-like growth factors, can permanently affect organ development and function, predisposing individuals to metabolic diseases.[35] Maternal high-fat diets can affect hypothalamic gene expression in the offspring, leading to leptin resistance and altered regulation of appetite and energy balance.[36] In essence, metabolic disturbances during critical windows of fetal development can trigger long-lasting structural and functional changes in key metabolic organs, such as the pancreas and liver, often mediated by epigenetic modifications.[37] These changes can impair glucose homeostasis, insulin sensitivity, and lipid metabolism, increasing the risk of developing metabolic diseases such as T2D, obesity, and metabolic syndrome in adulthood. If fetal metabolic disturbances are the root cause of adult-onset metabolic diseases, why is there a delay of several years to develop these chronic diseases? What epigenetic factors trigger or initiate the risks for the development of metabolic diseases? Answers to such questions are the key to our understanding of the "developmental origins of health and disease" (DOHaD) hypothesis.[38,39]

The delay between fetal programming and the onset of adult metabolic diseases is due to several interacting factors that cumulatively affect outcomes over time. Fetal programming causes permanent, often subtle, changes in the structure and function of key metabolic organs (like the pancreas, liver, and muscle) and systems.[40,41] These changes might not be severe enough to cause problems immediately, but they leave these organs with reduced capacity or altered responses to later environmental challenges. Epigenetic marks (like DNA methylation and histone modifications) can be permanently altered by the fetal environment, affecting gene expression throughout life.[42,43] These changes can prime genes involved in metabolic regulation to respond differently to stimuli, but the full impact may only become evident when combined with other factors over time. The postnatal environment plays a crucial role in triggering the manifestation of fetal programming effects. *Factors like diet*: An unhealthy diet, especially one high in fat and sugar, can place extra stress on organs already compromised by fetal programming.[36, 37] *Lifestyle:* A sedentary lifestyle further exacerbates the risks of developing metabolic disorders.[44] *Stress:* Chronic stress can disrupt hormonal balance and metabolic function, particularly in individuals with pre-existing vulnerabilities. [47] *Environmental factors:* Exposure to certain chemicals or toxins can interact with fetal programming, further increasing disease risk.[47,48]

Gradual Accumulation of Damage: Metabolic diseases often involve the gradual accumulation of damage to organs and tissues over time.[48,49] For example, insulin resistance develops progressively, leading to declining β-cell function and eventual diabetes.[50] Fetal programming creates a predisposition, but the full disease state requires the added impact of aging and other risk factors. *Compensatory Mechanisms*: In early life, the body's compensatory mechanisms may be able to mask the effects of fetal programming.[51,52] For instance, the pancreas may initially compensate for reduced β-cell mass by increasing insulin secretion.[53] However, these mechanisms may eventually be overwhelmed by the combined effects of aging, poor lifestyle choices, and other factors, leading to the development of metabolic diseases. In essence, delay is not a sign that the fetal insult is not the root cause, but rather that it sets the stage for future problems that unfold over time in combination with later-life exposures and the natural aging process.[50-53]

Fetal Origin of Adult Diseases

From 1934 onwards, the birth weight, length, and head circumference of all babies born in CSI Holdsworth Memorial Hospital (HMH), Mysore, India, were recorded in obstetric notes.[3,10-13,16-19] The studies with the 'Mysore Cohort' were among the first in a low-and middle-income country to test DOHaD concepts, with a predicted association between small size at birth and adult coronary heart disease, insulin resistance, and low lung function.[10] The Mysore Parthenon study findings suggest that exposure to maternal nutritional deficiencies, as well as overnutrition, may contribute to an increasing burden of cardiovascular disease in India, and that these two conditions may co-exist in the same mother, leading to dual insults to the offspring.[11] During 1993-2001, in a collaborative study with Barker's group at the Medical Research Council (MRC) Life course Epidemiology Unit, University of Southampton, UK, the records were used to trace people born in HMH, Mysore, India, between 1934 and 1966.[10] The FOAD, a concept first popularized by Dr. David Barker, has since led to many studies that have provided evidence that certain diseases have links to fetal origins. The concept of the fetal origin of adult disease has been extended well beyond cardiovascular disease (CVD) and now includes investigations into the development of the central nervous system and the early origins of adult mental health and cognitive function.[54-59] Given that epigenetic alterations during fetal development may cause several adult metabolic diseases, as well as diseases of the nervous system, we would like to see future research focus on possible intervention strategies to halt, reverse, or prevent these epigenetic modulations of fetal metabolism.

New Hypothesis on Fetal Origin of Adult Diseases

Obesity is a well-recognized risk factor for T2D. A landmark discovery from Children's National Hospital, Washington, DC, has been described as a potential "game changer" in detecting obesity-related complications. According to a hospital news release, physician-scientist Dr. Robert Freishtat and his colleagues have shown that "early intervention and prevention of obesity-related illness may soon be possible." It is well established that visceral adipose tissue (belly fat) is strongly associated with serious complications of obesity, including cardiovascular disease and insulin resistance leading to diabetes. What had remained unclear until recently, however, were the precise mechanisms by which excess visceral fat triggers these conditions. Dr. Freishtat's team demonstrated that as visceral fat accumulates, adipocytes undergo changes and begin releasing a distinct set of exosomes compared to those released by lean fat cells. These altered exosomal signals disrupt critical biological pathways, impairing the body's ability to regulate glucose and cholesterol. Dr. Freishtat has likened exosomes to "biological tweets"—brief molecular messages that enable cell-to-cell communication and influence gene expression. In their exploratory studies, the team collected adipose tissue from lean and obese female patients and used modified bead-based flow cytometry to isolate and compare exosomal miRNAs. They concluded that the successful identification of these exosomes paves the way for the development of diagnostic tests that could enable early intervention or even the prevention of obesity-related diseases.[60-62]

Similarly, microvesicles (MVs) released by multiple cell types carry mRNA and miRNA, remaining in the extracellular space to mediate intercellular signaling—functionally echoing Dr. Freishtat's "biological tweets." Importantly, these vesicles play a role in epigenetic reprogramming of host cell metabolism. Building on these findings, we contacted Dr. Freishtat to explore a potential US–India collaborative project on the role of maternal exosomal miRNAs in reprogramming fetal genetic material and gene expression. The Diabetes Research Group at King Edward Memorial (KEM) Hospital, Pune, had already established a large biobank of maternal and fetal tissues. With the leadership of Professor C.S. Yajnik, we initiated preliminary studies. Genotypic Technology, Bengaluru, partnered to provide rapid miRNA assays. Encouraging early results enabled the team to secure funding from the U.S. National Institutes of Health (NIH) for further research.[62] Based on these observations, a "new hypothesis" has emerged regarding the FOAD: maternal and cord blood adipocyte-derived exosomal miRNAs that regulate adipogenesis are associated with higher infant adiposity.[63] As body fat increases during obesity, fat cells change and release different exosomes than lean adipocytes. These altered signals interfere with key metabolic processes, ultimately reducing the body's capacity to manage sugar and cholesterol effectively.

Cardiometabolic Diseases

Cardiometabolic diseases, including hypertension, excess weight, obesity, T2D, and vascular disorders, have risen markedly in incidence and prevalence worldwide. [64-70] A cascade of pathological events contributes to the progression of these conditions and the onset of acute arterial complications. Key factors include oxidative stress, vascular inflammation, obesity, diabetes, endothelial dysfunction, arterial stiffness, subclinical atherosclerosis, growth and rupture of atherosclerotic plaques, arterial stenosis, and activation of platelet and coagulation pathways. Hypertension, obesity, and T2D are central drivers of this process. An imbalance between free radicals and antioxidants promotes widespread cellular and tissue damage, particularly in blood vessels. Persistent vascular inflammation is a critical mechanism that initiates structural changes in the arteries. Over time, vessel walls lose elasticity and become rigid—an independent predictor of cardiovascular risk. Fatty streaks and early lesions evolve into advanced lipid-rich plaques within the arterial wall. When these plaques rupture, thrombogenic material is exposed, triggering platelet activation and blood clot (thrombus) formation. Depending on the site of obstruction, this process can result in acute clinical events such as myocardial infarction (coronary arteries), ischemic stroke (cerebral arteries), or peripheral artery disease (limb arteries).

Altered Endothelial Metabolism: Vascular Dysfunction

Altered endothelial metabolism leading to vascular dysfunction is widely recognized as one of the earliest indicators for the progression of vascular disease. This damage to the endothelium—the thin layer of cells lining blood vessels—can precede and predict the onset of atherosclerosis and subsequent cardiovascular events.[71-73] Endothelial cells (ECs) adapt their metabolic pathways in response to stressors

like hyperglycemia, hyperlipidemia, and hypertension. This metabolic reprogramming disrupts vascular homeostasis, leading to inflammation, impaired vasodilation, and oxidative stress that characterize endothelial dysfunction. Endothelial cells typically favor glycolysis over mitochondrial oxidative phosphorylation, even in the presence of sufficient oxygen. However, under stressful conditions such as hypoxia or inflammation, this preference is heightened. This shift can promote the production of inflammatory and pro-atherogenic molecules. Excess reactive oxygen species (ROS) from metabolic shifts—such as from uncoupled endothelial nitric oxide synthase (eNOS) and NADPH oxidase activation—damage ECs and oxidize lipoproteins. ROS also react with nitric oxide (NO) to produce peroxynitrite, reducing NO bioavailability and inhibiting its anti-inflammatory and vasodilatory effects. NO, a key molecule for regulating vascular tone and inhibiting inflammation, is a metabolic product of the amino acid L-arginine through the eNOS enzyme. In metabolic disease, NO bioavailability is reduced due to reduced L-arginine, or eNOS coupling.

In metabolic disease, NO availability is reduced by reduced L-arginine availability and by inhibition of various endogenous enzymes by lipid hydroperoxides and oxidized lipoproteins (Figure 1). In hyperlipidemia, ECs exposed to oxidized LDL (ox-LDL) express adhesion molecules that cause platelets to adhere to the arterial wall. Macrophages consume these lipids to become foam cells, the earliest visible signs of atherosclerosis. Insulin resistance impairs the insulin-mediated signaling pathway(P13K/AKT/eNOS) that typically stimulates NO production. This causes an imbalance between vasoactive molecules such as prostacyclin and NO, and vasoconstrictive molecules such as endothelin-1, prostaglandins (PG), PGG2, PGH2, and thromboxane A2. In hyperglycemia, excess glucose reacts with proteins and lipids to form AGEs. When AGEs bind with ECs, they promote inflammation and oxidative stress. Hyperglycemia also alters the balance in the production of vasoconstrictive prostaglandins and vasodilatory metabolites.[74]

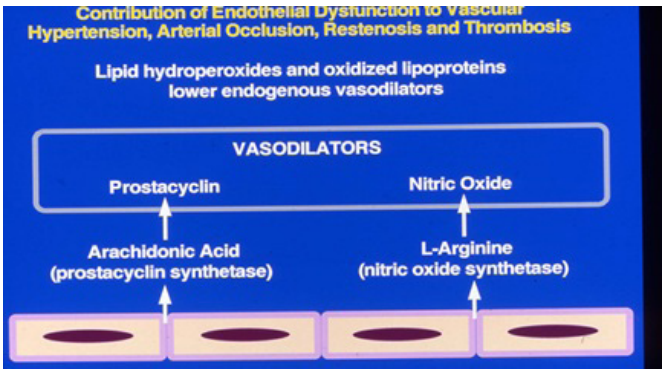

Figure 1. *Lipid Hydroperoxides and Oxidized lipoproteins lower endogenous Vasodilators (Schematic representation, prepared by the University of Minnesota Medical Artists).*

Hypertension

Intrauterine growth restriction (IUGR) leads to a reduced number of nephrons at birth, a condition that predisposes an individual to salt-sensitive hypertension later in life through compensatory hyperfiltration and epigenetic changes to the renin–angiotensin–aldosterone system (RAAS). This process is part of the «developmental origins of adult disease» theory, which posits that adverse events during critical periods of fetal development can have permanent effects on organ structure and function.[75] Endothelial dysfunction is a hallmark of programmed hypertension. Mitochondrial ROS production impairs nitric oxide (NO) bioavailability.[76] Excessive ROS production, often due to mitochondrial dysfunction, leads to endothelial activation, inflammation, and vascular disease by affecting NO release,[77] while histone modifications in endothelial nitric oxide synthase (eNOS) genes suppress vasodilatory capacity.[78] These changes, along with an altered balance between vasodilators and vasoconstrictors induced by hyperglycemia, lead to increased vascular stiffness and heightened sympathetic activity.[74]

Changes in signaling pathways in vascular endothelial cells and vascular smooth muscle cells (VSMCs) are key molecular mechanisms that trigger vascular dysfunction and promote the development of hypertension (Figure 2).[79]

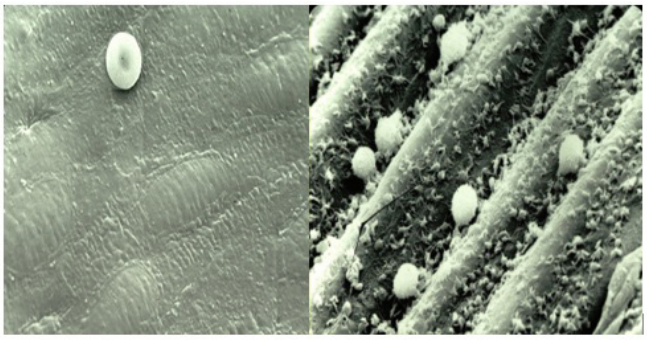

A B

Figure 2. *A: Healthy Endothelium. B: Dysfunctional Endothelium. (Courtesy: Professor (Late) James G White, University of Minnesota Medical School)*

Molecular pathways influencing blood vessels can be broadly categorized into two groups. The first indirectly regulates vascular sympathetic activity through mechanisms such as RAAS, immune signaling, and redox pathways. The second directly affects vascular functions, including calcium signaling, NO-(NOsGC)-cGMP pathways, and vascular remodeling. The indirect pathways form a complex network that primarily induces vasoconstriction via direct mechanisms. For instance, sympathetic disorders often promote vasoconstriction by activating calcium channels, while RAAS not only activates calcium channels but also drives vascular remodeling. While endothelial and smooth muscle cell signaling pathways are the primary drivers of vascular tone, platelets critically modulate this system. By tipping the PGI_2/TXA_2 balance toward vasoconstriction, platelet dysfunction directly contributes to hypertension and its cardiovascular complications (Figure 3).[74]

In terms of therapeutic application, molecular pathways involved in vascular regulation, such as calcium signaling, NO-(NOsGC)-cGMP, RAAS, and sympathetic activity, have demonstrated clear efficacy in clinical practice. [80-82] Modern

medicine increasingly views hypertension not as a standalone disease but as a significant risk factor for vascular disorders.[83] The primary goal of blood pressure management is to reduce cardiovascular events, much as controlling blood lipids or glucose levels. It is essential to recognize that the molecular basis of hypertension lies in vascular dysfunction and/or altered vascular volume. A deeper understanding of these mechanisms is crucial for advancing research on the signaling pathways underlying hypertension.

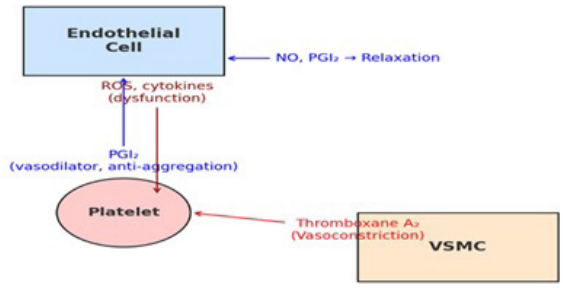

Figure 3. *Cros-talk between endothelial cells, vascular smooth muscle cells, and platelets (Prepared by Open AI-ChatGPT)*

Obesity

Compared to Europeans and Americans, South Asians and East Asians tend to develop central abdominal obesity and T2D at a lower body mass index (BMI). Advances in high-throughput genotyping technologies have enabled large-scale genome-wide association studies (GWAS), uncovering hundreds of genetic loci linked to BMI and waist-to-hip ratio (WHR), primarily in European populations. A major limitation of such studies is the overwhelming number of genes associated with these risks. For instance, a large meta-analysis of BMI-associated single-nucleotide polymorphisms (SNPs) identified more than 750 SNPs linked to susceptibility genes, including specific variants. Among them, the FTO (alpha-ketoglutarate-dependent dioxygenase) gene emerged as a strong contributor to polygenic obesity. Despite these findings, the molecular mechanisms driving this complex disorder remain poorly understood, and the variation in fat distribution across global populations is still unexplained. Obesity is now recognized as the leading public health challenge worldwide, yet the strikingly different fat distribution patterns in nearly half the global population remain a mystery. Central abdominal obesity is considered a major risk factor for T2D. Globally, the highest prevalence of T2D is observed in the United States, followed by China and India. This indicates that fat distribution alone is not the sole determinant; rather, factors such as poor dietary habits, poor nutritional quality, sedentary lifestyle, and broader socio-economic conditions contribute significantly to the development of metabolic disease.[84]

Brown fat and white fat are two distinct types of adipose tissue with opposite roles in energy metabolism, and their balance influences obesity and metabolic health (Figure 4, Table 1). (94). White adipose tissue (WAT) is the ‘storage fat’ that stores excess energy in the form of triglycerides. It is usually distributed subcutaneously and viscerally around internal organs. Excess visceral fat accumulation is strongly linked to insulin resistance, T2D, CVD, and chronic inflammation. These tissues secrete adipokines (leptin, adiponectin, resistin, TNF-α, IL-6). In obesity, secretion patterns shift towards the generation of pro-inflammatory signals, driving systemic metabolic dysfunction.[86,87] Whereas brown adipose tissue (BAT) burns energy to produce heat using uncoupling protein 1 (UCP1) in mitochondria.[88] More abundant in newborns, in adults, in areas like the neck, supraclavicular regions, and around large blood vessels. In obesity, BAT activity is reduced, leading to reduced energy expenditure and favoring fat accumulation. Active BAT helps maintain body weight by increasing energy expenditure, improving glucose and lipid metabolism, and insulin sensitivity. White fat cells can sometimes transform into beige adipocytes under certain stimuli (cold exposure, exercise, some hormones). This process, called “browning of white fat” is a potential therapeutic strategy against obesity.[89] Exercise increases irisin and other myokines that promote browning of fat. Dietary factors that promote this process include capsaicin, catechins, caffeine, and omega-3 fatty acids.

Excess maternal nutrition or gestational diabetes can also further aggravate obesity risk by enhancing adipogenesis through altered PPARγ and C/EBPα signaling, thereby expanding adipocyte progenitor pools.[29] Research from INSERM, France, highlights that dysregulated adipose progenitor cells (APCs) and abnormal perinatal adipogenesis, mediated by epigenetic mechanisms, are key drivers of long-term adipose dysfunction in offspring of obese mothers.[90]Additionally, mitogen-activated protein kinases (MAPKs), including ERK1/2, JNK, and p38MAPK, play critical roles in regulating appetite, adipogenesis, glucose homeostasis, and thermogenesis. While landmark studies on liraglutide, a GLP-1 receptor agonist, have demonstrated remarkable success in obesity management, such therapeutic strategies do not address the fundamental cellular and molecular mechanisms underlying obesity.[91]

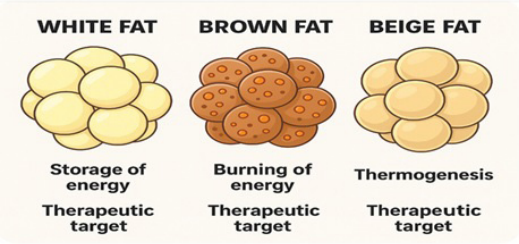

Figure 4*. Different types of adipose tissue. (Created by Open Ai-Chat GPT)*

Table 1.

Schematic diagram shows the differences between white fat, brown fat, and beige fat. (Developed by OpenAI ChatGPT).

Category	White Fat (WAT)	Brown Fat (BAT)	Beige Fat (Brite)
Main Function	Energy storage (triglycerides)	Energy burning (thermogenesis)	Intermediate; inducible thermogenesi
Color & Structure	White/yellow; large lipid droplets	Brown; multilocular lipid droplets	Light brown; appear within WAT
Mitochondria	Few	Very high	Moderate
UCP1 Presence	Absent	Abundant	Inducible
Effect on Obesity	Promotes obesity, insulin resistance	Protects against obesity, improves r	Can counteract obesity if activated
Therapeutic Target	Convert to beige fat (browning)	Activate to increase energy expendi	Induce browning via cold, exercise, d

Diabetes Mellitus

The combined effects, such as DNA methylation and histone modifications, can suppress pancreatic and duodenal homeobox 1 (PDX1) and hepatocyte nuclear factor 4 alpha (HNF4a), leading to oxidative stress and mitochondrial defects, and resulting in insufficient ATP generation in pancreatic β-cells.[92,93] This severely limits glucose-stimulated insulin release and contributes to the dysfunction seen in T2D.[94] Skeletal muscle is a major site for glucose uptake after meals, primarily facilitated by the glucose transporter type 4 (GLUT4). Programming of this tissue, often associated with insulin-resistant states, affects glucose metabolism through two main avenues. *Reduced mitochondrial oxidative capacity*: This refers to a decline in the mitochondria's ability to efficiently generate energy through oxidative phosphorylation. A lower oxidative capacity reduces the muscle's glucose demand, leaving more glucose in the bloodstream.[95] *Reduced GLUT4 expression*: Insulin and exercise typically trigger GLUT4 translocation from the cell's interior to the plasma membrane to facilitate glucose entry.[96] In programmed muscle, GLUT4 expression or translocation is reduced, limiting the cell's ability to clear glucose from the blood.

The liver is the primary organ responsible for endogenous glucose production, a process that is normally suppressed by insulin. In states of insulin resistance, this process becomes unregulated and contributes significantly to hyperglycemia, particularly during fasting. The two key proteins involved are: *FOXO1*: A transcription factor that activates the expression of genes involved in gluconeogenesis, such as glucose-6-phosphatase (G6Pc) and phosphoenolpyruvate carboxykinase (PEPCK).[97] Normally, insulin signaling via Akt phosphorylates FOXO1, sequestering it in the cytoplasm and inactivating it. In insulin resistance, this suppression is impaired, and active FOXO1 remains in the nucleus, promoting glucose production. *PGC-1α*: A transcriptional co-activator that collaborates with transcription factors like FOXO1 to boost the expression of gluconeogenic enzymes.[98] The combined effect of these dysfunctional pathways is systemic hyperglycemia. *In fasting states*: The liver increases its glucose production through hyperactivated gluconeogenesis, flooding the bloodstream with glucose. *Upon feeding*: The impaired glucose uptake by skeletal muscle means that ingested glucose is not efficiently cleared from the blood, further worsening hyperglycemia.[99] This vicious cycle demonstrates a central aspect of metabolic disorders like T2D, where tissue-specific defects converge to cause persistently high blood sugar.

FOXO1 activation: The transcription factor Forkhead box O1 (FOXO1) is a key regulator of hepatic gluconeogenesis (the production of glucose from non-carbohydrate sources).[100] Normally, insulin signaling activates Akt, which phosphorylates FOXO1 and sends it out of the cell's nucleus, effectively turning it off. In insulin-resistant states, this phosphorylation is impaired, and FOXO1 remains active in the nucleus. Active FOXO1 promotes the transcription of key gluconeogenic enzymes, such as phosphoenolpyruvate carboxykinase (PEPCK) and glucose-6-phosphatase (G6Pase), thereby increasing the liver's production of glucose.

PGC-1α hyperactivation: Peroxisome proliferator-activated receptor gamma coactivator 1-alpha (PGC-1α) is a transcriptional coactivator that works with FOXO1 to regulate gluconeogenesis.[98] Similar to FOXO1, PGC-1α is typically activated during fasting to stimulate hepatic glucose production. In the context of the described programming, increased activity leads to persistently elevated glucose production, contributing to fasting hyperglycemia. This cycle of reduced glucose uptake and increased production is a classic feature of insulin resistance and T2D.[101]

Hyperglycemia promotes a prothrombotic milieu by facilitating platelet activation, perturbing coagulation pathways, and impairing fibrinolytic mechanisms.[102] The underlying pathophysiological processes involve oxidative stress, endothelial dysfunction characterized by diminished nitric oxide bioavailability, accumulation of advanced glycation end products (AGEs), elevated circulating coagulation factors, augmented platelet aggregation, and decreased fibrinolytic enzyme activity.[103] *Endothelial Dysfunction*: Sustained hyperglycemia induces oxidative and inflammatory stress within the vascular endothelium, resulting in impaired endothelial function. This dysfunction is associated with reduced synthesis of nitric oxide (NO) and prostaglandin I_2, both of which inhibit platelet aggregation. Consequently, endothelial impairment contributes to a prothrombotic state. *Platelet Activation*: Hyperglycemia directly modulates platelet behavior by increasing their sensitivity to activating stimuli and promoting aggregation.[74,104] Additionally, it enhances the release of platelet-derived microparticles and strengthens the binding affinity for specific coagulation factors, collectively amplifying thrombotic potential.[105]

In a unique study conducted at the University of Minnesota, in collaboration with Dr. Jonathan Gerrard, we investigated alterations in arachidonic acid metabolism in drug-induced diabetic rats.[74] Diabetes was induced in these animals by streptozotocin injection. We assessed prostanoid production in platelets and vascular tissues by measuring stable metabolites of radiolabeled arachidonic acid, specifically thromboxane and prostacyclin. In diabetic rats, thromboxane production was elevated, whereas prostacyclin production was reduced compared with control animals (Figure 5). Remarkably, transplantation of pancreatic islet cells into diabetic rats restored prostaglandin production to normal levels, demonstrating that the shift in prostanoid balance toward a pro-thrombotic state was disease-specific.

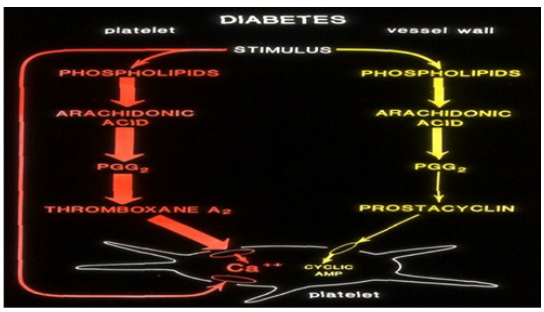

Figure 5. *Altered Prostanoid Metabolism in Drug-Induced Diabetes Rat Model (Courtesy: My Associate, Dr. Jonathan Gerrard, University of Minnesota).*

Clinical complications associated with chronic hyperglycemia include microvascular dysfunction that contributes to the development of peripheral neuropathy, retinopathy, and nephropathy, primarily as a result of arterial and capillary insufficiency.[106] Prolonged hyperglycemia activates multiple biochemical pathways that damage vascular endothelial cells.[104] Excess intracellular glucose increases flux through the polyol pathway, leading to sorbitol accumulation, osmotic stress, and depletion of NADPH, thereby reducing antioxidant defenses, including glutathione. Concurrently, hyperglycemia enhances the formation of advanced glycation end products (AGEs), which cross-link with proteins in the vascular basement membrane and interact with receptors for AGEs (RAGE) on endothelial and inflammatory cells, triggering oxidative stress and inflammatory signaling[107,108] Activation of protein kinase C (PKC), particularly the β-isoform, further promotes vasoconstriction, increased vascular permeability, and basement membrane thickening by upregulating endothelin-1, vascular endothelial growth factor (VEGF), and transforming growth factor-β (TGF-β).[109] Additionally, increased glucose auto-oxidation and mitochondrial overproduction of reactive oxygen species (ROS) exacerbate endothelial dysfunction by impairing nitric oxide (NO) bioavailability and promoting prothrombotic and proinflammatory states.[74,78] Collectively, these mechanisms result in capillary rarefaction, reduced tissue perfusion, and ischemic injury to nerves, retinal microvessels, and renal glomeruli, which are the pathological hallmarks of diabetic microangiopathy.

Occlusive Arterial Disease

Occlusive arterial disease develops primarily as a consequence of atherosclerosis, a chronic, progressive condition involving structural and functional alterations of the arterial wall.[110] The process begins with endothelial injury, often triggered by factors such as hypertension, hyperglycemia, dyslipidemia, smoking, or oxidative stress. [111] Damage to the endothelium leads to a loss of vascular homeostasis, characterized by reduced nitric oxide (NO) availability, increased permeability to lipids, and enhanced expression of adhesion molecules that promote the recruitment of circulating platelets, monocytes, and T lymphocytes (Figure 6).[112] Once within the intima, monocytes differentiate into macrophages, which engulf oxidized low-density lipoproteins (oxLDL) through scavenger receptors, transforming into foam cells—the hallmark of early fatty streak lesions.[113] This process is amplified by reactive oxygen species (ROS), which not only oxidize lipids but also activate redox-sensitive transcription factors such as NF-κB, leading to the production of inflammatory cytokines (e.g., TNF-α, IL-1β, and IL-6). These cytokines sustain local inflammation, attract more immune cells, and promote smooth muscle cell migration from the media to the intima.[114]

Vascular smooth muscle cells (VSMCs), once in the intimal layer, undergo phenotypic switching from a contractile to a synthetic state, enabling them to proliferate, secrete extracellular matrix components, and take up lipids.[115] Signaling pathways involving Bruton's tyrosine kinase (BTK) have been implicated in regulating macrophage activation, VSMC behavior, and lipid metabolism within the plaque microenvironment.[116] At the molecular level, microRNAs (miRNAs) play critical regulatory roles by modulating gene expression involved in inflammation, lipid metabolism, and cell survival. For instance, certain miRNAs suppress endothelial repair mechanisms or enhance pro-inflammatory signaling, further aggravating vascular dysfunction.[117] Over time, these processes culminate in the formation of fibroatheromatous plaques, composed of lipid cores, necrotic debris, inflammatory cells, and fibrotic tissue.[118] Continued oxidative and inflammatory stress may weaken the fibrous cap, predisposing it to rupture. Plaque rupture exposes thrombogenic material to circulating blood, triggering platelet activation and thrombus formation that can abruptly obstruct blood flow, manifesting clinically as myocardial infarction, stroke, or peripheral arterial occlusion.[119] In summary, occlusive arterial disease represents a complex interplay between endothelial dysfunction, oxidative stress, immune activation, lipid metabolism, and molecular signaling networks (including BTK and miRNAs). Together, these events perpetuate a self-amplifying cycle of inflammation and vascular injury that drives the progression from early atherosclerosis to advanced, clinically significant arterial occlusion.

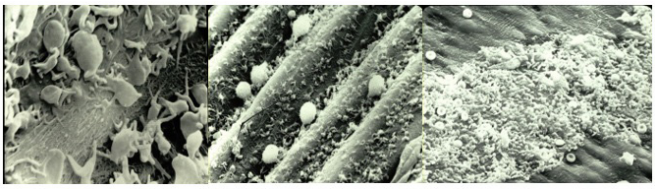

Figure 6. *Platelet Interactions with the arterial vessel wall. (Courtesy: My associate, (Late) Professor James G. White, University of Minnesota).*

Prothrombotic role of blood platelets

Prothrombotic conditions at the vascular wall arise from an imbalance between antithrombotic and prothrombotic mediators produced by endothelial cells and circulating platelets (Figure 7).

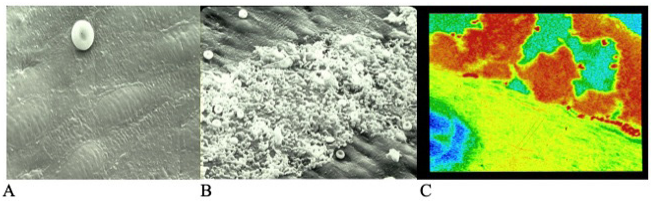

Figure 7. *Platelet Interaction with healthy endothelium (A), Platelet interaction with dysfunctional endothelium (B), and subendothelium (C).(Courtesy: My associate, (Late) Professor James G White, University of Minnesota).*

Under physiological conditions, vasodilators and antithrombotic agents such as prostacyclin (PGI_2), thrombomodulin, protein C, plasminogen activators, and heparin-like glycosaminoglycans maintain endothelial integrity and inhibit platelet aggregation and fibrin formation.[68-70] However, oxidative stress, inflammation, or hyperglycemia can disrupt this equilibrium, leading to

enhanced synthesis and release of prothrombotic factors, including platelet-activating factor (PAF), von Willebrand factor (vWF), plasminogen activator inhibitors, endothelial proteases, and tissue factor. These molecules promote platelet adhesion, activation, and aggregation, while concurrently stimulating the coagulation cascade through thrombin generation and fibrin deposition. Additionally, increased production of prostanoids such as prostaglandins G_2 and H_2, and thromboxane A_2, augments vasoconstriction and platelet aggregation, further amplifying the prothrombotic milieu that predisposes to vascular occlusion and ischemic events.[74]

Ionized calcium acts as the primary bioregulator, with numerous biochemical mechanisms modulating the availability of free cytosolic calcium.[120] Signal transduction begins when agonists bind to specific receptors, leading to the stimulation of effector enzymes via transmembrane GTP-binding proteins (Figure 8). Key enzymes that regulate calcium levels via secondary messengers include phospholipase C, phospholipase A2, phospholipase D, adenyl cyclases, and guanyl cyclases. Phospholipase-C activation results in the hydrolysis of phosphatidylinositol trisphosphate, generating the secondary messengers 1, 2-diacylglycerol (1, 2-DG) and inositol trisphosphate (IP3).[121] Signal transduction mechanisms are similar to agonist-induced transmembrane signaling. Platelet antagonists act at the membrane receptors, inducing transmembrane signals that result in the formation of second messengers, cyclic AMP (cAMP) and cyclic GMP (cGMP).[122] These second messengers lower cytosolic calcium levels and thereby limit the availability of free calcium needed for platelet activation, leading to the assembly of actin, contraction of cytoskeletal proteins, and secretion of granule contents.[120-122]

Figure 8. *Signal transduction, formation of second messengers. (Schematic representation prepared by the University of Minnesota Artists).*

Occlusive Arterial Events

All major arteries are susceptible to oxidative stress–induced endothelial injury, a fundamental initiating event in the pathogenesis of atherosclerosis.[123,124] Under normal physiological conditions, the vascular endothelium serves as a critical regulator of vascular homeostasis by maintaining vasodilation through nitric oxide (NO) production, inhibiting platelet aggregation, and preventing smooth muscle proliferation. However, chronic exposure to oxidative stress—arising from metabolic abnormalities such as hyperglycemia, dyslipidemia, hypertension, and smoking—leads to excessive generation of reactive oxygen species (ROS).[125] These reactive species rapidly inactivate NO, impairing endothelial-dependent vasodilation, and promoting a pro-inflammatory, pro-coagulant, and vasoconstrictive milieu.

Endothelial dysfunction enhances vascular permeability, facilitating subendothelial accumulation of LDL. Oxidative modification of LDL within the intima results in the formation of oxidized LDL (oxLDL), which acts as a potent chemoattractant for circulating monocytes and T lymphocytes.[126] Upon infiltration, monocytes differentiate into macrophages that internalize oxLDL via scavenger receptors, giving rise to foam cells, the earliest morphological feature of fatty streaks. The local inflammatory environment perpetuates the release of cytokines, chemokines, and growth factors that stimulate vascular smooth muscle cell (VSMC) migration and proliferation into the intima. These VSMCs contribute to extracellular matrix deposition, leading to the development of a fibrofatty atheromatous plaque.[127] As the lesion matures, persistent inflammation and oxidative stress weaken the fibrous cap via macrophage-derived matrix metalloproteinases (MMPs), rendering the plaque unstable and prone to rupture. Plaque rupture exposes thrombogenic core material to circulating blood, activating platelets and the coagulation cascade, culminating in thrombus formation and acute vascular occlusion. [128,129]

The clinical consequences of such occlusive arterial disease are determined by the vascular territory affected. In coronary arteries, it manifests as myocardial ischemia and infarction; in cerebral vessels, as transient ischemic attacks or ischemic stroke; and in peripheral arteries, as critical limb ischemia or gangrene.[130] Similarly, involvement of renal and retinal microvasculature results in ischemic nephropathy and retinopathy, respectively.[131] Collectively, oxidative stress–driven endothelial dysfunction integrates metabolic, inflammatory, and vascular mechanisms, forming the central axis of atherogenesis. This progressive process not only underlies the structural narrowing (stenosis) of arteries but also predisposes to acute ischemic events that compromise perfusion and the functional integrity of vital organs. Therapeutic implications: Understanding the molecular interplay between oxidative stress, inflammation, and endothelial dysfunction provides a strong rationale for targeted interventions.[132,133] Strategies that restore redox balance—such as antioxidants, NADPH oxidase inhibitors, and mitochondrial ROS modulators—alongside agents that enhance endothelial NO bioavailability or suppress vascular inflammation (e.g., statins, anti-cytokine therapies, and BTK inhibitors), hold promise in preventing or attenuating the progression of atherosclerotic vascular disease.[132,133]

Discussion

Cardiovascular diseases (CVDs) remain the foremost cause of death worldwide. Of the 20.5 million CVD-related deaths reported in 2021, nearly 80% occurred in low- and middle-income countries.[134] Much of the foundational understanding of CVD pathophysiology stems from the landmark Framingham Heart Study, which identified key risk factors such as hypertension, diabetes, and smoking. The study also underscored several critical contributors to heart disease—elevated cholesterol (particularly LDL or “bad”

cholesterol), obesity, physical inactivity, family history, age, and sex. It has been estimated that the complete elimination of cardiovascular diseases could extend average life expectancy by approximately 11 years.[135] The INTERHEART study further demonstrated that nine modifiable risk factors account for over 90% of the global risk of myocardial infarction across diverse regions and populations, implying that effective management of these factors could prevent most premature heart attacks.[136] Similarly, Khera and colleagues at Harvard University showed that even among individuals with a high genetic predisposition, adherence to a healthy lifestyle reduced the relative risk of coronary artery disease by nearly 50%.[137] Research from Imperial College London revealed a decline in cardiovascular mortality but a concurrent rise in diabetes-related deaths in high-income countries. Between 1980 and 2009, age-standardized cardiometabolic mortality decreased across 26 industrialized nations, with reductions in modifiable risk factors contributing to 49% of the decline in men and 40% in women. However, no country has yet succeeded in reversing or halting the increasing incidence of vascular diseases.[69]

In a monograph we published in 2001 titled "Coronary Artery Disease in South Asians," world-renowned cardiovascular epidemiologist Professor Henry Blackburn of the University of Minnesota emphasized, "The ultimate health goal is not merely to control disease or reduce high risk, but to prevent high risk from developing in the first place—both in individuals and across entire populations."[138] According to the Cleveland Clinic, healthy lifestyle habits could prevent up to 80% of chronic diseases, most of which are linked to modifiable risk factors—a finding supported by numerous studies and public health organizations. Despite this evidence, modern healthcare continues to focus largely on managing diagnosed conditions such as hypertension, T2D, obesity, and vascular diseases, rather than preventing them. The future of medicine, however, lies in proactive prevention, targeting modifiable risks and promoting a longer, healthier lifespan.[70,139] Our current understanding of the cellular and molecular mechanisms underlying cardiometabolic risk and the development of metabolic diseases has advanced substantially. In this review, we summarize these mechanisms, including oxidative stress, dysregulated lipid and glucose metabolism, endothelial dysfunction, arterial injury, atherosclerosis, and acute vascular events. In addition to lifestyle modification, early detection of metabolic dysfunction and targeted intervention at the cellular and molecular levels may significantly enhance the prevention and management of chronic metabolic diseases.

The concept of the FOAD, originally proposed by Dr. David Barker, has evolved into the DOHaD paradigm.[1-4] This hypothesis suggests that the intrauterine environment, including maternal nutrition, hormonal milieu, and metabolic status, profoundly influences fetal organ development and long-term health outcomes. Evidence from the Mysore Cohort and subsequent Mysore Parthenon Studies demonstrated that low birth weight, a marker of suboptimal fetal nutrition, was associated with an increased risk of coronary heart disease, insulin resistance, and metabolic dysfunction in adulthood.[10-12] Furthermore, maternal undernutrition or overnutrition—often coexisting in low- and middle-income countries—was found to exert dual adverse effects on offspring, predisposing them to metabolic and cardiovascular diseases. A new mechanistic hypothesis has emerged from studies led by Dr. Robert Freishtat's team at Children's National Hospital and collaborative work with Indian research institutions. Their work focuses on adipocyte-derived exosomal microRNAs (miRNAs) that mediate intercellular communication and epigenetic regulation.[60] In obesity, visceral adipocytes release altered exosomes that contain specific miRNAs, which reprogram metabolic pathways in distant tissues—impairing glucose and lipid homeostasis.[62,63] Extending this concept, maternal exosomal miRNAs may cross the placenta and modify fetal gene expression, influencing adipogenesis and lifelong susceptibility to obesity and T2D. This finding integrates epigenetic regulation into the DOHaD framework and opens avenues for early diagnosis and intervention.

The global rise in cardiometabolic diseases—including hypertension, obesity, T2D, and vascular dysfunction—reflects an interplay between metabolic, oxidative, and inflammatory processes.[64-70,140] ***Endothelial Dysfunction***: A pivotal early marker of vascular disease, characterized by reduced nitric oxide (NO) bioavailability due to oxidative stress and metabolic imbalance.[71-73] ***Hypertension***: Linked to fetal growth restriction, nephron deficit, and persistent activation of the renin–angiotensin–aldosterone system (RAAS), representing a developmental programming effect.[74-77] ***Obesity***: Differences in adipose tissue function—white (WAT), brown (BAT), and beige fat—determine metabolic efficiency. Maternal obesity and gestational diabetes further aggravate fetal adipogenesis via altered PPARγ and MAPK signaling, increasing long-term obesity risk.[84-87] ***Diabetes Mellitus***: Epigenetic modifications suppress critical pancreatic genes (PDX1, HNF4α), impairing β-cell function and insulin secretion. In peripheral tissues, reduced GLUT4 expression and mitochondrial dysfunction diminish glucose uptake, perpetuating hyperglycemia and insulin resistance.[92-99]

Atherosclerosis underlies occlusive arterial diseases through a cascade initiated by endothelial injury. Hyperglycemia, dyslipidemia, and hypertension increase oxidative stress, leading to lipid oxidation (ox-LDL formation), activation of inflammatory cytokines (TNF-α, IL-1β, IL-6), smooth muscle proliferation, and plaque formation.[123-127] Platelets play a prothrombotic role, amplifying vascular injury by promoting imbalanced prostanoid signaling and elevating thromboxane A_2. Experimental evidence, such as prostanoid imbalance in diabetic rats, confirms this metabolic-vascular linkage. In advanced stages, these mechanisms culminate in ischemic events—myocardial infarction, stroke, or peripheral artery disease—reflecting the systemic consequences of metabolic dysregulation. Despite advances in understanding molecular pathways—calcium signaling, NO–cGMP cascades, and redox regulation—clinical outcomes rely heavily on modifiable risk factor control. Historical and contemporary studies (Framingham, INTERHEART, Harvard's Khera et al.)[136,137] converge on the same conclusion: lifestyle modification—including balanced nutrition, physical activity, and smoking cessation—remains the most effective preventive strategy. Modern medicine must transition from a reactive model of disease management to a

proactive prevention model, emphasizing early identification of epigenetic and metabolic markers of disease susceptibility.

Conclusions

The cumulative evidence from decades of global and Indian research underscores that adult metabolic and cardiovascular diseases originate, in part, from adverse intrauterine environments that induce epigenetic reprogramming of key metabolic pathways. The integration of exosomal signaling, maternal nutrition, and oxidative stress into the DOHaD framework provides a unified model linking fetal events to adult pathology. Cardiometabolic diseases—spanning obesity, diabetes, hypertension, and vascular disorders—share a common axis of endothelial dysfunction, oxidative stress, and inflammation. While molecular research has identified numerous therapeutic targets, the greatest impact will come from early-life interventions and preventive strategies that address maternal and fetal health, aiming to halt the intergenerational transmission of disease risk. Ultimately, the future of medicine lies not merely in treating disease but in preventing high-risk states from developing, thereby promoting healthier aging and reducing the global burden of chronic cardiometabolic disorders.

Acknowledgments

Professor Gundu H. R. Rao is extremely grateful to the Department of Laboratory Medicine and Pathology, Lillehei Heart Institute, University of Minnesota, for its unwavering support for our research on thrombosis and hemostasis for more than 4 decades. He would also like to express his deep appreciation to the late Professor James G White of the University of Minnesota for his invaluable mentorship.

Funding

The author extends his gratitude to the National Heart, Blood, and Lung Institute (NHLBI) of the National Institutes of Health (NIH) for its continued financial support of our studies from 1970 to 2000. Furthermore, he expresses his sincere appreciation to the International Society on Thrombosis and Hemostasis (ISTH), USA, for their financial assistance to the South Asian Society on Atherosclerosis and Thrombosis (SASAT) from 1992 to 2000 for international educational initiatives in India. He also expresses his thanks to the National Science Foundation (NSF), USA, and the United Nations Development Program (UNDP) for providing travel grants to visit India for developing bilateral research projects from 1992 to 2000.

References

1. Barker DJ, Osmond C. Infant mortality, childhood nutrition, and ischaemic heart disease in England and Wales. Lancet. 1986 May 10;1(8489):1077-81. doi: 10.1016/s0140-6736(86)91340-1. PMID: 2871345.
2. Barker DJ, Winter PD, Osmond C, Margetts B, Simmonds SJ. Weight in infancy and death from ischaemic heart disease. Lancet. 1989 Sep 9;2(8663):577-80. doi: 10.1016/s0140-6736(89)90710-1. PMID: 2570282.
3. Barker DJ, Gluckman PD, Godfrey KM, Harding JE, Owens JA, Robinson JS. Fetal nutrition and cardiovascular disease in adult life. Lancet. 1993 Apr 10;341(8850):938-41. doi: 10.1016/0140-6736(93)91224-a. PMID: 8096277.
4. Barker DJ. The origins of the developmental origins theory. J Intern Med. 2007 May;261(5):412-7. doi: 10.1111/j.1365-2796.2007.01809.x. PMID: 17444880.
5. Junien C, Nathanielsz P. Report on the IASO Stock Conference 2006: early and lifelong environmental epigenomic programming of metabolic syndrome, obesity and type II diabetes. Obes Rev. 2007 Nov;8(6):487-502. doi: 10.1111/j.1467-789X.2007.00371.x. PMID: 17949354.
6. Reik W, Dean W, Walter J. Epigenetic reprogramming in mammalian development. Science. 2001 Aug 10;293(5532):1089-93. doi: 10.1126/science.1063443. PMID: 11498579.
7. Waterland RA, Jirtle RL. Early nutrition, epigenetic changes at transposons and imprinted genes, and enhanced susceptibility to adult chronic diseases. Nutrition. 2004 Jan;20(1):63-8. doi: 10.1016/j.nut.2003.09.011. PMID: 14698016.
8. Weaver IC, Champagne FA, Brown SE, Dymov S, Sharma S, Meaney MJ, Szyf M. Reversal of maternal programming of stress responses in adult offspring through methyl supplementation: altering epigenetic marking later in life. J Neurosci. 2005 Nov 23;25(47):11045-54. doi: 10.1523/JNEUROSCI.3652-05.2005. PMID: 16306417; PMCID: PMC6725868.
9. Wadhwa PD, Buss C, Entringer S, Swanson JM. Developmental origins of health and disease: brief history of the approach and current focus on epigenetic mechanisms. Semin Reprod Med. 2009 Sep;27(5):358-68. doi: 10.1055/s-0029-1237424. Epub 2009 Aug 26. PMID: 19711246; PMCID: PMC2862635.
10. Krishna M, Kumar GM, Veena SR, Krishnaveni GV, Kumaran K, Karat SC, et al. Birth size, risk factors across life and cognition in late life: protocol of prospective longitudinal follow-up of the MYNAH (MYsore studies of Natal effects on Ageing and Health) cohort. BMJ Open. 2017 Feb 16;7(2):e012552. doi: 10.1136/bmjopen-2016-012552. PMID: 28209604; PMCID: PMC5318644.
11. Krishnaveni GV, Veena SR, Hill JC, Karat SC, Fall CH. Cohort profile: Mysore parthenon birth cohort. Int J Epidemiol. 2015 Feb;44(1):28-36. doi: 10.1093/ije/dyu050. Epub 2014 Mar 7. PMID: 24609067; PMCID: PMC4266599.
12. Krishna M, Kalyanaraman K, Veena SR, Krishanveni GV, Karat SC, Cox V, et al. Cohort Profile: The 1934-66 Mysore Birth Records Cohort in South India. Int J Epidemiol. 2015 Dec;44(6):1833-41. doi: 10.1093/ije/dyv176. Epub 2015 Oct 7. PMID: 26445965; PMCID: PMC4690000.
13. Law CM, de Swiet M, Osmond C, Fayers PM, Barker DJ, Cruddas AM, Fall CH. Initiation of hypertension in utero and its amplification throughout life. BMJ. 1993 Jan 2;306(6869):24-7. doi: 10.1136/bmj.306.6869.24. PMID: 8435572; PMCID: PMC1676382.
14. Barker DJ, Gluckman PD, Godfrey KM, Harding JE, Owens JA, Robinson JS. Fetal nutrition and cardiovascular disease in adult life. Lancet. 1993 Apr 10;341(8850):938-41. doi: 10.1016/0140-6736(93)91224-a. PMID: 8096277.
15. Barker DJ. Fetal origins of coronary heart disease. BMJ. 1995 Jul 15;311(6998):171-4. doi: 10.1136/bmj.311.6998.171. PMID: 7613432; PMCID: PMC2550226.

16. Black RE, Victora CG, Walker SP, Bhutta ZA, Christian P, de Onis M, et al.; Maternal and Child Nutrition Study Group. Maternal and child undernutrition and overweight in low-income and middle-income countries. Lancet. 2013 Aug 3;382(9890):427-451. doi: 10.1016/S0140-6736(13)60937-X. Epub 2013 Jun 6. Erratum in: Lancet. 2013. 2013 Aug 3;382(9890):396. PMID: 23746772.
17. Fall CH, Stein CE, Kumaran K, Cox V, Osmond C, Barker DJ, Hales CN. Size at birth, maternal weight, and type 2 diabetes in South India. Diabet Med. 1998 Mar;15(3):220-7. doi: 10.1002/(SICI)1096-9136(199803)15:3<220::AID-DIA544>3.0.CO;2-O. PMID: 9545123.
18. Ward AM, Fall CH, Stein CE, Kumaran K, Veena SR, Wood PJ, Syddall HE, Phillips DI. Cortisol and the metabolic syndrome in South Asians. Clin Endocrinol (Oxf). 2003 Apr;58(4):500-5. doi: 10.1046/j.1365-2265.2003.01750.x. PMID: 12641634; PMCID: PMC3405820.
19. Kumaran K, Fall CHD. Fetal origins of coronary heart disease and hypertension and its relevance to India. Review of evidence from the Mysore studies. Int J Diab. Dev Countries 21:34-41, 2001.
20. Kuneš J, Hojná S, Mráziková L, Montezano A, Touyz RM, Maletínská L. Obesity, Cardiovascular and Neurodegenerative Diseases: Potential Common Mechanisms. Physiol Res. 2023 Jul 31;72(Suppl 2):S73-S90. doi: 10.33549/physiolres.935109. PMID: 37565414; PMCID: PMC10660578.
21. Nakamura M, Sadoshima J. Cardiomyopathy in obesity, insulin resistance and diabetes. J Physiol. 2020 Jul;598(14):2977-2993. doi: 10.1113/JP276747.
22. Giglio RV, Stoian AP, Haluzik M, Pafili K, Patti AM, Rizvi AA, et al. Novel molecular markers of cardiovascular disease risk in type 2 diabetes mellitus. Biochim Biophys Acta Mol Basis Dis. 2021 Aug 1;1867(8):166148. doi: 10.1016/j.bbadis.2021.166148. Epub 2021 Apr 20. PMID: 33892081.
23. Zhu Z, Cao F, Li X. Epigenetic Programming and Fetal Metabolic Programming. Front Endocrinol (Lausanne). 2019 Dec 3;10:764. doi: 10.3389/fendo.2019.00764. PMID: 31849831; PMCID: PMC6901800.
24. Barker DJ. In utero programming of chronic disease. Clin Sci (Lond). 1998 Aug;95(2):115-28. PMID: 9680492.
25. O'Dowd JF, Stocker CJ. Endocrine pancreatic development: impact of obesity and diet. Front Physiol. 2013 Jul 18;4:170. doi: 10.3389/fphys.2013.00170. PMID: 23882220; PMCID: PMC3714448.
26. Avrahami D, Kaestner KH. Epigenetic regulation of pancreas development and function. Semin Cell Dev Biol. 2012 Aug;23(6):693-700. doi: 10.1016/j.semcdb.2012.06.002. Epub 2012 Jun 21. PMID: 22728076; PMCID: PMC3423529.
27. Deodati A, Inzaghi E, Cianfarani S. Epigenetics and In Utero Acquired Predisposition to Metabolic Disease. Front Genet. 2020 Jan 29;10:1270. doi: 10.3389/fgene.2019.01270. PMID: 32082357; PMCID: PMC7000755.
28. Faa G, Fanos V, Manchia M, Van Eyken P, Suri JS, Saba L. The fascinating theory of fetal programming of adult diseases: A review of the fundamentals of the Barker hypothesis. J Public Health Res. 2024 Mar 1;13(1):22799036241226817. doi: 10.1177/22799036241226817. PMID: 38434579; PMCID: PMC10908242.
29. Lecoutre S, Maqdasy S, Lambert M, Breton C. The Impact of Maternal Obesity on Adipose Progenitor Cells. Biomedicines. 2023 Dec 8;11(12):3252. doi: 10.3390/biomedicines11123252. PMID: 38137473; PMCID: PMC10741630.
30. Boney CM, Verma A, Tucker R, Vohr BR. Metabolic syndrome in childhood: association with birth weight, maternal obesity, and gestational diabetes mellitus. Pediatrics. 2005 Mar;115(3):e290-6. doi: 10.1542/peds.2004-1808. PMID: 15741354.
31. Al Aboud NM, Tupper C, Jialal I. Genetics, Epigenetic Mechanism. 2023 Aug 14. In: StatPearls [Internet]. Treasure Island (FL): StatPearls Publishing; 2026 Jan–. PMID: 30422591.
32. Heijmans BT, Tobi EW, Stein AD, Putter H, Blauw GJ, Susser ES, Slagboom PE, Lumey LH. Persistent epigenetic differences associated with prenatal exposure to famine in humans. Proc Natl Acad Sci U S A. 2008 Nov 4;105(44):17046-9. doi: 10.1073/pnas.0806560105. Epub 2008 Oct 27. PMID: 18955703; PMCID: PMC2579375.
33. Kimura H. Histone modifications for human epigenome analysis. J Hum Genet. 2013 Jul;58(7):439-45. doi: 10.1038/jhg.2013.66. Epub 2013 Jun 6. PMID: 23739122.
34. Dupont C, Kappeler L, Saget S, Grandjean V, Lévy R. Role of miRNA in the Transmission of Metabolic Diseases Associated With Paternal Diet-Induced Obesity. Front Genet. 2019 Apr 18;10:337. doi: 10.3389/fgene.2019.00337. PMID: 31057600; PMCID: PMC6482346.
35. Chernausek SD. Update: consequences of abnormal fetal growth. J Clin Endocrinol Metab. 2012 Mar;97(3):689-95. doi: 10.1210/jc.2011-2741. Epub 2012 Jan 11. PMID: 22238390; PMCID: PMC3319209.
36. Harmancıoğlu B, Kabaran S. Maternal high fat diets: impacts on offspring obesity and epigenetic hypothalamic programming. Front Genet. 2023 May 11;14:1158089. doi: 10.3389/fgene.2023.1158089. PMID: 37252665; PMCID: PMC10211392.
37. Vaiserman A, Lushchak O. Prenatal Malnutrition-Induced Epigenetic Dysregulation as a Risk Factor for Type 2 Diabetes. Int J Genomics. 2019 Feb 28;2019:3821409. doi: 10.1155/2019/3821409. PMID: 30944826; PMCID: PMC6421750.
38. Bianco-Miotto T, Craig JM, Gasser YP, van Dijk SJ, Ozanne SE. Epigenetics and DOHaD: from basics to birth and beyond. J Dev Orig Health Dis. 2017 Oct;8(5):513-519. doi: 10.1017/S2040174417000733. Epub 2017 Sep 11. PMID: 28889823.
39. Barker DJ. The fetal and infant origins of adult disease. BMJ. 1990 Nov 17;301(6761):1111. doi: 10.1136/bmj.301.6761.1111. PMID: 2252919; PMCID: PMC1664286.
40. Heerwagen MJ, Miller MR, Barbour LA, Friedman JE. Maternal obesity and fetal metabolic programming: a fertile epigenetic soil. Am J Physiol Regul Integr Comp Physiol. 2010 Sep;299(3):R711-22. doi: 10.1152/ajpregu.00310.2010. Epub 2010 Jul 14. PMID: 20631295; PMCID: PMC2944425.
41. Fall CHD, Kumaran K. Metabolic programming in early life in humans. Philos Trans R Soc Lond B Biol Sci. 2019 Apr 15;374(1770):20180123. doi: 10.1098/rstb.2018.0123. PMID: 30966889; PMCID: PMC6460078.
42. Kundakovic M, Jaric I. The Epigenetic Link between Prenatal Adverse Environments and Neurodevelopmental Disorders. Genes (Basel). 2017 Mar 18;8(3):104. doi: 10.3390/genes8030104. PMID: 28335457; PMCID: PMC5368708.
43. Bale TL, Baram TZ, Brown AS, Goldstein JM, Insel TR, McCarthy MM, et al.. Early life programming and neurodevelopmental disorders. Biol Psychiatry. 2010 Aug 15;68(4):314-9. doi: 10.1016/j.biopsych.2010.05.028. PMID: 20674602; PMCID: PMC3168778.

44. Hill DJ, Hill TG. Maternal diet during pregnancy and adaptive changes in the maternal and fetal pancreas have implications for future metabolic health. Front Endocrinol (Lausanne). 2024 Sep 23;15:1456629. doi: 10.3389/fendo.2024.1456629. PMID: 39377073; PMCID: PMC11456468.
45. Park JH, Moon JH, Kim HJ, Kong MH, Oh YH. Sedentary Lifestyle: Overview of Updated Evidence of Potential Health Risks. Korean J Fam Med. 2020 Nov;41(6):365-373. doi: 10.4082/kjfm.20.0165. Epub 2020 Nov 19. PMID: 33242381; PMCID: PMC7700832.
46. Rabasa C, Dickinson SL. Impact of stress on metabolism and energy balance. Curr Opin Behavior Sci. 9:71-77,2016. doi:10.1016/cobeha.2016.01.011.
47. Lubrano C, Parisi F, Cetin I. Impact of Maternal Environment and Inflammation on Fetal Neurodevelopment. Antioxidants (Basel). 2024 Apr 11;13(4):453. doi: 10.3390/antiox13040453. PMID: 38671901; PMCID: PMC11047368.
48. Le Magueresse-Battistoni B, Vidal H, Naville D. Environmental Pollutants and Metabolic Disorders: The Multi-Exposure Scenario of Life. Front Endocrinol (Lausanne). 2018 Oct 2;9:582. doi: 10.3389/fendo.2018.00582. PMID: 30333793; PMCID: PMC6176085.
49. Baillie-Hamilton PF. Chemical toxins: a hypothesis to explain the global obesity epidemic. J Altern Complement Med. 2002 Apr;8(2):185-92. doi: 10.1089/107555302317371479. PMID: 12006126.
50. Le Magueresse-Battistoni B, Vidal H, Naville D. Lifelong consumption of low-dosed food pollutants and metabolic health. J Epidemiol Community Health. 2015 Jun;69(6):512-5. doi: 10.1136/jech-2014-203913. Epub 2014 Dec 3. PMID: 25472636.
51. Halban PA, Polonsky KS, Bowden DW, Hawkins MA, Ling C, Mather KJ, et al. β-cell failure in type 2 diabetes: postulated mechanisms and prospects for prevention and treatment. Diabetes Care. 2014 Jun;37(6):1751-8. doi: 10.2337/dc14-0396. Epub 2014 May 8. PMID: 24812433; PMCID: PMC4179518.
52. Zhang K, Ma Y, Luo Y, Song Y, Xiong G, Ma Y, Sun X, Kan C. Metabolic diseases and healthy aging: identifying environmental and behavioral risk factors and promoting public health. Front Public Health. 2023 Oct 13;11:1253506. doi: 10.3389/fpubh.2023.1253506. PMID: 37900047; PMCID: PMC10603303.
53. Cerf ME. Beta cell dysfunction and insulin resistance. Front Endocrinol (Lausanne). 2013 Mar 27;4:37. doi: 10.3389/fendo.2013.00037. PMID: 23542897; PMCID: PMC3608918.
54. Malhotra N, Malhotra J, Bora NM et al. Fetal origin of adult disease. Donald School J. Ultrasound Obstet. Gynecol.2014;8(2):164-177.
55. Shenkin SD, Starr JM, Deary IJ. Birth weight and cognitive ability in childhood: a systematic review. Psychol Bull. 2004 Nov;130(6):989-1013. doi: 10.1037/0033-2909.130.6.989. PMID: 15535745.
56. Shenkin SD, Deary IJ, Starr JM. Birth parameters and cognitive ability in older age: a follow-up study of people born 1921-1926. Gerontology. 2009;55(1):92-8. doi: 10.1159/000163444. Epub 2008 Oct 9. PMID: 18843177.
57. Gale CR, Walton S, Martyn CN. Foetal and postnatal head growth and risk of cognitive decline in old age. Brain. 2003 Oct;126(Pt 10):2273-8. doi: 10.1093/brain/awg225. Epub 2003 Jun 23. PMID: 12821508.
58. Craft S. The role of metabolic disorders in Alzheimer disease and vascular dementia: two roads converged. Arch Neurol. 2009 Mar;66(3):300-5. doi: 10.1001/archneurol.2009.27. PMID: 19273747; PMCID: PMC2717716.
59. Miller DB, O'Callaghan JP. Do early-life insults contribute to the late-life development of Parkinson and Alzheimer diseases? Metabolism. 2008 Oct;57 Suppl 2:S44-9. doi: 10.1016/j.metabol.2008.07.011. PMID: 18803966.
60. Ferrante SC, Nadler EP, Pillai DK, Hubal MJ, Wang Z, Wang JM, et al. Adipocyte-derived exosomal miRNAs: a novel mechanism for obesity-related disease. Pediatr Res. 2015 Mar;77(3):447-54. doi: 10.1038/pr.2014.202. Epub 2014 Dec 17. PMID: 25518011; PMCID: PMC4346410.
61. Camussi G, Deregibus MC, Bruno S, Grange C, Fonsato V, Tetta C. Exosome/microvesicle-mediated epigenetic reprogramming of cells. Am J Cancer Res. 2011;1(1):98-110. Epub 2010 Oct 22. PMID: 21969178; PMCID: PMC3180104.
62. Freishtat R. Maternal Adipocyte-derived Exosomes in the Thin-Fat Baby Paradox. Fogarty International Research Grant, National Institutes of Health (NIH), 1R21 HD094127-01. 2018-2020.
63. Rao GHR. Fetal Origin of Adult Cardiometabolic Diseases: Micronutrient and micro RNA Interventions. EC Endocrinol. Metab Res.2019; 4.1:07-16.
64. Mensah GA, Fuster V, Murray CJL, Roth GA; Global Burden of Cardiovascular Diseases and Risks Collaborators. Global Burden of Cardiovascular Diseases and Risks, 1990-2022. J Am Coll Cardiol. 2023 Dec 19;82(25):2350-2473. doi: 10.1016/j.jacc.2023.11.007. PMID: 38092509; PMCID: PMC7615984.
65. Huang X, Wu Y, Ni Y, Xu H, He Y. Global, regional, and national burden of type 2 diabetes mellitus caused by high BMI from 1990 to 2021, and forecasts to 2045: analysis from the global burden of disease study 2021. Front Public Health. 2025 Jan 23;13:1515797. doi: 10.3389/fpubh.2025.1515797. PMID: 39916706; PMCID: PMC11798972.
66. Islam ANMS, Sultana H, Nazmul Hassan Refat M, Farhana Z, Abdulbasah Kamil A, Meshbahur Rahman M. The global burden of overweight-obesity and its association with economic status, benefiting from STEPs survey of WHO member states: A meta-analysis. Prev Med Rep. 2024 Sep 5;46:102882. doi: 10.1016/j.pmedr.2024.102882. PMID: 39290257; PMCID: PMC11406007.
67. Global Burden of Cardiovascular Diseases and Risks 2023 Collaborators. Global, Regional, and National Burden of Cardiovascular Diseases and Risk Factors in 204 Countries and Territories, 1990-2023. J Am Coll Cardiol. 2025 Dec 2;86(22):2167-2243. doi: 10.1016/j.jacc.2025.08.015. Epub 2025 Sep 24. PMID: 40990886.
68. Rao GHR. Editorial: Insights in diabetes: molecular mechanisms 2022. Front Endocrinol (Lausanne). 2023 Aug 7;14:1242759. doi: 10.3389/fendo.2023.1242759. PMID: 37608793; PMCID: PMC10441663.
69. Rao GHR. Cardiometabolic Diseases: A Global Perspective. J Cardiol & Cardiovasc Ther. 2018;12(2):ID555834.
70. Tate A, Rao GHR. Cardiometabolic Diseases: Cellular and Molecular Mechanisms. Cardiol Cardiovasc Res.2025;3(2):1-15.
71. Verma S, Buchanan MR, Anderson TJ. Endothelial function testing as a biomarker of vascular disease. Circulation. 2003 Oct 28;108(17):2054-9. doi: 10.1161/01.CIR.0000089191.72957.ED. PMID: 14581384.
72. Corretti MC, Anderson TJ, Benjamin EJ, Celermajer D, Charbonneau F, Creager MA, Deanfield J, Drexler H, Gerhard-Herman M, Herrington D, Vallance P, Vita J, Vogel

R; International Brachial Artery Reactivity Task Force. Guidelines for the ultrasound assessment of endothelial-dependent flow-mediated vasodilation of the brachial artery: a report of the International Brachial Artery Reactivity Task Force. J Am Coll Cardiol. 2002 Jan 16;39(2):257-65. doi: 10.1016/s0735-1097(01)01746-6. Erratum in: J Am Coll Cardiol 2002 Mar 20;39(6):1082. PMID: 11788217.
73. Kasliwal RR, Bansal M, Mehrotra R, Yeptho KP, Trehan N. Effect of pistachio nut consumption on endothelial function and arterial stiffness. Nutrition. 2015 May;31(5):678-85. doi: 10.1016/j.nut.2014.10.019. Epub 2014 Nov 7. PMID: 25837212.
74. Gerrard JM, Stuart MJ, Rao GH, Steffes MW, Mauer SM, Brown DM, White JG. Alteration in the balance of prostaglandin and thromboxane synthesis in diabetic rats. J Lab Clin Med. 1980 Jun;95(6):950-8. PMID: 6445927.
75. Takeda Y, Demura M, Yoneda T, Takeda Y. Epigenetic Regulation of the Renin-Angiotensin-Aldosterone System in Hypertension. Int J Mol Sci. 2024 Jul 25;25(15):8099. doi: 10.3390/ijms25158099. PMID: 39125667; PMCID: PMC11312206.
76. Grossini E, Venkatesan S, Ola Pour MM. Mitochondrial Dysfunction in Endothelial Cells: A Key Driver of Organ Disorders and Aging. Antioxidants (Basel). 2025 Mar 21;14(4):372. doi: 10.3390/antiox14040372. PMID: 40298614; PMCID: PMC12024085.
77. Zhan Y, Cao J, Ji L, Zhang M, Shen Q, Xu P, et al. Impaired mitochondria of Tregs decreases OXPHOS-derived ATP in primary immune thrombocytopenia with positive plasma pathogens detected by metagenomic sequencing. Exp Hematol Oncol. 2022 Sep 1;11(1):48. doi: 10.1186/s40164-022-00304-y. PMID: 36050760; PMCID: PMC9434515.
78. Janaszak-Jasiecka A, Płoska A, Wierońska JM, Dobrucki LW, Kalinowski L. Endothelial dysfunction due to eNOS uncoupling: molecular mechanisms as potential therapeutic targets. Cell Mol Biol Lett. 2023 Mar 9;28(1):21. doi: 10.1186/s11658-023-00423-2. PMID: 36890458; PMCID: PMC9996905.
79. Ma J, Li Y, Yang X, Liu K, Zhang X, Zuo X, et al. Signaling pathways in vascular function and hypertension: molecular mechanisms and therapeutic interventions. Signal Transduct Target Ther. 2023 Apr 20;8(1):168. doi: 10.1038/s41392-023-01430-7. PMID: 37080965; PMCID: PMC10119183.
80. Suzuki Y, Giles WR, Zamponi GW, Kondo R, Imaizumi Y, Yamamura H. Ca2+ signaling in vascular smooth muscle and endothelial cells in blood vessel remodeling: a review. Inflamm Regen. 2024 Dec 27;44(1):50. doi: 10.1186/s41232-024-00363-0. PMID: 39731196; PMCID: PMC11673324.
81. Fajmut A. Molecular mechanisms and targets of cyclic guanosine monophosphate (cGMP) in vascular smooth muscles. [Internet]. In: Muscle Cell and Tissue-Novel molecular targets and advances. IntechOpen.2021Available from: http://doi.org/10.5772/intechopen.97708
82. Rao GHR. Role of cyclic AMP and cyclic GMP as modulators of platelet cytosolic calcium. K Clin Prevent Cardiol.2016;5(3):99-103. doi:10.4103/2250-3528.191101.
83. Ranadive SM, Dillon GA, Mascone SE, Alexander LM. Vascular Health Triad in Humans With Hypertension-Not the Usual Suspects. Front Physiol. 2021 Oct 1;12:746278. doi: 10.3389/fphys.2021.746278. PMID: 34658930; PMCID: PMC8517241.
84. Rao GHR. Obesity is a unique metabolic disease. EC Clin and Med Case Rep. 2023; 6(8):01-11.
85. Liu X, Zhang Z, Song Y, Xie H, Dong M. An update on brown adipose tissue and obesity intervention: Function, regulation and therapeutic implications. Front Endocrinol (Lausanne). 2023 Jan 11;13:1065263. doi: 10.3389/fendo.2022.1065263. PMID: 36714578; PMCID: PMC9874101.
86. Taylor EB. The complex role of adipokines in obesity, inflammation, and autoimmunity. Clin Sci (Lond). 2021 Mar 26;135(6):731-752. doi: 10.1042/CS20200895. PMID: 33729498; PMCID: PMC7969664.
87. Li M, Chi X, Wang Y, Setrerrahmane S, Xie W, Xu H. Trends in insulin resistance: insights into mechanisms and therapeutic strategy. Signal Transduct Target Ther. 2022 Jul 6;7(1):216. doi: 10.1038/s41392-022-01073-0. PMID: 35794109; PMCID: PMC9259665.
88. Ragni M, Ruocco C, Nisoli E. Mitochondrial uncoupling, energy substrate utilization, and brown adipose tissue as therapeutic targets in cancer. NPJ Metab Health Dis. 2025 Sep 22;3(1):37. doi: 10.1038/s44324-025-00080-3. PMID: 40983641; PMCID: PMC12454651.
89. Negroiu CE, Tudorașcu I, Bezna CM, Godeanu S, Diaconu M, Danoiu R, Danoiu S. Beyond the Cold: Activating Brown Adipose Tissue as an Approach to Combat Obesity. J Clin Med. 2024 Mar 28;13(7):1973. doi: 10.3390/jcm13071973. PMID: 38610736; PMCID: PMC11012454.
90. Wen X, Zhang B, Wu B, Xiao H, Li Z, Li R, Xu X, Li T. Signaling pathways in obesity: mechanisms and therapeutic interventions. Signal Transduct Target Ther. 2022 Aug 28;7(1):298. doi: 10.1038/s41392-022-01149-x. Erratum in: Signal Transduct Target Ther. 2022 Oct 21;7(1):369. doi: 10.1038/s41392-022-01188-4. PMID: 36031641; PMCID: PMC9420733.
91. Astrup A, Rössner S, Van Gaal L, Rissanen A, Niskanen L, Al Hakim M, Madsen J, Rasmussen MF, Lean ME; NN8022-1807 Study Group. Effects of liraglutide in the treatment of obesity: a randomised, double-blind, placebo-controlled study. Lancet. 2009 Nov 7;374(9701):1606-16. doi: 10.1016/S0140-6736(09)61375-1. Epub 2009 Oct 23. Erratum in: Lancet. 2010 Mar 20;375(9719):984. PMID: 19853906.
92. Liu J, Lang G, Shi J. Epigenetic Regulation of PDX-1 in Type 2 Diabetes Mellitus. Diabetes Metab Syndr Obes. 2021 Feb 2;14:431-442. doi: 10.2147/DMSO.S291932. PMID: 33564250; PMCID: PMC7866918.
93. Miura A, Yamagata K, Kakei M, Hatakeyama H, Takahashi N, Fukui K, et al. Hepatocyte nuclear factor-4alpha is essential for glucose-stimulated insulin secretion by pancreatic beta-cells. J Biol Chem. 2006 Feb 24;281(8):5246-57. doi: 10.1074/jbc.M507496200. Epub 2005 Dec 23. PMID: 16377800.
94. Kaimala S, Kumar CA, Allouh MZ, Ansari SA, Emerald BS. Epigenetic modifications in pancreas development, diabetes, and therapeutics. Med Res Rev. 2022 May;42(3):1343-1371. doi: 10.1002/med.21878. Epub 2022 Jan 4. PMID: 34984701; PMCID: PMC9306699.
95. Xiao Liang K. Interplay of mitochondria and diabetes: Unveiling novel therapeutic strategies. Mitochondrion. 2024 Mar;75:101850. doi: 10.1016/j.mito.2024.101850. Epub 2024 Feb 7. PMID: 38331015.
96. Wang T, Wang J, Hu X, Huang XJ, Chen GX. Current understanding of glucose transporter 4 expression and functional mechanisms. World J Biol Chem. 2020 Nov 27;11(3):76-98. doi: 10.4331/wjbc.v11.i3.76. PMID: 33274014; PMCID: PMC7672939.
97. Peng S, Li W, Hou N, Huang N. A Review of FoxO1-

Regulated Metabolic Diseases and Related Drug Discoveries. Cells. 2020 Jan 10;9(1):184. doi: 10.3390/cells9010184. PMID: 31936903; PMCID: PMC7016779.
98. Lee J, Salazar Hernández MA, Auen T, Mucka P, Lee J, Ozcan U. PGC-1α functions as a co-suppressor of XBP1s to regulate glucose metabolism. Mol Metab. 2018 Jan;7:119-131. doi: 10.1016/j.molmet.2017.10.010. Epub 2017 Oct 28. PMID: 29129613; PMCID: PMC5784318.
99. Sanvictores T, Casale J, Huecker MR. Physiology, Fasting. 2023 Jul 24. In: StatPearls [Internet]. Treasure Island (FL): StatPearls Publishing; 2026 Jan–. PMID: 30521298.
100. Tsuchiya K, Ogawa Y. Forkhead box class O family member proteins: The biology and pathophysiological roles in diabetes. J Diabetes Investig. 2017 Nov;8(6):726-734. doi: 10.1111/jdi.12651. Epub 2017 Apr 19. PMID: 28267275; PMCID: PMC5668485.
101. Solis-Herrera C, Triplitt C, Cersoimo E. DeFronzo RA: Pathogenesis of Type2 diabetes mellitus. In: Feingold KR Ahmed SF, Anawalt B et al;, editors. [Internet]. South Dartmouth (MA):MDtext.com Inc., 2000. https://www.ncbi.nlm.nih.gov/books/NBK279115.
102. Li X, Weber NC, Cohn DM, Hollmann MW, DeVries JH, Hermanides J, Preckel B. Effects of Hyperglycemia and Diabetes Mellitus on Coagulation and Hemostasis. J Clin Med. 2021 May 29;10(11):2419. doi: 10.3390/jcm10112419. PMID: 34072487; PMCID: PMC8199251.
103. Vaidya AR, Wolska N, Vara D, Mailer RK, Schröder K, Pula G. Diabetes and Thrombosis: A Central Role for Vascular Oxidative Stress. Antioxidants (Basel). 2021 Apr 29;10(5):706. doi: 10.3390/antiox10050706. PMID: 33946846; PMCID: PMC8146432.
104. Tian Y, Zong Y, Pang Y, Zheng Z, Ma Y, Zhang C, Gao J. Platelets and diseases: signal transduction and advances in targeted therapy. Signal Transduct Target Ther. 2025 May 16;10(1):159. doi: 10.1038/s41392-025-02198-8. PMID: 40374650; PMCID: PMC12081703.
105. Nomura S, Shimizu M. Clinical significance of procoagulant microparticles. J Intensive Care. 2015 Jan 7;3(1):2. doi: 10.1186/s40560-014-0066-z. PMID: 25705427; PMCID: PMC4336124.
106. Houben AJHM, Stehouwer CDA. Microvascular dysfunction: Determinants and treatment, with a focus on hyperglycemia. Endocrine Met Sci 2:100073. https://doi.org/10.1016/j.endmts.2020.1000073.
107. Taguchi K, Fukami K. RAGE signaling regulates the progression of diabetic complications. Front Pharmacol. 2023 Mar 16;14:1128872. doi: 10.3389/fphar.2023.1128872. PMID: 37007029; PMCID: PMC10060566.
108. Chen Y, Meng Z, Li Y, Liu S, Hu P, Luo E. Advanced glycation end products and reactive oxygen species: uncovering the potential role of ferroptosis in diabetic complications. Mol Med. 2024 Sep 9;30(1):141. doi: 10.1186/s10020-024-00905-9. PMID: 39251935; PMCID: PMC11385660.
109. Kant S, Feng J. Protein kinase C and endothelial dysfunction in select vascular diseases. Front Cardiovasc Med. 2025 Aug 25;12:1618343. doi: 10.3389/fcvm.2025.1618343. PMID: 40926896; PMCID: PMC12414950.
110. Belhoul-Fakir H, Brown ML, Thompson PL, Hamzah J, Jansen S. Connecting the Dots: How Injury in the Arterial Wall Contributes to Atherosclerotic Disease. Clin Ther. 2023 Nov;45(11):1092-1098. doi: 10.1016/j.clinthera.2023.10.004. Epub 2023 Oct 25. PMID: 37891144.
111. Jebari-Benslaiman S, Galicia-García U, Larrea-Sebal A, Olaetxea JR, Alloza I, Vandenbroeck K, Benito-Vicente A, Martín C. Pathophysiology of Atherosclerosis. Int J Mol Sci. 2022 Mar 20;23(6):3346. doi: 10.3390/ijms23063346. PMID: 35328769; PMCID: PMC8954705.
112. Feng Y, Li C, Liu B. Endothelial dysfunction in atherosclerosis: from classical pathways to emerging mechanisms. Vessel Plus. 2025; 9:8. Doi: 10.20517/2574-1209.2025.39 .
113. Jiang H, Zhou Y, Nabavi SM, Sahebkar A, Little PJ, Xu S, Weng J, Ge J. Mechanisms of Oxidized LDL-Mediated Endothelial Dysfunction and Its Consequences for the Development of Atherosclerosis. Front Cardiovasc Med. 2022 Jun 1;9:925923. doi: 10.3389/fcvm.2022.925923. PMID: 35722128; PMCID: PMC9199460.
114. Dash UC, Bhol NK, Swain SK, Samal RR, Nayak PK, Raina V, et al. Oxidative stress and inflammation in the pathogenesis of neurological disorders: Mechanisms and implications. Acta Pharm Sin B. 2025 Jan;15(1):15-34. doi: 10.1016/j.apsb.2024.10.004. Epub 2024 Oct 16. PMID: 40041912; PMCID: PMC11873663.
115. Chen R, McVey DG, Shen D, Huang X, Ye S. Phenotypic Switching of Vascular Smooth Muscle Cells in Atherosclerosis. J Am Heart Assoc. 2023 Oct 17;12(20):e031121. doi: 10.1161/JAHA.123.031121. Epub 2023 Oct 10. PMID: 37815057; PMCID: PMC10757534.
116. Bonetti J, Corti A, Lerouge L, Pompella A, Gaucher C. Phenotypic Modulation of Macrophages and Vascular Smooth Muscle Cells in Atherosclerosis-Nitro-Redox Interconnections. Antioxidants (Basel). 2021 Mar 26;10(4):516. doi: 10.3390/antiox10040516. PMID: 33810295; PMCID: PMC8066740.
117. Zapata-Martínez L, Águila S, de Los Reyes-García AM, Carrillo-Tornel S, Lozano ML, González-Conejero R, Martínez C. Inflammatory microRNAs in cardiovascular pathology: another brick in the wall. Front Immunol. 2023 May 18;14:1196104. doi: 10.3389/fimmu.2023.1196104. PMID: 37275892; PMCID: PMC10233054.
118. Li C, Deng C, Shi B, Zhao R. Thin-cap fibroatheroma in acute coronary syndrome: Implication for intravascular imaging assessment. Int J Cardiol. 2024 Jun 15;405:131965. doi: 10.1016/j.ijcard.2024.131965. Epub 2024 Mar 15. PMID: 38492863.
119. Baaten CCFMJ, Nagy M, Bergmeier W, Spronk HMH, van der Meijden PEJ. Platelet biology and function: plaque erosion vs. rupture. Eur Heart J. 2024 Jan 1;45(1):18-31. doi: 10.1093/eurheartj/ehad720. PMID: 37940193; PMCID: PMC10757869.
120. Rao GHR. Cellular Signaling Pathways and Vascular Dysfunctions. J Cardiol Cardiovasc Ther.12 (4):55844, 2018.
121. Rao GHR, Gerrard JM, Cohen I, Witkop CJ, White JG: Origin and role of calcium in platelet activation-contraction-secretion coupling. In: Fiskum, G (eds) Cell Calcium Metabolism. GWUMC Department of Biochemistry Annual Spring Symposia. Springer, Boston MA. https://doi.org/10.1007/978-1-4684-5598-4_44. ISBN 978-1-4684-5600-4. 1989.
122. Rao GHR. Role of cyclic AMP and cyclic GMP as modulators of platelet cytosolic calcium J. Clin Prevent Cardiol. 2016; 5(3):99-103. doi:10.4103/2250-3528.191101.
123. Higashi Y. Roles of Oxidative Stress and Inflammation in Vascular Endothelial Dysfunction-Related Disease. Antioxidants (Basel). 2022 Sep 30;11(10):1958. doi: 10.3390/antiox11101958. PMID: 36290681; PMCID: PMC9598825.

124. Batty M, Bennett MR, Yu E. The Role of Oxidative Stress in Atherosclerosis. Cells. 2022 Nov 30;11(23):3843. doi: 10.3390/cells11233843. PMID: 36497101; PMCID: PMC9735601.
125. Dilworth L, Facey A, Omoruyi F. Diabetes Mellitus and Its Metabolic Complications: The Role of Adipose Tissues. Int J Mol Sci. 2021 Jul 16;22(14):7644. doi: 10.3390/ijms22147644. PMID: 34299261; PMCID: PMC8305176.
126. Han KH, Chang MK, Boullier A, Green SR, Li A, Glass CK, Quehenberger O. Oxidized LDL reduces monocyte CCR2 expression through pathways involving peroxisome proliferator-activated receptor gamma. J Clin Invest. 2000 Sep;106(6):793-802. doi: 10.1172/JCI10052. PMID: 10995790; PMCID: PMC381395.
127. Poznyak AV, Nikiforov NG, Markin AM, Kashirskikh DA, Myasoedova VA, Gerasimova EV, Orekhov AN. Overview of OxLDL and Its Impact on Cardiovascular Health: Focus on Atherosclerosis. Front Pharmacol. 2021 Jan 11;11:613780. doi: 10.3389/fphar.2020.613780. PMID: 33510639; PMCID: PMC7836017.
128. Shah PK. Mechanisms of plaque vulnerability and rupture. J Am Coll Cardiol. 2003 Feb 19;41(4 Suppl S):15S-22S. doi: 10.1016/s0735-1097(02)02834-6. PMID: 12644336.
129. Mahdinia E, Shokri N, Taheri AT, Asgharzadeh S, Elahimanesh M, Najafi M. Cellular crosstalk in atherosclerotic plaque microenvironment. Cell Commun Signal. 2023 May 30;21(1):125. doi: 10.1186/s12964-023-01153-w. PMID: 37254185; PMCID: PMC10227997.
130. Rao GHR. Acute Vascular events: Cellular and Molecular Mechanisms. International Journal of Biomedicine. 2023;.13(3):9-16. doi:10.21103/Article13(3)_RA1.
131. Tang S, An X, Sun W, Zhang Y, Yang C, Kang X, et al. Parallelism and non-parallelism in diabetic nephropathy and diabetic retinopathy. Front Endocrinol (Lausanne). 2024 Feb 14;15:1336123. doi: 10.3389/fendo.2024.1336123.
132. Manful CF, Fordjour E, Ikumoinein E, Abbey L, Thomas R: Therapeutic strategies targeting Oxidative stress and inflammation: A narrative review. Biochem 5(4):35, 2025. https://doi.org/10.3390/biochem5040035
133. Xue J, Zhang Z, Sun Y, Jin D, Guo L, Li X, et al. Research Progress and Molecular Mechanisms of Endothelial Cells Inflammation in Vascular-Related Diseases. J Inflamm Res. 2023 Aug 23;16:3593-3617. doi: 10.2147/JIR.S418166. PMID: 37641702; PMCID: PMC10460614.
134. Di Cesare M, Perel P, Taylor S, Kabudula C, Bixby H, Gaziano TA, et al. The Heart of the World. Glob Heart. 2024 Jan 25;19(1):11. doi: 10.5334/gh.1288. PMID: 38273998; PMCID: PMC10809869.
135. Abohelwa M, Kopel J, Shurmur S, Ansari M, Awasthi Y, Awasthi S. The Framingham study of cardiovascular disease risks and stress -defenses: A Historical Review. J Vasc Dis. 2023;2(1):122-164.
136. Yusuf S, Hawken S, Ounpuu S, Dans T, Avezum A, Lanas F, et al.; INTERHEART Study Investigators. Effect of potentially modifiable risk factors associated with myocardial infarction in 52 countries (the INTERHEART study): case-control study. Lancet. 2004 Sep 11-17;364(9438):937-52. doi: 10.1016/S0140-6736(04)17018-9. PMID: 15364185.
137. Khera AV, Emdin CA, Drake I, Natarajan P, Bick AG, Cook NR, et al. Genetic Risk, Adherence to a Healthy Lifestyle, and Coronary Disease. N Engl J Med. 2016 Dec 15;375(24):2349-2358. doi: 10.1056/NEJMoa1605086. Epub 2016 Nov 13. PMID: 27959714; PMCID: PMC5338864.
138. Rao GHR, Kakkar VJ. Coronary artery disease in South Asians. Epidemiology, Risk Factors and Prevention. Jaypee Medical Publishers, India. 2001 ISBN# 81-7179-811-X.
139. Attia P, Gifford B. Outlive: The science and art of longevity. 2023. First Edition, Harmony, New York.
140. Tate AR, Rao GHR. Inflammation: Is It a Healer, Confounder, or a Promoter of Cardiometabolic Risks? Biomolecules. 2024 Aug 6;14(8):948. doi: 10.3390/biom14080948. PMID: 39199336; PMCID: PMC11352362.

International Journal of Biomedicine 16(2) (2026) 145-150
http://dx.doi.org/10.21103/Article16(2)_RA1

REVIEW ARTICLE

INTERNATIONAL JOURNAL OF BIOMEDICINE

Polymyalgia Rheumatica and Fibromyalgia: Similarities and Distinctions

Abdulrahman Ali M. Khormi[1*]

[1]*Department of Internal Medicine, College of Medicine, Prince Sattam bin Abdulaziz University, Al-Kharj, KSA*

Abstract

This review explores the similarities and distinctions between polymyalgia rheumatica (PMR) and fibromyalgia (FM), focusing on pain mechanisms, clinical features, diagnostic challenges, and individualized treatment strategies. Although both disorders manifest as musculoskeletal pain syndromes with overlapping features, PMR is characterized by inflammation and glucocorticoid responsiveness, while FM is dominated by central sensitization mechanisms. This article emphasizes the importance of differentiating between the two for accurate diagnosis and tailored therapy.(**International Journal of Biomedicine. 2026;16(2):145-150.**)

Keywords: polymyalgia rheumatica • fibromyalgia • central sensitization • inflammation • glucocorticoids • differential diagnosis

Main Points

- PMR and FM share symptoms but differ in that PMR is inflammatory and FM is centrally mediated.
- Distinguishing PMR from FM is very important to avoid misdiagnosis and inappropriate glucocorticoid use.
- Diagnosis depends on symptoms, inflammation markers, imaging (for PMR), and classification criteria.
- PMR is treated with glucocorticoids, while FM requires neuromodulators and non-drug therapies.
- PMR and FM can coexist, especially in older adults, requiring tailored multidisciplinary care.

For citation: Khormi AAM. Polymyalgia Rheumatica and Fibromyalgia: Similarities and Distinctions. International Journal of Biomedicine. 2026;16(2):145-150. doi:10.21103/Article16(2)_RA1

Abbreviations

CBT, cognitive behavioral therapy; **CRP**, C-reactive protein; **ESR**, erythrocyte sedimentation rate; **FM**, fibromyalgia; **FMS**, fibromyalgia syndrome; **GCA**, giant cell arteritis; **PMR**, polymyalgia rheumatica; **RA**, rheumatoid arthritis.

Introduction

Fibromyalgia (FM) is a chronic condition marked by pervasive musculoskeletal pain, accompanied by symptoms that significantly impact daily activities and diminish quality of life. The hallmark symptoms of FM encompass pervasive pain throughout the body, debilitating fatigue, sleep disturbances, and cognitive impairment, often termed "fibro-fog." Alongside psychological issues such as anxiety and depression, patients frequently endure headaches, irritable bowel syndrome, muscular and joint stiffness, and heightened pain sensitivity (allodynia and hyperalgesia). It is estimated that between 0.2% and 6.6% of the global population is afflicted by this condition, with a marked prevalence among women compared to men. A significant percentage of patients with inflammatory rheumatic diseases meet the fibromyalgia syndrome (FMS) criteria, complicating diagnosis, treatment, and follow-up. The coexistence of FMS may lead to superfluous laboratory and radiological evaluations.[1,2]

Polymyalgia rheumatica (PMR) is the most common inflammatory rheumatological disease in adults over 50,

***Corresponding author**:Dr. Abdulrahman Ali M Khormi. E-mail: isameldin2015@gmail.com*

occurring 2-3 times more frequently in women. PMR results in significant disabilities if inadequately managed. Symptoms include muscle rigidity and discomfort, predominantly in the cervical or shoulder regions and pelvic girdle, along with low-grade fever, depression, fatigue, anorexia, and weight reduction. Individuals affected often experience significant mobility restrictions due to discomfort, typically exacerbated in the mornings or after periods of inactivity. PMR is distinguished by increased inflammatory markers, including C-reactive protein (CRP) and erythrocyte sedimentation rate (ESR). It is typically administered with medium or low doses of oral glucocorticoids. The diagnosis of PMR depends on a synthesis of clinical assessment, medical history, physical examination, and laboratory tests. To diagnose PMR, conditions that may elicit similar symptoms must be excluded, according to the guidelines set forth by the American College of Rheumatology and the European League Against Rheumatism. The core exclusion disorders encompass infections, cancer, and giant cell arteritis (GCA), along with FM, hypothyroidism, rheumatoid arthritis, and drug-induced myalgia.[3]

The symptoms of FM and PMR often coincide, leading to potential misinterpretation or misdiagnosis, especially in elderly individuals presenting with fatigue and musculoskeletal pain. Muscle pain, stiffness, and fatigue are prevalent symptoms of both conditions, and distinguishing between them can be challenging because FM lacks definitive diagnostic tests, and symptoms vary. Certain criteria facilitate the differentiation between PMR and other pain disorders, such as FM, which typically manifests at a younger age than PMR. Furthermore, laboratory markers typically do not show elevation to indicate an inflammatory condition in FM. It is essential to differentiate between PMR and FM for accurate diagnosis and effective treatment, as well as to prevent the unwarranted administration of glucocorticoids in FM patients.[4]

This review paper examines pain mechanisms, clinical features, diagnostic techniques, and individualized therapies for PMR and FM. Furthermore, to demonstrate the similarities, intersections, and distinctions between the two conditions.

Pain Mechanisms

Polymyalgia Rheumatica

Common symptoms may include fatigue, fever, and weight loss. Pain is induced by systemic inflammation, primarily involving IL-6 and various cytokines. In certain studies, arthroscopic biopsies from the glenohumeral joints of untreated patients with PMR demonstrated synovitis characterized by leukocyte infiltration and vascular proliferation. Proximal pain is associated with synovitis and bursitis in the hip and shoulder regions. Most infiltrating cells were macrophages and memory T cells, with a minor presence of B cells. T cells exhibited elevated levels of major histocompatibility complex class II molecules, indicating activation. Inflamed tissues contain activated macrophages and T cells that sensitize peripheral nociceptors. Recent studies suggest that PMR patients experiencing persistent pain may exhibit low-grade central sensitization. Vascular endothelial activation may contribute to pathogenesis, as elevated expression of vascular endothelial growth factor (VEGF) in synovial biopsies is associated with GCA in 10-20% of cases, with vascular inflammation exacerbating pain. Elevated expression of adhesion molecules in endothelial and synovial lining cells may facilitate the recruitment of inflammatory cells to these lesions. Levels of vasoactive intestinal peptide (VIP) were elevated in the shoulder synovium of patients with PMR compared to those with rheumatoid arthritis (RA) or osteoarthritis. Nociception linked to local VIP production may contribute to the distinctive shoulder pain in PMR. A recent observation indicates that PMR may manifest as an adverse effect of cancer therapy utilizing checkpoint inhibitors.[5-9]

Fibromyalgia

Fibromyalgia is predominantly attributed to heightened pain signaling within the central nervous system. Neuroimaging research indicates modified brain connectivity in pain-processing areas, such as the insula and anterior cingulate cortex (10). Discrepancies in serotonin, norepinephrine, and substance P all enhance pain perception. Emerging evidence indicates low-grade inflammation and small-fiber neuropathy in certain FM patients, although it is less common than in polymyalgia rheumatica. Fibromyalgia-related pain has been linked to modifications in brain regions involved in pain processing, reduced activity of pain-inhibitory pathways, and heightened activity of pain-facilitating pathways. The precise pathogenetic mechanism underlying FM pain remains incompletely elucidated, yet it is thought to engage multiple peripheral and central pathways. Conditions such as FM can lead to sustained activation of glial cells and the ensuing release of proinflammatory agents.[10]

Thus, PMR pain is primarily inflammatory and peripheral, driven by cytokine-mediated activation of nociceptors. FM pain is centralized, with minimal inflammatory contribution, focusing on CNS amplification and neurochemical changes.

Clinical Differences

Polymyalgia rheumatica

The predominant symptoms include proximal pain and morning stiffness in the pelvic girdle and shoulders persisting for over 45 minutes, which may be acute or progress over several days to weeks, a swift response to glucocorticoids, and elevated ESR/CRP levels. Common symptoms may encompass fatigue, fever, and weight reduction. The nonspecific clinical presentation and absence of distinctive laboratory or serologic findings often result in diagnostic delays. PMR imposes a considerable burden on the daily lives of elderly individuals.[3,4]

Fibromyalgia

Fibromyalgia symptoms are persistent functional manifestations. Individuals exhibit a spectrum of symptoms and severity, ranging from mild and intermittent to persistent and debilitating. Clinical manifestations encompass diffuse pain, tender points, fatigue, sleep disturbances, and non-restorative sleep, alongside a form of cognitive impairment characterized by concentration difficulties and mental fog (“fibro fog”); headaches (e.g., migraines), paresthesia, memory deficits, abdominal discomfort or cramps, autonomic dysregulation,

xerostomia, xerophthalmia, visual disturbances, restless leg syndrome, and normal inflammatory markers. Fibromyalgia and other conditions with overlapping symptoms are not mutually exclusive and may coexist simultaneously.[2,5]

Demographics

Polymyalgia rheumatica

Polymyalgia rheumatica is the most common inflammatory rheumatic condition in individuals over 50, with a prevalence in women that is 2-3 times greater than in men. In Sweden, the prevalence of PMR among individuals aged 50 and older varies from 34 to 50 per 100,000. One review established that PMR is more prevalent among individuals of Northern European descent, while GCA and PMR are less prevalent in Asian populations. Polymyalgia rheumatica is 2 to 3 times more prevalent than GCA and manifests in approximately 50% of individuals diagnosed with GCA. Polymyalgia rheumatica may precede, coincide with, or succeed GCA.[4,11-13]

Fibromyalgia

This disease impacts individuals across all age groups and typically exacerbates with advancing age, reaching its zenith between 50 and 60 years old. Women are three times more likely to be affected than men. Global estimates vary from 0.2% to 6.6%. It is the third most prevalent musculoskeletal condition, following lumbar pain and osteoarthritis. The prevalence in Europe is 2.31%. Countries like the United States, Canada, and Japan report prevalence rates of 6.4%, 1.5%, and 2.1%, respectively. Y. Bawazir conducted a systematic review and meta-analysis regarding the prevalence of FMS in Saudi Arabia.[14] It disclosed that FMS is more prevalent among women, especially in Saudi Arabia, where its occurrence is 13.4%. Factors correlated with a heightened probability of developing FM encompass diagnoses of major depressive disorder, irritable bowel syndrome, and restless legs syndrome. A study conducted by AlOmair et al.[15] revealed that 15.2% (n= 47) of the 310 seropositive RA patients met the diagnostic criteria for FMS.[2,14,15]

Diagnostic Approaches

Polymyalgia Rheumatica

The diagnosis of PMR is difficult because there are no definitive findings on clinical evaluation, laboratory analysis, or imaging to validate the condition. Increased ESR (>40 mm/h) and CRP are prevalent but may be normal in 10-20% of instances. Ultrasound or MRI can identify bursitis or synovitis; PET-CT may be used to assess for GCA association; and a response to glucocorticoids (e.g., prednisone 15-20 mg/day) can serve as a diagnostic criterion. Chuang et al. and Healey et al. delineated diagnostic criteria for PMR, with the latter incorporating a swift response to less than 20 mg/day of prednisolone. Nevertheless, these criteria are not extensively utilized in standard clinical practice. The American College of Rheumatology and the European League Against Rheumatism recommend excluding conditions that mimic PMR symptoms, including core exclusion conditions (GCA, cancer, infections), rheumatoid arthritis (RA), FM, hypothyroidism, and drug-induced myalgia. The American College of Rheumatology and the European League Against Rheumatism recommend excluding conditions that mimic the symptoms of PMR, including core exclusion conditions (GCA, cancer, infections), RA, FM, hypothyroidism, and drug-induced myalgia. In 2012, the European League Against Rheumatism (EULAR) proposed new classification criteria for PMR. The American College of Rheumatology (ACR) developed a scoring algorithm incorporating factors such as morning stiffness exceeding 45 minutes (2 points), hip pain or restricted range of motion (1 point), absence of rheumatoid factor and/or anti-citrullinated protein antibodies (ACPA) (2 points), and absence of peripheral joint pain (1 point). A score of ≥4 demonstrates 68% sensitivity and 78% specificity for PMR. The inclusion of ultrasound results yields a score of ≥5, increasing sensitivity to 66% and specificity to 81%. Patients aged 50 and above presenting with bilateral shoulder pain of unexplained origin may be diagnosed with PMR if they exhibit morning stiffness exceeding 45 minutes, elevated CRP and/or ESR, and newly developed hip pain. These classification criteria mitigate heterogeneity among positive cases by emphasizing typical manifestations, thereby reducing the likelihood of false-positive diagnoses. Nonetheless, they may not be applicable in atypical instances of PMR. The majority of diagnostic criteria for PMR exhibit low sensitivity and specificity and were formulated for populations with a high prevalence of the disorder. Consequently, comprehensive clinical assessment and the exclusion of alternative potential causes are imperative for precise diagnosis. The functions of imaging studies in the diagnosis, treatment, and prognosis of PMR are inadequately documented and necessitate further elucidation.[16-20]

Fibromyalgia

The diagnosis is predicated on the persistence and extensive distribution of pain. The pain must persist for at least 3 consecutive months and be widespread. Sleep disturbances, fatigue, and mood disorders are typically evident. The diagnosis is established only after a comprehensive history and clinical examination have excluded peripheral pain of structural, inflammatory, or neuropathic origin, and after specific laboratory tests and clinical evaluations have excluded other conditions, such as normal inflammatory markers and negative autoimmune serologies. In 1990, the American College of Rheumatology (ACR) published the inaugural diagnostic criteria for fibromyalgia. In 2010, the ACR acknowledged "The American College of Rheumatology Preliminary Diagnostic Criteria for Fibromyalgia and Measurement of Symptom Severity" as "an alternative diagnostic method." The 1990 classification and 2010 diagnostic criteria were formulated among rheumatology patients and were physician-centric. Due to its nonspecific nature, it is no longer recommended to assess fibromyalgia based on pain at 11 of the 18 tender points. The tender point count relies on the patient's self-report, the physician examiner's assessment and interpretation, and the natural decrease in pain threshold. Gracely et al. characterized the tender count as "some unspecified combination of tenderness and distress" and referred to it as "a sedimentation rate for distress."[11] The 2011 criteria incorporated a fibromyalgia

severity (FS) score, derived from the sum of the Widespread Pain Index (WPI) and the Symptom Severity Scale (SSS), facilitating a quantitative evaluation of fibromyalgia symptom severity. Application of the 2010/2011 criteria to regional pain syndromes resulted in misclassification. Nevertheless, the incorporation of a modified widespread pain criterion, termed the "generalized pain criterion," eradicated misclassification. Fibromyalgia and other conditions with overlapping symptoms are not mutually exclusive and may coexist simultaneously. Consider testing for alternative conditions in patients with the appropriate history and distinctive clinical features. ACR 2016 criteria, highlighting the intensity of symptoms and extensive pain. This is an update to the fibromyalgia criteria from 2010 and 2011. Emerging tools for assessing fibromyalgia patients encompass Quantitative Sensory Testing and neuroimaging for research applications. A diagnosis of fibromyalgia is legitimate regardless of other diagnoses.[21-23] Adults can now be diagnosed with fibromyalgia if they meet all of the following criteria:

- There is widespread pain, which is characterized by pain in at least four out of five areas.
- For at least three months, the symptoms have persisted at a comparable level.
- Symptom severity scale (SSS) score ≥5 and widespread pain index (WPI) ≥7 or SSS score ≥9 and WPI of 4-6.
- A diagnosis of fibromyalgia is valid irrespective of other diagnoses. A diagnosis of fibromyalgia does not exclude the presence of other clinically important illnesses.

Diagnostic Challenges

Overlap: Both may present stiffness, fatigue, and generalized pain, leading to misdiagnosis.

Tools: Polymyalgia rheumatica diagnosis relies on clinical criteria (e.g., EULAR/ACR 2012 classification) and inflammatory markers. FM diagnosis uses ACR 2016 criteria (widespread pain index, symptom severity scale).

Comorbidity: Fibromyalgia may coexist with PMR, complicating pain assessment. Up to 20% of PMR patients may meet FM criteria. Yu Yokota et al reported a 92-year-old woman with polymyalgia rheumatism who had been treated with prednisolone for 18 years and was later diagnosed with coexisting fibromyalgia based on two physical examinations and her personal history of general pain. Pregabalin was prescribed, and her pain gradually disappeared.[24]

Differentiation

Inflammatory markers and glucocorticoid response are key to distinguishing PMR from FM. Fibromyalgia requires assessment of non-pain symptoms (headaches, paresthesia, memory deficits, abdominal discomfort or cramps, autonomic dysregulation, xerostomia, xerophthalmia, visual disturbances, restless leg syndrome) to ensure an accurate diagnosis. Table 1 for summarizing diagnostic features of PMR vs. FM.

Table 1.

Diagnostic Features of PMR vs. FM.

Diagnostic Feature	PMR	FM
Inflammatory markers	Elevated CRP, ESR	Normal
Age relevance	>50 years	Any age (peak 50–60)
Imaging	Ultrasound, MRI (bursitis/synovitis)	Not useful clinically
Classification criteria	EULAR/ACR 2012	ACR 2016 (WPI + SSS)
Response to glucocorticoids	Rapid and significant	None

Treatment Approaches

Polymyalgia Rheumatica

The management of PMR emphasizes symptom relief, reduction in inflammation, and enhancement of overall function. Corticosteroid therapy is the foundation of PMR treatment. Nonsteroidal anti-inflammatory drugs (NSAIDs) may be prescribed to augment corticosteroid therapy and alleviate symptoms. Physical therapy is crucial for managing PMR. Glucocorticoids generally elicit a rapid response to all PMR symptoms. The latest ACR/EULAR guideline for the initial daily dosage of prednisolone in PMR is 12.5–25 mg. The diagnosis is corroborated by the patient's rapid response to treatment and alleviation of pain within 1-2 weeks. It is recommended to gradually reduce dosage over a period of 6 to 12 months to mitigate side effects. A suboptimal treatment response should necessitate a reevaluation of alternative diagnoses, especially malignancy or other rheumatic disorders. To mitigate long-term toxicity, supportive measures must be employed alongside GC treatment. Calcium, vitamin D, and bisphosphonate supplements are utilized to prevent osteoporosis. A daily dosage of 10 mg or greater is associated with an increased risk of injury. When evaluating the extent of harm associated with a daily dose of 5–10 mg, it is essential to consider patient characteristics and comorbidities. The prognosis for PMR is generally positive, and the condition usually resolves within a few years. A meta-analysis by Floris et al. included 21 studies, revealing that 77%, 51%, and 25% of participants remained on glucocorticoids at 1, 2, and 5 years post-diagnosis, respectively. While further research is necessary, intramuscular MP is probably an effective alternative to oral GC for specific patients, including the elderly and those with adherence issues. Patients with PMR necessitate GC-sparing strategies due to the myriad adverse effects associated with prolonged GC therapy. The ACR/EULAR panel conditionally recommended the early initiation of MTX, particularly for patients at elevated risk of relapse and/or those necessitating extended treatment. Numerous case reports and series indicate the effectiveness of intravenous tocilizumab in individual patients with PMR. TNF inhibitors are contraindicated for the management of PMR. The most prevalent comorbidity reported following a PMR diagnosis is vascular disease. The vascular disorders encompass strokes, myocardial infarction, and peripheral vascular disease.[25-28] Table 2 presents a treatment comparison of PMR and FM.

Table 2.

Treatment Comparison of PMR and FM.

Treatment Feature	PMR	FM
First-line therapy	Glucocorticoids (prednisone)	SNRIs, anticonvulsants, TCAs
Treatment response time	Rapid (days)	Gradual (weeks to months)
Non-pharmacologic approaches	Physical therapy, taper monitoring	CBT, exercise, sleep hygiene
Other medications	Methotrexate, tocilizumab	Low-dose naltrexone, ketamine (experimental)
Steroid use	Essential for remission	Ineffective and not recommended
Comorbidity focus	Osteoporosis, GCA, vascular risk	Depression, anxiety, IBS, sleep disorders

Fibromyalgia

Individualized and multidisciplinary treatment is necessary. It is crucial to manage comorbid conditions like psychiatric disorders and sleep disturbances and to educate patients. Aerobic cardiovascular fitness exercises are beneficial. For certain patients, tai chi and/or water exercise may be more beneficial. FDA-approved drugs include a dual uptake inhibitor, such as duloxetine 20 to 30 mg at breakfast, gradually increased to 60 mg/day, or milnacipran 12.5 mg each morning, gradually increased as tolerated to 50 mg twice daily. Pregabalin (anticonvulsant) for centralized pain taken at bedtime. Treatment is initiated at a dose of 25 to 50 mg at bedtime and is adjusted upwards as tolerated to 300 to 450 mg/day. Gabapentin is an acceptable alternative for patients for whom cost or regulatory constraints limit the availability of pregabalin. Amitriptyline (low dose) and/or cyclobenzaprine can also be used. Emerging treatment low-dose naltrexone (1-4.5 mg/day) shows promise in reducing pain and fatigue. Lidocaine infusions could give an alternative option for patients who have not responded well to conventional therapies. A 2024 systematic review by de Carvalho and de Sena[30] demonstrates the effectiveness and safety of ketamine in FM patients in the short term. More studies, including long-term follow-up studies, are still needed. Recently, the FDA approved cyclobenzaprine HCL sublingual (Tonmya) as a treatment for fibromyalgia in adults. Non-pharmacological options also include cognitive behavioral therapy (CBT) and mindfulness-based stress reduction for pain coping.[29-31]

Comparison

PMR treatment targets inflammation, with a rapid response to steroids. FM treatment focuses on neuromodulation and symptom management, with a slower, variable response. Overlap management: If PMR and FM coexist, combine anti-inflammatory and neuromodulation strategies.

Conclusion

It is important to diagnose both FM and PMR accurately and early. Additionally, clinicians should be aware of the distinct pain mechanisms in both conditions (inflammatory vs. central), differences in clinical features, and the possibility of both conditions coexisting. Tailored therapy is needed to improve the outcomes. Integrating rheumatology, pain medicine, and psychology is needed for holistic management. Longitudinal studies to understand the development of FM in PMR patients are needed.

Author Contribution Statement

Abdulrahman Ali M. Khormi confirms sole responsibility for all aspects of the research.

Conflict of Interest

The author has declared no conflict of interest.

Acknowledgements

The author is grateful to the Deanship of Scientific Research, Prince Sattam bin Abdulaziz University, Al-Kharj, Saudi Arabia, for its support and encouragement in conducting the research and publishing this report.

References

1. Kocyigit BF, Akyol A. Coexistence of fibromyalgia syndrome and inflammatory rheumatic diseases, and autonomic cardiovascular system involvement in fibromyalgia syndrome. Clin Rheumatol. 2023 Mar;42(3):645-652. doi: 10.1007/s10067-022-06385-8. Epub 2022 Sep 23. PMID: 36151442.
2. García-Domínguez M. Fibromyalgia and Inflammation: Unrevealing the Connection. Cells. 2025 Feb 13;14(4):271. doi: 10.3390/cells14040271. PMID: 39996743; PMCID: PMC11853252.
3. Partington R, Muller S, Mallen CD, Abdul Sultan A, Helliwell T. Comorbidities in patients with polymyalgia rheumatica prior to and following diagnosis: A case control and cohort study. Semin Arthritis Rheum. 2020 Aug;50(4):663-672. doi: 10.1016/j.semarthrit.2020.05.003. Epub 2020 May 26. PMID: 32512261.
4. Lundberg IE, Sharma A, Turesson C, Mohammad AJ. An update on polymyalgia rheumatica. J Intern Med. 2022 Nov;292(5):717-732. doi: 10.1111/joim.13525. Epub 2022 Jun 11. PMID: 35612524; PMCID: PMC9796644.
5. Sarzi-Puttini P, Giorgi V, Marotto D, Atzeni F. Fibromyalgia: an update on clinical characteristics, aetiopathogenesis and treatment. Nat Rev Rheumatol. 2020 Nov;16(11):645-660. doi: 10.1038/s41584-020-00506-w. Epub 2020 Oct 6. PMID: 33024295.
6. Sarzi-Puttini P, Giorgi V, Marotto D, Atzeni F. Fibromyalgia: an update on clinical characteristics, aetiopathogenesis and treatment. Nat Rev Rheumatol. 2020 Nov;16(11):645-660. doi: 10.1038/s41584-020-00506-w. Epub 2020 Oct 6. PMID: 33024295.
7. Meliconi R, Pulsatelli L, Dolzani P, Boiardi L, Macchioni P, Salvarani C, et al. Vascular endothelial growth factor production in polymyalgia rheumatica. Arthritis Rheum. 2000 Nov;43(11):2472-80. doi:

10.1002/1529-0131(200011)43:11<2472::AID-ANR14>3.0.CO;2-B. PMID: 11083270.
8. Meliconi R, Pulsatelli L, Melchiorri C, Frizziero L, Salvarani C, Macchioni P, et al. Synovial expression of cell adhesion molecules in polymyalgia rheumatica. Clin Exp Immunol. 1997 Mar;107(3):494-500. doi: 10.1046/j.1365-2249.1997.d01-946.x. PMID: 9067523.
9. Pulsatelli L, Dolzani P, Silvestri T, De Giorgio R, Salvarani C, Macchioni P, et al. Synovial expression of vasoactive intestinal peptide in polymyalgia rheumatica. Clin Exp Rheumatol. 2006 Sep-Oct;24(5):562-6. PMID: 17181926.
10. Vatvani AD, Patel P, Hariyanto TI, Yanto TA. Efficacy and safety of low-dose naltrexone for the management of fibromyalgia: a systematic review and meta-analysis of randomized controlled trials with trial sequential analysis. Korean J Pain. 2024 Oct 1;37(4):367-378. doi: 10.3344/kjp.24202. Erratum in: Korean J Pain. 2026 Jan 1;39(1):147-149. doi: 10.3344/kjp.25393. PMID: 39344363; PMCID: PMC11450306.
11. Noltorp S, Svensson B. High incidence of polymyalgia rheumatica and giant cell arteritis in a Swedish community. Clin Exp Rheumatol. 1991 Jul-Aug;9(4):351-5. PMID: 1934682.
12. Schaufelberger C, Bengtsson BA, Andersson R. Epidemiology and mortality in 220 patients with polymyalgia rheumatica. Br J Rheumatol. 1995 Mar;34(3):261-4. doi: 10.1093/rheumatology/34.3.261. PMID: 7728403.
13. Sharma A, Mohammad AJ, Turesson C. Incidence and prevalence of giant cell arteritis and polymyalgia rheumatica: A systematic literature review. Semin Arthritis Rheum. 2020 Oct;50(5):1040-1048. doi: 10.1016/j.semarthrit.2020.07.005. Epub 2020 Jul 14. PMID: 32911281.
14. Bawazir Y. Prevalence of fibromyalgia syndrome in Saudi Arabia: a systematic review and meta-analysis. BMC Musculoskelet Disord. 2023 Aug 30;24(1):692. doi: 10.1186/s12891-023-06821-z. PMID: 37649080; PMCID: PMC10466693.
15. AlOmair M, AlMalki H, Sarhan L, Shweel M, Asiri A, Almhjani E, et al. Fibromyalgia concomitant with seropositive RA in a tertiary Saudi hospital. Open Rheumatol J. 25 Nov 2022. DOI: 10.2174/18743129-v16-e2209290
16. Butt NI, Ghoauri MSA, Riaz MW, Aiman. Polymyalgia Rheumatica Presenting as Nocturnal Pyrexia of Unknown Origin: A Case Report. Galician Med J. 2024;31(3).
17. Chuang TY, Hunder GG, Ilstrup DM, Kurland LT. Polymyalgia rheumatica: a 10-year epidemiologic and clinical study. Ann Intern Med. 1982 Nov;97(5):672-80. doi: 10.7326/0003-4819-97-5-672. PMID: 6982645.
18. Healey LA. Long-term follow-up of polymyalgia rheumatica: evidence for synovitis. Semin Arthritis Rheum. 1984 May;13(4):322-8. doi: 10.1016/0049-0172(84)90012-x. PMID: 6729485.
19. Macchioni P, Boiardi L, Catanoso M, Pazzola G, Salvarani C. Performance of the new 2012 EULAR/ACR classification criteria for polymyalgia rheumatica: comparison with the previous criteria in a single-centre study. Ann Rheum Dis. 2014 Jun;73(6):1190-3. doi: 10.1136/annrheumdis-2013-204167. Epub 2013 Dec 2. PMID: 24297384.
20. Dasgupta B, Cimmino MA, Maradit-Kremers H, Schmidt WA, Schirmer M, Salvarani C, et al. 2012 provisional classification criteria for polymyalgia rheumatica: a European League Against Rheumatism/American College of Rheumatology collaborative initiative. Ann Rheum Dis. 2012 Apr;71(4):484-92. doi: 10.1136/annrheumdis-2011-200329. PMID: 22388996; PMCID: PMC3298664.
21. Wolfe F, Clauw DJ, Fitzcharles MA, Goldenberg DL, Häuser W, Katz RL, Mease PJ, Russell AS, Russell IJ, Walitt B. 2016 Revisions to the 2010/2011 fibromyalgia diagnostic criteria. Semin Arthritis Rheum. 2016 Dec;46(3):319-329. doi: 10.1016/j.semarthrit.2016.08.012. Epub 2016 Aug 30. PMID: 27916278.
22. Wolfe F, Clauw DJ, Fitzcharles MA, Goldenberg DL, Katz RS, Mease P, et al. The American College of Rheumatology preliminary diagnostic criteria for fibromyalgia and measurement of symptom severity. Arthritis Care Res (Hoboken). 2010 May;62(5):600-10. doi: 10.1002/acr.20140. PMID: 20461783.
23. Aggarwal R, Ringold S, Khanna D, Neogi T, Johnson SR, Miller A, et al. Distinctions between diagnostic and classification criteria? Arthritis Care Res (Hoboken). 2015 Jul;67(7):891-7. doi: 10.1002/acr.22583. PMID: 25776731; PMCID: PMC4482786.
24. Yokota Y, Namiki H. Pitfalls in diagnosing geriatric general pain: coexistence of polymyalgia rheumatism and fibromyalgia. BMJ Case Rep. 2019 Jul 23;12(7):e230078. doi: 10.1136/bcr-2019-230078. PMID: 31340948; PMCID: PMC6663217.
25. Lundberg IE, Sharma A, Turesson C, Mohammad AJ. An update on polymyalgia rheumatica. J Intern Med. 2022 Nov;292(5):717-732. doi: 10.1111/joim.13525. Epub 2022 Jun 11. PMID: 35612524; PMCID: PMC9796644.
26. Dejaco C, Singh YP, Perel P, Hutchings A, Camellino D, Mackie S, et al.; European League Against Rheumatism; American College of Rheumatology. 2015 recommendations for the management of polymyalgia rheumatica: a European League Against Rheumatism/American College of Rheumatology collaborative initiative. Arthritis Rheumatol. 2015 Oct;67(10):2569-80. doi: 10.1002/art.39333. PMID: 26352874.
27. Floris A, Piga M, Chessa E, Congia M, Erre GL, Angioni MM, Mathieu A, Cauli A. Long-term glucocorticoid treatment and high relapse rate remain unresolved issues in the real-life management of polymyalgia rheumatica: a systematic literature review and meta-analysis. Clin Rheumatol. 2022 Jan;41(1):19-31. doi: 10.1007/s10067-021-05819-z. Epub 2021 Aug 20. PMID: 34415462; PMCID: PMC8724087.
28. Buckley L, Guyatt G, Fink HA, Cannon M, Grossman J, Hansen KE, et al. 2017 American College of Rheumatology Guideline for the Prevention and Treatment of Glucocorticoid-Induced Osteoporosis. Arthritis Care Res (Hoboken). 2017 Aug;69(8):1095-1110. doi: 10.1002/acr.23279. Epub 2017 Jun 6. Erratum in: Arthritis Care Res (Hoboken). 2017 Nov;69(11):1776. doi: 10.1002/acr.23441. PMID: 28585410.
29. Macfarlane GJ, Kronisch C, Dean LE, Atzeni F, Häuser W, Fluß E, et al. EULAR revised recommendations for the management of fibromyalgia. Ann Rheum Dis. 2017 Feb;76(2):318-328. doi: 10.1136/annrheumdis-2016-209724. Epub 2016 Jul 4. PMID: 27377815.
30. de Carvalho JF, de Sena EP. Ketamine in fibromyalgia: a systematic review. Adv Rheumatol. 2024 Jul 29;64(1):54. doi: 10.1186/s42358-024-00393-9. PMID: 39075628.
31. Lederman S, Arnold LM, Vaughn B, Engels JM, Kelley M, Sullivan GM. Pain relief by targeting nonrestorative sleep in fibromyalgia: a phase 3 randomized trial of bedtime sublingual cyclobenzaprine. Pain Med. 2026 Jan 1;27(1):86-94. doi: 10.1093/pm/pnaf089.

International Journal of Biomedicine 16(2) (2026) 151-156
http://dx.doi.org/10.21103/Article16(2)_RA2

REVIEW ARTICLE

INTERNATIONAL JOURNAL OF BIOMEDICINE

Plant-Derived Bioactive Compounds Mitigate Diabetes Globally: An Updated Mini Review

Faiza Siddique[1], Duaa Qaiser[2], Tahir Mehmood[2*]

[1]*AGAT Labs, 2910 12 St NE, Calgary, Canada*
[2]*Institute of Microbiology and Molecular Genetics, (IMMG), University of the Punjab, 54590-Lahore, Pakistan*

Abstract

Diabetes mellitus (DM) is one of the most vital health crises across the world in the 21st century, as it affects more than 537 million adults in the world and is projected to increase to 783 million individuals by 2045. The existing pharmacological treatments, such as metformin, sulfonylureas, and insulin therapy, though effective, have significant drawbacks, including gastrointestinal adverse effects, hypoglycemic events, weight gain, and diminishing efficacy over time. Bioactive compounds of plant origin have emerged as new therapeutic options, offering multi-targeted supplementation with a good safety profile. This review provides an in-depth analysis of key groups of antidiabetic phytochemicals, including phenolics (gallic acid, chlorogenic acid), flavonoids (quercetin, kaempferol, anthocyanins), alkaloids (berberine, trigonelline), and terpenoids (ginsenosides, oleanolic acid). Recent discoveries between 2024 and 2026 show significant potential to modulate glucose homeostasis through AMP-activated protein kinase (AMPK), α-glucosidase, β-cell protection, and the anti-inflammatory pathway. Potential drugs such as *Gymnema sylvestre*, *Momordica charantia*, *Azadirachta indica*, and *Celtis tetrandra* have good preclinical and clinical results. Although bioavailability, standardization, and clinical translation are challenging, plant-based bioactive compounds are promising next-generation antidiabetic therapeutic agents, as monotherapy or as a supplement to the current treatment.(**International Journal of Biomedicine. 2026;16(2):151-156.**)

Keywords: diabetes mellitus • bioactive compounds • phenolics • flavonoids • alkaloids • AMP-activated protein kinase • medicinal plants

For citation: Siddique F, Qaiser D, Mehmood T. Plant-Derived Bioactive Compounds Mitigate Diabetes Globally: An Updated Mini Review. International Journal of Biomedicine. 2026;16(2):151-156. doi:10.21103/Article16(2)_RA2

Introduction

Diabetes mellitus (DM) is a heterogeneous group of metabolic diseases characterized by chronic hyperglycemia resulting from defects in insulin secretion, insulin action, and both.[1] The prevalence of diabetes nowadays is at epidemic levels, and the International Diabetes Federation (IDF) estimates 537 million cases in 2021, and it will reach 783 million by 2045.[2] This increasing rate of prevalence has high economic costs, as the global healthcare spending reaches USD 966 billion yearly.

There are multiple pathophysiological entities associated with diabetes. Type 1 diabetes mellitus (T1DM) is an autoimmune destruction of β-cells in the pancreas, requiring lifelong insulin replacement. Type 2 diabetes mellitus (T2DM) is a progressive insulin resistance disease associated with defective β-cells and 90-95% of all diseases. Gestational diabetes mellitus (GDM) is an illness that arises during pregnancy, placing both mother and child at risk of developing serious metabolic disorders. Maturity-onset diabetes of the young (MODY) is a monogenic disorder caused by mutations in genes that regulate β-cell function.[3]

Existing treatment approaches are largely limited. The pharmacotherapy of T2DM, which is the first-line option, Metformin, is most commonly associated with gastrointestinal intolerance, manifesting as diarrhea and nausea, and thus discontinuations are as high as 5-10% in patients. Sulfonylureas encourage hypoglycemia and weight gain, and thiazolidinediones heighten cardiovascular risks and fluid retention. T1DM and advanced T2DM insulin therapy are vital and necessitate close observation and carry the threat of hypoglycemia. Moreover, several traditional agents have shown a decreasing efficacy with time owing to progressive β-cell failure.[4]

Such restrictions have prompted the exploration of medicinal plants and their bioactive compounds. The use

of botanical preparations in the management of diabetes has a history of thousands of years in traditional medicine, which includes Ayurveda, Traditional Chinese Medicine, and Arabic medicine. In modern pharmacognosy, some bioactive molecules responsible for the aforementioned antidiabetic effects have been identified, enabling mechanistic evaluation of these effects and the application of therapeutic strategies in a standardized manner. The mentioned effects of plant-derived compounds include the following: multi-targeted activity, reduced toxicity, and potential β-cell protection.[5]

This review aims to present a timely overview of recent developments (2024-2026) in the field of plant-derived bioactive compounds for the management of diabetes, with a focus on mechanistic insights, clinical trials, and potential therapeutic implications.

Plant-Derived Bioactive Compounds with Antidiabetic Potential

Phytochemicals are secondary metabolites produced by plants to protect against external stressors. These compounds have developed complex molecular structures that facilitate interaction with mammalian biological targets, including glucose homeostatic biological targets. The significant classes that have antidiabetic effects are:

The phenolic compounds are aromatic secondary metabolites with hydroxylated benzene rings. This heterogeneous group consists of phenolic acids (gallic acid, caffeic acid, chlorogenic acid), stilbenes (resveratrol), and lignans. Their antidiabetic effect is mediated by antioxidant activity, enzyme inhibition, and alterations in glucose transporters.[6]

The largest group of polyphenols is the flavonoids, which share the diphenylpropane (C6-C3-C6) skeleton. They have subclasses of flavonols (quercetin, kaempferol), flavones (apigenin), flavanols (catechins), and anthocyanins (cyanidin-3-glucoside). Such compounds show insulin secretagogue effects, β-cell protection, and anti-inflammatory properties.

Alkaloids are nitrogen-based basic compounds that are based on the amino acid precursors. Some well-known antidiabetic alkaloids include berberine (isoquinoline type), trigonelline (pyridine type), and piperine. These molecules first and foremost activate AMP-activated protein kinase (AMPK), which regulates cellular energy metabolism.[7]

Saponins and terpenoids are derivatives of isoprene, such as triterpenes (oleanolic acid, ursolic acid) and saponins that are steroids (ginsenosides). These chemicals improve insulin sensitivity, maintain lipid metabolism, and prevent diabetic complications.[7]

The general mechanisms underlying the antidiabetic effects of these compounds are: (1) blockage of carbohydrate-digesting enzymes (α-amylase, α-glucosidase); (2) enhancement of insulin secretion and regeneration of β-cells; (3) promotion of peripheral glucose uptake through GLUT4 translocation; (4) inhibition of hepatic gluconeogenesis; (5) inhibition of oxidative stress and inflammation; and (6) alteration of gut microbiota.[8]

Major Classes of Antidiabetic Bioactive Compounds

Phenolic Compounds

Phenolic acids are important antidiabetic agents, and their mechanisms are well documented. Chlorogenic acid, which is present in large quantities in coffee, apples, and blueberries, exhibits strong hypoglycemic and hypolipidemic properties. Recent reports show that chlorogenic acid inhibits α-amylase and enhances insulin action in antioxidant and anti-inflammatory mechanisms. Gallic acid and caffeic acid exhibit similar enzyme-inhibitory profiles; caffeic acid shows stronger α-glucosidase inhibitory activity (IC50 8.00 ± 0.40 mg/mL) than the standard drugs. Rosmarinic acid, a compound extracted from *Rosmarinus officinalis* and other species of the *Lamiaceae* family, increases insulin sensitivity by regulating the expression of GLUT4 and suppressing phosphoenolpyruvate carboxykinase (PEPCK). The molecular docking studies show that rosmarinic acid binds to the α-glucosidase active site, forming stable hydrogen bonds with binding energies similar to those of acarbose. According to recent studies, rosmarinic acid modulates the activity of glycogen phosphorylase and glycogen synthase in diabetic animals and restores hepatic and muscular glycogen levels after 30 days of administration.

Phenolic antioxidant capacity is very instrumental in alleviating diabetic complications. These scavenge reactive oxygen species (ROS), prevent the formation of advanced glycation end-products (AGEs), and chelate transition metals (Fe^{2+}, Cu^{2+}) that catalyze oxidative reactions. Quercetin and resveratrol, in particular, exhibit AGE-inhibitory activity, trapping reactive dicarbonyl compounds and inhibiting protein glycation.[6]

Flavonoids

The variety of antidiabetic mechanisms of flavonoids is impressive. Quercetin, which is rich in onions, apples, and broccoli, exhibits a variety of activities, including inhibition of DPP-4 (IC50 1.150 mg/mL), α-glucosidase, and β-cell apoptosis. According to recent mechanistic research, quercetin alleviates endoplasmic reticulum stress and oxidative harm in pancreatic β-cells, maintaining insulin production and secretion.[9]

Among the flavonols with a promising future is kaempferol, according to research in 2024-2025. In vitro experiments indicate that kaempferol inhibits α-glucosidase and α-amylase with IC 50 values of 2.33 mg/mL and 52.95mg/mL, respectively. Kaempferol enhances hexokinase activity in both skeletal muscle and liver in streptozotocin-induced diabetic mice but inhibits hepatic gluconeogenesis through the inhibition of pyruvate carboxylase. It is important to note that kaempferol upregulates autophagy in β-cells, which helps defend against lipotoxic injury by maintaining lipid homeostasis.[10]

The pigmented flavonoids, anthocyanins, that color berries and grape plants blue, purple, and red have shown specific protective effects on pancreatic β-cell function. A

systematic review of in vitro studies of cyanidin-3-glucoside (C3G) found that the compound can enhance β-cell function under conditions of glucotoxicity and oxidative stress, alleviating endoplasmic reticulum (ER) stress, decreasing apoptosis, and promoting insulin production. Cyanidin-3-rutinoside (C3R) stimulates insulin release by elevating intracellular Ca^{2+} and raising ATP synthesis by glucokinase up-regulation.

Anthocyanins at the transcriptional level activate genes essential to β-cells (Ins1/Ins2, Slc2a2 (GLUT2), Gck (glucokinase), and the transcription factor PDX-1) and regulate ion channel genes (Cav1.2, Kir6.2), thereby affecting membrane excitability and insulin exocytosis. These data are consistent with larger studies on dietary polyphenols that protect β-cells against metabolic stress, but not by acting on individual molecular targets.[11]

Alkaloids

One of the most studied plant-derived antidiabetic agents is berberine, an isoquinoline alkaloid found in *Coptis chinensis*, *Berberis* species, and the bark of *Phellodendron (Phellodendron amurense tree*). New 2024-2025 studies have clarified the advanced mechanisms of action underlying berberine's therapeutic effects. The compound triggers the AMP-activated protein kinase (AMPK) via LKB1-mediated phosphorylation, thereby regulating several metabolic processes simultaneously.

Berberine-induced increases in AMPK activity in skeletal muscle and adipose tissue stimulate GLUT4 translocation to the plasma membrane to enable glucose uptake, irrespective of insulin receptor signaling, and are significantly beneficial in insulin-resistant conditions. Berberine inhibits gluconeogenesis hepatically through the AMPK-TORC2 pathway by reducing PEPCK and glucose-6-phosphatase (G6Pase). Recent randomized clinical trials with the gut-targeted berberine ursodeoxycholate co-crystal (HTD1801) showed AMPK activation and inhibition of the gluconeogenic gene signature, with 0.5 percentage point reductions in HbA1c compared to placebo.[12]

In addition to glucose homeostasis, berberine has lipid-lowering effects distinct from those of statins, enhancing LDR expression and cholesterol clearance. Berberine affects adipokine profiles as well, lowering pro-inflammatory leptin and MCP-1 levels and increasing adiponectin levels, thereby improving insulin sensitivity.

The main alkaloid of fenugreek (*Trigonella foenum-graecum)*, trigonelline, is the antidiabetic material that activates AMPK and regulates carbohydrate metabolism. Recent results suggest that trigonelline improves glucose tolerance and insulin sensitivity in experimental animals, although clinical evidence is less robust than that for berberine.[13]

Terpenoids and Saponins

Panax ginseng contains triterpene saponins (ginsenosides), which have a complex metabolism. These substances enhance insulin sensitivity by stimulating the AMPK system and PI3K/Akt pathway. Recent network pharmacology research indicates that ginsenosides Rb1 and Rg1 are among the most important bioactive compounds that interact with various proteins, such as PPAR-g, IRS-1, and GLUT4, in diabetes.

Oleanolic acid is a pentacyclic triterpene that is abundant in olive leaves, garlic, and other medicinal plants, which has been shown to have an antidiabetic effect by both increasing insulin secretion by pancreatic β-cells and reducing peripheral insulin resistance. The compound binds to the TGR5 receptor, activating GLP-1 release and energy consumption while preventing β-cell oxidative stress-related apoptosis.

Momordica charantia (bitter melon) saponins, such as charantin and momordicosides, have insulin-like properties and inhibit intestinal glucose absorption. Recent molecular docking studies show that these compounds also bind several targets in diabetes, such as β-glucosidase and protein tyrosine phosphatase 1B (PTP1B).

Antidiabetic Medicinal Plants

Gymnema sylvestre

Gymnemic acids and gurmarin peptides are present in *Gymnema sylvestre* (an herb used in Ayurvedic medicine), which has potent antidiabetic effects, as the plant is known as gurmar (sugar destroyer). Recent network pharmacology and molecular docking studies in 2024 have identified bioactive substances and their molecular targets. Gymnemic acids exhibit α-glucosidase-inhibitory action and restore the pancreatic β-cells in rodent diabetic models. The intestinal glucose absorption is decreased, and the endogenous insulin secretion is increased by the plant extracts, which act by modulating ATP-sensitive potassium channels.[14]

Momordica charantia

Momordica charantia is among the most widely researched antidiabetic plants worldwid. It has charantin (steroidal saponin), vicine, and polypeptide-p (insulin of the plants) in its fruit.[15] Recent combined computational analysis based on network pharmacology and molecular docking has helped elucidate the molecular pathophysiology underlying its antidiabetic action by identifying key targets, including PI3K, Akt, and MAPK signaling pathways. Some trials show substantial decreases in fasting blood glucose and HbA1c values comparable to those with metformin.

Azadirachta indica

Neem (*Azadirachta indica*) is a plant that incorporates azadirachtin, nimbin, and nimbidin with proven hypoglycemic properties. The extracts of leaves and bark enhance insulin sensitivity and are powerful antioxidants and anti-inflammatory agents. Recent studies have focused on neem's capacity to regulate the Nrf2/ARE antioxidant pathway and to prevent NF-kB-mediated inflammation in diabetic tissues.[5]

Celtis tetrandra

Celtis tetrandra Roxb. is a member of the Cannabaceae family and a promising antidiabetic plant according to recent 2024-2025 studies. Profiling of gas chromatography-mass spectrometry has revealed the presence of various

bioactive compounds, including flavonoids, phenolic acids, and terpenoids, with antimicrobial, anti-inflammatory, and cytotoxic properties.[16] Leaf extracts showed strong antidiabetic and antihyperlipidemic effects in diabetic rats, improving lipid profiles and characterized by protective histopathological changes in pancreatic tissue. The results contribute to the established use of *C. tetrandra* in the management of diabetes and warrant further clinical study.

Other medicinal plants, their bioactive compounds, and reported antidiabetic activity are shown in Table 1.

Mechanisms of Antidiabetic Action

Plant-derived bioactive compounds exert antidiabetic effects through multiple organ-specific mechanisms, as illustrated in Figure 1, and the details are described next.

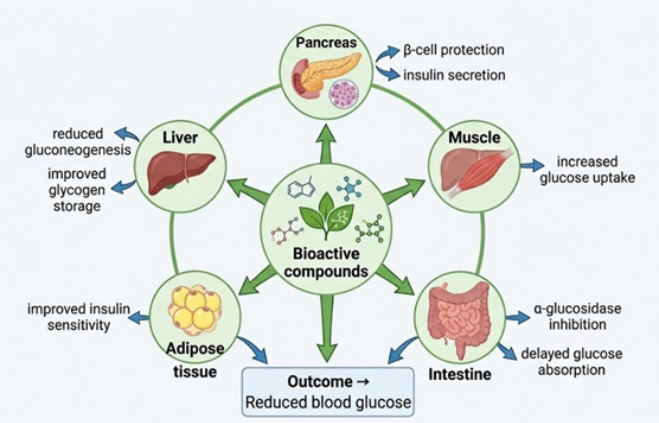

Fig. 1. *Organ-specific mechanisms of antidiabetic action of plant-derived bioactive compounds. Bioactive phytochemicals induce antihyperglycemic effects in the body by acting on several mechanisms, such as stimulation of insulin secretion and β-cells in the pancreas, and enhancing glucose uptake in skeletal muscle, α -glucosidase inhibition and slowed glucose absorption in the intestine, decreased hepatic gluconeogenesis and glycogen storage in the liver, and enhanced insulin sensitivity of adipose tissue, which results in low levels of blood glucose.*

Insulin Secretion Stimulation

Plant bioactive compounds stimulate insulin secretion through multiple pathways. Sulfonylurea-like mechanisms involve closure of ATP-sensitive potassium (KATP) channels on β-cell membranes, causing depolarization and calcium influx. However, unlike synthetic sulfonylureas, phytochemicals such as gymnemic acids and naringenin exhibit glucose-dependent insulin secretion, thereby reducing the risk of hypoglycemia. Recent studies reveal that anthocyanins upregulate glucokinase (GCK) expression, enhancing glucose sensing and ATP production in β-cells.[17]

β-Cell Regeneration and Protection

Chronic hyperglycemia induces β-cell apoptosis through oxidative stress, ER stress, and inflammation. Flavonoids, including quercetin and kaempferol, protect β-cells by upregulating antioxidant enzymes (SOD, CAT, GPx), suppressing caspase-3 activation, and promoting autophagy. Berberine stimulates mitochondrial biogenesis through the AMPK-SIRT1-PGC-1α axis, restoring β-cell energy metabolism.

Enzyme Inhibition

Inhibition of α-glucosidase and α-amylase enzymes slows carbohydrate digestion, thereby lowering blood glucose levels. The phenolic compounds exhibit non-competitive inhibition, unlike acarbose, and are not affected by substrate concentration. The structure-activity relationship shows that hydroxylation of the flavonoids is responsible for the increased inhibitory potential.[7]

Glucose Uptake Enhancement

Activation of the AMPK signaling pathway is a core mechanism for improving glucose uptake. Berberine, resveratrol, and galegine activate the AMPK signaling pathway by inhibiting mitochondrial Complex I and increasing the AMP/ATP ratio. Activated AMPK increases GLUT4 translocation to the plasma membrane in skeletal muscle and adipose tissue, thereby increasing glucose uptake independently of insulin action. Moreover, rosmarinic acid activates the AMPK signaling pathway in L6 muscle cells and increases glucose uptake.[18]

Antioxidant Activity

Hyperglycemia-induced oxidative stress drives diabetic complications through ROS generation and AGE formation. Phenolic compounds scavenge free radicals, chelate metal ions, and inhibit lipid peroxidation. Quercetin and resveratrol specifically inhibit the Maillard reaction, preventing protein glycation and AGE accumulation.

Anti-Inflammatory Pathways

Chronic low-grade inflammation characterizes T2DM, with elevated TNF-α, IL-6, and IL-1β contributing to insulin resistance. Flavonoids suppress NF-κB activation and MAPK signaling, reducing proinflammatory cytokine production. Berberine activates the AMPK-SIRT1 axis, suppressing NF-κB and limiting MCP-1 production in adipose tissue.[17]

Many medicinal plants and their bioactive compounds have demonstrated significant antidiabetic activity and exhibit diverse mechanisms of action, as shown in Table 1.

Challenges and Future Perspectives

Although preclinical evidence of the ability of plant-derived antidiabetic compounds to be translated into clinical settings appears promising, a number of obstacles hinder such translation:

Revealing Clinical Trials: Although berberine has been extensively studied in clinical trials, most plant compounds have not undergone rigorous randomized controlled trials across various population groups. Most of the evidence has been based on in vitro research and small-animal models, which require large-scale human studies to determine efficacy and safety profiles.

Standardization Problems: Botanical extracts exhibit high batch-to-batch variation in bioactive compound content

due to geographical location, harvest timing, and processing procedures. Phytochemical profile standardization and the implementation of quality control markers remain the keys to consistent therapeutic responses.

Bioavailability Limits: Oral bioavailability of many polyphenols and alkaloids is also low due to low aqueous solubility, high first-pass metabolism, and P-glycoprotein-mediated efflux. This is one such instance of berberine in which oral bioavailability is less than 1%. High-tech drug delivery systems—such as nanoparticles, liposomes, and phospholipid complexes—can enhance absorption and ensure targeted delivery to tissues.

Toxicity and Dosage Concerns: High doses can cause hepatotoxicity, nephrotoxicity, or drug interactions, though these are considered safe. It is necessary to obtain systematic toxicological profiling and calculate therapeutic indices.

Regulatory Frameworks: The regulatory pathways for Herbal medicines have become complicated, with specifications for consistency, purity, and stability similar to those for synthetic pharmaceuticals.

The future directions include (1) applying network pharmacology and systems biology to identify synergistic combinations of compounds; (2) developing semi-synthetic analogs with improved pharmacokinetics; (3) combining metabolomics analysis with gut microbiome analysis to personalize phytotherapy; (4) adopting the precision medicine-based approaches that are based on genetic variants of drug metabolism.

Conclusion

Plant-derived bioactive compounds offer a useful therapeutic pool for the management of diabetes, providing multi-target effects that address the complex pathophysiology of metabolic disease. Recent developments between 2024 and 2026 have greatly enhanced our understanding of the mechanisms by which phenolics, flavonoids, alkaloids, and terpenoids regulate glucose homeostasis by activating AMPK, inhibiting enzymes, protecting β cells, and mediating anti-inflammatory responses. Medicinal plants, such as *Gymnema sylvestre*, *Momordica charantia*, and newer ones which show clinical promise through mechanistic research, include *Celtis tetrandra*. Although bioavailability, standardization, and clinical validation remain challenging, these natural compounds offer promising opportunities for developing safer, more effective treatments for diabetes. To maximize the therapeutic potential of plant-derived bioactive compounds for managing diabetes worldwide, future studies should focus on rigorous clinical trials, sophisticated formulations, and their combination with precision medicine to achieve the desired outcome.

Table 1.

An overview of plant-based bioactive compounds with documented antidiabetic properties, their sources, key phytochemical compounds, experimental models, and mechanism of action, and significant results of major studies.

Plant source	Bioactive compound(s)	Experimental model	Mechanism of action	Key findings	Reference
Momordica charantia	Charantin, polypeptide-p	Diabetic animal models	Insulin secretion, glucose uptake	Reduced blood glucose	15
Gymnema sylvestre	Gymnemic acids	Animal models	β-cell regeneration	Improved insulin secretion	14
Azadirachta indica	Nimbin, flavonoids	In vitro / in vivo	α-glucosidase inhibition	Reduced hyperglycemia	5
Celtis tetrandra	Phenolics, flavonoids	Alloxan-induced rats	Antioxidant, β-cell protection	Improved pancreatic histology	16
Berberis vulgaris	Berberine	Clinical & animal	AMPK activation	Reduced HbA1c	12
Camellia sinensis	Catechins (EGCG)	Animal studies	Antioxidant, insulin signaling	Improved glucose metabolism	19
Curcuma longa	Curcumin	Animal models	Anti-inflammatory	Reduced insulin resistance	5
Allium sativum	Allicin	Diabetic rats	Insulin secretion	Lower blood glucose	20
Trigonella foenum-graecum	Trigonelline	Human & animal	Insulin sensitivity	Reduced fasting glucose	5
Panax ginseng	Ginsenosides	Animal model	β-cell protection	Improved glycemic control	19
Aloe vera	Aloin	Animal model	Glucose uptake	Reduced blood glucose	20
Ocimum sanctum	Eugenol	Animal model	Antioxidant	Improved glucose tolerance	20
Zingiber officinale	Gingerols	Animal model	Insulin sensitivity	Lower glucose levels	19

Author Contributions

Faiza Siddique: Data curation and analysis, Writing – review and editing.
Duaa Qaiser: Data curation and analysis, Writing – review and editing.
Tahir Mehmood: Supervision, Writing – review and editing.
Faiza Siddique and **Duaa Qaiser** contributed equally and share first authorship.
All authors have approved the final article.

Conflict of Interest

The authors have declared no conflict of interest.

References

1. Jadon AS, Kaushik MP, Anitha K, Bhatt S, Bhadauriya P, Sharma M. Types of diabetes mellitus, mechanism of insulin resistance and associated complications. Biochemical immunology of diabetes and associated complications: Elsevier; 2024. p. 1-18.
2. Rooney MR, Fang M, Ogurtsova K, Ozkan B, Echouffo-Tcheugui JB, Boyko EJ, Magliano DJ, Selvin E. Global Prevalence of Prediabetes. Diabetes Care. 2023 Jul 1;46(7):1388-1394. doi: 10.2337/dc22-2376. PMID: 37196350; PMCID: PMC10442190.
3. Patel DK, Kumar R, Laloo D, Hemalatha S. Diabetes mellitus: an overview on its pharmacological aspects and reported medicinal plants having antidiabetic activity. Asian Pac J Trop Biomed. 2012 May;2(5):411-20. doi: 10.1016/S2221-1691(12)60067-7. PMID: 23569941; PMCID: PMC3609313.
4. Kaur S, Gadpayale D, Kumari A, Kaur G, Kumar A, Seem K, et al. Antidiabetic potential of underutilized crops: Nutritional, phytochemical insights, and prospects for diabetes management. Applied Food Research. 2025;5(2):101127.
5. Vishwakarma A, Biswas V, Hasan F, Praveen A, Sharma D. Diabetes mellitus: An updated overview and role of medicinal plants in modern treatment. Innovative Medicines & Omics. 2025;2(2):20.
6. Aryal D, Joshi S, Thapa NK, Chaudhary P, Basaula S, Joshi U, et al. Dietary phenolic compounds as promising therapeutic agents for diabetes and its complications: A comprehensive review. Food Sci Nutr. 2024 Jan 30;12(5):3025-3045. doi: 10.1002/fsn3.3983. PMID: 38726403; PMCID: PMC11077226.
7. Alhajje K, Golushko N, Erofeeva N, Romanovskaya E, Tupe R, Frolov A. Anti-Diabetic Effects of Plant-Derived Natural Products–Where We Are and Where to Go. 2024.
8. Kashtoh H, Baek KH. New Insights into the Latest Advancement in α-Amylase Inhibitors of Plant Origin with Anti-Diabetic Effects. Plants (Basel). 2023 Aug 14;12(16):2944. doi: 10.3390/plants12162944. PMID: 37631156; PMCID: PMC10458243.
9. Coskun O, Kanter M, Korkmaz A, Oter S. Quercetin, a flavonoid antioxidant, prevents and protects streptozotocin-induced oxidative stress and beta-cell damage in rat pancreas. Pharmacol Res. 2005 Feb;51(2):117-23. doi: 10.1016/j.phrs.2004.06.002. PMID: 15629256.
10. Lee YJ, Suh KS, Choi MC, Chon S, Oh S, Woo JT, et al. Kaempferol protects HIT-T15 pancreatic beta cells from 2-deoxy-D-ribose-induced oxidative damage. Phytother Res. 2010 Mar;24(3):419-23. doi: 10.1002/ptr.2983.
11. Kumkum R, Pathiranage TR, McNeill BA, Rivera LR, Aston-Mourney K. Antidiabetic Effects of Anthocyanins on Pancreatic β-Cell Function: A Systematic Review of *In Vitro* Studies. Int J Mol Sci. 2026 Jan 30;27(3):1415. doi: 10.3390/ijms27031415. PMID: 41683835; PMCID: PMC12898225.
12. Chimaeze MK, Stephen KP, Clemence T. Targeting AMPK signaling: The therapeutic potential of berberine in diabetes and its complications. Pharmacological Research-Modern Chinese Medicine. 2025:100689.
13. Rasouli H, Yarani R, Pociot F, Popović-Djordjević J. Anti-diabetic potential of plant alkaloids: Revisiting current findings and future perspectives. Pharmacol Res. 2020 May;155:104723. doi: 10.1016/j.phrs.2020.104723. Epub 2020 Feb 24. PMID: 32105756.
14. Mayyas A, Al-Samydai A, Oraibi AI, Debbabi N, Hassan SS, Al-Hussainy HA, et al. Deciphering the Anti-Diabetic Potential of Gymnema Sylvestre Using Integrated Computer-Aided Drug Design and Network Pharmacology. J Cell Mol Med. 2025 Jan;29(1):e70349. doi: 10.1111/jcmm.70349. PMID: 39810481; PMCID: PMC11733079.
15. Yedjou CG, Grigsby J, Mbemi A, Nelson D, Mildort B, Latinwo L, Tchounwou PB. The Management of Diabetes Mellitus Using Medicinal Plants and Vitamins. Int J Mol Sci. 2023 May 22;24(10):9085. doi: 10.3390/ijms24109085. PMID: 37240430; PMCID: PMC10218826.
16. Yousaf S, Nawaz S, Saeed S, Mujahid H, Ullah A, Qaiser D, Mehmood T. Antidiabetic potential of *Celtis tetrandra* Roxb. leaf extracts in alloxan-induced diabetic rats, lipid profile, and histopathological analysis of pancreas. Eur J Mass Spectrom (Chichester). 2025 Oct;31(5-6):182-188. doi: 10.1177/14690667251370487. Epub 2025 Aug 21. PMID: 40836893.
17. Husak V, Shvadchak V, Bobrova O, Faltus M, Hryhoriv Y, Karbivska U, et al. Plant-Derived Strategies for Glycemic Management in Diabetes: A Narrative Review. Diabetology. 2026;7(2):29.
18. Li M, Ding L, Cao L, Zhang Z, Li X, Li Z, et al. Natural products targeting AMPK signaling pathway therapy, diabetes mellitus and its complications. Front Pharmacol. 2025 Feb 3;16:1534634. doi: 10.3389/fphar.2025.1534634. Erratum in: Front Pharmacol. 2025 Apr 14;16:1604573. doi: 10.3389/fphar.2025.1604573. PMID: 39963239; PMCID: PMC11830733.
19. El-Saadony MT, Saad AM, Mohammed DM, Alkafaas SS, Abd El-Mageed TA, Fahmy MA, et al. Plant bioactive compounds: extraction, biological activities, immunological, nutritional aspects, food application, and human health benefits-A comprehensive review. Front Nutr. 2025 Dec 19;12:1659743. doi: 10.3389/fnut.2025.1659743. PMID: 41487672; PMCID: PMC12757306.
20. Chahrour JA, Abdel Baki Z, El Badan D, Nasser G, Maresca M, Hijazi A. Herbal Medicines in the Management of Diabetes Mellitus: Plants, Bioactive Compounds, and Mechanisms of Action. Biomolecules. 2025 Dec 1;15(12):1674. doi: 10.3390/biom15121674. PMID: 41463330; PMCID: PMC12731053.

***Corresponding author**:
Prof. Dr. Tahir Mehmood, PhD. E-mail: tahir.mmg@pu.edu.pk

International Journal of Biomedicine 16(2) (2026) 157-162
http://dx.doi.org/10.21103/Article16(2)_OA1

ORIGINAL ARTICLE

INTERNATIONAL JOURNAL OF BIOMEDICINE

Preliminary Study on the Anti-Proliferative Mechanism of Hesperetin against MDA-MB-231 Cells Based on RNA-Seq Analysis

Yu-Zhen Ma[1], Shuang-Shuang Sun[2], Guang-Zhou Zhou[2*]

[1]*Dengzhou Zhen-Yu Hospital of Traditional Chinese Medicine, Dengzhou 474150, China*
[2]*College of Bioengineering, Henan University of Technology, Zhengzhou 450001, China*

Abstract

Background: Hesperetin is a natural dihydroflavonoid compound with multiple pharmacological activities. Previous studies have shown that hesperetin targets multiple cellular proteins, such as cell cycle regulation, apoptosis, metastasis, tyrosine kinases, growth factor receptors, estrogen metabolism, and antioxidant-related proteins, to inhibit tumor formation.
Methods and Results: In this study, we treated the triple-negative breast cancer cell line MDA-MB-231 with hesperetin for 24 h and extracted total RNA for RNA-seq analysis, which revealed that 1203 genes were up-regulated and 1997 genes were down-regulated. GO clustering and KEGG enrichment analysis indicated that most of these genes played important roles in tumorigenesis and various cellular signaling pathways. Four genes related to tumor cell apoptosis and migration, including *NR4A1*, *CSF2*, *KDR*, and *LRRK2*, were selected for real-time RT-PCR analysis for validation. The mRNA level changes were consistent with the transcriptome sequencing results. Further western blot analysis of changes in the expression of the orphan nuclear receptor NR4A1 and the apoptosis-related protein Bcl-2 showed that they may be involved in hesperetin-induced apoptosis in MDA-MB-231 cells. The current research results provide a preliminary basis for further elucidating the molecular mechanism of hesperetin against breast cancer and for developing future clinical drugs based on hesperetin.(**International Journal of Biomedicine. 2026;16(2):157-162.**)

Keywords: breast cancer • hesperetin • transcriptome sequencing • orphan nuclear receptor • molecular mechanism

For citation: Ma Y-Z, Sun S-S, Zhou G-Z. Preliminary Study on the Anti-Proliferative Mechanism of Hesperetin against MDA-MB-231 Cells Based on RNA-Seq Analysis. International Journal of Biomedicine. 2026;16(2):157-162. doi:10.21103/Article16(2)_OA1

Introduction

As a naturally occurring dihydroflavonoid compound commonly found in citrus fruits, hesperetin (4-methoxy-3,5',7'-trihydroxyflavanone, C16H14O6, MW 304.2713) has been demonstrated to possess various pharmacological activities, including antitumor, anti-inflammatory, antioxidant, antiviral, antibacterial, antifibrotic, anti-aging, and neuroprotective effects.[1] In recent years, it has garnered widespread attention from numerous researchers. Hesperetin effectively scavenges hydroxyl radicals and singlet oxygen in the human body, upregulates or downregulates dysfunctional immune cells, and activates or inhibits multiple target molecules such as p38/MAPK, reactive oxygen species, Bcl-2, as well as related cellular signaling pathways, thereby inducing various programmed cell death pathways including apoptosis, autophagy and necroptosis, exerting its diverse pharmacological functions.[2-4] However, due to its low bioavailability, relatively poor solubility, and instability, there have been increasing reports in recent years on coating, modification, and solubilization technologies for hesperetin.[5] These studies provide further support for enhancing the higher application value and clinical development prospects of hesperetin.

Breast cancer is a heterogeneous disease involving multiple genetic and environmental factors. In recent years, it has become one of the tumors with the highest incidence and mortality rates globally, and it has been the most diagnosed malignant neoplasm and the second leading cause of cancer mortality among Chinese females in 2020.[6] Current treatments for breast cancer primarily involve surgical interventions, antibody-drug conjugate (ADC) therapy, immunotherapy, and chemoradiotherapy, based on specific diagnostic biomarkers and prognostic criteria.[7] Although these approaches show certain efficacy for patients with early-stage detection, the high individual heterogeneity of breast cancer, particularly in triple-negative breast cancer (TNBC, characterized by negative estrogen receptor and progesterone receptor expression, and HER2 expression below 2+ or FISH-negative), presents significant challenges. Due to the strong drug resistance and high metastasis risk in these cases, effective therapeutic targets

remain scarce, leading to limited survival outcomes. Research on the molecular mechanisms influencing the proliferation and migration of breast cancer cells, especially TNBC, is now urgently needed to identify new treatment targets for this aggressive subtype.

As a natural compound with broad-spectrum antitumor effects, hesperetin can exert cytotoxicity against various tumor cells while exhibiting minimal toxicity to normal cells.[8,9] In preliminary studies, we treated a triple-negative breast cancer cell line MDA-MB-231 with hesperetin and observed its dose- and time-dependent inhibition of tumor cell proliferation and migration, along with induction of autophagy and apoptotic cell death. Based on this, this study employed transcriptome sequencing (RNA-Seq) to analyze differentially expressed genes, aiming to identify functional genes influencing cell proliferation, migration, and apoptosis, and to further validate their roles through experimental validation, with the expectation of uncovering the cellular signaling pathways mediating hesperetin's anticancer effects. This research could provide more data and theoretical insights for molecular-level exploration of its mechanisms.

Materials and Methods

Cell Culture and Hesperetin Stock

Breast cancer MDA-MB-231 cells were preserved at Henan University of Technology. The cells were cultured with RPMI 1640 medium containing 10% FBS at 37°C in a 5% CO2 incubator. Hesperetin was purchased from Macklin Inc. (Shanghai, China) and dissolved in DMSO solution to prepare a concentration of 600 mM as a storage solution.

Cell RNA Extraction and Purification

MDA-MB-231 cells were treated with hesperetin (400 μM final concentration), and after 24 hours of drug treatment, total RNA was extracted from the cells using the TRIzol reagent (Thermo Fisher, no. 15596018, CA, USA) according to the manufacturer's instructions. An untreated blank group was set up. Three replicates were set for each sample group. The extracted RNA was measured for concentration using a NanoDrop 2000 (Thermo Fisher Scientific), and its integrity was assessed using an Agilent 2100 and a LabChip GX (PerkinElmer LabChip GX).

Transcriptome Sequencing

After binding mRNA with oligo (dT) magnetic beads twice, interrupting mRNA, synthesizing the first strand of cDNA, synthesizing the second strand of cDNA, purifying the product, repairing the end of the cDNA strand and adding an A base, purifying the linker product and fragment selection, PCR amplification and product purification, the library was subjected to quality inspection. Double-end sequencing was performed using Illumina Novaseq 6000 (transcriptome sequencing process was entrusted to Beijing Tsingke Biotech Co., Ltd., China).

Data Filtering and Quality Control

The raw image data files obtained from high-throughput sequencing are converted into sequencing raw data (Raw Data) using CASAVA Base Calling analysis. The base quality value (Quality Score or Q-score) is an integer that maps to the probability of base-calling errors. This experiment requires an average Q30 ratio of 85% or above. mRNA fragmentation results were simulated by mapping read positions across various mRNA transcripts, and the randomness of mRNA fragmentation was assessed. Furthermore, the saturation of gene numbers with different expression levels was simulated using the Mapped Data for each sample, and saturation testing was performed on transcriptome sequencing data.

Data Assembly and Gene Expression Analysis

We applied HISAT2 (Hierarchical Indexing for Spliced Alignment of Transcripts, https://daehwankimlab.github.io/hisat2/,version:hisat2-2.2.1) to align Clean Reads with the reference genome to obtain positional information on the reference genome or gene, as well as unique sequence features of the sequencing sample. The number of Mapped Reads in different regions (exons, introns, and intergenic regions) of the specified reference genome was counted. StringTie (version number stringtie-2.1.6, developed by Johns Hopkins University in collaboration with the University of Texas Southwestern Medical Center) was used for transcript assembly and prediction of expression levels, and FPKM (Fragment Per Kilobase of transcript per Million fragment mapped, per kilobase transcript fragment/million mapped reads) was used as an indicator to measure transcript or gene expression levels.

Screening and Analysis of Differentially Expressed Genes

The DESeq2 software was applied to perform differential gene expression analysis between sample groups. A fold change greater than 2 and a false discovery rate (FDR) parameter less than 0.05 was used as the screening criteria (using the Benjamin Hochberg correction method to correct the significance p-values obtained from the original hypothesis test, and using FDR as the key indicator for differential gene screening). Moreover, hierarchical clustering analysis and functional annotation of the selected differentially expressed genes were performed, along with GO functional and KEGG pathway enrichment analyses of the expressed genes.

RT-qPCR

Based on transcriptome sequencing analysis, four differentially expressed functional genes, *CSF2*, *KDR*, *NR4A1*, and *LRRK2*, which affect cell proliferation, apoptosis, and autophagy, were randomly selected for RT-qPCR validation analysis. The brief process is to collect MDA-MB-231 cells treated with hesperetin and extract total RNA using a cell total RNA extraction kit (Beijing Qingke Biotechnology Co., Ltd., Beijing). After reverse-transcribing it into cDNA, the RT-qPCR reaction system was prepared according to the procedures of the SYBR qPCR Master Mix kit (Nanjing Novozymes Biotechnology Co., Ltd.), and the reaction was detected using the Eppendorf PCR System instrument. The data were calculated using the $2^{-\triangle\triangle Ct}$ method (experiment was repeated three times in parallel). The primer sequences required for the experiment were as follows:

CSF2-F: GCCTCACCAAGCTCAAGGG, *CSF2*-R: TCATCTGGCCGGTCTCACTC

KDR-F: CGGTCAACAAAGTCGGGAGA, *KDR*-R: TCCCACATGGATTGGCAGAG

NR4A1-F: CCTCGCCTTGGTTGGAGG, *NR4A1*-R: CTCGGTGCTGGTGTCCCATA

LRRK2-F: CCTGGATCTTTCAACTCGTCG, *LRRK2*-R: GTCCCAAACGGTCAAGCAAG

Western Blot

After protein extraction from MDA-MB-231 cells treated with hesperetin, subsequent immunoblotting was performed using conventional methods.[10] The brief procedures are as follows: The proteins were first analyzed by SDS-PAGE (labeled with color prestained markers) and then transferred onto nitrocellulose membranes (NC membrane, Beijing Solarbio Technology Co., Ltd.). After blocking the NC membranes with a 5% skim milk powder solution diluted with TBS buffer for 1 h, the membranes were incubated with primary antibodies against NA4R1 or Bcl-2 for 16-18 h at 4 ℃, respectively. After washing three times with TBS buffer, the NC membranes were further incubated with secondary antibody (sheep anti-mouse IgG produced by LiCOR Bioscience, USA) for 4 h at 4 ℃. After washing with TBST buffer three times (7 minutes each time), the blots in the NC membranes were scanned and saved using an Odyssey infrared laser imager.

Results

Quality Control of Sequencing Data

To investigate the effect of hesperetin treatment on gene expression in MDA-MB-231 cells, we set up three blank control groups (C1, C2, and C3) and three MDA-MB-231 cell groups (T1, T2, and T3) treated with hesperetin (400 μ M) for 24 h each for RNA-seq analysis in this study. The correlation analysis of biological replicates showed that the r-values between the dosing groups T1, T2, and T3, and the blank groups C1, C2, and C3 were close to 1.000, while the r-values between the two groups were 0.773~0.681 (Figure 1) (according to the Pearson correlation coefficient r-index, r>0.95 is significant correlation, and 0.5 ≤ r < 0.8 is moderate correlation). The results indicated a strong correlation between intra-group duplicate samples in the hesperetin treatment group and the control group, while the correlation between the two groups was weak, indicating that the experimental sample selection is reasonable and the conditions are reliable.

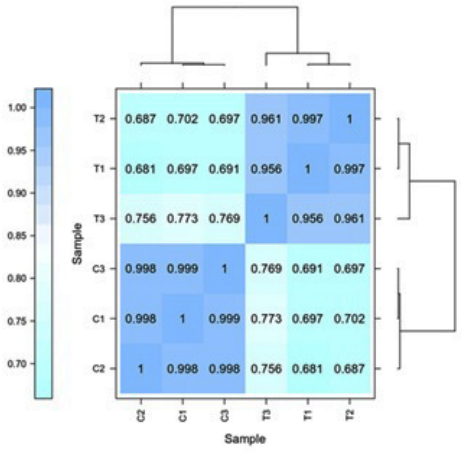

Fig. 1. *Correlation analysis of gene expression between different samples. C1, C2, and C3 denote different control duplicates, while T1, T2, and T3 stand for three hesperetin treatment samples, respectively.*

In addition, by comparing the sequencing base information with the human genome, the total Clean data of the sequencing samples was 37.71 Gb, and the average Q30 ratio was above 93.64% (Table 1). The sequencing results indicate that the data quality of this study is qualified, and all samples meet the basic requirements for library sequencing.

Table 1.
Statistical analysis of sequencing data quality control.

Sample ID	Clean reads	Clean bases	GC(%) GC Content	Q30 value% ≥ Q30
Control 1 (C1)	21563838	6464239479	49.70	93.64
Control 2 (C2)	21278783	6377945170	50.01	95.03
Control 3 (C3)	20657474	6192076317	49.83	94.31
Test 1 (T1)	20275484	6077236081	49.56	94.94
Test 2 (T2)	19147049	5739575817	49.28	95.00
Test 3 (T3)	22887520	6860538159	49.48	95.36

Note: Clean reads, total number of pair-end reads in Clean Data; GC content, the percentage of G and C bases in the total bases in Clean Data; ≥Q30%, the percentage of bases with a Clean Data quality value greater than or equal to 30.

Overall Analysis of Differentially Expressed Genes

The screening criteria for differentially expressed genes were based on a multiple difference of ≥ 2 (equivalent to an absolute value of log2FC ≥ 1) and a q-value<0.05 (p-value correction). The number of differentially expressed genes between the experimental and control groups was counted. Among them, 3200 genes were differentially expressed (DEGs), including 1203 up-regulated and 1997 down-regulated genes, indicating that hesperetin affects the transcription levels of multiple genes. Cluster analysis was performed on genes with the same or similar expression patterns (Figure 2A), and the control and experimental groups showed good reproducibility. The volcano plot (Figure 2B) visually displays the overall distribution of differential gene expression levels and fold differences between two groups.

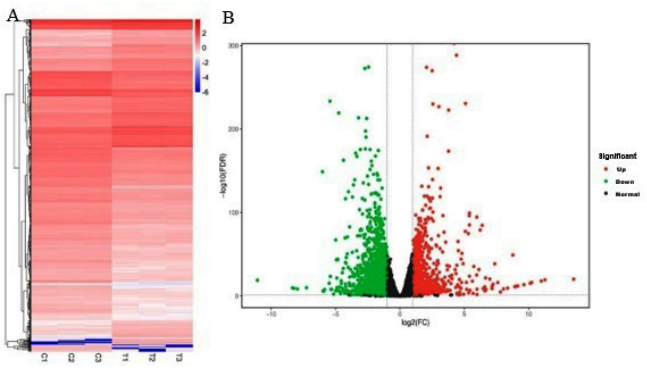

Fig. 2. *Cluster heatmap of differentially expressed genes in hesperetin-treated MDA-MB-231 cells (**A**, Different columns represent different samples and different rows represent different genes. Colors represent the log10 expression levels of genes in the samples) and volcano plot (**B**, Green dots represent down-regulated differentially expressed genes, red dots represent up-regulated differentially expressed genes, and black dots represent non-differentially expressed genes).*

Clustering of Differentially Expressed Genes and KEGG Annotation

Further Gene Ontology analysis was conducted on 3200 differentially expressed genes induced by hesperetin in MDA-MB-231 cells, which were classified into three functional categories: Molecular Function (MF), Cellular Component (CC), and Biological Process (BP). Among them, there are relatively more differentially expressed genes involved in intracellular metabolic processes and molecular functions such as cell membrane binding, catalysis, and regulation of molecular signaling pathways.

On this basis, further KEGG (Kyoto Encyclopedia of Genes and Genomes) annotation analysis was performed on differentially expressed genes in MDA-MB-231 cells treated with hesperetin. The results showed that the differentially expressed genes had the highest number of genes involved in anti-tumor related pathways, with 105 genes, accounting for 8.95% (Figure 3, marked in red). In addition, 29 genes (2.47%) were related to cell apoptosis. There are 60 genes related to the MAPK signaling pathway, all of which can regulate cell proliferation and apoptosis. Besides that, hesperetin treatment of cells also led to differential expression of 70 genes (5.97%) in the PI3K-Akt pathway, most of which are related to cellular autophagy, migration, and apoptosis. These data provide direction for further in-depth study on the molecular anti-proliferative mechanism of hesperetin on MDA-MB-231 cells.

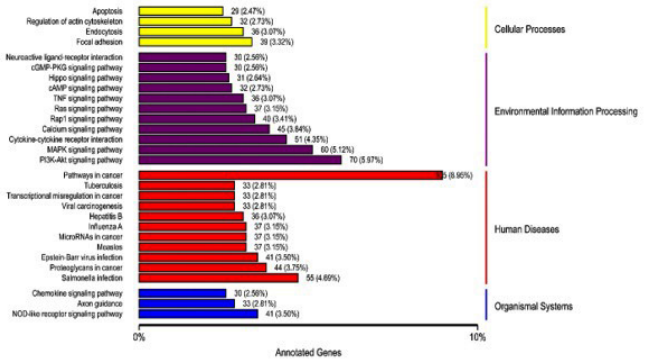

Fig. 3. *Classification of differentially expressed genes KEGG in hesperetin-treated MDA-MB-231 cells. The vertical axis shows the name of the KEGG metabolic pathway, and the horizontal axis shows the number of genes annotated to this pathway and their proportion to the total number of annotated genes.*

Enrichment Analysis of Differentially Expressed Genes in KEGG Pathway

Using the metabolic pathways represented in the KEGG database as units of analysis, hypergeometric testing was applied to identify pathways that are significantly enriched in differentially expressed genes compared to the entire genome background. Figure 4 shows the top 20 pathways with the lowest Q-values in the KEGG enrichment analysis (the lower the Q-value, the more significant the enrichment). These pathways involve TGF-β signaling pathway, NOD like receptor signaling pathway, microRNAs in cancer, longevity regulation pathway (multi species), JAK-STAT signaling pathway, anti-folate resistance, ECM receptor interaction, toxoplasmosis, steroid biosynthesis, relaxin signaling pathway, Kaposi sarcoma associated herpesvirus infection, cancer pathway, IL-17 signaling pathway, measles, small cell lung cancer, herpes simplex virus 1 infection, whooping cough, TNF signaling pathway, legionellosis, AGE-RAGE signaling pathway in diabetes complications, etc. Among them, the proportion of differentially expressed genes involved in pathways in cancer is the highest (Figure 4), which again confirms the disturbance of MDA-MB-231 tumor cell-related signaling pathways caused by hesperetin treatment, providing guidance for further identification of functional genes that affect tumor cell proliferation and death.

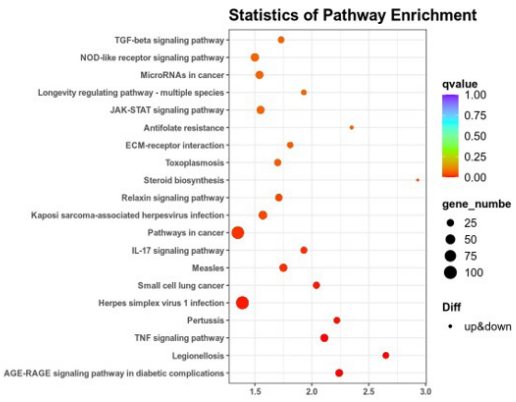

Fig. 4. *Scatter plot of KEGG pathway enrichment for differentially expressed genes in hesperetin-treated MDA-MB-231 cells.*

RT-qPCR and Western Blot Validation of Differentially Expressed Genes

Based on the differential gene GO clustering and KEGG pathway enrichment analysis results, we further selected four genes related to tumor cell apoptosis and migration, including nuclear receptor 4A1 (NR4A1), colony stimulating factor 2 (CSF2), kinase insert domain receptor (KDR), and leucine rich repeat kinase 2 (LRRK2), for RT-qPCR analysis to further verify the reliability of transcriptome sequencing. The results showed that after treatment with hesperetin in MDA-MB-231 cells for 24 h, the mRNA levels of NR4A1, CSF2, and KDR were upregulated, while the mRNA level of LRRK2 decreased (Figure 5A), which were consistent with the trend of RNA-seq analysis, proving the high reliability of sequencing in this study.

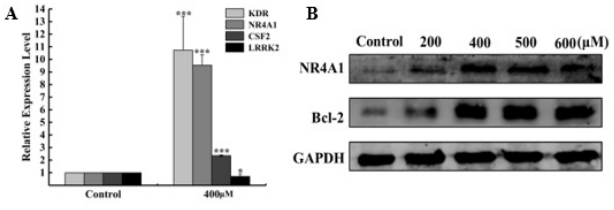

Fig. 5. A*. Changes in mRNA level (CSF, LRRK2, KDR, and NR4A1) of relevant differential genes detected by fluorescence quantitative PCR in hesperetin-treated MDA-MB-231 cells (*p<0.05, ***p<0.001).* ***B****. Western blot analysis of NR4A1 and Bcl-2 protein expression. tect protein expression.*

To further verify the expression changes of key functional genes and the potential anti-proliferative mechanism in

hesperetin-treated MDA-MB-231 cells, the NR4A1 gene was selected for western blot analysis to assess its expression. Previous research confirmed that the orphan nuclear receptor NR4A1 can induce mitochondrial apoptosis by exposing the BH3 domain of the anti-apoptotic protein Bcl-2, leading to conformational changes in Bcl-2. This study found that after hesperetin treatment, NR4A1 and Bcl-2 expressions increased in a dose-dependent manner (Figure 5B). It is speculated that the synergistic effect of the two proteins is involved in the hesperetin-induced apoptosis process of MDA-MB-231 cells.

Discussion

As an important natural dihydroflavonoid compound, hesperetin has been shown to exhibit strong anti-tumor effects, although the specific molecular mechanisms remain to be further explored. Previous studies showed that hesperetin can inhibit the proliferation of breast cancer cells by acting as an epigenetic modulator of gene expression.[12,13] In addition, hesperetin can inhibit breast cancer stem cells and, when combined with other agents, achieve a synergistic anti-tumor effect by targeting p53, PPARG, Notch, and other signal transduction pathways.[14]

In order to further explore the anti-proliferative molecular mechanism on breast cancer cells, we selected the triple-negative breast cancer cell line, MDA-MB-231, as a cell model, and used transcriptome sequencing to study the differential expression of functional genes after hesperetin treatment, aiming to screen important functional proteins involved in regulating cell proliferation, migration, and influencing various cell signal pathways. As a mature high-throughput RNA sequencing technology, RNA-seq can obtain millions of readings in each experimental sample, enabling high-resolution study of any cellular transcriptome changes and obtaining valuable clues about the organism's response to specific stimuli.[15,16] Our current research showed that, compared with the blank control group, the numbers of upregulated and downregulated genes were 1203 and 1997, respectively, in hesperetin-treated cells. Subsequent gene cluster analysis and KEGG pathway enrichment analysis revealed that the largest number of genes are involved in tumorigenesis; furthermore, numerous genes are involved in modulating signaling pathways, such as tumor cell proliferation and apoptosis. This suggested that hesperetin treatment can affect tumor cell survival-related functional genes, thereby inhibiting the proliferation of MDA-MB-231 cells.

Previous studies have shown that hesperetin targets multiple cellular proteins, such as cell cycle regulation, apoptosis, metastasis, tyrosine kinases, growth factor receptors, estrogen metabolism, and antioxidant-related proteins, to inhibit tumor formation.[17] Based on transcriptome sequencing data analysis, four differentially expressed genes (*NR4A1*, *CSF2*, *KDR*, and *LRRK2*) related to tumor cell proliferation, migration, and apoptosis were further screened and validated by RT-qPCR. The trends in mRNA levels were consistent with transcriptomic sequencing, further demonstrating the reliability of RNA-seq in this study. On this basis, the orphan nuclear receptor NR4A1 was also selected for western blot analysis to assess its translation level. We found that in hesperetin-treated MDA-MB-231 cells, both NR4A1 and the apoptosis-related protein Bcl-2 were upregulated in a dose-dependent manner. Previous literature has shown that NR4A1 can be located in the gene body and 3'UTR regions of immediate early genes in cells, inhibits the transcriptional elongation of RNA polymerase II, and that its ectopic expression enhances the tumorigenesis of breast cancer cells.[18] Preliminary studies on retinoids and apoptosis inducers have suggested that their cytotoxic activity is NR4A1 dependent and involves drug-induced NR4A1 nuclear export and mitochondrial pro-apoptotic NR4A1-Bcl-2 complex formation.[19,20] Orphan members of the nuclear receptor family, lacking the BH3 domain, can bind to Bcl-2 and regulate its effects on cell apoptosis and autophagy.[21]The endogenous apoptotic pathway of cells (also known as the mitochondrial pathway) is initiated by various intracellular signals, mainly regulated by the Bcl-2 family, which comprises pro-apoptotic and anti-apoptotic proteins that together control the permeability of the mitochondrial outer membrane.[22] In this study, we found that NR4A1 and Bcl-2 exhibit a dose-dependent upregulation, which may play an important role in hesperetin's anti-proliferative effect on breast cancer cells. In fact, our recent study has shown that hesperetin indeed induces apoptosis and autophagy in MDA-MB-231 cells. In the future, further exploration can be conducted to determine whether the two proteins exhibit a synergistic effect and participate in hesperetin-induced mitochondrial apoptosis in MDA-MB-231 cells. However, current research undoubtedly lays the foundation for such future study.

Conclusion

Through RNA-seq analysis, combined with RT-qPCR and western blot validation, we preliminarily identified several differential gene expression changes that affect the death of breast cancer cells MDA-MB-231 induced by hesperetin, discussed the possible functional role of NR4A1 protein in it, and provided a preliminary basis for the future in-depth study of the molecular mechanism of hesperetin's anti-tumor effect and the development of clinical drugs based on hesperetin.

Author Contributions

Yu-Zhen Ma: Investigation, Methodology, Data curation, Writing – original draft.
Shuang-Shuang Sun: Investigation, Methodology, Data curation, Writing – original draft.
Guang-Zhou Zhou: Conceptualization, Supervision, Funding acquisition. Writing – review and editing.
All authors have approved the final article.

Conflict of Interest

The authors have declared no conflict of interest.

Acknowledgments

This research was supported, in part, by the Science and Technology Planning Project of Henan Province, China (No. 262102311263).

References

1. Song B, Hao M, Zhang S, Niu W, Li Y, Chen Q, Li S, Tong C. Comprehensive review of Hesperetin: Advancements in pharmacokinetics, pharmacological effects, and novel formulations. Fitoterapia. 2024 Dec;179:106206. doi: 10.1016/j.fitote.2024.106206.
2. Elango R, Athinarayanan J, Subbarayan VP, Lei DKY, Alshatwi AA. Hesperetin induces an apoptosis-triggered extrinsic pathway and a p53- independent pathway in human lung cancer H522 cells. J Asian Nat Prod Res. 2018 Jun;20(6):559-569. doi: 10.1080/10286020.2017.1327949. Epub 2017 May 24. PMID: 28537448.
3. Li Q, Miao Z, Wang R, Yang J, Zhang D. Hesperetin Induces Apoptosis in Human Glioblastoma Cells via p38 MAPK Activation. Nutr Cancer. 2020;72(3):538-545. doi: 10.1080/01635581.2019.1638424. Epub 2019 Jul 11. PMID: 31295040.
4. Wu D, Li J, Hu X, Ma J, Dong W. Hesperetin inhibits Eca-109 cell proliferation and invasion by suppressing the PI3K/AKT signaling pathway and synergistically enhances the anti-tumor effect of 5-fluorouracil on esophageal cancer in vitro and in vivo. RSC Adv. 2018 Jul 6;8(43):24434-24443. doi: 10.1039/c8ra00956b. PMID: 35539191; PMCID: PMC9082046.
5. Davodabadi F, Nasri N, Valizadeh N, Haji Ali B, Ghotekar S, Sargazi S, Barani M, Rahman MM. Nanotechnology-enhanced delivery systems for bioactive citrus compounds: a comprehensive review. Crit Rev Food Sci Nutr. 2025 Nov 20:1-45. doi: 10.1080/10408398.2025.2584454. Epub ahead of print. PMID: 41262037.
6. Tao X, Li T, Gandomkar Z, Brennan PC, Reed WM. Incidence, mortality, survival, and disease burden of breast cancer in China compared to other developed countries. Asia Pac J Clin Oncol. 2023 Dec;19(6):645-654. doi: 10.1111/ajco.13958. Epub 2023 Apr 7. PMID: 37026375.
7. Barzaman K, Karami J, Zarei Z, Hosseinzadeh A, Kazemi MH, Moradi-Kalbolandi S, Safari E, Farahmand L. Breast cancer: Biology, biomarkers, and treatments. Int Immunopharmacol. 2020 Jul;84:106535. doi: 10.1016/j.intimp.2020.106535. Epub 2020 Apr 29. PMID: 32361569.
8. He P, Ma J, Liu Y, Deng H, Dong W. Hesperetin Promotes Cisplatin-Induced Apoptosis of Gastric Cancer In Vitro and In Vivo by Upregulating PTEN Expression. Front Pharmacol. 2020 Aug 27;11:1326. doi: 10.3389/fphar.2020.01326. PMID: 32973533; PMCID: PMC7482524.
9. Chen X, Wei W, Li Y, Huang J, Ci X. Hesperetin relieves cisplatin-induced acute kidney injury by mitigating oxidative stress, inflammation and apoptosis. Chem Biol Interact. 2019 Aug 1;308:269-278. doi: 10.1016/j.cbi.2019.05.040. Epub 2019 May 31. PMID: 31153982.
10. Zhao YY, Li J, Wang HQ, Zheng HB, Ma SW, Zhou GZ. Activation of autophagy promotes the inhibitory effect of curcumin analog EF-24 against MDA-MB-231 cancer cells. J Biochem Mol Toxicol. 2024 Feb;38(2):e23642. doi: 10.1002/jbt.23642. PMID: 38348710.
11. Payapilly A, Guilbert R, Descamps T, White G, Magee P, Zhou C, Kerr A, Simpson KL, Blackhall F, Dive C, Malliri A. TIAM1-RAC1 promote small-cell lung cancer cell survival through antagonizing Nur77-induced BCL2 conformational change. Cell Rep. 2021 Nov 9;37(6):109979. doi: 10.1016/j.celrep.2021.109979. PMID: 34758330; PMCID: PMC8595642.
12. Sun YS, Zhao Z, Yang ZN, Xu F, Lu HJ, Zhu ZY, Shi W, Jiang J, Yao PP, Zhu HP. Risk Factors and Preventions of Breast Cancer. Int J Biol Sci. 2017 Nov 1;13(11):1387-1397. doi: 10.7150/ijbs.21635. PMID: 29209143; PMCID: PMC5715522.
13. Hasan AK, Babaei E, Al-Khafaji ASK. Hesperetin effect on MLH1 and MSH2 expression on breast cancer cells BT-549. J Adv Pharm Technol Res. 2023 Jul-Sep;14(3):241-247. doi: 10.4103/japtr.japtr_277_23. Epub 2023 Jul 28. PMID: 37692022; PMCID: PMC10483912.
14. Hermawan A, Ikawati M, Khumaira A, Putri H, Jenie RI, Angraini SM, Muflikhasari HA. Bioinformatics and *In Vitro* Studies Reveal the Importance of p53, PPARG and Notch Signaling Pathway in Inhibition of Breast Cancer Stem Cells by Hesperetin. Adv Pharm Bull. 2021 Feb;11(2):351-360. doi: 10.34172/apb.2021.033. Epub 2020 Apr 19. PMID: 33880358; PMCID: PMC8046396.
15. Withanage MHH, Liang H, Zeng E. RNA-Seq Experiment and Data Analysis. Methods Mol Biol. 2022;2418:405-424. doi: 10.1007/978-1-0716-1920-9_22. PMID: 35119677.
16. Gill N, Dhillon B. RNA-seq Data Analysis for Differential Expression. Methods Mol Biol. 2022;2391:45-54. doi: 10.1007/978-1-0716-1795-3_4. PMID: 34686975.
17. Sohel M, Sultana H, Sultana T, Al Amin M, Aktar S, Ali MC, Rahim ZB, Hossain MA, Al Mamun A, Amin MN, Dash R. Chemotherapeutic potential of hesperetin for cancer treatment, with mechanistic insights: A comprehensive review. Heliyon. 2022 Jan 23;8(1):e08815. doi: 10.1016/j.heliyon.2022.e08815. PMID: 35128104; PMCID: PMC8810372.
18. Guo H, Golczer G, Wittner BS, Langenbucher A, Zachariah M, Dubash TD, et al. NR4A1 regulates expression of immediate early genes, suppressing replication stress in cancer. Mol Cell. 2021 Oct 7;81(19):4041-4058.e15. doi: 10.1016/j.molcel.2021.09.016. PMID: 34624217; PMCID: PMC8549465.
19. Safe S, Karki K. The Paradoxical Roles of Orphan Nuclear Receptor 4A (NR4A) in Cancer. Mol Cancer Res. 2021 Feb;19(2):180-191. doi: 10.1158/1541-7786.MCR-20-0707. Epub 2020 Oct 26. PMID: 33106376; PMCID: PMC7864866.
20. Xiong J, Kuang X, Lu T, Liu X, Cheng B, Wang W, Wei D, Li X, Zhang Z, Fang Q, Wu D, Wang J. Fenretinide-induced Apoptosis of Acute Myeloid Leukemia Cells via NR4A1 Translocation into Mitochondria and Bcl-2 Transformation. J Cancer. 2019 Nov 1;10(27):6767-6778. doi: 10.7150/jca.32167. PMID: 31839811; PMCID: PMC6909957.
21. Godoi PHC, Wilkie-Grantham RP, Hishiki A, Sano R, Matsuzawa Y, Yanagi H, et al. Orphan Nuclear Receptor NR4A1 Binds a Novel Protein Interaction Site on Anti-apoptotic B Cell Lymphoma Gene 2 Family Proteins. J Biol Chem. 2016 Jul 1;291(27):14072-14084. doi: 10.1074/jbc.M116.715235. Epub 2016 Apr 19. PMID: 27129202; PMCID: PMC4933167.
22. Cooper KF. Till Death Do Us Part: The Marriage of Autophagy and Apoptosis. Oxid Med Cell Longev. 2018 May 8;2018:4701275. doi: 10.1155/2018/4701275. PMID: 29854084; PMCID: PMC5964578.

***Corresponding author:** Dr. Guang-Zhou Zhou. College of Bioengineering, Henan University of Technology, Zhengzhou 450001, China. E-mail: gzzhou@163.com*

International Journal of Biomedicine 16(2) (2016) 163-168
http://dx.doi.org/10.21103/Article16(2)_OA2

ORIGINAL ARTICLE

INTERNATIONAL JOURNAL OF BIOMEDICINE

An Integrated Analysis of NF-κB, MMP-9 Expression, and Tumor-Infiltrating Lymphocytes Density in Correlation with TNM Stage of Colorectal Cancer

Heru Fajar Trianto[1,2], Gondo Mastutik[3*], Desak Gede Agung Suprabawati[4], Mitra Handini[5], Mahyarudin Mahyarudin[6]

[1]*Doctoral Program of Medical Science, Faculty of Medicine, Universitas Airlangga, Surabaya, Indonesia*
[2]*Department of Anatomical Pathology, Faculty of Medicine, Universitas Tanjungpura, Pontianak, Indonesia*
[3]*Department of Anatomical Pathology, Faculty of Medicine, Universitas Airlangga, Surabaya, Indonesia*
[4]*Oncology Division, Surgery Department, Faculty of Medicine, Universitas Airlangga, Surabaya, Indonesia*
[5]*Department of Physiology, Faculty of Medicine, Universitas Tanjungpura, Pontianak, Indonesia*
[6]*Department of Microbiology and Immunology, Faculty of Medicine, Universitas Tanjungpura, Pontianak, Indonesia*

Abstract

Background: Colorectal cancer progression is influenced by interactions between tumor cells and the stromal area. Nuclear factor kappa B (NF-κB) and matrix metalloproteinase-9 (MMP-9) contribute to cancer expansion, while tumor-infiltrating lymphocyte (TIL) density influences the host immune response. However, their complexity remains unclear. Therefore, this study aimed to integrate an analysis of the correlation between NF-κB, MMP-9, and TIL density with TNM stage in colorectal cancer.

Methods and Results: Fifty colorectal cancer paraffin blocks were analyzed. NF-κB and MMP-9 expression were evaluated by immunohistochemistry, while TIL density was assessed using hematoxylin-eosin (HE) staining. Correlations with TNM stage and its components were analyzed using Spearman's correlation test. NF-κB expression correlated positively with N stage (p = 0.013). MMP-9 expression had a positive correlation with T stage (p = 0.000), M stage (p = 0.036), and TNM stage (p = 0.001). In contrast, TIL density showed an inverse correlation with T stage (p = 0.010), N stage (p = 0.003), and TNM stage (p = 0.001). NF-κB expression correlated positively with MMP-9 (p = 0.021), but not with TIL density.

Conclusion: NF-κB and MMP-9 expressions contribute to progression, while TIL density contributes to the antitumor response in colorectal cancer. An integrated analysis of the biomarkers showed a dynamic interaction between tumor molecular changes and the host immune response.(**International Journal of Biomedicine. 2026;16(2):163-168.**)

Keywords: transcription factor • matrix metalloproteinase • immune response • cancer

For citation: Trianto HF, Mastutik G, Suprabawati DGA, Handini M, Mahyarudin M. An Integrated Analysis of NF-κB, MMP-9 Expression, and Tumor-Infiltrating Lymphocytes Density in Correlation with TNM Stage of Colorectal Cancer. International Journal of Biomedicine. 2026;16(2):163-168. doi:10.21103/Article16(2)_OA2

Abbreviations

NF-κB, nuclear factor kappa B; **MMP-9**, matrix metalloproteinase-9; **TILs**, tumor-infiltrating lymphocytes.

Introduction

Colorectal cancer is ranked second with the highest mortality rate worldwide.[1] Several examination variables can be used to predict outcomes and therapy options, including the TNM (tumor, lymph nodes, metastasis) stage established by the American Joint Committee on Cancer (AJCC).[2,3] The TNM stage reflects the biological and molecular conditions of the tumor associated with the proliferation and progression of cancer cells.[4]

Nuclear factor kappa B (NF-κB) is a transcription factor associated with the immune response, apoptosis regulation, and progression of various cancers, including colorectal cancer.[5,6] Its activation can trigger various molecules that enhance the ability of cancer cells to migrate, invade, and metastasize.[6,7] Among the kinds of molecules is matrix metalloproteinase-9 (MMP-9), which has matrix degradation capabilities and facilitates tumor invasion.[8] Increased MMP-9 expression is associated with advanced stage and high-grade tumors.[9]

In addition to influencing cancer progression, NF-κB plays a crucial role in inflammation and the immune response.[7,10] A component of the immune response in cancer is tumor-infiltrating lymphocytes (TIL), which are discovered in the tumor stroma.[11] Several studies have shown a relationship between TIL density and clinicopathological characteristics with survival rates in colorectal cancer patients.[12,13]

Although NF-κB activation, MMP-9 expression, and TIL density have been studied individually in colorectal cancer, an integrated analysis of their interrelationships and correlations with clinicopathological characteristics remains limited. The interaction between the inflammatory process and cancer progression remains poorly understood. Therefore, this study aims to evaluate the correlation between NF-κB, MMP-9 expression, and TIL density with TNM stage in colorectal cancer. Clarifying the associations may provide a more comprehensive understanding of the interplay between inflammation, invasion, and immune response in the progression.

Materials and Methods

This observational analytical study used 50 colorectal cancer paraffin blocks from the Anatomical Pathology Laboratory of Dr. Soedarso General Hospital, Pontianak, West Kalimantan, Indonesia, between 2020 and 2023. Inclusion criteria included paraffin blocks from resection specimens, a diagnosis of adenocarcinoma, and data on depth of invasion (T stage), lymph node spread (N stage), distant metastasis (M stage), and TNM stage. Observations were conducted on hematoxylin-eosin (HE) slides and by immunohistochemistry (IHC) using two blinded pathologists. Ethical approval was obtained from the Health Research Ethics Committee of Dr. Soedarso General Hospital (No. 96/RSUD/KEPK/XI/2024).

Immunohistochemistry (IHC)

Paraffin blocks were sectioned at 4 µm, deparaffinized using xylene, and rehydrated with alcohol. Antigen retrieval was performed at 95°C in a decloaking chamber with pH 9 for 30 minutes. Slides were then incubated with NF-κB (Cat#BF0466, Affinity Biosciences, USA; dilution 1:200) and MMP-9 primary monoclonal antibodies (IHC109, GenomeMe, Canada; dilution 1:200) at room temperature for 60 minutes. Washing was conducted twice with phosphate-buffered saline, followed by polymer and 3,3′-diaminobenzidine for 5 minutes each. Counterstaining was performed with hematoxylin. This was followed by dehydration in graded alcohol concentrations and clearing with xylene.

TIL Density Assessment

TIL density was assessed based on the percentage of mononuclear cells (lymphocytes and plasma cells) in the entire tumor stroma on HE slides. Observation criteria were based on a modification of the TIL working group method.[14] TIL was observed at 10x objective magnification and classified into three groups, namely low (0-10%), moderate (11-50%), and high (51-100%).

NF-κB and MMP-9 Expression Evaluation

NF-κB and MMP-9 expression were examined using IHC staining. NF-κB expression was observed in the nucleus, while MMP-9 expression was observed in the cytoplasm of tumor cells. NF-κB and MMP-9 expressions were assessed using the semiquantitative H-Score method. This combined the intensity and number of stained tumor cells across the entire field of view. H-Score assessment results were categorized as negative (0-49), weak (50-99), moderate (100-199), and strong (200-300).[15]

Statistical Analysis

Observation data were presented as frequencies and percentages. Furthermore, statistical analysis was performed using SPSS 25 software. The Spearman's correlation test was used to assess the strength and direction of a monotonic relationship between two variables. A p-value of < 0.05 was considered statistically significant.

Results

The sample consisted of 50 colorectal cancer patients, comprising 29 men and 21 women, with the majority aged 51-60 (36%). The histopathological types were Adenocarcinoma NOS (86%) and Mucinous Adenocarcinoma (14%), with the most common grade being well-differentiated (58%). In this study, the most common T Stage was T3 (64%), while the most common N and M Stages were N0 (54%) and M0 (76%). The most common TNM stage was Stage II (26%) and III (26%), with sample characteristics presented in Table 1.

The entire sample showed NF-κB expression, as evidenced by nuclear staining in tumor cells (Figure 1). Most of the expressions were moderate (56%) as detailed in Table 1. There was a significant relationship between NF-κB expression and N stage ($p = 0.013$) with a correlation coefficient (r) of 0.350. No significant relationship was observed between NF-κB expression and T stage ($p = 0.160$), M stage ($p = 0.468$), and TNM stage ($p = 0.086$) (Table 2).

This study showed that MMP-9 expression was predominantly moderate (56%) (Table 1) and was observed in the cytoplasm of tumor cells. Spearman's correlation test results showed a significant, positive correlation between MMP-9 expression and T stage ($r = 0.580$, $p = 0.000$), M stage ($r = 0.298$, $p = 0.036$), and TNM stage ($r = 0.446$, $p = 0.001$). MMP-9 was not significantly correlated with N stage ($p = 0.050$) (Table 2).

Most TIL density in this study was in the moderate category (76%) as detailed in Table 1. TIL was assessed in the stromal area surrounding the tumor, as presented in

Figure 1. TIL showed significant negative correlations with T (r = -0.361, p = 0.010), N (r = -0.418, p = 0.003), and TNM stage (r = -0.454, p = 0.001). TIL was not significantly correlated with M stage (p = 0.056) (Table 2).

Spearman's test showed a positive correlation between NF-κB and MMP-9 (r = 0.325, p = 0.021). These results suggest that increasing NF-κB expression is associated with elevating MMP-9 expression. NF-κB was not significantly correlated with TIL (r = -0.117, p = 0.418) (Table 3).

Table 1.

Sample Characteristics

Parameters	n (%)
Age (Years)	
21-30	2 (4)
31-40	2 (4)
41-50	5 (10)
51-60	18 (36)
61-70	14 (28)
>70	9 (18)
Sex	
Men	29 (58)
Women	21 (42)
Histopathological type	
Adenocarcinoma, NOS	43 (86)
Mucinous adenocarcinoma	7 (14)
T Stage	
T1	3 (6)
T2	10 (20)
T3	32 (64)
T4	5 (10)
N Stage	
N0	27 (54)
N1	12 (24)
N2	11 (22)
M Stage	
M0	38 (76)
M1	12 (24)
TNM Stage	
I	12 (24)
II	13 (26)
III	13 (26)
IV	12 (24)
NF-κB Expression	
Negative	0 (0)
Weak	12 (24)
Moderate	28 (56)
Strong	10 (20)
MMP-9 Expression	
Negative	0 (0)
Weak	19 (38)
Moderate	28 (56)
Strong	3 (6)
TIL Density	
Low	2 (4)
Moderate	38 (76)
High	10 (20)

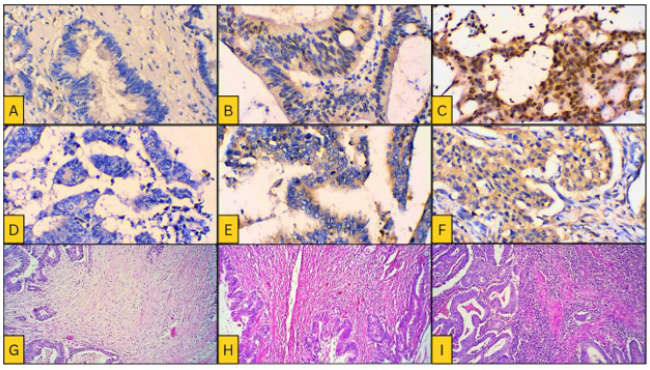

Fig 1. *Immunohistochemical staining of NF-κB and MMP-9 (Objective, 40x) and hematoxylin-eosin staining of TILs (Objective, 10x). (A) Weak expression of NF-κB; (B) Moderate expression of NF-κB; (C) Strong expression of NF-κB; (D) Weak expression of MMP-9; (E) Moderate expression of MMP-9; (F) Strong expression of MMP-9; (G) Low TILs density; (H) Moderate TILs density; (I) High TILs density.*

Table 2.

Correlation between NF-κB, MMP-9, and TIL density with clinicopathological parameters.

Parameters	NF-κB (n=50)		MMP-9 (n=50		TILs (n=50)	
	p-value	r	*p*-value	r	*p*-value	r
T Stage	0.160	0.202	0.000	0.580	0.010	-0.361
N Stage	0.013	0.350	0.050	0.279	0.003	-0.418
M Stage	0.468	0.105	0.036	0.298	0.056	-0.272
TNM Stage	0.086	0.245	0.001	0.446	0.001	-0.454

Table 3.

Correlation between NF-κB with MMP-9 expression and TIL density.

Parameters	NF-κB			r	*p*-value
	Weak	Moderate	Strong		
MMP-9					
Weak	6	7	1	0.325	0.021
Moderate	3	18	9		
Strong	1	3	2		
TIL density					
Low	0	3	2	-0.117	-0.418
Moderate	8	19	8		
High	2	6	2		

Discussion

The majority of the sample were male (58%) and aged 51-60 years (36%). The change from precancerous lesions to colorectal cancer takes approximately 10-25 years, and most incidents occur in people over the age of 50 years.[1,16,17] Furthermore, men have a 20.4% higher risk of colorectal

cancer than women. This is related to various factors such as tobacco exposure, mutations of several tumor suppressor genes linked to sex chromosomes, and a lower immune response around the tumor.[18]

The TNM stage is a classification system that assesses tumor invasion, lymph node involvement, and distant metastasis related to prognosis and therapy options in colorectal cancer.[3,19] The five-year survival rate decreases with increasing stage, from 0.85 in Stage I to 0.30 in Stage IV.[20] Based on observation, most of the samples were T3 (64%), N0 (54%), and M0 (76%). Tsabit et al.[21] and Yao et al.[22] also showed that most tumors were T3. Patients with T3 tumors had a 1.29 times greater risk of death compared to T1.[22] Metastatic colorectal cancer is related to several gene mutations, such as KRAS, PIK3CA, BRAF, and ERBB2, which are associated with a poor prognosis.[23]

The expression of NF-κB in this study shows a positive correlation with N stage. This signified that NF-κB expression increases with increasing lymph node metastasis. The result is in line with studies conducted by Farhat et al.[24] in patients with nasopharyngeal carcinoma and Berkovich et al.[25] in colonic cancer. A relationship was observed between NF-κB overexpression and the occurrence of lymph node metastasis. NF-κB plays an important role in tumor cell invasion and migration by activating transcription factors in epithelial-mesenchymal transition (EMT), such as TWIST1 and SNAIL.[7,26] Furthermore, it can increase the degradation of the extracellular matrix by upregulating various types of degradation enzymes, including MMP-9.[7,8,26] The results of this study support the above theory by obtaining a positive correlation between NF-κB and MMP-9 expression, featuring a biological relationship and signaling pathway between the two molecules. The NF-κB and MMP-9 signaling pathways, which influence tumor progression and metastasis, are related to reactive oxygen species (ROS) as well as the PI3K and AKT pathways.[8,26]

Matrix metalloproteinase-9 expression in this study correlated with cancer progression. Its significant positive correlation with tumor depth, distant metastasis, and TNM stage emphasized the crucial role in both local invasion and metastatic spread. The results are consistent with previous studies showing a relationship between MMP-9 and various clinicopathological factors in colorectal cancer.[9,27] MMP-9 degrades gelatin and collagen, facilitating tumor cell passage through the basement membrane and extracellular matrix to other sites.[27,28] It can influence vascular endothelial growth factor (VEGF) in angiogenesis, thereby increasing the incidence of metastasis.[7,28] Tumor-infiltrating lymphocytes density showed significant inverse correlations with tumor depth, lymph node status, and TNM stage, suggesting a protective role for antitumor immune responses in colorectal cancer. The results are supported by several other studies that show significant relationships between TIL and depth of invasion, lymphovascular invasion, lymph node status, and grading.[12,13] The TIL components are mostly CD8+ T lymphocytes, which can destroy tumor cells.[11,29] This destruction is mediated by the secretion of perforin and granzyme and the production of various pro-inflammatory cytokines, such as tumor necrosis factor α (TNF-α) and interferon-γ (IFN-γ).[11] Additionally, a subset of lymphocytes, namely CD4+ T lymphocytes, enhances the immune response by activating B lymphocytes, T lymphocytes, and macrophages.[11,30]

Although NF-κB plays a crucial role in the inflammatory process, this study discovered no significant association with TIL density. The NF-κB-mediated antitumor immune response in cancer is a complex process that involves various factors in the tumor microenvironment (TME), including TILs, dendritic cells (DCs), macrophages, natural killer (NK) cells, and cytokines such as interleukin-6 (IL-6) and TNF-α.[7,26,31] The nuclear factor can indirectly influence TIL by activating DCs, which act as antigen-presenting cells (APCs), presenting tumor antigens to CD8+ T lymphocytes.[31] Additionally, activation of B and T lymphocytes by NF-κB is influenced by activation of surface immune receptors such as the B-cell receptor (BCR) and T-cell receptor (TCR).[7,31]

In conclusion, this study showed that tumor-promoting signaling pathways were mediated by NF-κB and MMP-9, and protective immune responses were reflected in TIL density. The opposing correlations of MMP-9 expression and TIL density with TNM stage supported the concept that colorectal cancer progression is determined by the dynamic interaction between molecular drivers of invasion and the host immune response. This integrated analysis provided a more comprehensive understanding of tumor behavior than the assessment of individual biomarkers.

Ethics Statement

All procedures of this study were approved by the Health Research Ethics Committee of Dr. Soedarso General Hospital (No. 96/RSUD/KEPK/XI/2024).

Author Contributions

Heru Fajar Trianto: Investigation, Data curation, Formal analysis, Literature search, Writing – original draft.
Gondo Mastutik: Supervision, Methodology, Validation, Writing – review & editing.
Desak Gede Agung Suprabawati: Supervision, Methodology, Writing – review & editing.
Mitra Handini: Visualization, Software, Writing – original draft.
Mahyarudin Mahyarudin: Investigation, Data curation, Literature search.
All authors have read and approved the final manuscript and agree to be accountable for all aspects of the work.

Conflicts of Interest

The authors have declared no conflict of interest.

Acknowledgments

The author is grateful to all staff of the Anatomical Pathology Laboratory at Dr. Soedarso General Hospital for granting permission to collect data.

References

1. Roshandel G, Ghasemi-Kebria F, Malekzadeh R. Colorectal Cancer: Epidemiology, Risk Factors, and Prevention. Cancers (Basel). 2024 Apr 17;16(8):1530. doi: 10.3390/cancers16081530. PMID: 38672612; PMCID: PMC11049480.
2. Weiser MR. AJCC 8th Edition: Colorectal Cancer. Ann Surg Oncol. 2018 Jun;25(6):1454-1455. doi: 10.1245/s10434-018-6462-1. Epub 2018 Apr 3. PMID: 29616422.
3. Fleming M, Ravula S, Tatishchev SF, Wang HL. Colorectal carcinoma: Pathologic aspects. J Gastrointest Oncol. 2012 Sep;3(3):153-73. doi: 10.3978/j.issn.2078-6891.2012.030. PMID: 22943008; PMCID: PMC3418538.
4. Coebergh van den Braak RRJ, Ten Hoorn S, Sieuwerts AM, Tuynman JB, Smid M, Wilting SM, et al. Interconnectivity between molecular subtypes and tumor stage in colorectal cancer. BMC Cancer. 2020 Sep 4;20(1):850. doi: 10.1186/s12885-020-07316-z. PMID: 32887573; PMCID: PMC7473811.
5. Sadati S, Khalaji A, Bonyad A, Khoshdooz S, Hosseini Kolbadi KS, Bahrami A, et al. NF-κB and apoptosis: colorectal cancer progression and novel strategies for treatment. Eur J Med Res. 2025 Jul 14;30(1):616. doi: 10.1186/s40001-025-02734-w. PMID: 40660346; PMCID: PMC12261797.
6. Lukas K, Nguyen J, Necas C, Dave K, Venketaraman V. Targeting the NF-κB Pathway in Cancer: Mechanisms, Resistance, and Therapeutic Potential Across Tumor Types. Pharmaceuticals (Basel). 2025 Nov 20;18(11):1764. doi: 10.3390/ph18111764. PMID: 41305005; PMCID: PMC12655786.
7. Mao H, Zhao X, Sun SC. NF-κB in inflammation and cancer. Cell Mol Immunol. 2025 Aug;22(8):811-839. doi: 10.1038/s41423-025-01310-w. Epub 2025 Jun 25. PMID: 40562870; PMCID: PMC12310982.
8. Veljkovic A, Stanojevic G, Brankovic B, Roumeliotis S, Leivaditis K, Djordjevic B, et al. MMP-9 Activation via ROS/NF-κB Signaling in Colorectal Cancer Progression: Molecular Insights and Prognostic-Therapeutic Perspectives. Curr Issues Mol Biol. 2025 Jul 17;47(7):557. doi: 10.3390/cimb47070557. PMID: 40729026; PMCID: PMC12293130.
9. Mudatsir, Labeda I, Uwuratuw JA, Hendarto J, Warsinggih, Lusikooy RE, et al. Relationship between metalloproteinase-9 (MMP-9) expression and clinicopathology in colorectal cancer: a cross-sectional study. Ann Med Surg (Lond). 2023 Jul 25;85(9):4277-4282. doi: 10.1097/MS9.0000000000000892. PMID: 37663709; PMCID: PMC10473300.
10. Antonangeli F, Natalini A, Garassino MC, Sica A, Santoni A, Di Rosa F. Regulation of PD-L1 Expression by NF-κB in Cancer. Front Immunol. 2020 Nov 25;11:584626. doi: 10.3389/fimmu.2020.584626. PMID: 33324403; PMCID: PMC7724774.
11. Bai Z, Zhou Y, Ye Z, Xiong J, Lan H, Wang F. Tumor-Infiltrating Lymphocytes in Colorectal Cancer: The Fundamental Indication and Application on Immunotherapy. Front Immunol. 2022 Jan 14;12:808964. doi: 10.3389/fimmu.2021.808964. PMID: 35095898; PMCID: PMC8795622.
12. Iseki Y, Shibutani M, Maeda K, Nagahara H, Fukuoka T, Matsutani S, Kashiwagi S, Tanaka H, Hirakawa K, Ohira M. A new method for evaluating tumor-infiltrating lymphocytes (TILs) in colorectal cancer using hematoxylin and eosin (H-E)-stained tumor sections. PLoS One. 2018 Apr 26;13(4):e0192744. doi: 10.1371/journal.pone.0192744. PMID: 29698402; PMCID: PMC5919485.
13. Karki S, Pariyar S. Tumor-infiltrating lymphocytes in colorectal carcinoma. J Pathol Nepal. 2021;11(2):1859–63. doi: 10.3126/jpn.v11i2.38227.
14. Salgado R, Denkert C, Demaria S, Sirtaine N, Klauschen F, Pruneri G, et al.; International TILs Working Group 2014. The evaluation of tumor-infiltrating lymphocytes (TILs) in breast cancer: recommendations by an International TILs Working Group 2014. Ann Oncol. 2015 Feb;26(2):259-71. doi: 10.1093/annonc/mdu450. Epub 2014 Sep 11. PMID: 25214542; PMCID: PMC6267863.
15. Soraya F, Sandhika W, Wiratama PA. 8-OHdG and Nrf2 Protein are Expressed Consistently in Various T Stages of Invasive Breast Carcinoma. Asian Pac J Cancer Prev. 2025 Jan 1;26(1):301-307. doi: 10.31557/APJCP.2025.26.1.301. PMID: 39874013; PMCID: PMC12082425.
16. Nguyen LH, Goel A, Chung DC. Pathways of Colorectal Carcinogenesis. Gastroenterology. 2020 Jan;158(2):291-302. doi: 10.1053/j.gastro.2019.08.059. Epub 2019 Oct 14. PMID: 31622622; PMCID: PMC6981255.
17. Malki A, ElRuz RA, Gupta I, Allouch A, Vranic S, Al Moustafa AE. Molecular Mechanisms of Colon Cancer Progression and Metastasis: Recent Insights and Advancements. Int J Mol Sci. 2020 Dec 24;22(1):130. doi: 10.3390/ijms22010130. PMID: 33374459; PMCID: PMC7794761.
18. Tsokkou S, Konstantinidis I, Papakonstantinou M, Chatzikomnitsa P, Liampou E, Toutziari E, et al. Sex Differences in Colorectal Cancer: Epidemiology, Risk Factors, and Clinical Outcomes. J Clin Med. 2025 Aug 6;14(15):5539. doi: 10.3390/jcm14155539. PMID: 40807160; PMCID: PMC12347225.
19. Chen K, Collins G, Wang H, Toh JWT. Pathological Features and Prognostication in Colorectal Cancer. Curr Oncol. 2021 Dec 13;28(6):5356-5383. doi: 10.3390/curroncol28060447. PMID: 34940086; PMCID: PMC8700531.
20. Wang R, Lian J, Wang X, Pang X, Xu B, Tang S, et al. Survival rate of colorectal cancer in China: A systematic review and meta-analysis. Front Oncol. 2023 Mar 3;13:1033154. doi: 10.3389/fonc.2023.1033154. PMID: 36937415; PMCID: PMC10020492.
21. Tsabit SS, Trianto HF, Pratiwi SE, Hartono H. Clinicopathological Profile of Colorectal Adenocarcinoma in the Anatomical Pathology Laboratory of Dr . Soedarso Hospital Pontianak. Indones J Cancer. 2023;17 (4):292–8. doi: https://doi.org/10.33371/ijoc.v17i4.1004.
22. Yao N, Li W, Wang J, Chu H, Duan N, Niu X, et al. Prognostic implications of T stage in different pathological types of colorectal cancer: an observational study using SEER population-based data. BMJ Open. 2024 Feb 29;14(2):e076579. doi: 10.1136/bmjopen-2023-076579. PMID: 38423773; PMCID: PMC10910631.
23. Testa U, Castelli G, Pelosi E. Genetic Alterations of Metastatic Colorectal Cancer. Biomedicines. 2020 Oct

13;8(10):414. doi: 10.3390/biomedicines8100414. PMID: 33066148; PMCID: PMC7601984.
24. Farhat F, Daulay ER, Chrestella J, Williamson O, Syari RP. Expressions of Nuclear Factor-kappa B and Peroxisome Proliferator-activated Receptor-Gamma Proportional with Clinical Staging of Nasopharyngeal Carcinoma. Open Access Maced J Med Sci. 2021;9(B):1347–51. doi: 10.3889/oamjms.2021.6261.
25. Berkovich L, Gerber M, Katzav A, Kidron D, Avital S. NF-kappa B expression in resected specimen of colonic cancer is higher compared to its expression in inflammatory bowel diseases and polyps. Sci Rep. 2022 Oct 5;12(1):16645. doi: 10.1038/s41598-022-21078-7.
26. Bahrami A, Khalaji A, Bahri Najafi M, Sadati S, Raisi A, Abolhassani A, et al. NF-κB pathway and angiogenesis: insights into colorectal cancer development and therapeutic targets. Eur J Med Res. 2024 Dec 19;29(1):610. doi: 10.1186/s40001-024-02168-w. PMID: 39702532; PMCID: PMC11658081.
27. Ghadyani R, Mozooni Z, Sohbatzadeh Z, Gachkar L, Sepehr Kahrizi, Movafagh A. Expression patterns and clinical significance of MMP-8, MMP-9 and MMP-13 in colorectal cancer. Cell Mol Biol (Noisy-le-grand). 2025 Oct 7;71(9):111-116. doi: 10.14715/cmb/2025.71.9.14. PMID: 41054365.
28. Shoari A, Ashja Ardalan A, Dimesa AM, Coban MA. Targeting Invasion: The Role of MMP-2 and MMP-9 Inhibition in Colorectal Cancer Therapy. Biomolecules. 2024 Dec 30;15(1):35. doi: 10.3390/biom15010035. PMID: 39858430; PMCID: PMC11762759.
29. Matsutani S, Shibutani M, Maeda K, Nagahara H, Fukuoka T, Iseki Y, et al. Tumor-infiltrating Immune Cells in H&E-stained Sections of Colorectal Cancer Tissue as a Reasonable Immunological Biomarker. Anticancer Res. 2018 Dec;38(12):6721-6727. doi: 10.21873/anticanres.13041. PMID: 30504382.
30. Kraja FP, Jurisic VB, Hromić-Jahjefendić A, Rossopoulou N, Katsila T, Mirjacic Martinovic K, et al. Tumor-infiltrating lymphocytes in cancer immunotherapy: from chemotactic recruitment to translational modeling. Front Immunol. 2025 May 22;16:1601773. doi: 10.3389/fimmu.2025.1601773. PMID: 40475782; PMCID: PMC12137109.
31. Lalle G, Twardowski J, Grinberg-Bleyer Y. NF-κB in Cancer Immunity: Friend or Foe? Cells. 2021 Feb 9;10(2):355. doi: 10.3390/cells10020355. PMID: 33572260; PMCID: PMC7914614.

***Corresponding author**: Prof. Gondo Mastutik, PhD. E-mail: gondomastutik@fk.unair.ac.id*

International Journal of Biomedicine 16(2) (2026) 169-177
http://dx.doi.org/10.21103/Article16(2)_OA3

ORIGINAL ARTICLE

INTERNATIONAL JOURNAL OF BIOMEDICINE

Relapse-Free Survival and Prognostic Factors in Gastric Cancer Patients in Albania: A Prospective Longitudinal Observational Cohort Study

Bledi Kreka[1], Ervin Toçi[2], Arvit Llazani[1], Drini Shehi[1], Albana Shahini[3], Dorina Canaku[4], Enkelejda Cuedari[1], Fatjona Kraja[1,2], Alba Agaraj[1], Martiola Kola[2], Dea Kreka[2], Meri Vasha[2], Arvin Dibra[1,2*], Manika Face[1,2*]

[1]*University Hospital Cener "Mother Teresa", Tirana, Albania*
[2]*Faculty of Medicine, University of Medicine, Tirana, Albania*
[3]*Faculty of Medical Technical Sciences, University of Medicine, Tirana, Albania*
[4]*Institute of Public Health, Tirana, Albania*

Abstract

Background: In Eastern Europe, where late cancer diagnoses are frequent and survival rates are low, gastric cancer continues to be a leading cause of cancer-related death. The data on relapse-free survival (RFS) and the factors that influence it in Albania are scarce.

Methods and Results: A total of 221 adult patients with histologically confirmed gastric cancer at the Oncology Service at the University Hospital Center "Mother Teresa" participated in this 60-month follow-up prospective longitudinal observational study. The Kaplan-Meier method was used to estimate relapse-free survival, and multivariate Cox proportional hazards regression was used to evaluate prognostic factors.

Relapses occurred in 37.1% of patients during follow-up. The median relapse-free survival was 28.0 months (95% CI: 25.04–30.96). When compared to diffuse gastric cancer, the intestinal type was independently linked to a lower risk of relapse (HR = 0.32; 95% CI: 0.19–0.53). Relapse risk was strongly correlated with increasing lymph node involvement (N1: HR = 5.31; N2: HR = 6.53; N3: HR = 9.59). Age, radiotherapy, adjuvant therapy, and tumor depth did not independently correlate with RFS. A higher risk of relapse was linked to a positive family history of gastric cancer (HR = 10.87).

Conclusion: The histopathological subtype and lymph node status at diagnosis were the main factors influencing relapse-free survival in this group of gastric cancer patients in Albania. These findings highlight the importance of early detection, accurate staging, and follow-up strategies adapted to the risk level in gastric cancer care.(**International Journal of Biomedicine. 2026;16(2):169-177.**)

Keywords: Albania • cohort study • gastric cancer • prognostic factors • relapse-free survival

For citation: Kreka B, Toçi E, Llazani A, Shehi D, Shahini A, Canaku D, Cuedari E, Kraja F, Agaraj A, Kola M, Kreka D, Vasha M, Dibra A, Face M. Relapse-Free Survival and Prognostic Factors in Gastric Cancer Patients in Albania: A Prospective Longitudinal Observational Cohort Study. International Journal of Biomedicine. 2026;16(2):169-177. doi:10.21103/Article16(2)_OA3

Introduction

Gastric cancer is one of the most frequent causes of cancer morbidity and mortality. In several high-income countries, the incidence of this health condition is gradually declining. However, in most parts of Eastern Europe, Asia, and Latin America, the burden of gastric cancer remains high.[1] Currently, gastric cancer is responsible for over a million new cancer cases and is one of the most frequent causes of cancer-related mortality.[1] It is also important to note that most patients are diagnosed at a late stage, and the survival outcomes are dismal. In this context, there is no doubt that gastric cancer is a global health concern, deserving increased attention.

The variability of gastric cancer prognosis is one of the most complicated problems in this field. Each specific case of gastric cancer prognosis is the result of a tumor-specific, patient-

specific, and treatment-specific set of parameters. The extent of tumor infiltration and the presence of lymphatic spread at the time of diagnosis are the most important survival determinants and those that most consistently impact prognostic outcomes.[2,3]

Additionally, there are also different histopathological subtypes of gastric cancer. A commonly used histopathological classification of gastric cancer is the Lauren classification. Based on this classification, there are 2 groups: the intestinal and diffuse types. The diffuse type is the one that usually results in a more negative gastric cancer prognosis, as it is characterized by poorer outcomes and more advanced tumor aggressiveness.[4,5] Still, how each of these factors affects cancer progression likely varies across populations, health care environments, and treatment strategies.

The relapse of the disease after intentional clinical treatment continues to be a critical inflection point in the disease's trajectory and is closely correlated to long-term survival. For this reason, the oncology community has recognized relapse-free survival (RFS) as a critically important indicator for assessing outcomes in both clinical trials and observational studies; this clinical endpoint reflects both the malignancy's characteristics and the efficacy (or lack thereof) of the surgical and adjuvant interventions performed.[6] Most studies published in the international literature in this field suggest that the greatest risk of relapse seems to be within the first two to three years after diagnosis or surgical intervention, highlighting the need for careful monitoring of these patients and the prompt diagnosis of patients within the highest risk categories.[7] There is a relative scarcity of evidence from real-world cohorts in Southeastern and Eastern Europe, as most relevant literature stems from large international studies on relapse-free survival and its prognostic factors conducted in developed countries. Data from Albania is particularly troubling, as gastric cancer is still being diagnosed at very advanced stages. Despite this, it seems that there is still a considerable lack of scientific systematic analyses of survival outcomes and prognostic determinants of gastric cancer in Albania. Local scientific data is necessary, as it is likely that diagnostic and treatment pathways, including access to neoadjuvant and adjuvant therapies, diagnostic and follow-up strategies, as well as differing patient control parameters, may significantly impact the clinical outcomes and limit the applicability potential of various findings and/or interventions from other settings.[8,9]

Relapse patterns and predictors of relapse-free survival in Albanian patients with gastric cancer bear clinical and public health significance. Such knowledge can improve risk stratification and assist in the development of tailored follow-up plans and cancer care enhancements at the national level. In this context, the objective of the present study was to assess relapse-free survival rates in a cohort of patients with gastric cancer in Albania and to identify independent prognostic factors for disease recurrence within 60 months (5 years) of diagnosis

Methods

Study Design

This is a prospective, longitudinal, observational cohort study conducted among patients diagnosed with gastric cancer and managed at the Oncology Service at the University Hospital Center "Mother Teresa" (UHCT) in Tirana, Albania. Participating gastric cancer patients were followed from the time of diagnosis and/or initiation of treatment and were observed longitudinally for the occurrence of disease relapse for a maximum follow-up period of 60 months.

Study Setting

UHCT "Mother Teresa" is Albania's largest tertiary referral hospital and the only public reference center for cancer diagnosis and treatment. The Oncology Service at UHCT delivers care to cancer patients from all regions of the country, providing multidisciplinary cancer care that includes medical oncology, surgical oncology, and radiotherapy, as well as imaging and pathology services. Hence, the study participants represent the standard clinical routine nationwide.

Study Population

The study population for this study was adult patients with a confirmed diagnosis of gastric cancer who were treated and/or followed at the Oncology Service of UHCT during the study period.

The inclusion criteria were as follows: histologically confirmed gastric cancer, age ≥18 years, cancer diagnosis and/or treatment initiated at UHCT "Mother Teresa", availability of baseline clinicopathological data, and at least one follow-up evaluation after diagnosis.

Exclusion criteria were patients with incomplete diagnostic confirmation, patients who were lost to follow-up immediately after diagnosis, patients who declined to participate, or patients who did not provide informed consent.

The inclusion criteria were met by 221 gastric cancer patients, and they were therefore included in the study.

Data Collection, Data Sources, and Variables

A structured data-collection form developed specifically for this project was used to collect the necessary information from participants. Various information sources were used, including medical records, oncology and surgery reports, pathology and histopathology reports, imaging records, and follow-up visits and outpatient oncology notes.

The following categories of variables were collected and analyzed: demographic and clinical variables (age at diagnosis, sex); family history of gastric cancer; tumor-related variables such as histopathological type; status of presence of signet-ring cells; TNM tumor stage at diagnosis; treatment-related variables, including neoadjuvant therapy, adjuvant therapy, radiotherapy, surgery, etc., and outcome-related variables such as relapse status. Relapses were defined based on clinical, radiological, and/or histological evidence of disease recurrence. When a relapse was first detected, we noted down the date of this event. This allowed us to calculate the time to relapse (defined as the interval of time between diagnosis and the first documented recurrence of the disease). Obviously, patients without documented relapses were censored at the date of last follow-up.

Follow-Up Period

Patients were followed under routine clinical practice at UHCT. During this time, periodic clinical evaluations, imaging studies, and laboratory assessments were performed as needed. Follow-up duration ranged from 7 to 60 months.

Statistical Analysis

All statistical analyses were carried out using IBM SPSS Statistics (version 21). Baseline characteristics were summarized as frequencies and percentages for categorical variables and mean ± standard deviation (SD) and additional statistical parameters for continuous variables. The Kaplan-Meier method was used to estimate relapse-free survival, and survival curves were constructed using the log-rank (Mantel-Cox) test. The median RFS was considered the most robust survival measure, as it is unaffected by censored observations. A univariate Cox proportional hazards regression test was used to identify independent predictors of RFS; those achieving clinical relevance were entered into a multivariate Cox proportional hazards regression model to adjust for potential confounding factors. Hazard ratios (HRs) and their respective 95% confidence intervals (CIs) were reported. The adequacy and goodness-of-fit of the multivariate model were assessed as well, through omnibus tests and likelihood-based statistics. A 2-sided *P*-value of less than 0.05 was considered statistically significant.

Results

Table 1 shows the information on various characteristics of the 221 patients included in the study. The dominant sex was male (71.5%), and the mean age of participants was 64.0 ± 9.9 years. More than 7 in 10 patients (78.7%) were aged 50–74 years, while patients younger than 50 years accounted for a relatively small proportion of cases.

Family history of gastric cancer was reported in only 3.7% of participating patients. From a histopathological perspective, diffuse and intestinal types were almost equally represented, together accounting for more than 95% of patients, while indeterminate histology was rare. Signet-ring cell features were identified in fewer than 1 in 10 patients.

At diagnosis, more than 85% of patients presented with locally advanced tumors (T3–T4), and nearly four out of five showed regional lymph node involvement (N1–N3). Distant metastases were present in approximately 20% of cases. Regarding treatment, neoadjuvant therapy was rarely administered, despite the advanced stage at presentation, whereas adjuvant therapy was given to about two-thirds of patients. Radiotherapy was used in a minority of cases (14.5%).

Table 2 presents information on relapse and the timing of events during the follow-up period. In 37.1% of patients, a relapse occurred, while the remaining 62.9% remained relapse-free until the end of follow-up. Among those patients who experienced a relapse, the mean time to relapse was approximately 19 months, with a median relapse-free survival of 16 months. Relapse time distribution showed substantial variability, with events occurring as early as 7 months and as late as 45 months in this cohort of patients. The follow-up period was slightly longer than the observed time to relapse, with a mean duration of about 22 months and a median duration of 19 months. Follow-up ranged from 7 to 60 months.

Table 3 summarizes the overall estimates of relapse-free survival for the study cohort, calculated using the Kaplan-Meier method. The mean time to relapse-free survival was 32.78 months (95% CI: 29.15–36.42), reflecting the average duration patients remained free of recurrence during the follow-up. In clinical terms, the median relapse-free survival was 28.0 months (95% confidence interval: 25.04–30.96). Half of the patients experienced relapse within approximately 28 months, while the remaining half remained relapse-free for a longer period of time. Because it is resistant to censoring and has a clear clinical interpretation, the median relapse-free survival is the most reliable summary measure of the outcome in this cohort.

Table 1.

Baseline demographic, clinicopathological, and treatment characteristics of the study population.

Variable	Absolute number	Percentage
Total	221	100.0
Sex		
Male	158	71.5
Female	63	28.5
Age (mean ± SD)	64.04 ± 9.92	
Age group		
<50 years	18	8.1
50-64 years	92	41.6
65-74 years	82	37.1
≥75 years	29	13.1
Family history for gastric cancer*		
No	210	96.3
Yes	8	3.7
Histopathological type of cancer*		
Diffuse	107	49.1
Intestinal	104	47.7
Indeterminate	7	3.2
Status of signet cell presence		
No	200	91.3
Yes	19	8.7
T stage*		
T0	1	0.5
T1	5	2.7
T2	20	10.9
T3	110	59.8
T4	48	26.1
N stage*		
N0	39	21.3
N1	41	22.4
N2	54	29.5
N3	49	26.8
M stage*		
M0	173	80.1
M1	43	19.9
Neoadjuvant therapy*		
No	213	96.8
Yes	7	3.2
Adjuvant therapy*		
No	67	30.5
Yes	153	69.5
Radiotherapy*		
No	189	85.5
Yes	32	14.5

* *Any discrepancy with the total number is due to missing information.*

Table 2.

Relapse status and relapse-free survival outcomes.

Variable	Absolute number	Percentage
Relapse		
No	139	62.9
Yes	82	37.1
Statistical parameter	Relapse-free survival (in months)	Follow-up period (months)
Mean	19.05	21.56
Median	16.00	19.00
Moda	9	14
Standard deviation	9.17	10.23
Range	38	53
Minimum	7	7
Maximum	45	60

Table 3.

Mean and median relapse-free survival in the study population.

RFS mean time			
Time (months)	Standard error	95% CI	
		Lower limit	Upper limit
32.78	1.85	29.15	36.42
RFS median time			
Time (months)	Standard error	95% CI	
		Lower limit	Upper limit
28.00	1.51	25.04	30.96

Figure 1 shows the Kaplan–Meier curve of relapse-free survival, showing a more pronounced decline in survival during the first years of follow-up, a slowdown in the decline after about 30 months, and a relatively horizontal final segment, indicating a subgroup of patients with longer relapse-free survival. This means that the risk of relapse is highest in the first 2-3 years of follow-up, while patients who survive these periods have a lower chance of later relapse. Censored cases (the + signs) are reasonably distributed, implying there is no massive early censoring, an indication of adequate follow-up, and the absence of serious bias in follow-up.

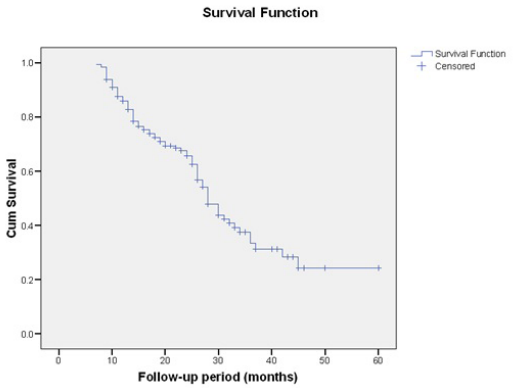

Figure 1. *Relapse-free survival.*

Relapse-Free Survival Analysis by Histopathological Type of Gastric Cancer

Relapse-free survival was analyzed using the Kaplan–Meier method to assess whether the histopathological type of gastric cancer affects RFS (Table 4). The analysis data show that the RFS median differs significantly between groups. In patients with intestinal type – 31 months (95% CI: 26.149 – 35.851); in those with diffuse type –18 months, and in those with indeterminate type – 11 months (95% CI: 8.434 – 13.566). The intestinal type was associated with the longest RFS, while the indeterminate type was associated with the shortest survival. On the other hand, the mean survival follows the same trend, but this indicator has a secondary role due to censoring (Table 4). The respective p-value from the Log Rank (Mantel-Cox) test = 0.001 (chi-square = 13.914, df = 2) indicates a statistically significant difference in relapse-free survival between histopathological types of gastric cancer.

Table 4.

RFS according to histopathological type of gastric cancer.

Variable	RFS mean time				RFS median time			
Type of cancer	Time*	SE	95% CI		Time*	SE	95% CI	
			Lower limit	Upper limit			Lower limit	Upper limit
Diffuse	30.081	2.111	25.944	34.218	18.000	-	-	+
Intestinal	36.183	2.166	31.937	40.429	31.000	2.475	26.149	35.851
Indeterminate	23.143	5.850	11.677	34.609	11.000	1.309	8.434	13.566

*SE- Standard Error; * - Time in months.*

This is confirmed by the RFS curves shown in Figure 2. The intestinal type curve remains higher during the first 2-3 years of follow-up, suggesting a better prognosis. The diffuse type presents a more rapid decline in survival in the early stages. The indeterminate type shows the fastest decline and the poorest relapse-free survival.

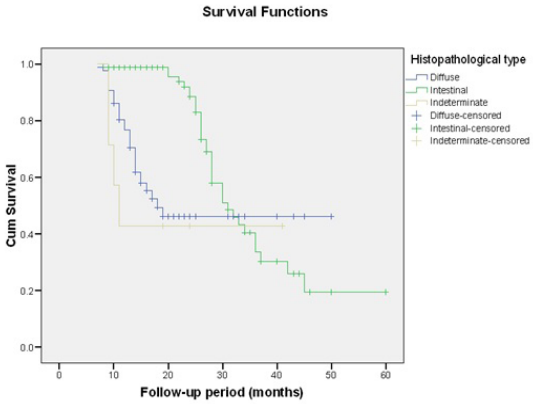

Figure 2. *Relapse-free survival by histopathological type of gastric cancer*

Relapse-Free Survival Analysis by the Nodal (N) Stage of Gastric Cancer

According to Table 5, the RFS median shows a clear downward trend with increasing level of N stage. In patients with N1 stage – 28 months (95% CI: 26.350–29.650); in patients with N2 stage – 26 months (95% CI: 17.543–34.457); in patients with N3 stage – 25 months (95% CI: 18.404–31.596). These differences were highly statistically significant (chi-square = 16.672, df = 3; Log Rank (Mantel-Cox) test $P = 0.001$). For patients with stage N0, the median was not reported, suggesting a low relapse rate or high censoring, reflecting a more favorable prognosis. On the other hand, the mean survival is highest in N0 and decreases progressively in N1–N3, supporting the prognostic importance of lymph node involvement (Table 5). On the other hand, the mean survival is highest in N0 and decreases progressively in N1–N3, supporting the prognostic importance of lymph node involvement (Table 5).

Table 5.

Relapse-free survival according to the N stage of gastric cancer.

Variable	RFS mean time				RFS median time			
N stage	Time*	SE	95% CI		Time*	SE	95% CI	
			Lower limit	Upper limit			Lower limit	Upper limit
N0	43.561	2.924	37.831	49.292	.	.	.	.
N1	27.763	1.955	23.932	31.594	28.000	.842	26.350	29.650
N2	26.875	2.988	21.020	32.731	26.000	4.315	17.543	34.457
N3	26.819	2.236	22.437	31.201	25.000	3.365	18.404	31.596

*SE - Standard Error; *- Time in months.*

This is confirmed by the RFS curves for N stages of gastric cancer (Figure 3). The N0 stage shows the highest RFS throughout the entire follow-up period. With increasing stage N (from N1 to N3), a more rapid decline in survival and an increasingly lower probability of remaining relapse-free are observed.

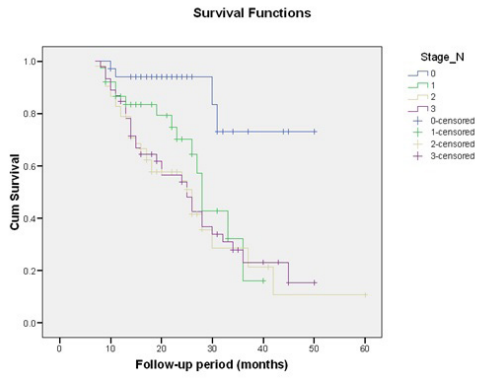

Figure 3. *Relapse-free survival by N stages of gastric cancer.*

Multivariate Analyses of Relapse-Free Survival (Cox Proportional Model)

The overall performance and adequacy of the multivariate Cox proportional hazards model used to analyze RFS were assessed. The model demonstrated a good fit to the data, as indicated by a statistically significant omnibus test ($P < 0.001$). The substantial improvement in model likelihood (coefficient –2 Log Likelihood = 641.319; chi square = 42.140, df = 12, $P < 0.001$) compared with the baseline model (change in chi square = 51.702, $P < 0.001$) without covariates confirmed that the set of variables included meaningfully explains variation in the risk of relapse. These results supported the appropriateness of the model for identifying independent prognostic factors associated with relapse-free survival.

Table 6 presents the results of the multivariate Cox regression analysis, identifying independent predictors of relapse-free survival after adjustment for potential confounders. Histopathological type emerged as a strong prognostic factor. Compared with diffuse-type tumors, intestinal-type gastric cancer was associated with a significantly lower risk of relapse (HR = 0.32), indicating a more favorable prognosis, while indeterminate histology did not show an independent effect.

Table 6.

Multivariate Cox Proportional Hazards analysis of factors associated with relapse-free survival.

Variable	B	SE	Wald	df	*P*-value	HR	95.0% CI for HR	
							Lower limit	Upper limit
Histopathological type (overall)			19.627	2	0.000			
Intestinal type	-1.156	0.264	19.201	1	0.000	0.315	0.188	0.528
Indeterminate type	-0.213	0.557	0.146	1	0.702	0.808	0.271	2.409
N stage (overall)			15.387	3	0.002			
N1 stage	1.670	0.589	8.046	1	0.005	5.310	1.675	16.833
N2 stage	1.876	0.557	11.362	1	0.001	6.528	2.193	19.431
N3 stage	2.260	0.583	15.024	1	0.000	9.587	3.057	30.067
T stage (overall)			4.494	3	0.213			
T1 stage	0.135	1.049	0.017	1	0.898	1.144	0.146	8.947
T2 stage	-1.643	0.780	4.442	1	0.035	0.193	0.042	0.891
T3 stage	-0.137	0.272	0.256	1	0.613	0.872	0.512	1.485
AT, Yes	-0.145	0.405	0.129	1	0.719	0.865	0.391	1.911
Radiotherapy, Yes	-0.534	0.361	2.180	1	0.140	0.586	0.289	1.191
Age (numeric)	0.010	0.011	0.764	1	0.382	1.010	0.988	1.032
Family history, Yes	2.386	1.041	5.254	1	0.022	10.872	1.413	83.644

AT - Adjuvant Therapy; SE - Standard Error.

Regional lymph node involvement was the most powerful predictor of relapse. Compared with node-negative disease (N0), progressively higher N stages were associated with a marked and stepwise increase in relapse risk, with hazard ratios rising from N1 to N3, reflecting a clear biological gradient.

Tumor depth (T stage) was not significant overall; however, patients with T2 tumors had a significantly lower risk of relapse compared with those with T4 disease, even after multivariable adjustment. Adjuvant therapy, radiotherapy, and patient age were not independently associated with relapse-free survival in this model. Notably, a positive family history of gastric cancer was associated with a substantially higher risk of relapse, although the wide confidence interval suggests limited precision and warrants cautious interpretation.

Discussion

This prospective cohort study is one of the first attempts to scientifically assess the relapse-free survival among a group of cancer patients in Albania and the factors associated with it. The findings suggest that the gastric cancer population in Albania is characterized by advanced disease at the time of diagnosis, heterogeneous relapse patterns, and a survival course that seems to be largely impacted by tumor histopathology rather than treatment modalities. These results provide a very interesting, clinically relevant insight into the course of gastric cancer patients at a national tertiary referral center.

A major finding was the relatively high proportion of patients experiencing relapse during the follow-up period (37.1%), with a median RFS of 28 months. The median time to relapse reported in this study is in accordance with the international research suggesting that the period with the highest risk of cancer relapse is within the first two to three years following the diagnosis or treatment.[6,7,10] The Kaplan–Meier curve in our gastric cancer cohort showed a steeper decline at the start of follow-up, followed by a plateau, suggesting that patients who do not relapse after this point may have a more favorable profile, including histopathological tumor type or treatment response. These findings are similar to those observed in various randomized controlled trials or large observational studies,[2,11] further highlighting the clinical importance of careful surveillance of these patients right after treatment.

The findings of this study reported the histopathological type of gastric cancer to be a strong and independent prognostic factor for the relapse-free survival of these patients. The intestinal type of gastric cancer was associated with significantly longer relapse-free survival compared to the diffuse type of cancer, in both univariate and multivariate analysis. This finding is in accordance with reports from international literature.[12] More specifically, the international literature has consolidated the fact that biological distinctions between Lauren subtypes of gastric cancers are key determinants of RFS among affected patients,[13] with the intestinal type being associated more frequently with glandular differentiation, predominantly localized growth models and better response to treatment modalities, in contrast with the diffuse type which often exhibit more spread or infiltrative growth patterns, early dissemination[4,5,14] and are more resistant to treatment schemes.[15,16] On the other hand, the worst median RFS observed among patients with an indeterminate type of gastric cancer needs to be carefully considered, given the small number of patients with this type of gastric cancer available for analysis; however, this could be an indication that this histopathological type could be associated with more aggressive tumor dynamics and/or diagnostic uncertainty at baseline.[17]

The spreading of the tumor and the involvement of regional lymph nodes emerged as one of the strongest predictors of RFS in the actual study, as shown by the strong and positive association of Hazard Ratios with the N stage of gastric cancer: the more advanced the cancer (the higher the N stage), the higher the HRs (Table 6). This modality and gradient of the association highlight the critical role of lymphatic involvement in the progression of gastric cancer.[18] The association between the N stage of gastric cancer and the RFS is in accordance with reports from international literature consistently reporting the level of lymph nodes infiltration as a major factor in the recurrence of disease and survival of patients.[19-21] The critical role of lymph node involvement in the prognosis of gastric cancer is also supported by the finding that patients with intact lymph nodes (stage N0) had a much more favorable RFS, with a considerable percentage remaining free of disease throughout the follow-up period. This once again highlights the importance of early detection of the lymph node involvement for the prognosis of gastric cancer.

On the other hand, the depth of the tumor, measured by the T stage of it, was, overall, not significantly associated with RFS in the multivariable adjusted model, even though patients with a T2 stage tumor showed a significantly lower risk of relapse compared to patients with a T4 stage gastric cancer. This pattern might suggest that lymph node status overrides the prognostic information provided by local tumor extension, meaning that the N stage, per se, is more informative than the T stage, potentially because of the strong correlation between tumor depth and nodal involvement, as reported in the international literature.[22-24]

It was interesting to note that, even after all the adjustments, variables such as adjuvant therapy and radiotherapy did not appear to be significantly associated with RFS. Even though this finding may seem counterintuitive, it could mean that patients who receive adjuvant treatment are more likely to have more serious illnesses. On the other hand, the low application of neoadjuvant therapy in this group of patients, despite the presence of advanced cancer in the overwhelming majority of patients, may have contributed to masking the treatment-related survival differences in this case. Finally, this observation highlights the very limited application of contemporary multimodal treatment strategies among gastric cancer patients in Albania and indicates a potential area for future improvement.[25,26]

With regard to family history, it is well established that it is a risk factor for developing gastric cancer, with odds ratios fluctuating between 2 and 10 among different studies and population groups.[27] However, we detected a significant association between family history of gastric cancer and the risk of relapse, an association that has not been much explored in the international arena. Amid the uncertainty of this association due to the small number of patients having this trait and wide confidence intervals in our case, the finding

however aligns well with some literature reports that have reported family history to be a risk factor associated with specific molecular characteristics that might influence cancer aggressiveness, poorer outcomes and less favorable response to treatment,[28,29] potentially negatively affecting their relapse-free survival. Obviously, there is a need for further research to better understand and explore the association between family history and risk of relapses among gastric cancer patients.

Looking from a broader angle, the results of our study point out the many difficulties and challenges that gastric cancer patients encounter in a health system where late diagnosis is often the norm. A relatively high proportion of patients we see in our oncology practice present with quite advanced cancer, both in the primary tumor size and how much it's spread to lymph nodes. This is a common finding in Eastern European countries.[30,31] This situation highlights the need to improve early detection strategies, better identify who is at higher risk, and ensure people reach the right doctors faster by reviewing and improving referral pathways and modalities.[32,33] The survival patterns observed in this study among a group of gastric cancer patients in Albania are comparable to those reported elsewhere, once again confirming the critical role of cancer biology in patient outcomes across settings.

This study has several limitations. For example, we observed patients recruited from a single medical center; such an approach may limit the study's ability to identify regional differences in healthcare delivery and narrow the scope for generalizing the results. However, the fact that cancer patients in UHCT come from all over the country might dilute these potential biases. On the other hand, we did not have access to information on tumor molecular characteristics or details of chemotherapy regimens, thus further limiting the potential of prognostic analysis.

Despite its weaknesses, this study has some strengths as well. These include a prospective observational design, a relatively long follow-up period, full standardization, and the inclusion of many background variables, such as sociodemographic and clinicopathological factors, which enhance the robustness of the survival analysis. In addition, we have used powerful statistical tests to assess relapse-free survival and the factors associated with it, and have adjusted for potential confounding effects of various variables. Lastly, this is among the few studies that explore relapse-free survival among gastric cancer patients in Albania and the factors associated with it.

Conclusion

This study demonstrated that the relapse-free survival among gastric cancer patients in Albania is mainly influenced by the histopathological type of the tumor and lymph node involvement at the time of diagnosis. These findings underscore the critical importance of early detection and staging of cancer, as well as the application of follow-up strategies tailored to the risk of relapse. In addition, the findings of this study could serve to inform field professionals, policymakers, and decision-makers to further improve the management of gastric cancer in Albania.

Ethical Considerations

The study was conducted in accordance with the principles of the WMA Declaration of Helsinki (1964, ed. 2013) and approved by the Ethics Committee of the University of Medicine, Tirana; Approval number: 2235/2 dated 08.30.2024. All potential candidates were fully informed about the study's aim and procedures. All participants granted their informed consent to participate in the study. We ensured patient data anonymization before analysis. Access to the database was restricted only to authorized members of the research team.

Disclaimer

The current study was conducted within the framework of an institutional research project aimed at establishing a structured hospital-based database for gastric cancer to evaluate real-world clinical outcomes and prognostic factors among Albanian patients.
Project Title: "Foundation of a University Clinic Database on Gastric Cancer—A Necessity for Ensuring Optimal Treatment in Light of New Therapeutic Protocols." Professor Arvin Dibra serves as the Project Coordinator (with a copy of the letter) and Principal Investigator.

Author Contributions

Bledi Kreka: Conceptualization, Methodology, Data analysis/interpretation, Writing – original draft.
Ervin Toçi: Conceptualization, Methodology, Data analysis/interpretation, Writing – review and editing.
Arvit Llazani: Investigation, Data curation.
Drini Shehi: Investigation, Data curation.
Albana Shahini: Investigation, Data curation
Dorina Canaku: Methodology, Data analysis/interpretation, Writing – original draft
Enkelejda Cuedari: Investigation, Data curation
Fatjona Kraja: Methodology, Data analysis/interpretation, Writing – original draft.
Alba Agaraj: Investigation, Data curation
Martiola Kola: Methodology, Data analysis/interpretation, Writing – original draft.
Dea Kreka: Investigation, Data curation.
Meri Vasha: Investigation, Data curation.
Arvin Dibra: Supervision, Conceptualization, Writing – review and editing.
Manika Face: Conceptualization, Methodology, Writing – review and editing.

All authors have approved the final manuscript.

Conflicts of Interest

The authors have declared no conflict of interest.

References

1. Sung H, Ferlay J, Siegel RL, Laversanne M, Soerjomataram I, Jemal A, Bray F. Global Cancer Statistics

2020: GLOBOCAN Estimates of Incidence and Mortality Worldwide for 36 Cancers in 185 Countries. CA Cancer J Clin. 2021 May;71(3):209-249. doi: 10.3322/caac.21660. Epub 2021 Feb 4. PMID: 33538338.
2. Smyth EC, Nilsson M, Grabsch HI, van Grieken NC, Lordick F. Gastric cancer. Lancet. 2020 Aug 29;396(10251):635-648. doi: 10.1016/S0140-6736(20)31288-5. PMID: 32861308.
3. Ajani JA, D'Amico TA, Almhanna K, Bentrem DJ, Chao J, Das P, Denlinger CS, Fanta P, Farjah F, Fuchs CS, Gerdes H, Gibson M, Glasgow RE, Hayman JA, Hochwald S, Hofstetter WL, Ilson DH, Jaroszewski D, Johung KL, Keswani RN, Kleinberg LR, Korn WM, Leong S, Linn C, Lockhart AC, Ly QP, Mulcahy MF, Orringer MB, Perry KA, Poultsides GA, Scott WJ, Strong VE, Washington MK, Weksler B, Willett CG, Wright CD, Zelman D, McMillian N, Sundar H. Gastric Cancer, Version 3.2016, NCCN Clinical Practice Guidelines in Oncology. J Natl Compr Canc Netw. 2016 Oct;14(10):1286-1312. doi: 10.6004/jnccn.2016.0137. PMID: 27697982.
4. Lauren P. The two histological main types of gastric carcinoma: diffuse and so-called intestinal-type carcinoma. An attempt at a histo-clinical classification. Acta Pathol Microbiol Scand. 1965;64:31-49. doi: 10.1111/apm.1965.64.1.31. PMID: 14320675.
5. Berlth F, Bollschweiler E, Drebber U, Hoelscher AH, Moenig S. Pathohistological classification systems in gastric cancer: diagnostic relevance and prognostic value. World J Gastroenterol. 2014 May 21;20(19):5679-84. doi: 10.3748/wjg.v20.i19.5679. PMID: 24914328; PMCID: PMC4024777.
6. Paoletti X, Oba K, Bang YJ, Bleiberg H, Boku N, Bouché O, Catalano P, Fuse N, Michiels S, Moehler M, Morita S, Ohashi Y, Ohtsu A, Roth A, Rougier P, Sakamoto J, Sargent D, Sasako M, Shitara K, Thuss-Patience P, Van Cutsem E, Burzykowski T, Buyse M; GASTRIC group. Progression-free survival as a surrogate for overall survival in advanced/recurrent gastric cancer trials: a meta-analysis. J Natl Cancer Inst. 2013 Nov 6;105(21):1667-70. doi: 10.1093/jnci/djt269. Epub 2013 Oct 9. PMID: 24108811; PMCID: PMC4994928.
7. Dikken JL, van de Velde CJ, Coit DG, Shah MA, Verheij M, Cats A. Treatment of resectable gastric cancer. Therap Adv Gastroenterol. 2012 Jan;5(1):49-69. doi: 10.1177/1756283X11410771. PMID: 22282708; PMCID: PMC3263979.
8. Torre LA, Bray F, Siegel RL, Ferlay J, Lortet-Tieulent J, Jemal A. Global cancer statistics, 2012. CA Cancer J Clin. 2015 Mar;65(2):87-108. doi: 10.3322/caac.21262. Epub 2015 Feb 4. PMID: 25651787.
9. Allemani C, Matsuda T, Di Carlo V, Harewood R, Matz M, Nikšić M, Bonaventure A, Valkov M, Johnson CJ, Estève J, Ogunbiyi OJ, Azevedo E Silva G, Chen WQ, Eser S, Engholm G, Stiller CA, Monnereau A, Woods RR, Visser O, Lim GH, Aitken J, Weir HK, Coleman MP; CONCORD Working Group. Global surveillance of trends in cancer survival 2000-14 (CONCORD-3): analysis of individual records for 37 513 025 patients diagnosed with one of 18 cancers from 322 population-based registries in 71 countries. Lancet. 2018 Mar 17;391(10125):1023-1075. doi: 10.1016/S0140-6736(17)33326-3. Epub 2018 Jan 31. PMID: 29395269; PMCID: PMC5879496.
10. Tanaka K, Kawano M, Iwasaki T, Itonaga I, Tsumura H. Surrogacy of intermediate endpoints for overall survival in randomized controlled trials of first-line treatment for advanced soft tissue sarcoma in the pre- and post-pazopanib era: a meta-analytic evaluation. BMC Cancer. 2019 Jan 11;19(1):56. doi: 10.1186/s12885-019-5268-2. PMID: 30634944; PMCID: PMC6330427.
11. Boilève J, Touchefeu Y, Matysiak-Budnik T. Clinical Management of Gastric Cancer Treatment Regimens. Curr Top Microbiol Immunol. 2023;444:279-304. doi: 10.1007/978-3-031-47331-9_11. PMID: 38231223.
12. Wang Q, Wang T. Comparison of survival between diffuse type and intestinal type early-onset gastric cancer patients: A large population-based study. Medicine (Baltimore). 2023 Nov 24;102(47):e36261. doi: 10.1097/MD.0000000000036261. PMID: 38013337; PMCID: PMC10681446.
13. Lee JH, Chang KK, Yoon C, Tang LH, Strong VE, Yoon SS. Lauren Histologic Type Is the Most Important Factor Associated With Pattern of Recurrence Following Resection of Gastric Adenocarcinoma. Ann Surg. 2018 Jan;267(1):105-113. doi: 10.1097/SLA.0000000000002040. PMID: 27759618; PMCID: PMC5515689.
14. Ergenç M, Uprak TK, Akın Mİ, Hekimoğlu EE, Çelikel ÇA, Yeğen C. Prognostic significance of metastatic lymph node ratio in gastric cancer: a Western-center analysis. BMC Surg. 2023 Aug 7;23(1):220. doi: 10.1186/s12893-023-02127-y. PMID: 37550669; PMCID: PMC10408136.
15. Lee JY, Gong EJ, Chung EJ, Park HW, Bae SE, Kim EH, Kim J, Do YS, Kim TH, Chang HS, Song HJ, Choe J, Jung HY. The Characteristics and Prognosis of Diffuse-Type Early Gastric Cancer Diagnosed during Health Check-Ups. Gut Liver. 2017 Nov 15;11(6):807-812. doi: 10.5009/gnl17033. PMID: 28798286; PMCID: PMC5669596.
16. van der Kaaij RT, Koemans WJ, van Putten M, Snaebjornsson P, Luijten JCHBM, van Dieren JM, Cats A, Lemmens VEPP, Verhoeven RHA, van Sandick JW. A population-based study on intestinal and diffuse type adenocarcinoma of the oesophagus and stomach in the Netherlands between 1989 and 2015. Eur J Cancer. 2020 May;130:23-31. doi: 10.1016/j.ejca.2020.02.017. Epub 2020 Mar 11. PMID: 32171106.
17. Zheng HC, Li XH, Hara T, Masuda S, Yang XH, Guan YF, Takano Y. Mixed-type gastric carcinomas exhibit more aggressive features and indicate the histogenesis of carcinomas. Virchows Arch. 2008 May;452(5):525-34. doi: 10.1007/s00428-007-0572-7. PMID: 18266006; PMCID: PMC2329735.
18. Kinami S, Saito H, Takamura H. Significance of Lymph Node Metastasis in the Treatment of Gastric Cancer and Current Challenges in Determining the Extent of Metastasis. Front Oncol. 2022 Jan 7;11:806162. doi: 10.3389/fonc.2021.806162. PMID: 35071010; PMCID: PMC8777129.
19. Japanese Gastric Cancer Association. Japanese gastric cancer treatment guidelines 2018. Gastric Cancer. 2021;24(1):1–21.
20. Biffi R, Botteri E, Cenciarelli S, Luca F, Pozzi S, Valvo M, Sonzogni A, Chiappa A, Leal Ghezzi T, Rotmensz N, Bagnardi V, Andreoni B. Impact on survival of the number of lymph nodes removed in patients with node-negative

gastric cancer submitted to extended lymph node dissection. Eur J Surg Oncol. 2011 Apr;37(4):305-11. doi: 10.1016/j.ejso.2011.01.013. Epub 2011 Feb 1. PMID: 21288685.
21. Alatengbaolide, Lin D, Li Y, Xu H, Chen J, Wang B, Liu C, Lu P. Lymph node ratio is an independent prognostic factor in gastric cancer after curative resection (R0) regardless of the examined number of lymph nodes. Am J Clin Oncol. 2013 Aug;36(4):325-30. doi: 10.1097/COC.0b013e318246b4e9. PMID: 22547011.
22. Lee EW, Lee WY, Koo HS. Prognostic Factors for Node-Negative Advanced Gastric Cancer after Curative Gastrectomy. J Gastric Cancer. 2016 Sep;16(3):161-166. doi: 10.5230/jgc.2016.16.3.161. Epub 2016 Sep 30. PMID: 27752393; PMCID: PMC5065945.
23. Hu X, Cao L, Yu Y. Prognostic prediction in gastric cancer patients without serosal invasion: comparative study between UICC 7(th) edition and JCGS 13(th) edition N-classification systems. Chin J Cancer Res. 2014 Oct;26(5):596-601. doi: 10.3978/j.issn.1000-9604.2014.10.09. PMID: 25400426; PMCID: PMC4220259.
24. Deng JY, Liang H. Clinical significance of lymph node metastasis in gastric cancer. World J Gastroenterol. 2014 Apr 14;20(14):3967-75. doi: 10.3748/wjg.v20.i14.3967. PMID: 24744586; PMCID: PMC3983452.
25. Cunningham D, Allum WH, Stenning SP, Thompson JN, Van de Velde CJ, Nicolson M, Scarffe JH, Lofts FJ, Falk SJ, Iveson TJ, Smith DB, Langley RE, Verma M, Weeden S, Chua YJ, MAGIC Trial Participants. Perioperative chemotherapy versus surgery alone for resectable gastroesophageal cancer. N Engl J Med. 2006 Jul 6;355(1):11-20. doi: 10.1056/NEJMoa055531. PMID: 16822992.
26. Van Cutsem E, Sagaert X, Topal B, Haustermans K, Prenen H. Gastric cancer. Lancet. 2016 Nov 26;388(10060):2654-2664. doi: 10.1016/S0140-6736(16)30354-3. Epub 2016 May 5. PMID: 27156933.
27. Yaghoobi M, Bijarchi R, Narod SA. Family history and the risk of gastric cancer. Br J Cancer. 2010 Jan 19;102(2):237-42. doi: 10.1038/sj.bjc.6605380. Epub 2009 Nov 3. PMID: 19888225; PMCID: PMC2816643.
28. Guilford P, Blair V, More H, Humar B. A short guide to hereditary diffuse gastric cancer. Hered Cancer Clin Pract. 2007 Dec 15;5(4):183-94. doi: 10.1186/1897-4287-5-4-183. PMID: 19725995; PMCID: PMC2736978.
29. Oliveira C, Seruca R, Carneiro F. Genetics, pathology, and clinics of familial gastric cancer. Int J Surg Pathol. 2006 Jan;14(1):21-33. doi: 10.1177/106689690601400105. PMID: 16501831.
30. Elmadani M, Mokaya PO, Omer AAA, Kiptulon EK, Klara S, Orsolya M. Cancer burden in Europe: a systematic analysis of the GLOBOCAN database (2022). BMC Cancer. 2025 Mar 12;25(1):447. doi: 10.1186/s12885-025-13862-1. PMID: 40075331; PMCID: PMC11905646.
31. Ferlay J, Colombet M, Soerjomataram I, Dyba T, Randi G, Bettio M, Gavin A, Visser O, Bray F. Cancer incidence and mortality patterns in Europe: Estimates for 40 countries and 25 major cancers in 2018. Eur J Cancer. 2018 Nov;103:356-387. doi: 10.1016/j.ejca.2018.07.005. Epub 2018 Aug 9. PMID: 30100160.
32. Dana J, Meyer A, Paisant A, Rode A, Sartoris R, Séror O, Cassinotto C, Milot L, Grégory J, Cœur J, Lebigot J, Schembri V, Villeret F, Takeda AN, Ronot M, Vilgrain V, Baumert TF, Gallix B, Padoy N, Nahon P. Improving risk stratification and detection of early HCC using ultrasound-based deep learning models. JHEP Rep. 2025 Jul 5;7(10):101510. doi: 10.1016/j.jhepr.2025.101510. PMID: 40980161; PMCID: PMC12448012.
33. AlHarthy SH, Al-MoundhrI M, Al-Mahmoodi W, Ibrahim R, Ayaad O, Al Baimani K. Referral Process Enhancement: Innovative Approaches and Best Practices. Asian Pac J Cancer Prev. 2024 May 1;25(5):1691-1698. doi: 10.31557/APJCP.2024.25.5.1691. PMID: 38809641; PMCID: PMC11318818.

Corresponding authors:
Professor Arvin Dibra, MD, PhD. E-mail: arvindibra@gmail.com
Professor Manika Face, MD, PhD. E-mail: manika.kreka@umed.edu.al

International Journal of Biomedicine 16(2) (2026) 178-186
http://dx.doi.org/10.21103/Article16(2)_OA4

ORIGINAL ARTICLE

INTERNATIONAL JOURNAL OF BIOMEDICINE

Laparoscopic Surgery for Benign Gynecological Conditions: Perioperative Characteristics and Short-term Outcomes at a Private Hospital in Bangladesh: A Prospective Cross-sectional Study

Isameldin Medani[1*]

[1]*Department of Obstetrics and Gynecology, Faculty of medicine, Jazan University, Jazan, Saudi Arabia*

Abstract

Background: Laparoscopic surgery is widely recommended for benign gynecological conditions because it minimizes surgical trauma and accelerates postoperative recovery. Prospective evidence from low- and middle-income settings, particularly detailing operative determinants and short-term outcomes, remains limited. Our objective is to describe perioperative characteristics, identify predictors of operative complexity, and evaluate short-term outcomes among women undergoing laparoscopic surgery for benign gynecological conditions at a tertiary hospital in Bangladesh.

Methods and Results: A prospective observational study was conducted at Feni PVT Hospital and Laparoscopy Institute in Bangladesh from July to September 2025. Consecutive women aged 18–70 years undergoing elective laparoscopic surgery (hysterectomy, myomectomy, ovarian cystectomy, or diagnostic laparoscopy) for benign indications were included. Demographic, clinical, intraoperative, and postoperative data were collected prospectively. Descriptive statistics summarized outcomes. Multiple linear regression identified predictors of operative time, and binary logistic regression assessed factors associated with intra-abdominal adhesions.

A total of 181 women were included, with a mean age of 42.2±9.0 years and a mean parity of 2.5±0.6. Abnormal uterine bleeding was the most frequent indication (67.4%). Mean operative time was 47.9±4.8 minutes, and estimated blood loss was <50mL in 99.4% of cases. No intraoperative complications, conversions, or transfusions occurred. All participants were discharged after one day, and 97.2% were mobilized on the day of surgery. Intra-abdominal adhesions were identified in 37.0% of cases. Increased operative time was independently associated with higher parity, comorbidities, previous surgery, abnormal uterine bleeding, and adenomyosis, while age showed a modest inverse association. Adhesions were strongly associated with prior surgery, increasing age, and uterine fibroids.

Conclusion: In this experienced center, laparoscopic surgery for benign gynecological conditions was associated with a consistent safety profile, minimal blood loss, and rapid recovery. Patient- and pathology-related factors influence operative complexity but do not compromise short-term outcomes.(**International Journal of Biomedicine. 2026;16(2):178-186.**)

Keywords: adhesions • benign gynecological conditions • laparoscopic surgery • operative time• perioperative outcomes.

For citation: Medani I. Laparoscopic Surgery for Benign Gynecological Conditions: Perioperative Characteristics and Short-term Outcomes at a Private Hospital in Bangladesh: A Prospective Cross-sectional Study.. International Journal of Biomedicine. 2026;16(2):178-186. doi:10.21103/Article16(2)_OA4

Introduction

Contemporary clinical guidelines recommend hysterectomy for benign gynecological disease via a minimally invasive route whenever feasible, supported by more than three decades of comparative evidence.[1] Randomized trials and meta-analyses consistently show that laparoscopic and vaginal hysterectomy reduce postoperative pain, febrile morbidity, and hospital stay compared with abdominal hysterectomy.[2, 3] These benefits translate into earlier mobilization, faster return to normal activity, and improved patient satisfaction within enhanced recovery pathways.

The advantages of minimally invasive surgery arise from pneumoperitoneum and optical magnification, which facilitate precise dissection and hemostasis while minimizing tissue trauma and blood loss. Smaller incisions also attenuate inflammatory and endocrine stress responses associated with laparotomy.[2,3] Limitations of conventional laparoscopy, including restricted instrument articulation and two-dimensional imaging, have driven interest in robot-assisted

surgery. Robotic platforms offer enhanced dexterity, tremor filtration, and three-dimensional visualization, potentially facilitating complex pelvic procedures.[4]However, population-based analyses have not demonstrated consistent reductions in morbidity with robotic surgery compared with conventional laparoscopy for benign indications.[5]A systematic review of more than 4,000 procedures concluded that the cost-effectiveness of robotic surgery remains unproven, supporting selective rather than routine use.[6]Large registry data reinforce the benefits of minimally invasive approaches. In over 450,000 benign hysterectomies, laparoscopic access halved transfusion requirements and reduced mortality by nearly 40% compared with abdominal hysterectomy.[7] Single-center audits similarly report lower blood loss and shorter operating times once proficiency is achieved.[8] Meta-analyses also support vaginal hysterectomy, demonstrating faster recovery and non-inferior complication rates compared with total laparoscopic hysterectomy.[9] Randomized comparisons indicate that the ergonomic advantages of robotic surgery do not translate into superior early quality-of-life outcomes relative to vaginal or laparoscopic hysterectomy.[10] These findings highlight surgeon experience and appropriate case selection as key determinants of outcome.

Similar patterns are observed in myomectomy. Randomized evidence shows that laparoscopic myomectomy results in less postoperative pain and earlier discharge than open surgery without compromising uterine integrity.[11] Cochrane reviews confirm reduced febrile morbidity, lower transfusion rates, and faster recovery following minimally invasive approaches.[12] Multicenter cohorts demonstrate reduced blood loss with laparoscopic myomectomy,[13] while laparo-endoscopic single-site surgery provides cosmetic benefits without prolonging operative time.[14] Economic analyses suggest higher costs without clear differences in clinical outcomes,[15] while matched studies report comparable fertility and symptom relief between minimally invasive and open techniques.[16] Although abdominal myomectomy is associated with longer recovery and higher adhesion-related morbidity,[17] outcomes improve with increasing minimally invasive experience,[18] and meta-analyses confirm lower febrile morbidity across all minimally invasive routes.[19,20]

Benign ovarian surgery has similarly transitioned toward minimally invasive management. Randomized trials and Cochrane reviews demonstrate reduced analgesic requirements, shorter hospital stay, and comparable complication rates with laparoscopy compared with laparotomy.[21,22] Advances such as single-port laparoscopy allow removal of large ovarian cysts (>10 cm) while preserving ovarian reserve and achieving fertility outcomes comparable to those of open surgery.[23–26] Deep infiltrating endometriosis remains technically challenging, yet minimally invasive surgery predominates. Randomized trials show faster recovery with laparoscopic compared with open colorectal resection,[27] while large series report durable pain relief and acceptable complication rates even in advanced disease.[28,29] Registry analyses attribute major complications primarily to prolonged operative time rather than surgical access.[29,30] Overall, minimally invasive surgery for benign gynecological conditions accelerates recovery and reduces morbidity but often incurs higher costs with largely comparable clinical outcomes, particularly for robotic platforms. Selective application based on patient characteristics and anatomical complexity is therefore appropriate. Accordingly, this study aims to prospectively describe perioperative characteristics, identify predictors of operative complexity, and evaluate short-term postoperative outcomes among women undergoing laparoscopic surgery for benign gynecological conditions at a tertiary private hospital in Bangladesh.

Methods

Study Design and Setting

This was a prospective, single-arm, observational study conducted from July 9 to September 8, 2025, at Feni PVT Hospital and Laparoscopy Institute in Feni District, Chattogram Division, Bangladesh (Figure 1, Table 1). The hospital is a private multidisciplinary facility providing routine inpatient and outpatient care as well as advanced minimally invasive laparoscopic gynecological services. It serves a large number of patients from Feni and neighboring areas, achieving favorable surgical outcomes with short recovery times. The institution also functions as a training center for surgeons in minimally invasive gynecological techniques. The study aimed to evaluate perioperative characteristics and short-term postoperative outcomes of women undergoing laparoscopic surgery for benign gynecological conditions.

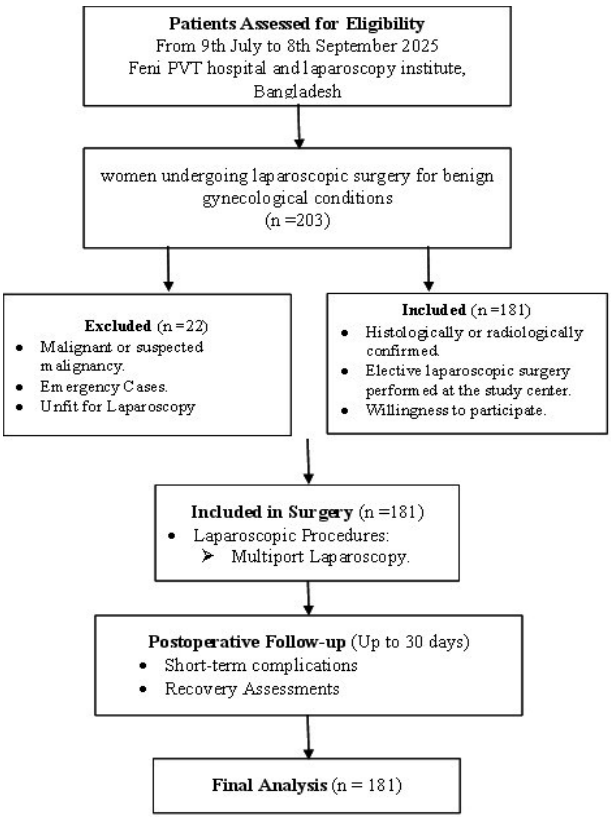

Figure 1. *A flow diagram showing patient inclusion, surgery types, and follow-up.*

Table 1.

Summarizing variables, their definitions, measurement methods, and timing.

Variable Category	Variable	Definition / Measurement	Timing	Notes
Demographic & Baseline	Age	Years, obtained from patient records	At enrollment	All participants
	Body Mass Index (BMI)	Weight (kg) / Height (m^2)	Preoperative assessment	All participants
	Parity	Number of previous births	At enrollment	All participants
	Comorbidities	Chronic conditions (e.g., diabetes, hypertension)	Preoperative assessment	All participants
Clinical Presentation	Primary Complaint	Main presenting symptom	At enrollment	All participants
	Diagnosis	Confirmed via imaging or histopathology	Preoperative assessment	All participants
	Imaging Findings	Size, number, or location of lesions	Preoperative assessment	All participants
Surgical Characteristics	Type of Laparoscopic Procedure	Multiport	Intraoperative	All participants
	Operative Time	Minutes from incision to closure	Intraoperative	All participants
	Intraoperative Blood Loss	mL measured via suction and sponge weight	Intraoperative	All participants
	Conversion to Open Surgery	Noted if conversion occurs	Intraoperative	Included as part of laparoscopic cohort
	Intraoperative Complications	Bleeding, organ injury, anesthesia events	Intraoperative	All participants
Postoperative Outcomes	Length of Hospital Stay	Days from surgery to discharge	Postoperative	All participants
	Pain Score	VAS 0–10 at 6, 12, 24, 48 hours	Postoperative	All participants
	Analgesic Requirement	Total dose of analgesics (mg)	Postoperative	All participants
	Febrile Morbidity	Temperature >38°C sustained >24 hours	Postoperative	All participants
	Wound Complications	Infection, dehiscence, seroma	Postoperative & 30-day follow-up	All participants
Follow-up Outcomes	Short-term Complications	Readmission, reoperation, other complications	30-day follow-up	All participants
	Recovery Parameters	Return to normal activity, symptom resolution	30-day follow-up	All participants

Study Population

Consecutive women aged 18–70 years undergoing elective laparoscopic surgery for benign gynecological conditions were enrolled. The primary procedures included total laparoscopic hysterectomy, laparoscopic myomectomy, laparoscopic ovarian cystectomy, and diagnostic laparoscopy with biopsy.

Inclusion criteria

- Histologically or radiologically confirmed benign gynecological pathology.
- Elective laparoscopic surgery performed at the study center.
- Willingness to participate and provide written informed consent.

Exclusion criteria

- Malignant or suspected malignant gynecological pathology.
- Emergency surgical cases.
- Previous extensive pelvic surgery making laparoscopic surgery unfeasible.
- Severe comorbidities contraindicating general anesthesia.

Sampling Technique

A total population (consecutive) sampling approach was used: all women meeting the inclusion criteria who underwent laparoscopic surgery during the study period were included in the study. No formal sample size calculation was performed, as the study aimed to capture the entire laparoscopic cohort available at the center.

Data Collection

Data were collected prospectively using a structured proforma and included:

- Demographic characteristics: age, BMI, parity, comorbidities.
- Clinical presentation: primary complaint, diagnosis, imaging findings.
- Surgical characteristics: type of laparoscopic procedure, operative time, intraoperative blood loss, intraoperative complications, conversion to open surgery (if any).
- Postoperative outcomes: length of hospital stay, postoperative pain (Visual Analog Scale at 6, 12, 24, and 48 hours), analgesic requirements, febrile morbidity, wound complications, readmissions within 30 days.
- Follow-up outcomes: short-term complications

and recovery parameters assessed up to 30 days postoperatively.

All data collection was performed by trained surgical residents and research assistants, supervised by senior gynecologists to ensure accuracy and standardization.

Surgical Procedures

- Laparoscopic surgery: Standard multiport technique was employed depending on case complexity. Pneumoperitoneum was established using a Veress needle or an open technique. Bipolar and monopolar energy devices were used for hemostasis.
- Conversion to open surgery: Cases requiring conversion were noted and analyzed as part of the laparoscopic cohort.

All procedures followed institutional perioperative protocols, including prophylactic antibiotics, thrombo-prophylaxis, and standardized anesthesia care.

Primary Outcomes

- Operative time (minutes)
- Intraoperative blood loss (mL)
- Length of hospital stay (days)

Secondary Outcomes

- Postoperative pain (VAS scores)
- Analgesic consumption
- Febrile morbidity
- Wound infection or dehiscence
- Conversion to open surgery
- Short-term complications within 30 days

Data Analysis

All data were coded with serial numbers, so personal information was removed during analysis, and privacy was maintained. Data were entered into an Excel sheet and transferred to SPSS (IBM 28.0). Descriptive statistics were calculated: means ± standard deviation for continuous variables and frequencies/percentages for categorical variables. Multiple linear regression was performed to identify predictors of operative time. All candidate predictors (age, parity, comorbidities, prior surgery, specific indications, and adhesions) were entered into the model simultaneously. Model assumptions, including linearity, normality of residuals, homoscedasticity, and the absence of problematic multicollinearity, were assessed and found satisfactory. Binary logistic regression was performed to identify factors associated with intra-abdominal adhesions, using the same entry method. Model fit was assessed using the Hosmer-Lemeshow test (P=0.62) and classification accuracy. Model assumptions, including the absence of multicollinearity and the adequacy of model fit, were assessed and found to be satisfactory.

Results

Participant Demographics and Clinical Characteristics

A total of 181 participants were included, all of Bangladeshi nationality. The cohort was predominantly married (99.4%), with only one participant reporting divorce (0.6%). Educational attainment was primarily at the primary level (97.8%), while a minority had secondary education (2.2%). Employment was rare, with only two participants (1.1%) employed.

The mean age was 42.2±9.0 years (range 25–75), and participants had an average parity of 2.5 ± 0.6 children (median 3, range 1–4). The mean operative time for the entire cohort was 47.9±4.8 minutes (median 46, range 40–75) (Table 2).

Table 2.

Descriptive statistics of numerical variables.

Variable	n	Mean	SD	Median	Min	Max
Age (years)	181	42.2	9.0	40.0	25	75
Number of children		2.5	0.6	3.0	1	4
Operative time (minutes)		47.9	4.8	46.0	40	75

Comorbidities were reported in 32 participants (17.7%), with hypertension being most common (10.5%), followed by diabetes (8.8%) and obesity (3.3%) (Figure 2). Regarding prior surgery, 56.4% of participants (n=102) had no surgical history, while 43.6% (n=79) had a previous cesarean section (Figure 3).

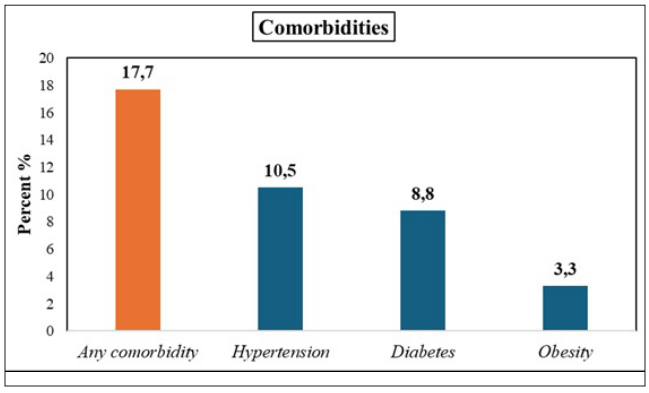

Figure 2. *Comorbidities among study participants (n=181). Bar chart showing the prevalence of comorbid conditions in participants undergoing laparoscopic hysterectomy. Overall, 32 participants (17.7%) reported at least one comorbidity. Hypertension was the most frequent (10.5%, n=19), followed by diabetes (8.8%, n=16) and obesity (3.3%, n=6). The majority (82.3%, n=149) had no comorbidities.*

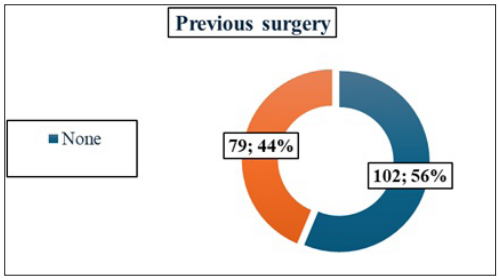

Figure 3. *History of previous surgery among study participants (n=181). Illustration of prior surgical history in the cohort. More than half of participants (56%, n=102) had no history of previous surgery, whereas 44% (n=79) reported a prior cesarean section. This distribution highlights the prevalence of prior lower abdominal surgery in the study population.*

Indications for Surgery

Abnormal uterine bleeding was the most frequent indication for laparoscopic hysterectomy, reported in 122 participants (67.4%), followed by chronic pelvic pain in 76 participants (42.0%). Uterine fibroids were identified in 56 participants (30.9%), and adenomyosis in 27 participants (14.9%). Less frequent indications included ovarian cysts (8.8%) and uterine prolapse (6.1%) (Figure 4).

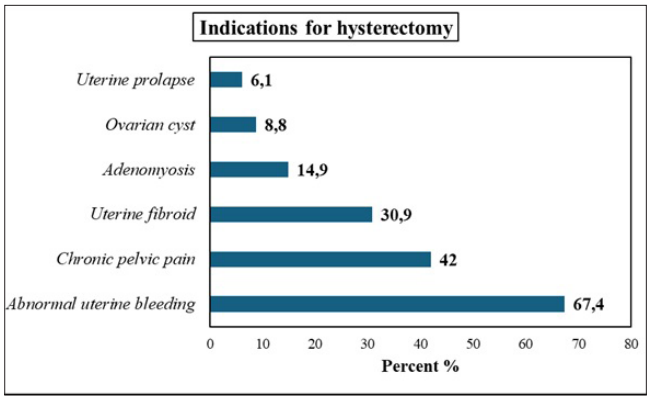

Figure 4. *Indications for laparoscopic hysterectomy (n=181). Bar chart depicting the primary clinical indications for hysterectomy. Abnormal uterine bleeding was the most common indication (67.4%, n=122), followed by chronic pelvic pain (42.0%, n=76), uterine fibroids (30.9%, n=56), and adenomyosis (14.9%, n=27). Less common indications included ovarian cysts (8.8%, n=16) and uterine prolapse (6.1%, n=11). Percentages exceed 100% in some cases due to overlapping indications.*

Intraoperative and Postoperative Outcomes

All procedures were laparoscopic and performed by senior consultants. No intraoperative complications, tissue injuries, or conversions to open surgery occurred, and no participants required blood transfusion. Estimated blood loss was <50 mL in 99.4% of participants and <100 mLin 0.6%. Early mobilization was achieved on the same day in 97.2% of participants and on the first postoperative day in 2.8% of participants. Hospital stay was uniformly one day, and all participants resumed normal activities within one week. Postoperative pain during the first 48 hours was mild in all participants, with 98.9% requiring analgesics. Only one participant (0.6%) required reoperation, and there were no 30-day readmissions. Intra-abdominal adhesions were identified in 67 participants (37.0%), while 114 participants (63.0%) had no adhesions (Figure 5).

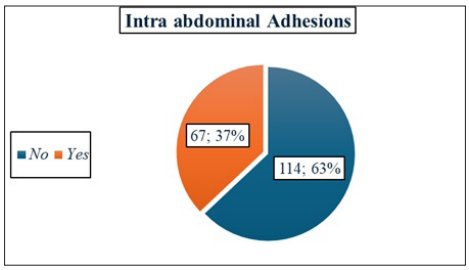

Figure 5. *Frequency of intra-abdominal adhesions identified during laparoscopic hysterectomy (n=181). Pie chart illustrating the presence of intra-abdominal adhesions. Adhesions were observed in 37.0% of participants (n=67), while 63.0% (n=114) had no adhesions identified intraoperatively.*

Predictors of Operative Time

Multiple linear regression analysis evaluated the relationship between demographic and clinical variables and operative time. The model was statistically significant ($F(11,167)=3.11$, $P=0.001$) and explained 17.0% of the variance ($R^2=0.170$; adjusted $R^2=0.115$).

Significant predictors of increased operative time included:

- Higher parity (B=1.947, 95% CI: 0.556–3.338, $P=0.006$)
- Presence of comorbidities (B=2.164, 95% CI: 0.178–4.151, $P=0.033$)
- History of previous surgery (B=2.522, 95% CI: 0.580–4.464, $P=0.011$)
- Abnormal uterine bleeding (B=2.421, 95% CI: 0.758–4.084, $P=0.005$)
- Adenomyosis (B=2.717, 95% CI: 0.277–5.157, $P=0.029$)

Conversely, increasing age was associated with a slight reduction in operative time (B=−0.116, 95% CI: −0.214 to −0.018, $P=0.020$). Chronic pelvic pain, uterine fibroid, ovarian cyst, uterine prolapse, and intra-abdominal adhesions were not significant predictors (Table 3).

Table 3*.*

Demographic and clinical predictors of operative time in patients undergoing laparoscopic hysterectomy.

Predictors	B	Std. Error	*P*-value	95.0% CI for B	
				L. Bound	U. Bound
Age	-0.116	0.050	0.020	-0.214	-0.018
Parity	1.947	0.705	0.006	0.556	3.338
Comorbidities	2.164	1.006	0.033	0.178	4.151
History of previous Surgery	2.522	0.984	0.011	0.580	4.464
Abnormal uterine bleeding	2.421	0.843	0.005	0.758	4.084
Chronic pelvic pain	-1.704	0.920	0.167	-3.520	0.113
Uterine fibroid	-1.320	0.973	0.177	-3.241	0.601
Adenomyosis	2.717	1.236	0.029	0.277	5.157
Ovarian cyst	1.474	1.326	0.268	1.143	4.092
Uterine prolapse	-2.316	1.686	0.171	-5.646	1.013
Intra-abdominal Adhesions	1.658	1.056	0.118	-0.426	3.742

** All listed variables were entered simultaneously into the multiple linear regression model.*

Predictors of Intra-Abdominal Adhesions

Binary logistic regression assessed factors associated with intra-abdominal adhesions. The model was significant ($\chi^2(10)=121.74$, $P<0.001$), explaining 49.2–67.2% of the variance (Cox & Snell $R^2=0.492$; Nagelkerke $R^2=0.672$) and achieving an overall classification accuracy of 87.2%.

Significant predictors included:

- Age (OR=1.11, 95% CI: 1.03–1.20, $P=0.006$)
- History of previous surgery (OR=45.21, 95% CI: 15.19–134.58, $P<0.001$)
- Presence of uterine fibroids (OR=5.22, 95% CI: 1.18–23.05, $P=0.029$)

Other variables—including parity, comorbidities, abnormal uterine bleeding, chronic pelvic pain, adenomyosis, ovarian cyst, and uterine prolapse—were not significantly associated (Table 4).

Table 4.

Demographic and clinical predictors of intra-abdominal adhesions in patients undergoing laparoscopic hysterectomy.*

Predictor	B	SE	*P*-value	OR (Exp(B))	95% CI for OR
Age	0.105	0.038	0.006	1.11	1.03–1.20
Parity	0.669	0.474	0.157	1.95	0.77–4.94
Comorbidities	0.067	0.664	0.920	1.07	0.29–3.93
History of previous surgery	3.811	0.557	<0.001	45.21	15.19–134.58
Abnormal uterine bleeding	0.646	0.628	0.304	1.91	0.56–6.54
Chronic pelvic pain	0.527	0.707	0.456	1.70	0.42–6.77
Uterine fibroid	1.652	0.758	0.029	5.22	1.18–23.05
Adenomyosis	0.846	0.971	0.384	2.33	0.35–15.64
Ovarian cyst	1.736	0.937	0.064	5.68	0.91–35.61
Uterine prolapse	0.663	1.159	0.567	1.94	0.20–18.81

** All listed variables were entered simultaneously into the binary logistic regression model.*

Patient-Reported Outcomes

Patient satisfaction was uniformly high. All participants reported being very satisfied with the surgical outcomes, perceived faster-than-expected recovery, and indicated they would recommend laparoscopic hysterectomy to others or choose the same procedure again if required.

Discussion

This prospective cross-sectional study demonstrates that laparoscopic surgery for benign gynecological conditions can be delivered with consistently favorable peri-operative performance and excellent short-term recovery in a real-world, resource-constrained private hospital setting. Without reiterating specific outcome measures, the collective pattern of findings reflects a highly standardized surgical pathway characterized by procedural efficiency, minimal physiological insult, and rapid functional recovery. Importantly, the absence of major intraoperative adversity and the uniformly short convalescence underscore the maturity of laparoscopic practice at the study center and reinforce the premise that surgical outcomes are primarily driven by case selection, surgeon experience, and perioperative systems rather than by patient demographics alone.

The observed determinants of operative duration highlight the interaction between patient-related complexity and surgical workload rather than technical failure. Factors such as prior pelvic surgery, higher parity, and specific uterine pathologies were associated with longer procedures, reflecting expected anatomical distortion and the demands of adhesiolysis. This aligns closely with large observational data reported by Wright et al.,[5] where increased operative time in minimally invasive hysterectomy correlated with prior surgery and case complexity but did not translate into higher morbidity. Unlike Wright et al., whose population-level analysis identified variability in outcomes across institutions, the present study demonstrates consistency, suggesting that standardized surgical teams may mitigate complexity-related risks.

Similarly, Aboulfotouh et al.[8] reported that operative efficiency improves substantially once laparoscopic proficiency is established, with case-mix factors—not surgical access—being the primary drivers of operative duration. The present study extends this observation by quantifying patient-level predictors within a homogeneous laparoscopic cohort, rather than by comparing surgical routes.

Intra-abdominal adhesions emerged as a clinically relevant intraoperative finding, predominantly associated with age and prior surgery. This mirrors findings from Clark et al.,[30] who identified previous abdominal surgery as the strongest predictor of intraoperative complexity and major complications during laparoscopic treatment of endometriosis. However, unlike Clark et al., in which adhesions increased the risk of complications, the present study did not observe downstream adverse outcomes, suggesting that experienced surgical teams can neutralize adhesion-related risk in benign gynecological surgery.

Comparable observations were reported by Khazali et al.,[29] who demonstrated that operative difficulty in advanced endometriosis was more strongly associated with duration and extent of dissection than with incision type. The present study broadens this concept beyond endometriosis, supporting adhesions as a marker of technical demand rather than a determinant of poor outcome.

The uniformly favorable short-term postoperative course observed in this cohort is concordant with high-quality evidence synthesized by Aarts et al.,[2] who demonstrated that minimally invasive hysterectomy consistently reduces postoperative morbidity compared with open approaches. Unlike randomized trials included in the Cochrane review, which often involve heterogeneous surgeons and centers, this study reflects outcomes within a single, high-volume laparoscopic institute, highlighting the potential for optimized outcomes when procedural standardization is achieved.

Furthermore, the findings resonate with the population-based analysis by Wiser et al.,[7] which showed substantial reductions in transfusion and mortality with laparoscopic hysterectomy. While Wiser et al. focused on national-level morbidity and mortality, the present study complements these data by detailing patient-reported recovery and early functional outcomes, areas often underrepresented in administrative datasets.

High patient satisfaction and rapid return to normal activity observed in this study parallel findings from Sandberg et al.,[9] who demonstrated that minimally invasive routes—particularly vaginal and laparoscopic hysterectomy—are associated with superior patient-reported recovery compared with abdominal surgery. However, unlike Sandberg et al., which compared different minimally invasive routes, the present study isolates laparoscopic surgery, thereby providing

a focused assessment of its patient-centered value in routine practice.

The consistency of satisfaction across all participants suggests that expectation management, peri-operative counseling, and early mobilization protocols may be as influential as surgical technique itself—an insight not explicitly addressed in comparative trials.

The uniformly positive short-term outcomes, including rapid mobilization and high patient satisfaction, mirror the benefits of minimally invasive surgery demonstrated in randomized trials and large registries from high-income countries.[2,7] This study confirms that these benefits are achievable in an LMIC setting with appropriate expertise and infrastructure. In contrast to concerns raised by Gala et al.[6] regarding the cost-effectiveness of advanced platforms, the present study demonstrates that standard laparoscopy—without reliance on costly technologies—can achieve outcomes comparable to those reported in high-income settings. This has particular relevance for South Asian and other LMIC contexts, where scalability and sustainability are critical.

By focusing exclusively on laparoscopic surgery and examining predictors of operative complexity and short-term recovery within this cohort, the study avoids the confounding inherent in route-comparison designs. Its prospective nature, comprehensive peri-operative assessment, and integration of patient-reported outcomes strengthen its contribution to the literature. When interpreted alongside comparable studies,[2,5,7,8,30] the findings position laparoscopic surgery not merely as a technically superior alternative, but as a mature, reproducible standard of care when delivered within an optimized institutional framework.

In summary, this study adds contextualized, practice-based evidence supporting the safety, efficiency, and patient-centered benefits of laparoscopic surgery for benign gynecological conditions, reinforcing global recommendations while offering practical insights relevant to similar healthcare settings.

Limitations

This study has several limitations. First, as a single-arm descriptive study, it lacks a direct comparator group (e.g., open surgery). Therefore, while outcomes are excellent, we cannot make comparative claims of superiority. Second, the study was conducted at a single, specialized private center with highly experienced surgeons, which may limit the generalizability of the results to public hospitals or less-experienced teams. Third, follow-up was limited to 30 days, precluding assessment of long-term complications or recurrence. Finally, the cohort was predominantly comprised of hysterectomy patients; outcomes for less common procedures (myomectomy, cystectomy) should be interpreted with caution due to small numbers.

Conclusion

This prospective study demonstrates that laparoscopic surgery for benign gynecological conditions can be performed safely and efficiently in an experienced tertiary center in Bangladesh. Operative performance and early postoperative outcomes were driven primarily by patient-related complexity, including prior surgery and underlying uterine pathology, rather than by the laparoscopic approach itself. The favorable peri-operative outcomes and high patient-reported satisfaction observed reinforce laparoscopy as a reliable standard of care for benign gynecological disease in routine clinical practice. Importantly, these findings provide context-specific evidence from a South Asian setting, supporting the feasibility and reproducibility of high-quality minimally invasive gynecological surgery beyond high-income health systems. Sustained investment in structured surgical training, appropriate case selection, and standardized perioperative pathways is essential to maximize the benefits of laparoscopy. Future studies should incorporate longer follow-up, cost-effectiveness analyses, and comparative designs to further inform evidence-based surgical planning in resource-constrained environments.

Ethical Considerations

The implementation of this study adhered to the ethical principles outlined in the Declaration of Helsinki. Ethical approval was obtained from the Institutional Review Board (IRB) of Feni PVT Hospital and Laparoscopy Institute, Bangladesh (Approval No 202501/FPHLI). Written informed consent was obtained from all participants. Confidentiality was maintained, and participants could withdraw at any time without affecting their treatment

Data Availability Statement

The data that support the findings of this study are available on request from the corresponding author.

Author Contribution Statement

Isameldin Medani confirms sole responsibility for all aspects of the research.

Conflict of Interest

The author declares that he has no known competing financial interests or personal relationships that could have appeared to influence the work reported in this paper.

Acknowledgments

We express our sincere gratitude to Prof. Dr. Mohammad Abdul Quayyum, Chief Consultant and Chairman of Feni Private Hospital & Laparoscopy Institute, for his invaluable support and guidance during this research. We also thank all the medical, nursing, and administrative staff for their dedicated assistance and cooperation. In addition, we gratefully acknowledge the Deanship of Scientific Research and Postgraduate Studies at Jazan University for their continuous support.
The author acknowledges QuillBot for providing proofreading support during the writing process.

References

1. Committee Opinion No 701: Choosing the Route of Hysterectomy for Benign Disease. Obstet Gynecol. 2017 Jun;129(6):e155-e159. doi: 10.1097/AOG.0000000000002112. PMID: 28538495.
2. Aarts JW, Nieboer TE, Johnson N, Tavender E, Garry R, Mol BW, Kluivers KB. Surgical approach to hysterectomy for benign gynaecological disease. Cochrane Database Syst Rev. 2015 Aug 12;2015(8):CD003677. doi: 10.1002/14651858.CD003677.pub5. Update in: Cochrane Database Syst Rev. 2023 Aug 29;8:CD003677. doi: 10.1002/14651858.CD003677.pub6. PMID: 26264829; PMCID: PMC6984437.
3. Johnson N, Barlow D, Lethaby A, Tavender E, Curr L, Garry R. Methods of hysterectomy: systematic review and meta-analysis of randomised controlled trials. BMJ. 2005 Jun 25;330(7506):1478. doi: 10.1136/bmj.330.7506.1478. PMID: 15976422; PMCID: PMC558455.
4. O'Neill M, Moran PS, Teljeur C, O'Sullivan OE, O'Reilly BA, Hewitt M, Flattery M, Ryan M. Robot-assisted hysterectomy compared to open and laparoscopic approaches: systematic review and meta-analysis. Arch Gynecol Obstet. 2013 May;287(5):907-18. doi: 10.1007/s00404-012-2681-z. Epub 2013 Jan 5. PMID: 23291924
5. Wright JD, Ananth CV, Lewin SN, Burke WM, Lu YS, Neugut AI, Herzog TJ, Hershman DL. Robotically assisted vs laparoscopic hysterectomy among women with benign gynecologic disease. JAMA. 2013 Feb 20;309(7):689-98. doi: 10.1001/jama.2013.186. PMID: 23423414.
6. Gala RB, Margulies R, Steinberg A, Murphy M, Lukban J, Jeppson P, et al.; Society of Gynecologic Surgeons Systematic Review Group. Systematic review of robotic surgery in gynecology: robotic techniques compared with laparoscopy and laparotomy. J Minim Invasive Gynecol. 2014 May-Jun;21(3):353-61. doi: 10.1016/j.jmig.2013.11.010. Epub 2013 Dec 1. PMID: 24295923.
7. Wiser A, Holcroft CA, Tulandi T, Abenhaim HA. Abdominal versus laparoscopic hysterectomies for benign disease: morbidity and mortality among 465 798 cases. Gynecol Surg. 2013;10:117-122. doi:10.1007/s10397-013-0781-9.
8. Aboulfotouh ME, Chaalan F, Mohammed ABF. Laparoscopic hysterectomy versus total abdominal hysterectomy: a retrospective study at a tertiary hospital. Gynecol Surg. 2020;17:1. doi:10.1186/s10397-020-01068-1
9. Sandberg EM, Twijnstra ARH, Driessen SRC, Jansen FW. Total Laparoscopic Hysterectomy Versus Vaginal Hysterectomy: A Systematic Review and Meta-Analysis. J Minim Invasive Gynecol. 2017 Feb;24(2):206-217.e22. doi: 10.1016/j.jmig.2016.10.020. Epub 2016 Nov 17. PMID: 27867051.
10. Lönnerfors C, Reynisson P, Persson J. A randomized trial comparing vaginal and laparoscopic hysterectomy vs robot-assisted hysterectomy. J Minim Invasive Gynecol. 2015 Jan;22(1):78-86. doi: 10.1016/j.jmig.2014.07.010. Epub 2014 Jul 19. PMID: 25045857.
11. Mais V, Ajossa S, Guerriero S, Mascia M, Solla E, Melis GB. Laparoscopic versus abdominal myomectomy: a prospective, randomized trial to evaluate benefits in early outcome. Am J Obstet Gynecol. 1996 Feb;174(2):654-8. doi: 10.1016/s0002-9378(96)70445-3. PMID: 8623802.
12. Bhave Chittawar P, Franik S, Pouwer AW, Farquhar C. Minimally invasive surgical techniques versus open myomectomy for uterine fibroids. Cochrane Database Syst Rev. 2014 Oct 21;2014(10):CD004638. doi: 10.1002/14651858.CD004638.pub3. PMID: 25331441; PMCID: PMC10961732.
13. Barakat EE, Bedaiwy MA, Zimberg S, Nutter B, Nosseir M, Falcone T. Robotic-assisted, laparoscopic, and abdominal myomectomy: a comparison of surgical outcomes. Obstet Gynecol. 2011 Feb;117(2 Pt 1):256-266. doi: 10.1097/AOG.0b013e318207854f. PMID: 21252737.
14. Song T, Kim TJ, Lee SH, Kim TH, Kim WY. Laparoendoscopic single-site myomectomy compared with conventional laparoscopic myomectomy: a multicenter, randomized, controlled trial. Fertil Steril. 2015 Nov;104(5):1325-31. doi: 10.1016/j.fertnstert.2015.07.1137. Epub 2015 Aug 8. PMID: 26263079.
15. Advincula AP, Xu X, Goudeau S 4th, Ransom SB. Robot-assisted laparoscopic myomectomy versus abdominal myomectomy: a comparison of short-term surgical outcomes and immediate costs. J Minim Invasive Gynecol. 2007 Nov-Dec;14(6):698-705. doi: 10.1016/j.jmig.2007.06.008. PMID: 17980329.
16. Gargiulo AR, Srouji SS, Missmer SA, Correia KF, Vellinga TT, Einarsson JI. Robot-assisted laparoscopic myomectomy compared with standard laparoscopic myomectomy. Obstet Gynecol. 2012 Aug;120(2 Pt 1):284-91. doi: 10.1097/AOG.0b013e3182602c7d. Erratum in: Obstet Gynecol. 2012 Nov;120(5):1214. Erratum in: Obstet Gynecol. 2013 Sep;122(3):698. Vellinga, Thomas [corrected to Vellinga, Thomas T]. PMID: 22825086.
17. Ascher-Walsh CJ, Capes TL. Robot-assisted laparoscopic myomectomy is an improvement over laparotomy in women with a limited number of myomas. J Minim Invasive Gynecol. 2010 May-Jun;17(3):306-10. doi: 10.1016/j.jmig.2010.01.011. Epub 2010 Mar 19. PMID: 20303834.
18. Özbaşlı E, Güngör M. Comparison of perioperative outcomes among robot-assisted, conventional laparoscopic, and abdominal/open myomectomies. J Turk Ger Gynecol Assoc. 2021 Dec 6;22(4):312-318. doi: 10.4274/jtgga.galenos.2021.2021.0049. Epub 2021 Oct 12. PMID: 34634858; PMCID: PMC8666999.
19. Nezhat C, Lavie O, Hsu S, Watson J, Barnett O, Lemyre M. Robotic-assisted laparoscopic myomectomy compared with standard laparoscopic myomectomy--a retrospective matched control study. Fertil Steril. 2009 Feb;91(2):556-9. doi: 10.1016/j.fertnstert.2007.11.092.
20. Wang T, Tang H, Xie Z, Deng S. Robotic-assisted vs. laparoscopic and abdominal myomectomy for treatment of uterine fibroids: a meta-analysis. Minim Invasive Ther Allied Technol. 2018 Oct;27(5):249-264. doi: 10.1080/13645706.2018.1442349.
21. Yuen PM, Yu KM, Yip SK, Lau WC, Rogers MS, Chang A. A randomized prospective study of laparoscopy and laparotomy in the management of benign ovarian masses. Am J Obstet Gynecol. 1997 Jul;177(1):109-14. doi: 10.1016/s0002-9378(97)70447-2. PMID: 9240592.
22. Medeiros LR, Rosa DD, Bozzetti MC, Fachel JM, Furness S, Garry R, Rosa MI, Stein AT. Laparoscopy versus laparotomy for benign ovarian tumour. Cochrane Database Syst Rev. 2009 Apr 15;(2):CD004751. doi: 10.1002/14651858.CD004751.pub3. PMID: 19370607.

23. Wang X, Li Y. Comparison of perioperative outcomes of single-port laparoscopy, three-port laparoscopy and conventional laparotomy in removing giant ovarian cysts larger than 15 cm. BMC Surg. 2021 Apr 21;21(1):205. doi: 10.1186/s12893-021-01205-3. PMID: 33882918; PMCID: PMC8061010.
24. Benezra V, Verma U, Whitted RW. Comparison of Laparoscopy versus Laparotomy for the Surgical Treatment of Ovarian Dermoid Cysts. Gynecol Surg. 2005;2(2):89-92. doi:10.1007/s10397-005-0091-y
25. Somigliana E, Ragni G, Infantino M, Benedetti F, Arnoldi M, Crosignani PG. Does laparoscopic removal of nonendometriotic benign ovarian cysts affect ovarian reserve? Acta Obstet Gynecol Scand. 2006;85(1):74-7. doi: 10.1080/00016340500334802. PMID: 16521684.
26. Sethi N, Agrawal M, Patel A, Reddy LS, Bhatt DM. Surgical Technique and Fertility Outcomes: A Comprehensive Review of Open and Laparoscopic Cystectomy in Women of Reproductive Age. Cureus. 2024 Oct 10;16(10):e71179. doi: 10.7759/cureus.71179.
27. Daraï E, Dubernard G, Coutant C, Frey C, Rouzier R, Ballester M. Randomized trial of laparoscopically assisted versus open colorectal resection for endometriosis: morbidity, symptoms, quality of life, and fertility. Ann Surg. 2010 Jun;251(6):1018-23. doi: 10.1097/SLA.0b013e3181d9691d.
28. Magrina JF, Espada M, Kho RM, Cetta R, Chang YH, Magtibay PM. Surgical Excision of Advanced Endometriosis: Perioperative Outcomes and Impacting Factors. J Minim Invasive Gynecol. 2015 Sep-Oct;22(6):944-50. doi: 10.1016/j.jmig.2015.04.016. Epub 2015 Apr 24. PMID: 25917276
29. Khazali S, Gorgin A, Mohazzab A, Kargar R, Padmehr R, Shadjoo K, Minas V. Laparoscopic excision of deeply infiltrating endometriosis: a prospective observational study assessing perioperative complications in 244 patients. Arch Gynecol Obstet. 2019 Jun;299(6):1619-1626. doi: 10.1007/s00404-019-05144-6. Epub 2019 Apr 5. PMID: 30953187
30. Clark NV, Dmello M, Griffith KC, Gu X, Ajao MO, Cohen SL, Einarsson JI. Laparoscopic treatment of endometriosis and predictors of major complications: A retrospective cohort study. Acta Obstet Gynecol Scand. 2020 Mar;99(3):317-323. doi: 10.1111/aogs.13762.

***Corresponding author:** Dr. Isameldin Medani. E-mail: isameldin2015@gmail.com*

International Journal of Biomedicine 16(2) (2026) 187-196
http://dx.doi.org/10.21103/Article16(2)_OA5

ORIGINAL ARTICLE

INTERNATIONAL JOURNAL OF BIOMEDICINE

Quantitative Analysis of Computed Tomography Image Acquisition Factors and Demographic Characteristics in Pediatric Brain and Head Scans

Nouf Abuhadi[1*]

[1]*Department of Diagnostic Radiography Technology, College of Nursing and Health Sciences, Jazan University, Jazan, Saudi Arabia*

Abstract

Background: While computed tomography (CT) imaging is vital for diagnosing brain issues, it can expose children to unnecessary risks if not optimized. The aim of this study was to identify the key predictors of radiation dose in pediatric head and brain CT scans, including patient age, scan type, kilovoltage, and field of view (FOV), so that these assessed technical and demographic factors could be used to help radiologists develop dose-optimized protocols for pediatric populations in ways that will minimize radiation doses while maintaining diagnostic image quality.

Methods and Results: We investigated a sample of 138 patients aged 18 years or younger from a single institution who had undergone pediatric brain and head CT scans. Descriptive statistics and data visualization, including correlation tests, were initially performed to explore the data and assess the significance of relationships between the radiation dose indices (CT dose index volume [CTDIvol] and dose-length product [DLP]) and the associated predictors of radiation dose (age, scan type, peak kilovoltage [kVp], tube current, and FOV). The radiation dose indices were found to be higher for the head than for the brain CT scans, which indicated that the patients who underwent head CT were exposed to higher radiation doses. The diagnostic reference levels were set at the 75th percentile of the radiation dose indices for both test sites and age groups, as shown in the box plots. Highly significant linear relationships were found between patient age and the radiation dose indices, (CTDIvol and DLP), (P<0.000 for both), indicating that the required radiation dose tended to increase with age. In this study, the main radiation dose parameters in pediatric neuroimaging were significantly influenced by patient age, scan type, tube current, and kilovoltage. These findings underscore the critical need for age- and indication-adjusted CT protocols to minimize radiation exposure in children without compromising diagnostic utility. The most important finding of this study is the derivation of best-fit model equations for radiation dose indices using our patients' scan parameters. These equations can be used to predict (calculate) the optimal scan parameters for a single variable of the radiation dose indices, while keeping other variables constant. Insights obtained can help radiologists create safer, child-specific scanning protocols, improve radiology practices, and perform more research to minimize risks worldwide.(**International Journal of Biomedicine. 2026;16(2):187-196.**)

Keywords: computed tomography • children • brain scan • radiation dose

For citation: Abuhadi N. Quantitative Analysis of Computed Tomography Image Acquisition Factors and Demographic Characteristics in Pediatric Brain and Head Scans. International Journal of Biomedicine. 2026;16(2):187-196. doi:10.21103/Article16(2)_OA5

Abbreviations

CT, computed tomography; **CTDIvol**, CT dose index volume; **DLP**, dose-length product; **DRLs**, diagnostic reference levels; **FOV**, field of view; **kVp**, peak kilovoltage; **VIF**, variance inflation factor.

Introduction

Diagnostic radiology is a critical practice in medicine. Computed tomography (CT) is widely used in pediatric and adult patients and has transformed medical diagnostics through its fast, precise imaging capabilities, which can be applied to a range of clinical conditions.[1] Unlike other radiological imaging techniques, CT poses a high risk of radiation exposure because multiple thin slices of the target tissue must be captured, leading to multiple exposures in a

single session to enable high-detail, multiplanar computer-generated reconstructions and 3D rendering of the image.

CT scans deliver significantly higher ionizing radiation doses, often 50 to 1,000 times more than conventional X-rays, making them a major contributor (up to 50% or more) to medical radiation exposure. This high-dose exposure increases risks for cancer, with some estimates suggesting a one in 1,000 to 2,000 chances of cancer per scan and a potential contribution to 2% of all cancers.[2]

Because CT doses are initially high, medical imaging optimization is particularly important in pediatrics to reduce radiation exposure for high-risk pediatric patients. As the clinical use of this technique continues to rise, optimization has become a critical requirement. One of the most serious concerns for individuals, specifically children, who undergo diagnostic CT is the elevated risk associated with ionizing radiation.[3,4] Several studies have shown that children are more vulnerable to radiation hazards than adults, as their rapidly developing tissues and longer life expectancy make them more prone to developing radiation-induced cancers later in life.[5] They also have smaller body sizes and receive a higher radiation dose per unit of tissue when conventional adult protocols are used.[6,7]

A troubling trend is the use of adult protocols for children in some radiology departments, as this leads to higher levels of radiation exposure in these patients.[8,9] Pediatric CT scans, such as brain scans, are often employed to diagnose neurological issues, so radiation exposure remains a major concern in pediatric brain CT despite its known clinical benefits. Minimizing radiation exposure in pediatric CT is thus essential to prevent or lessen its radiogenic effects.

According to El-Nachef et al.,[10] scan parameters should be optimized for pediatric patients to ensure diagnostic image quality while maintaining safety. In so doing, the basic goal of radiation safety should be adhered to, that is, to achieve quality diagnostic images using the principle of radiation doses that are "as low as reasonably achievable" (ALARA) Outdated protocols and equipment are still being widely used in many hospitals, particularly in those in low-resource settings, so patients are continuing to be unnecessarily exposed to high radiation.[11] Although the literature provides a solid foundation for radiation risks and dose-reduction practices, several critical research gaps persist. First, quantitative modeling is rarely used. In most studies, researchers have relied on descriptive analyses rather than multivariate regression to determine the independent contributions of scan parameters to radiation dose. Second, researchers in only a few studies have considered the radiation impact of specific scan types (brain or head) within controlled datasets, despite known differences in radiation exposure. Third, the volume of dose optimization research in low-resource settings, where outdated equipment and poorly standardized procedures continue to pose serious challenges, is significantly lacking.[12,13] Therefore, there is a need for empirical research to examine how various technical factors affect radiation dose in pediatric CT scans.

The aim of this study was to identify the key predictors of radiation dose in pediatric head and brain CT scans, including patient age, scan type, kilovoltage, and field of view (FOV), so that these assessed technical and demographic factors could be used to help radiologists develop dose-optimized protocols for pediatric populations in ways that will minimize radiation doses while maintaining diagnostic image quality.

Materials and Methods

Subjects

In this retrospective cross-sectional study, we evaluated CT head and brain procedures performed on 138 patients aged 18 years or younger (average age of 7.42 years) at a single hospital (Southern Hospital, Saudi Arabia).[14] The patients selected for this study met strict selection criteria. The basic inclusion criteria were:

•Patients ≤18 years of age

•Patients who have a brain or head CT scan for non-emergency diagnostic purposes

•Patients for whom complete data were available (patient age, peak kilovoltage [kVp], tube current [mA], FOV, CT dose index volume [CTDIvol], and dose-length product [DLP])

The basic exclusion criteria were:

•Patients who were <18 years of age but had incomplete data

•Patients who had scans performed in the emergency department

•Patients who were originally planned to receive a low-dose CT scan.

Relationship between Image Acquisition Factors and Radiation Dose in CT Scanners

Management of the radiation dose is required to optimize imaging protocols. In CT scans, two radiation dose indices (CTDIvol and DLP) are used in radiation dose management.[1,2]

The technical image acquisition factors applied during the CT scans in this study were X-ray, tube current (mA), peak kilovoltage (kVp), the size of the scanned area or FOV, and scan type (head or brain), in addition to age as a demographic factor. We therefore identified these factors as the key determinants of radiation dose for pediatric brain CT scans. The effects of these factors on CTDIvol and DLP, and thus the radiation dose, were subsequently determined.

Image Protocol (Imaging Procedures)

This study was primarily designed to evaluate the effects of demographic and technical factors in 138 pediatric patients, of whom 26 had pediatric CT head scans, and 112 had pediatric CT brain scans.

CT head scans are primarily requested for bone structure assessment (trauma, sinusitis, pre-surgical planning, and bony lesions) to allow clear visualization of fracture lines and bony architecture, while CT scans of the brain are indicated for soft tissue in the brain to diagnose various pathological conditions, including stroke, tumor, and bleeding within the brain substance. The protocol for CT head imaging typically begins with a non-contrast scan to rule out hemorrhaging, followed by a contrast injection, which is referred to as CT angiography

or CT perfusion. Thinner slices are preferred to enable high-detail, multiplanar reconstructions and 3D rendering of bone structures.

CT Equipment

Brain CT scans were obtained using three scanners: a Toshiba Aquilion 128-slice CT scanner (Japan), a GE Discovery CT750 HD (64 slices), and a GE Revolution HD6 long CTM (128 slices) (USA). All the procedures were performed in accordance with the department's standard protocols.

Methods of Quantification of the Impact of Technical and Demographic Variables on the Radiation Dose

To assess the impact of the deterministic technical variables kVp, mA, and FOV on the two radiation dose indices (CTDIvol and DPL), we performed descriptive statistics, as well as correlation and multiple linear regression analyses.

The data obtained for the 138 patients concerning each factor in relation to radiation dose indices was presented in scatter plots to visualize (identify) the trend (positive or negative impact) and generate the regression line (the best-fit line between the scattered points) in the form of:

$$y = a + bx$$

where, y is the dependent variable (CTDIvol or DLP-the radiation dose indices); x is an independent variable (tube current, kilovoltage or FOV); a, the interception of the regression line with the x-axis which is the constant; b, is a factor of the independent variable (i.e., how many times, the independent variable changes with each change in the dependent variable).

The regression line has slope showing the trend of the correlation (whether positive or negative).

The objective of this study was to identify and quantify the impact of key technical and demographic factors on radiation dose in pediatric brain and head CT scans to inform the development of optimized, low-dose protocols.To be more specific, we examined the impact of the technical factors (mA, kVp, and FOV) on the radiation dose in terms of the radiation dose indices (CTDIvol and DPL) and, in doing so, derived the optimization equations for these parameters.

Statistical analyses were performed using IBM SPSS Statistics for Windows, version 26 (IBM Corporation, Armonk, NY, USA). For all analyses, $P<0.05$ was considered statistically significant.

Results

To identify and quantify the impact of key technical and demographic factors on radiation dose in pediatric brain and head CT, we recorded and analyzed 138 CT scan results of the brain and head.

Impact of Demographic Factors on Radiation Dose

In addition to the descriptive statistics, box and scatter plots were generated to visualize the relationships between the independent variable, age, and the related scan type, with CTDIvol and DLP as the dependent variables. The majority of patients (112) underwent brain volume CT scans (Table 1), with most in the 5–9-year age group. Twenty-six patients had CT head scans.

Table 1.

Data summary of the scan types for the different age groups.

Age	Brain CT scan	Head CT scan
≤4 years	24	9
5–9 years	58	7
10–14 years	27	9
≥15 years	3	1
Total (138 patients)	112 (81.2%)	26(18.8%)

In Table 2, we present summary statistics for the demographic (age) and technical data during the CT scans under analysis, namely, X-ray tube current (mA), kVp, FOV, CTDIvol, and DLP.

Table 2.

Summary statistics for the variables under study.

Statistics	Age	mA	kVp	FOV	CTDIvol	DLP
Mean	7.7329	228.3425	112.6027	26	33.8166	643
Std. Deviation	4.20064	73.33884	9.68859	8	9.48062	208
Median	7.0000	222.0000	120.0000	32	31.6350	601
Maximum	17.00	378.00	120.00	32	73.84	1380
Minimum	1.00	50.00	100.00	16	6.00	157

Impact of Age as a Demographic Factor and Scan Type on CTDIvol

CTDIvol was one of the radiation-dose dependent variables affected by age and scan type. For various test sites and age groups—as well as for the reference points used in establishing the DRLs that fell within the 75th percentile—the median CTDIvol values consistently proved to be lower than the corresponding DRLs. As a radiation-dose index, CTDIvol was higher for the head CT than for the brain CT (Table 3).

Impact of Age and Scan Type on DLP

The DLP (the second radiation dose-dependent variable) for both the head and brain CT were always higher than the median levels for both. DPL, an index of radiation dose, was again higher for the head CT than for the brain CT, indicating that the head CT had a higher radiation dose than the brain CT (Table 4).

Figures 1–4 present box plots of CTDIvol and DLP levels for the different test sites and age groups.. The line in

the middle of each box represents the median, while all the values above and below the plots are extreme values.

Table 3.

CTDIvol values for the different types of test sites, age groups, and diagnostic reference levels (75th percentile).

CTDIvol	Category	Mean±SD	Median	75th percentile
Test type	CT brain CT head	33.8073±9.45791 34.3333±10.05273	30.9000 35.0000	41.7750 43.0000
Age group	≤4 years 5–9 years 10–14 years ≥15 years	28.0824±7.06307 34.4283±8.96909 38.0679±9.42357 33.1111±11.82629	26.8850 31.3000 38.8900 35.0000	30.6725 43.1050 43.0825 39.5000

Table 4.

DLP statistics for the different test sites and age groups.

DLP	Category	Mean± SD	Median	75th percentile
Test type	CT brain CT head CT sinus	632.4475±196.72692 703.8000±243.86279 474.0000±74.74624	593.4000 783.0000 467.0000	771.0000 898.2500 -
Age group	≤4 years 5–9 years 10–14 years ≥15 years	500.8838±151.78631 639.6946±172.00276 756.6150±216.82333 737.8889±280.03636	451.0000 593.4000 766.5000 821.0000	585.9750 798.3950 932.0275 944.0000

With respect to the median CTDIvol for each age group (Figure 1), it was lowest for the age group ≤4 years; however, it increased in the next age group (5–9 years) and continued to rise with increasing age. It was highest in the 10–14-year age group, but declined slightly in the> 15-year age group. Irrespective of the decline, the median for the group aged ≥15 years remained higher than that of the other age groups. The same trend of CTDIvol with age was observed for the 75th percentile.

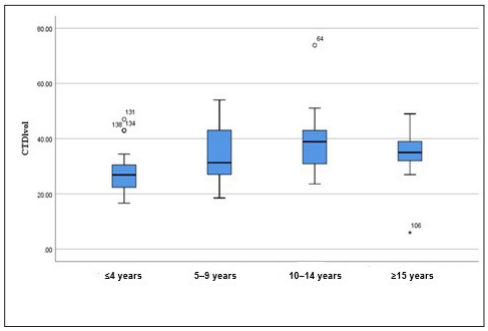

Fig. 1. *Box plot illustrating the CTDIvol levels for the different age groups.*

It can be clearly observed from Figure 2 that the median CTDIvol for the different test sites was highest for head CT, followed by brain and then sinus CT.

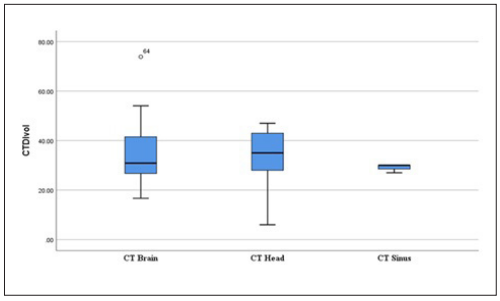

Fig. 2. *Box plot illustrating the CTDIvol levels for the different test sites.*

Unlike variations in CTDIvol with age, the median DLP across age groups continued to rise with increasing age (Figure 3).

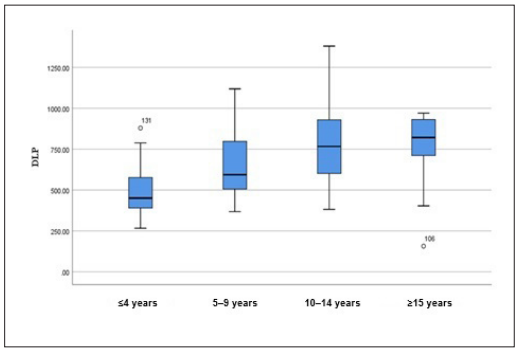

Fig. 3. *Box plot illustrating the DLP levels for the different age groups.*

As for CTDIvol, the median DLP for the different test sites was highest for head CT, followed by brain and then sinus CT (Figure 4).

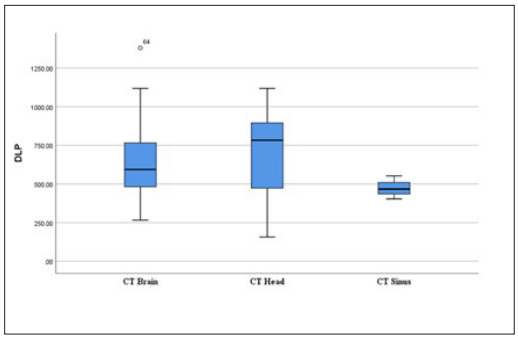

Fig. 4. *Box plot illustrating the levels of DLP for the different test sites.*

Correlation of Age with the Radiation Dose-Dependent Indices

The descriptive statistics for the demographic factor patient age and the image acquisition variables are presented in tables and illustrative figures to reflect the depth of the data. To better visualize the relationships between the variables, a correlation test was performed to investigate how the radiation

dose indices (CTDIvol and DLP) varied with changes in age and a deterministic dose factor (milliamperage). The results are shown in Tables 5–6 and illustrated in the scatter diagrams with their associated regression lines (Figs. 5–6).

Table 5.

Correlation of CTDIvol with age and tube current.

Variables	*r* (Correlation Coefficient)	*P*-value
Age	0 .325	0.000
Tube current (mA)	−0.127	0.127

Table 6.

Correlation of DPL with age and tube current.

Variables	*r* (Correlation Coefficient)	*P*-value
Age	0.455	0.000
Tube current (mA)	−0.109	0.190

As for CTDIvol, the median DLP for the different test sites was highest for head CT, followed by brain and then sinus CT (Figure 4).

The highly significant, but moderately positive, linear relationship between patient age and CTDIvol (Table 5 and Figure 5) indicates that radiation dose tended to increase with increasing patient age. The same trend applied to the highly significant, moderately positive relationship (r=0.455) between patient age and DLP (Table 6 and Figure 6).

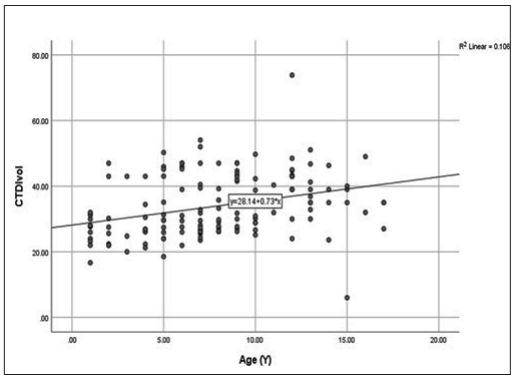

Fig. 5. *Scatter plot showing the correlation of CTDIvol with age.*

However, no significant correlations were observed between tube current (mA), a deterministic radiation dose factor, and radiation dose as measured by CTDIvol and DLP (Table 5 and Table 6, respectively). In both cases, the correlation was weakly negative, which indicated an inverse relationship between radiation dose and tube current. This inverse relationship was weak and insignificant, so increasing tube current would not reduce radiation dose. Accordingly, the regression was meaningless, and the scatter plots are not shown.

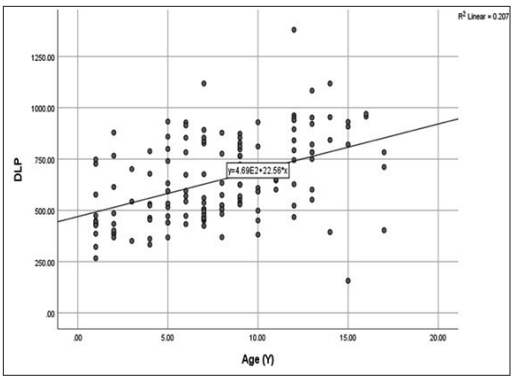

Fig. 6. *Scatter plot showing correlation of DPL with age.*

Impact of Technical Factors on Radiation Dose

We aimed to determine the impact of the technical radiation dose determinants, milliamperage, kVp, and FOV, on radiation dose in terms of the radiation-dose indices (CTDIvol and DLP).

Correlations between CTDIvol and the technical predictors mA, kVp, and FOV:

• The correlation between the X-ray tube current and CTDIvol was found to be insignificant (Table 5).

• In the scatter plot showing the correlation between kVp and CTDIvol, the upward-sloping trend line indicates a moderately positive relationship between kVp and CTDIvol.

• In the scatter plot showing the correlation between the FOV and CTDIvol, the moderate upward trend line indicates a moderately positive relationship between FOV and CTDIvol.

Correlations between DLP and the technical predictors mA, kVp, and FOV:

• The correlation between the X-ray tube current and DLP was found to be insignificant (Table 6).

• In the scatter plot showing the correlation between kVp and DLP, the upward-sloping trend line indicates a moderately positive relationship between kVp and DLP.

• In the scatter plot showing the correlation between the FOV and DLP, the moderate upward trend line indicates a moderately positive relationship between FOV and DLP.

Multiple Linear Regression Analysis

To check the effect of the deterministic technical variables identified (kVp, tube current, and FOV) on CT dose index and DPL, multiple linear regression analysis was performed.

Multiple linear regression for the dependent variable was formulated as a regression line equation comprising an intercept and a set of independent variables, each associated with a specific coefficient (slope). Models were constructed—analogous to a line of best fit—to forecast future values based on existing data.

CT Dose Index Volume

To obtain the regression coefficient for a CTDIvol regression line, standard linear regression methods were used

to estimate the slope and intercept that best fit a dataset of CT imaging parameters and corresponding dose values.

The regression coefficient table showed that the independent variables named kVp and tube current have a statistically significant impact on CTDIvol (P<0.05), but FOV did not (P=0.559) (Table 7).

Table 7.

Regression Coefficients Base Model for the dependent variable CTDIvol.

Coefficients[a]							
Model	Unstandardized Coefficients		Standard. Coeffic.	T	*P.*	Collinearity Statistics	
	B	Std. Error	Beta			Tolerance	VIF
(Constant)	-65.744	11.855		-5.546	<.001		
Peak kilovoltage applied during CT	.758	.128	.774	5.919	<.001	.221	4.526
Tube current (mA) used during CT	.051	.011	.394	4.775	<.001	.555	1.801
FOV the size of the scanned area	.100	.171	.082	.586	.559	.193	5.188
a. Dependent Variable: CTDIvol							

The variance inflation factor (VIF) for FOV was 5.188, exceeding 5, indicating multicollinearity among the independent variables. Thus, it was removed from the regression model due to its insignificant effect and multicollinearity. After removing the FOV, the regression coefficients of the optimal model for the dependent variable, CTDIvol, were obtained (Table 7).

The optimal model showed (Table 8) that the p-values of kVp and tube current are less than 0.05. At the 5% significance level, it can be concluded that the two variables have a statistically significant impact on CTDIvol. Furthermore, the VIF values are below 5, providing further evidence that there is no multicollinearity among the independent variables.

Next, we examined the regression coefficients to discuss the direction and magnitude of their effect on the dependent variable, CTDIvol.

•The kVp regression coefficient is 0.818, which means that CTDIvol will go up by 0.818 units for every kilovoltage increase, assuming that all other factors stay the same.

•The tube current regression coefficient is 0.049, meaning that CTDIvol increases by 0.049 units for every milliampere increase, assuming all other factors remain constant.

The model summary table showed an adjusted R^2 of 0.454, indicating that 45.4% of the total variation in CTDIvol is explained by the independent variables (Table 9).

The ANOVA table showed that the P-value for the F statistic is <0.001. At the 5% significance level, we can say that the fitted model is statistically significant and provides a good fit (Table 10).

Table 8.

Regression Coefficients Optimal Model for the dependent variable CTDIvol.

Coefficients[a]							
Model	Unstandardized Coefficients		Standard. Coeff.	T	*P*	Collinearity Statistics	
	B	Std. Error	Beta			Tolerance	VIF
(Constant)	-69.438	10.013		-6.935	<.001		
Peak kilovoltage applied during CT	.818	.075	.836	10.884	<.001	.638	1.569
Tube current (mA) used during CT	.049	.010	.377	4.902	<.001	.638	1.569
a. Dependent variable: CTDIvol							

Table 9.

Model Summary.

Model Summary				
Model	R	R^2	Adjusted R^2	Std. Error of the estimate
1	.680	.462	.454	7.00308

Table 10.

Analysis of Variance (ANOVA).

Model	Sum of Squares	Df	Mean Square	F	*P*-value
Regression	6019.760	2	3009.880	61.372	<.001
Residual	7013.162	143	49.043		
Total	13032.921	145			

Fitted Equation

CTDIvol = -69.438 + 0.818 × Peak Kilovoltage Applied + 0.049 × Tube Current (in mA)

Therefore, the above CTDIvol best-fitting equation can be solved to obtain the peak kilovoltage to be applied for any tube current and vice versa.

Dose-Length Product

The research aims to assess the impact of peak voltage, tube current, and FOV on DLP. Here, DLP is the dependent variable, and peak voltage, tube current, and FOV are the independent variables. As the dependent variable is continuous, we can perform multiple linear regressions to check the impact. Table 11 presents the regression coefficients for the base model of the dependent variable DLP.

The regression coefficients indicated that the independent variables, peak kilovoltage and tube current, have a statistically significant impact on DLP (P<0.05).

But FOV does not have a significant impact on DLP (*P*=0.399).

Table 11.

Regression Coefficients Base Model for the dependent variable DLP.

Coefficients[a]							
Model	Unstandardized Coefficients		Standard. Coeff.	T	*P*	Collinearity Statistics	
	B	Std. Error	Beta			Tolerance	VIF
(Constant)	-1421.676	268.944		-5.286	<.001		
Peak kilovoltage applied during CT	15.277	2.904	.711	5.261	<.001	.221	4.526
Tube current (mA) used during CT	1.137	.242	.401	4.699	<.001	.555	1.801
FOV the size of the scanned area	3.286	3.886	.122	.846	.399	.193	5.188
a. Dependent Variable: DLP							

The variance inflation factor (VIF) for FOV was 5.188, exceeding 5, indicating multicollinearity among the independent variables. Thus, it was removed from the regression model due to its insignificant effect and multicollinearity. After removal of the FOV, the regression coefficients of the optimal model for the dependent variable, DLP, were obtained (Table 12).

Table 12.

Regression Coefficients Optimal Model for the dependent variable DLP.

Coefficients[a]							
Model	Unstandardized Coefficients		Standard. Coeff.	T	*P*	Collinearity Statistics	
	Std. Error	Beta	B			Tolerance	VIF
(Constant)	-1542.729	227.456		-6.783	<.001		
Peak kilovoltage applied during CT	17.262	1.708	.804	10.108	<.001	.638	1.569
Tube current (mA) used during CT	1.063	.226	.375	4.713	<.001	.638	1.569
a. Dependent Variable: DLP							

The optimal model showed (Table 12) that the *P*-values of kVp and tube current are less than 0.05. At the 5% significance level, it can be concluded that the two variables have a statistically significant impact on DLP. Furthermore, the VIF values are below 5, providing further evidence that there is no multicollinearity among the independent variables.

The obtained regression coefficient values indicate the direction and magnitude of the influence on the dependent variable DLP.

•The kVp regression coefficient is 17.262, which means that DLP will go up by 17.262 units for every kilovoltage increase, assuming that all other factors stay the same.

•The tube current regression coefficient is 1.063, meaning that DLP will increase by 1.063 units for every milliamperage increase, assuming all other factors remain constant.

The model summary table shows that the adjusted R^2 is 0.416, indicating that 41.6% of the total variation in DLP is explained by the independent variables (Table 13).

Table 13.

Model summary.

Model summary				
Model	R	R^2	Adjusted R^2	Std. Error of the estimate
1	.651	.424	.416	159.08418

The ANOVA table showed that the *P*-value for the F statistic is <0.001. At the 5% significance level, we can say that the fitted model is statistically significant and provides a good fit (Table 14).

Table 14.

Analysis of Variance (ANOVA).

Model	Sum of Squares	Df	Mean Square	F	*P*
Regression	2660389.611	2	1330194.805	52.561	<.001
Residual	3619012.235	143	25307.778		
Total	6279401.845	145			

Fitted Equation

DLP = -1542.729 + 17.262 × Peak Kilovoltage Applied + 1.063 × Tube Current (in mA)

Therefore, the DLP best-fit equation can be solved to obtain the kVp to apply for any tube current, and vice versa. Coefficients can be calculated using statistical software (for example, Excel, Python, etc) or manually.

Discussion

Given that the objective of this study was to identify and quantify the impact of key technical and demographic

factors on radiation dose during CT of the brain and head in children, this task was addressed by quantitatively assessing the influence of these determining factors on CTDIvol and DLP. Any factor affecting these indices will, in turn, influence the overall radiation dose. It follows, therefore, that the precise adjustment of key parameters affecting these indices will enable the optimization of radiation dose.

In this study, we identified several key variables that significantly impacted radiation dose in pediatric brain and head CT scans: age, kVp, and scan type. From the regression coefficients (Tables 7 and 11), we observed clearly that the independent variables kVp and mA had a statistically significant impact on dependent variables, CTDIvol and DLP, $P<0.05$ in both cases. However, FOV did not have a significant impact on the CT dose index ($P=0.559$). Accordingly, FOV was excluded from the best-fit equations for CTDIvol and DLP.

The best-fit equations for CTDIvol and DLP in this study were derived from multiple linear regression analysis, which facilitated the determination of mA and kVp values corresponding to the manual CTDIvol settings.

Our findings suggest that as pediatric patients grow older, their exposure to radiation increases due to larger head size, underscoring the importance of age-adjusted protocols. In our study, radiation exposure was significantly dependent on scan type, with brain CT scans generally yielding lower exposure than head CT scans. This finding has direct implications for clinical practice, underscoring the importance of pediatric-specific protocols to minimize radiation exposure during head and brain scans. For instance, reducing the milliamperage and adjusting the scan parameters based on patient size and age can significantly reduce the radiation dose, as shown by the best-fit equation in our study and by previous studies.[15] The findings of this study agree with those of previous studies that used targeted brain scan protocols (which restrict the scan range to the brain) rather than broader adult head scan protocols (which may include the skull base and upper neck) and significantly reduced radiation exposure. Accordingly, we recommend that pediatric institutions establish specific protocols tailored to individual characteristics to improve patient care and safety. Additionally, automatic exposure control systems can minimize radiation exposure by automatically adjusting the milliamperage based on the patient's size.[16]

According to previous studies, pediatric patients are readily affected by radiation-induced effects and may receive up to three times more radiation per unit of body weight than adults.[17] This calls for urgent measures that utilize existing protocols to reduce radiation exposure while other accurate diagnostic tools are being developed. In the present study, we examined the various technical and demographic parameters that affect radiation dose levels in head and brain CT scans in children by analyzing CTDIvol and DLP. We found that brain scan procedures developed for children reduced their radiation exposure more effectively than those for the head alone, demonstrating the relevance of these procedures through appropriate naming and standardization. Statistical analyses have shown that applying age-adjusted dose changes can reduce the overall radiation exposure to young patients by up to 30% when automated exposure control systems are used.[18]

One important consideration in this study was selecting reference points to establish DRLs that fell within the 75th percentile at our hospital. The 75th percentile values of our local dose distribution were determined in accordance with the European guidelines on diagnostic reference levels for pediatric imaging (ACR, 2015). The third quartiles of the local CTDIvol and DLP values for both pediatric brain and head CT scans will be continuously refined and incorporated into the national diagnostic reference levels for pediatric CT imaging, once developed.

The pediatric diagnostic reference levels in this study were established for children grouped by age (e.g., 1–4-year-olds); however, groupings should preferably be based on body weight (e.g., 5–15 kg group),[19,5] as weight better reflects body size than age. Weight-based groupings are therefore recommended to establish diagnostic reference levels in body CT. Nevertheless, age-based groupings are recommended for brain CT scans because weight does not reflect head size.

Study Limitations

This study had several limitations. Its retrospective design introduced the potential for selection bias and unmeasured confounding. Furthermore, the single-center design may have limited the generalizability of the findings to other institutions with different CT equipment and patient demographics. Consequently, these results should be interpreted in the context of the present study, and future multicenter, prospective studies are warranted to validate and extend our findings. Finally, the influence of certain technical parameters, such as scan time and contrast use, warrants further investigation to build a more comprehensive model for dose optimization. The application of advanced imaging techniques, such as iterative reconstruction algorithms, should be considered to reduce radiation exposure without compromising image quality.[20]

This study underscores the need for patient-specific dose adjustment, particularly with respect to age, and affirms the value of automated exposure control in minimizing radiation exposure. By aligning with global safety initiatives, such as the Image Gently campaign, our findings provide an evidence-based strategy to enhance safety in pediatric neuroimaging and support the dual development of standardized low-dose CT protocols and individualized procedures based on patient age and clinical indications. To translate these findings into practice, future research should prioritize validating these protocols, and policymakers are urged to integrate this evidence into formal guidelines and regulations for pediatric imaging.

Conclusions

In this study, age, milliamperage, peak kilovoltage, field of view, and scan type emerged as the key determinants

of radiation dose in pediatric brain CT scans, as shown by their effects on CTDIvol and DLP. The positive relationships among age, milliamperage, and field of view with radiation dose underscore the importance of strict pediatric optimization protocols. While the patient data revealed key CT measurement parameters, the regression analysis showed that patient age, peak kilovoltage, and mA readings significantly impacted the CTDIvol levels (P-values <0.05). Our results affirm the need for effective reforms in CT protocol standardization, personnel training, and national dose regulations, especially in regions where pediatric diagnostic reference levels do not exist. The necessity of a diagnostic test should be weighed repeatedly against the associated radiation risk in the pursuit of safer imaging. As Salah et al.[21] noted, "Optimizing CT techniques is important, primarily for pediatrics, being more radiosensitive to radiation than adults." This study contributes to that optimization by highlighting the levels at which doses can be applied scientifically and safely and thus controlled effectively.

Institutional Review Board Statement

The study was approved by the Standing Committee for Scientific Research at Jazan University, reference No: REC-46/07/1357.

Informed Consent Statement

Patient consent was waived due to the retrospective nature of this study, which involved no direct interaction with human subjects or new data collection; the research used existing deidentified patient data from hospital records, qualifying for a waiver under minimal risk and retrospective data criteria.

Data Availability Statement

The datasets used in this study are available on request from the corresponding author.

Author Contribution Statement

Nouf Abuhadi confirms sole responsibility for all aspects of the research.

Conflicts of Interest

The author has declared no conflict of interest.

References

1. Hsieh J, Flohr T. Computed tomography recent history and future perspectives. J Med Imaging (Bellingham). 2021 Sep;8(5):052109. doi: 10.1117/1.JMI.8.5.052109. Epub 2021 Aug 11. PMID: 34395720; PMCID: PMC8356941.
2. Cao CF, Ma KL, Shan H, Liu TF, Zhao SQ, Wan Y, Jun-Zhang, Wang HQ. CT Scans and Cancer Risks: A Systematic Review and Dose-response Meta-analysis. BMC Cancer. 2022 Nov 30;22(1):1238. doi: 10.1186/s12885-022-10310-2. PMID: 36451138; PMCID: PMC9710150.
3. Abalo KD, Rage E, Leuraud K, Richardson DB, Le Pointe HD, Laurier D, Bernier MO. Early life ionizing radiation exposure and cancer risks: systematic review and meta-analysis. Pediatr Radiol. 2021 Jan;51(1):45-56. doi: 10.1007/s00247-020-04803-0. Epub 2020 Sep 10. Erratum in: Pediatr Radiol. 2021 Jan;51(1):157-158. doi: 10.1007/s00247-020-04883-y. PMID: 32910229.
4. Sulieman A. Establishment of diagnostic reference levels in computed tomography for paediatric patients in Sudan: a pilot study. Radiat Prot Dosimetry. 2015 Jul;165(1-4):91-4. doi: 10.1093/rpd/ncv109. Epub 2015 Apr 1. PMID: 25836694.
5. The 2007 Recommendations of the International Commission on Radiological Protection. ICRP publication 103. Ann ICRP. 2007;37(2-4):1-332. doi: 10.1016/j.icrp.2007.10.003. PMID: 18082557.
6. Constine LS, Olch AJ, Jackson A, Hua CH, Ronckers CM, Milano MT, Marcus KJ, Yorke E, Hodgson DC, Howell RM, Hudson MM, Williams JP, Marples B, C M Kremer L, Marks LB, Bentzen SM. Pediatric Normal Tissue Effects in the Clinic (PENTEC): An International Collaboration to Assess Normal Tissue Radiation Dose-Volume-Response Relationships for Children With Cancer. Int J Radiat Oncol Biol Phys. 2024 Jun 1;119(2):316-320. doi: 10.1016/j.ijrobp.2020.10.040. Epub 2021 Mar 30. PMID: 33810949.
7. Sulieman A, Adam H, Elnour A, Tamam N, Alhaili A, Alkhorayef M, et al. Patient radiation dose reduction using a commercial iterative reconstruction technique package. Radiation Physics and Chemistry. 2021;178, 108996.
8. Dudhe SS, Mishra G, Parihar P, Nimodia D, Kumari A. Radiation Dose Optimization in Radiology: A Comprehensive Review of Safeguarding Patients and Preserving Image Fidelity. Cureus. 2024 May 22;16(5):e60846. doi: 10.7759/cureus.60846. PMID: 38910606; PMCID: PMC11191847.
9. Sulieman A, Elnour A, Mahmoud MZ, Alkhorayef M, Hamid O, Bradley DA. Diagnostic reference level for computed tomography abdominal examinations: A multicentre study. Radiation Physics and Chemistry. 2020;174, 108963.
10. El-Nachef L, Al-Choboq J, Restier-Verlet J, Granzotto A, Berthel E, Sonzogni L, Ferlazzo ML, Bouchet A, Leblond P, Combemale P, Pinson S, Bourguignon M, Foray N. Human Radiosensitivity and Radiosusceptibility: What Are the Differences? Int J Mol Sci. 2021 Jul 2;22(13):7158. doi: 10.3390/ijms22137158. PMID: 34281212; PMCID: PMC8267933.
11. Akinwande AM, Ugwuanyi DC, Chiegwu HU, Idigo F, Ogolodom MP, Anakwenze CP, Abi R, Odukoya O. Radiotherapy services in low resource settings: The situation in Nigeria. SAGE Open Med. 2023 Feb 7;11:20503121231153758. doi: 10.1177/20503121231153758. PMID: 36778199; PMCID: PMC9909043.
12. Malchair F, Maccia C. Practical advice for optimal CT scanner dose in children. Radioprotection. 2020;55(2):117–122. Doi: 10.1051/radiopro/2020046
13. Manssor E, Abuderman A, Osman S, Alenezi SB, Almehemeid S, Babikir E, et al. Radiation doses in chest, abdomen and pelvis CT procedures. Radiation protection

dosimetry. 2015;165(1-4):194–198. doi:10.1093/rpd/ncv107
14. Althammer A, Prückner S, Gehring GC, Lieftüchter V, Trentzsch H, Hoffmann F. Systemic review of age brackets in pediatric emergency medicine literature and the development of a universal age classification for pediatric emergency patients - the Munich Age Classification System (MACS). BMC Emerg Med. 2023 Jul 25;23(1):77. doi: 10.1186/s12873-023-00851-5. Erratum in: BMC Emerg Med. 2024 Aug 9;24(1):145. doi: 10.1186/s12873-024-01064-0. PMID: 37491219; PMCID: PMC10369835.
15. ICRP; Khong PL, Ringertz H, Donoghue V, Frush D, Rehani M, Appelgate K, Sanchez R. ICRP publication 121: radiological protection in paediatric diagnostic and interventional radiology. Ann ICRP. 2013 Apr;42(2):1-63. doi: 10.1016/j.icrp.2012.10.001. Erratum in: Ann ICRP. 2020 Oct 5:146645320966413. doi: 10.1177/0146645320966413. Erratum in: Ann ICRP. 2021 Mar 25:1466453211000254. doi: 10.1177/01466453211000254. PMID: 23218172.
16. Singh S, Kalra MK, Thrall JH, Mahesh M. Automatic exposure control in CT: applications and limitations. J Am Coll Radiol. 2011 Jun;8(6):446-9. doi: 10.1016/j.jacr.2011.03.001. PMID: 21636062.
17. Huda W, Vance A. Patient radiation doses from adult and pediatric CT. AJR Am J Roentgenol. 2007;188(2), 540–546. doi:10.2214/AJR.06.0101
18. Greffier J, Pereira F, Macri F, Beregi JP, Larbi A. CT dose reduction using Automatic Exposure Control and iterative reconstruction: A chest paediatric phantoms study. Phys Med. 2016 Apr;32(4):582-9. doi: 10.1016/j.ejmp.2016.03.007. Epub 2016 Apr 4. PMID: 27056436.
19. European Commission. European guidelines on diagnostic reference levels for paediatric imaging (Radiation Protection 185). Publications Office of the European Union; 2018
20. Brady SL, Yee BS, Kaufman RA. Characterization of adaptive statistical iterative reconstruction algorithm for dose reduction in CT: A pediatric oncology perspective. Med Phys. 2012 Sep;39(9):5520-31. doi: 10.1118/1.4745563. PMID: 22957619.
21. Salah H, Rabbaa M, Abuljoud M, Babikir E, Alkhorayef M, Tamam N, Tahir D, Sulieman A, Bradley DA. Paediatric effective radiation doses during brain computed tomography angiography procedure. Appl Radiat Isot. 2023 Feb;192:110610. doi: 10.1016/j.apradiso.2022.110610. Epub 2022 Dec 7. PMID: 36525913.

***Correspondence:** Nouf Hussain Abuhadi. E-mail: nabuhadi@jazanu.edu.sa*

International Journal of Biomedicine 16(2) (2026) 197-200
http://dx.doi.org/10.21103/Article16(2)_OA6

ORIGINAL ARTICLE

INTERNATIONAL JOURNAL OF BIOMEDICINE

Ultrasound Evaluation of Renal Measurements in Type 1 Diabetes Patients: Impact of Disease Duration

Elrashed AbdElrahim[1], Raghad Jemeen Al-Malki[1], Rehab Ali Al-Kathiri[1], Jana Awad Al-Thobaity[1], Shahad Abdullah Al-Kaabi[1], Ibtihal Saud Al-Withainani[1], Mona Elhaj[1], Bahaaedin A. Elkhader[1], Hamid Osman[1*]

[1]*Department of Radiological Sciences, College of Applied Medical Sciences, Taif University, Taif, Saudi Arabia*

Abstract

Background: Type 1 diabetes mellitus (T1DM) is a chronic metabolic disorder associated with progressive renal complications, often leading to diabetic nephropathy. Early detection of renal morphological changes is essential for prevention and management. This study aimed to evaluate the impact of T1DM duration on renal size and morphology using ultrasound, with a focus on kidney length, width, thickness, and cortical characteristics.

Methods and Results: A retrospective cross-sectional study was conducted on 94 patients with T1DM in Taif, Saudi Arabia, between November 2024 and May 2025. Patients of both sexes, aged 1–70 years, underwent renal ultrasound in accordance with standard hospital protocols. Kidney dimensions (length, width, thickness) and cortical echogenicity were measured and compared across different disease durations and age groups.

Slight renal enlargement was observed in 73.7% of patients, predominantly in younger age groups (10–20 years), while 26.3% demonstrated slight renal atrophy, more frequent among older patients. The length and width of the kidneys gradually decreased 10 years after disease onset, reflecting progressive loss of parenchyma. The duration of longer diabetes appears to increase the likelihood of kidney atrophy, especially in older patients.

Conclusion: Ultrasound is a non-invasive and effective tool for monitoring renal morphological changes in patients with T1DM. Early-stage kidney hypertrophy trend appears to progress toward atrophy with longer disease duration, especially in older patients. underscoring the importance of routine renal monitoring to identify early diabetic nephropathy and guide timely intervention. (**International Journal of Biomedicine. 2026;16(2):197-200.**)

Keyword: ultrasound • kidney dimensions • type 1 diabetes mellitus

For citation: AbdElrahim E, Al-Malki RJ, Al-Kathiri RA, Al-Thobaity JA, Al-Kaabi SA, Al-Withainani IS, Elkhader ME, Osman BAH. Ultrasound Evaluation of Renal Measurements in Type 1 Diabetes Patients: Impact of Disease Duration. International Journal of Biomedicine. 2026;16(2):197-200. doi:10.21103/Article16(2)_OA6

Introduction

Type 1 diabetes mellitus (T1DM), also known as insulin-dependent diabetes mellitus, is a chronic autoimmune disease characterized by the immune-mediated destruction of the insulin-producing β-cells of the pancreas, leading to an insulin deficiency. This deficiency impairs the proper regulation of blood glucose levels, leading to hyperglycemia and lifelong dependence on daily exogenous insulin therapy.

Type 1 diabetes mellitus often appears in childhood or young adulthood, though it can develop at any age.[1] Patients with T1DM often experience symptoms such as increased thirst, frequent urination, and weight loss. In acute cases, patients may present with diabetic ketoacidosis, a serious complication. Early diagnosis depends on detecting specific antibodies that signal an immune response against the pancreas.[1]

In Saudi Arabia, the incidence of diabetes is rising, including in younger populations. The high rates of diabetes make it essential to understand the impact on other organs, especially the kidneys, which are often affected by long-term high blood glucose.

This research examined how kidney size and shape change over time in patients with T1DM, using ultrasound to track these changes and considering how disease duration may affect kidney health and size. Ultrasound diagnostics enable

the detection of anomalies in kidney shape and size. However, kidney dimensions may vary not only with pathology but also with the patient's physique, age, and race.[2]

Normal kidney measurements, the length of the kidney is between 9-12 cm, more than 2 cm is diagnosed with abnormal kidney enlargement, as for the width, it is between 4-6 cm, and the thickness is 3.5 cm, and a slight difference in measurement is not considered abnormal due to the difference in measurements according to the scanning angle.[3]

The renal sinus is a highly echogenic region due to the presence of calyces, vessels, and fat.[4] The measurement of cortical thickness to determine the well-being of the kidneys. The echogenicity of the kidney tissue assesses changes in echotexture to determine the presence of fibrosis or scarring. One important evaluation method for the renal system is Doppler ultrasound, which can be used to compute resistance index values, useful for assessing vascular resistance. Doppler also assesses blood flow, which can detect flow disorders. As regards most patients with advanced chronic kidney disease (CKD), cysts or calcifications are typically present in X-rays.[5]

Diabetes mellitus causes chronic hyperglycemia, leading to secondary microvascular complications through endothelial damage, capillary thickening, and tissue ischemia. Both maladaptive and adaptive responses are possible from the damaged kidney. The size and function of the remaining tubules, as well as glomerular pressure, increase in response to early adaptive reactions that increase blood flow to the remaining glomeruli.[6] A section of the kidney dies; however, increased glomerular pressure causes each nephron to generate more filtration (hyperfiltration), resulting in overall organ hypertrophy. If injury to normal nephrons progresses, the early adaptive response becomes more pronounced, leading to a gradual reduction in kidney size and function.[7] Diabetic nephropathy is described as the combination of structural and functional problems in the kidneys caused by diabetes. This involves atrophy (reduction in size), hypertrophy (abnormal increase in size), thickening of glomerular and tubular basement membranes, formation of extracellular matrix in the glomerulus (glomerulosclerosis), and tubular atrophy.[8]

Although diabetes is highly prevalent in Saudi Arabia, limited data exist on how T1DM affects renal dimensions across different age groups using ultrasound. The objective of this study was to investigate the impact of T1DM duration on kidney measurements using ultrasound across different age groups.

Materials and Methods

A retrospective cross-sectional study was conducted in Taif city from November 2024 to May 2025. The study population comprises 94 T1DM patients. The study included males and females aged 1 to 70 years. The patient's kidneys were scanned by ultrasound at Taif hospitals, following the hospital's routine scan protocols. The ultrasound technique started with preparation and position.[9]

For kidney scanning, a 3.5 MHz transducer is used, while the 5.0 MHz transducer is used for children or thin patients.[9] The transducer was placed on the upper right or left side and started with a longitudinal scan, then a transverse scan, with the liver acting as an acoustic window for the right kidney. The lateral position was used in cases of gas retention, or the patient was asked to drink water, thus filling the stomach with fluid as an acoustic window that allows us to see the kidneys.[9]

Researchers measured the kidney size (length, width, thickness) and the shape (echogenicity and cortical thickness). Data collection was conducted using a specialized registration form developed by the researchers, which included all variables necessary for this study.

Statistical analysis was performed using SPSS v.25.0 (SPSS Inc., Armonk, NY; IBM Corp.). Baseline characteristics were summarized as frequencies and percentages. Group comparisons were performed using the chi-square test. A *P*-value <0.05 was considered statistically significant.

Results

The distribution of kidney measurements across different age groups is summarized in Table 1. The majority of T1DM patients (73.7%) showed slight kidney enlargement, while 26.3% had slight atrophy (Figure 1). Among younger patients (10–19 years and 20-29 years), slight enlargement was predominant, with 100% and 88.2% of cases, respectively. In contrast, the frequency of slight atrophy increased progressively with advancing age, reaching 50% in the 70-79 age group. Despite this apparent trend toward increased atrophy with age, the difference in kidney measurements among the age groups was not statistically significant (P = 0.105) (Table 1).

Table 1.

Distribution of kidney measurement changes across age groups in T1DM patients.

Age Range (years)	Slight Atrophy n (%)	Slight Enlargement n (%)	Total n (%)
10–19	0 (0.0%)	14 (100.0%)	14 (100.0%)
20–29	2 (11.8%)	15 (88.2%)	17 (100.0%)
30–39	4 (40.0%)	6 (60.0%)	10 (100.0%)
40–49	4 (30.8%)	9 (69.2%)	13 (100.0%)
50–59	6 (33.3%)	12 (66.7%)	18 (100.0%)
60–69	8 (38.1%)	13 (61.9%)	21 (100.0%)
70–79	1 (50.0%)	1 (50.0%)	2 (100.0%)
Total	25 (26.3%)	70 (73.7%)	95 (100.0%)

Chi-square test: P = 0.105

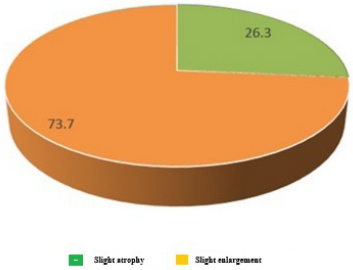

Fig. 1. *Kidney dimensions.*

Ultrasound measurements of renal dimensions in patients with T1DM demonstrated distinct trends correlated with disease duration (Figure 2). Both kidney length and width were assessed over a disease span of 1 to 20 years.

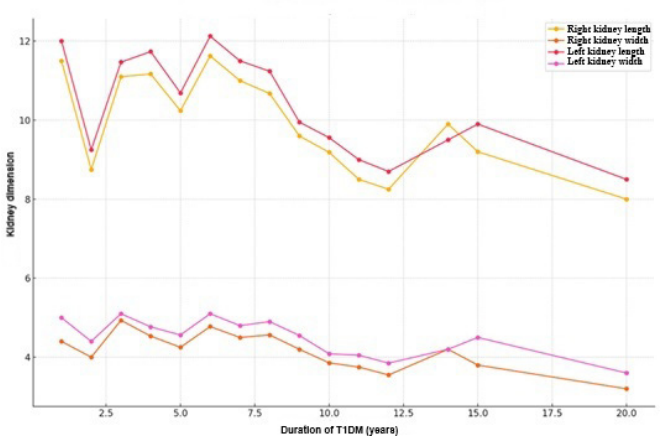

Fig. 2. *Changes in kidney length and width over time in T1DM patients as measured by ultrasound.*

By Year 1 of disease onset, both kidneys were slightly enlarged, with the left measuring approximately 12 cm in length, slightly exceeding the right. This finding is consistent with early-stage diabetic renal hypertrophy, likely reflecting compensatory glomerular hyperfiltration.

By Year 2, a notable reduction in kidney dimensions was observed, particularly in the right kidney. This abrupt decrease may indicate early parenchymal changes or variability in individual physiological responses during the initial phase of glycemic control.

Between Years 3 and 10, renal measurements remained relatively stable, with only minor fluctuations. The left kidney consistently measured longer and wider than the right, consistent with established anatomical asymmetry. Beginning around Year 10, a gradual and sustained decline in both renal length and width was evident bilaterally. By Year 20, renal dimensions had markedly decreased, with the right kidney width approaching 3.5 cm. These findings are indicative of progressive nephron loss and chronic parenchymal damage associated with diabetic nephropathy.

Discussion

Our findings support the hypothesis that the duration of T1DM influences kidney morphology through gradual, measurable changes in size and shape that could ultimately affect kidney health. In our sample of 95 T1DM patients, the majority exhibited slight renal enlargement (73.7%), while a smaller proportion demonstrated slight renal atrophy (26.3%). These findings are consistent with previous studies, including those by Tonneijc et al.,[10] which identified early-stage renal hypertrophy associated with glomerular hyperfiltration in patients with T1DM. With a mean duration of diabetes of approximately 7.4 years in our cohort, early renal enlargement predominates in most patients, supporting the idea that, in the initial stages, kidney changes may be associated with hyperfiltration and compensatory enlargement.[11] As the disease progresses, however, the prevalence of renal atrophy increases, suggesting that long-term hyperglycemia may eventually lead to kidney structural deterioration. This aligns with our hypothesis that kidney size and shape change gradually and measurably as the duration of diabetes increases, with these changes potentially having a lasting effect on kidney health.[12] Further analysis of age groups revealed a trend toward greater renal atrophy in older patients, though this association was not statistically significant (P=0.105). Interestingly, patients in the age of 30-39 years showed a 40%of renal atrophy, hinting that those with longer disease duration, even at a relatively young age, may be more susceptible to kidney structural changes. While the results were not statistically conclusive, they reinforce the hypothesis that kidney morphology in younger patients, particularly those in the early stages of T1DM, tends to be either preserved or enlarged. In contrast, older patients, or those with longer disease duration, are more likely to exhibit signs of renal atrophy.[13] Overall, this study highlights the utility of ultrasonography as an effective, non-invasive tool for detecting early morphological changes in diabetic kidneys. These changes, particularly with longer diabetes duration, may be critical in assessing kidney health and the potential risk for chronic kidney disease.[14] Our results suggest that monitoring kidney size and shape over time could provide valuable insights into the progression of kidney damage in T1DM patients, emphasizing the importance of early intervention and regular assessment to prevent long-term renal complications.[15]

The major strength of this study is the fact that it used ultrasound. Ultrasound is a non-invasive, practical, and widely available imaging technique for the early detection of morphological changes in the kidneys of individuals with diabetes. This will allow follow-up and early intervention strategies to be implemented in time to prevent long-term kidney complications.

However, some limitations should be noted. Primarily, generalizing the findings to the whole population is somewhat hampered by the relatively small sample size and the study's limited scope to one center. Second, it cannot be proven that a direct link exists between structural changes and kidney dysfunction due to the lack of biochemical correlates, such as serum creatinine, glomerular filtration rate, and urinary albumin.

Nevertheless, the results we obtained are clinically significant. Monitoring kidney size and shape over time using ultrasound is an effective tool for detecting diabetic nephropathy. Integrating ultrasound with kidney biomarkers may contribute to future studies, improve risk assessment, and enable timely intervention. Ultimately, these strategies may play a crucial role in reducing the burden of chronic kidney disease in patients with T1DM.

Conclusion

Ultrasound imaging is an effective and safe way to measure the kidneys, detect early changes, and monitor and intervene in kidney health in T1DM. To determine the correct kidney measurements, it is necessary to know the measurements of healthy adults, as they are affected by various factors. Our

study supports the hypothesis that the duration of T1DM leads to gradual changes, and most of them showed renal hypertrophy (73.7%), with some showing renal dystrophy (26.3%).

In this study, these changes are in line with previous studies on early-stage renal hypertrophy and glomerular hyperfiltration. The duration of longer diabetes appears to increase the likelihood of kidney atrophy, especially in older patients. We found at King Abdulaziz Specialist Hospital (KASH) in Taif city and at King Faisal that there is a need to study the normal values of kidney size among Saudis, and we recommend expanding the scope of this study throughout Saudi Arabia.

Since T1DM is a growing problem in Saudi Arabia, more research is needed in other parts of the country to better understand its complications and risk factors to reduce its burden.

Authors Contributions

Elrashed AbdElrahim: Supervision, Conceptualization, Methodology, Data analysis and interpretation, Writing – review and editing.
Raghad Jemeen Al-Malki: Methodology, Writing – original draft.
Rehab Ali Al-Kathiri: Methodology, Writing – original draft.
Jana Awad Al-Thobaity: Investigation, Data curation
Shahad Abdullah Al-Kaabi: Investigation, Data curation
Ibtihal Saud Al-Withainani: Investigation, Data curation
Mona Elhaj: Data analysis and Interpretation, Writing – original draft .
Bahaaedin A. Elkhader: Methodology, Writing – original draft.
Hamid Osman: Supervision, Conceptualization, Methodology, Writing – review and editing.

All authors have read and approved the final manuscript.

Ethical Statement

The Local Bioethics Committee and Research Administration of Taif Health Cluster, Saudi Arabia, accepted this study (approval number: E-32-2025; IRB registration number: H-02-T-123). All patients, their parents, or legal guardians provided informed consent before participation.

Conflict of Interest

The authors have declared no conflict of interest.

References

1. Sacks DB, Arnold M, Bakris GL, Bruns DE, Horvath AR, Lernmark Å, et al. Guidelines and Recommendations for Laboratory Analysis in the Diagnosis and Management of Diabetes Mellitus. Diabetes Care. 2023 Oct 1;46(10):e151-e199. doi: 10.2337/dci23-0036.
2. American Diabetes Association. Diagnosis and classification of diabetes mellitus. Diabetes Care. 2014 Jan;37 Suppl 1:S81-90. doi: 10.2337/dc14-S081. PMID: 24357215.
3. International Expert Committee. International Expert Committee report on the role of the A1C assay in the diagnosis of diabetes. Diabetes Care. 2009 Jul;32(7):1327-34. doi: 10.2337/dc09-9033.
4. Meijnikman AS, De Block CEM, Dirinck E, Verrijken A, Mertens I, Corthouts B, Van Gaal LF. Not performing an OGTT results in significant underdiagnosis of (pre)diabetes in a high risk adult Caucasian population. Int J Obes (Lond). 2017 Nov;41(11):1615-1620. doi: 10.1038/ijo.2017.165.
5. Knowler WC, Barrett-Connor E, Fowler SE, Hamman RF, Lachin JM, Walker EA, Nathan DM; Diabetes Prevention Program Research Group. Reduction in the incidence of type 2 diabetes with lifestyle intervention or metformin. N Engl J Med. 2002 Feb 7;346(6):393-403. doi: 10.1056/NEJMoa012512.
6. Tuomilehto J, Lindström J, Eriksson JG, Valle TT, Hämäläinen H, Ilanne-Parikka P, et al.; Finnish Diabetes Prevention Study Group. Prevention of type 2 diabetes mellitus by changes in lifestyle among subjects with impaired glucose tolerance. N Engl J Med. 2001 May 3;344(18):1343-50. doi: 10.1056/NEJM200105033441801.
7. Diabetes Prevention Program Research Group. HbA1c as a predictor of diabetes and as an outcome in the diabetes prevention program: a randomized clinical trial. Diabetes Care. 2015 Jan;38(1):51-8. doi: 10.2337/dc14-0886.
8. Echouffo-Tcheugui JB, Selvin E. Prediabetes and What It Means: The Epidemiological Evidence. Annu Rev Public Health. 2021 Apr 1;42:59-77. doi: 10.1146/annurev-publhealth-090419-102644.
9. Chadha C, Pittas AG, Lary CW, Knowler WC, Chatterjee R, Phillips LS, et al.; D2d Research Group. Reproducibility of a prediabetes classification in a contemporary population. Metabol Open. 2020 Mar 7;6:100031. doi: 10.1016/j.metop.2020.100031.
10. Tonneijck L, Muskiet MH, Smits MM, van Bommel EJ, Heerspink HJ, van Raalte DH, Joles JA. Glomerular Hyperfiltration in Diabetes: Mechanisms, Clinical Significance, and Treatment. J Am Soc Nephrol. 2017 Apr;28(4):1023-1039. doi: 10.1681/ASN.2016060666.
11. Expert Committee on the Diagnosis and Classification of Diabetes Mellitus. Report of the expert committee on the diagnosis and classification of diabetes mellitus. Diabetes Care. 2003 Jan;26 Suppl 1:S5-20. doi: 10.2337/diacare.26.2007.s5.
12. Klein KR, Walker CP, McFerren AL, Huffman H, Frohlich F, Buse JB. Carbohydrate Intake Prior to Oral Glucose Tolerance Testing. J Endocr Soc. 2021 Mar 29;5(5):bvab049. doi: 10.1210/jendso/bvab049.
13. Mottl AK, Alicic R, Argyropoulos C, Brosius FC, Mauer M, Molitch M, et al. KDOQI US Commentary on the KDIGO 2020 Clinical Practice Guideline for Diabetes Management in CKD. Am J Kidney Dis. 2022 Apr;79(4):457-479. doi: 10.1053/j.ajkd.2021.09.010.
14. Kidney Disease: Improving Global Outcomes (KDIGO) Diabetes Work Group. KDIGO 2022 Clinical Practice Guideline for Diabetes Management in Chronic Kidney Disease. Kidney Int. 2022 Nov;102(5S):S1-S127. doi: 10.1016/j.kint.2022.06.008.
15. Afkarian M, Zelnick LR, Hall YN, Heagerty PJ, Tuttle K, Weiss NS, de Boer IH. Clinical Manifestations of Kidney Disease Among US Adults With Diabetes, 1988-2014. JAMA. 2016 Aug 9;316(6):602-10. doi: 10.1001/jama.2016.10924.

Correspondence:
Prof. Hamid Osman Hamid. E-mail: hamidsssan@yahoo.com

International Journal of Biomedicine 16(2) (2026) 201-206
http://dx.doi.org/10.21103/Article16(2)_OA7

ORIGINAL ARTICLE

INTERNATIONAL JOURNAL OF BIOMEDICINE

Impact of Vitamin D Levels on Disease Control Across Asthma Subtypes in Mixed-Care Settings

Mehmet Hoxha[1,2*], Eralda Lekli[1,3], Dorian Shkembi[1], Ester Ndreu[1], Xhein Hajrulla[1], Etleva Qirko[1,2]

[1]*Department of Internal Medicine, Faculty of Medicine, University of Medicine, 1005 Tirana, Albania*
[2]*Service of Allergology, University Hospital Center Mother Teresa, 1005 Tirana, Albania*
[3]*Salus Hospital Tirana, 1000 Tirana, Albania*

Abstract

Background: Vitamin D has been implicated in asthma pathophysiology through immunomodulatory and anti-inflammatory mechanisms, although evidence regarding its association with asthma control remains inconsistent. There are no data for the Albanian population that we can use to investigate the level of serum 25(OH)D and its correlation with clinical variables in asthma patients

Methods and Results: This cross-sectional study included 163 adult patients diagnosed with bronchial asthma who were ambulatory, consulted, or hospitalized in the University Hospital Center Tirana, Albania, between November 2024 and October 2025. Asthma control was assessed using the Asthma Control Visual Analogue Scale (AC-VAS; 0-25). Serum 25(OH)D concentration was measured by chemiluminescent immunoassay (CLIA). The primary outcome variable was asthma control measured by the AC-VAS score. Serum 25(OH)D (ng/mL) was analyzed both as a continuous variable and as a categorical variable. Associations were examined using non-parametric tests, linear regression analysis, and moderation analysis (PROCESS macro) to explore potential effect modification by vitamin D status.

Serum 25(OH)D levels were 18.35±8.72 ng/mL, indicating a high prevalence of deficiency. Spearman's rank correlation analysis demonstrated a statistically significant negative correlation between age and serum 25(OH)D levels ($\rho = -0.24$, $P = 0.003$). Serum 25(OH)D levels were positively associated with AC-VAS scores, although this association did not reach statistical significance ($P = 0.097$). Spearman's rank correlation analysis demonstrated a statistically significant negative correlation between AC-VAS scores and age ($\rho = -0.19$, $P = 0.015$), as well as between AC-VAS scores and body mass index (BMI) ($\rho = -0.17$, $P = 0.031$). In the multivariable-adjusted general linear model, age remained independently and negatively associated with AC-VAS scores (B = −0.048, SE = 0.022; $P = 0.030$). Serum 25(OH)D levels (B = 0.039, SE = 0.036; $P = 0.269$) and BMI (B = −0.065, SE = 0.057; $P = 0.253$) were not significantly associated with asthma control after adjustment. Asthma phenotype remained statistically significantly associated with AC-VAS scores in the adjusted model (global test $P = 0.031$). Among the phenotype categories, phenotype 6 was independently associated with higher AC-VAS scores than phenotype 1 (B = 3.612, SE = 1.198; $P = 0.003$). The moderation analysis indicated that the association between BMI and asthma control differed according to 25(OH)D category, with a significant conditional effect observed only at serum 25(OH)D levels ≥ 20 ng/mL.

Conclusion: Vitamin D deficiency was highly prevalent among Albanian adults with asthma but was not independently associated with asthma control. Asthma control was associated with age, body mass index, and asthma phenotype. Vitamin D did not show a direct effect but appeared to modify the association between BMI and asthma control, suggesting a context-dependent role. Further longitudinal and interventional studies are required to confirm these findings and clarify their clinical implications. (**International Journal of Biomedicine. 2026;16(2):201-206.**)

Keywords: vitamin D • asthma control • body mass index • asthma phenotype • moderation analysis

For citation: Hoxha M, Lekli E, Shkembi D, Ndreu E, Hajrulla X, Qirko E. Impact of Vitamin D Levels on Disease Control Across Asthma Subtypes in Mixed-Care Settings. International Journal of Biomedicine. 2026;16(2):201-206. doi:10.21103/Article16(2)_OA7

Introduction

Asthma is a clinically heterogeneous syndrome characterized by chronic airway inflammation and airway hyperresponsiveness, its hallmark features. Distinct aggregations of demographic and clinical attributes have been delineated as "clinical asthma phenotypes," generally showing limited correlation with discrete underlying pathobiological mechanisms or differential therapeutic responsiveness.[1] Vitamin D may influence asthma through effects on lung development, immune regulation, and airway smooth-muscle remodeling. Many studies suggest that lower vitamin D levels are linked to more severe asthma, though results are not always consistent. These potential effects have led to interest in using vitamin D as a preventive or therapeutic option in children with asthma.[2]Recent investigations have identified a correlation between vitamin D deficiency and an elevated risk of both asthma onset and exacerbation.[3,4] Vitamin D deficiency was associated with increased risk of asthma, current wheezing, and reduced lung function in a large study of British adults, suggesting that higher vitamin D levels may reduce asthma risk and improve disease control.[5] A systematic review of randomized controlled trials up to November 2022 examined the effects of vitamin D supplementation in children and adults with asthma. While vitamin D did not reduce type 2 inflammatory markers such as IgE or eosinophils, it was associated with increased serum IL-10, an anti-inflammatory cytokine. These findings suggest that vitamin D may modulate anti-inflammatory pathways rather than directly affecting type 2 inflammation.[6] Biomarkers indicative of type 2-driven airway inflammation have particular clinical utility, especially for phenotyping, stratifying, and managing refractory and severe asthma.

There are no data for the Albanian population that we can use to investigate the level of serum 25(OH)D and its correlation with clinical variables in asthma patients. This study provides evidence for a potential association between serum vitamin D levels and reported asthma control, potentially linked to disease severity, laying the groundwork for future research and informing possible preventive and therapeutic strategies in the Albanian population.

Materials and Methods

This cross-sectional study included 163 adult patients diagnosed with bronchial asthma who were ambulatory, consulted, or hospitalized in the University Hospital Center Tirana, Albania, between November 2024 and October 2025. Demographic and clinical data were collected, including age, gender, body mass index (BMI), smoking status, skin prick test results, comorbidities such as rhinosinusitis, nasal polyposis, and asthma phenotype classification. Asthma control was assessed using the Asthma Control Visual Analogue Scale (AC-VAS; 0-25) (Figure 1).

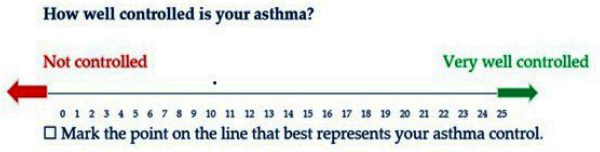

Figure 1. *AC-VAS; 0-25 for asthma control.*

Serum 25(OH)D concentration was measured by chemiluminescent immunoassay (CLIA). Serum 25(OH) D values were available for 155 participants. The primary outcome variable was asthma control measured by the AC-VAS score. Serum 25(OH)D (ng/mL) was analyzed both as a continuous variable and as a categorical variable. For moderation analyses, 25(OH)D status was dichotomized (<20 ng/mL vs ≥20 ng/mL), while for subgroup analyses, 25(OH) D levels were categorized into three groups (<20, 20–30, and >30 ng/mL). Independent variables included age, age at asthma diagnosis, BMI, gender, asthma phenotype, smoking status, rhinosinusitis, nasal polyposis, and skin prick test categories. Asthma clinical phenotypes were classified into six subtypes based on available anamnestic and clinical data (Tables 1 and 2).

Table 1.

Characteristics of classification for probably T2-high phenotypes.

Key Characteristics for likely T2-High phenotypes	
Phenotype 1	Childhood onset; atopy-positive, positive skin allergy tests, ↑ specific IgE
Phenotype 2	Adulthood onset steroid-resistant, blood eosinophilia, sputum eosinophils/neutrophils, CRSwNP
Phenotype 3	Adulthood onset, CRSwNP + NSAID sensitivity

Table 2.

Characteristics of classification for probably T2 -low phenotypes.

Key Characteristics for Likely T2-Low Phenotypes	
Phenotype 4	Middle-aged, non-atopic woman, severe symptoms, perimenopausal
Phenotype 5	Adults, smoking history, steroid resistance, neutrophils in sputum, fixed airflow obstruction
Phenotype 6	Older adults >55 years, non-atopic, severe symptoms, frequent exacerbations, more comorbidities, misdiagnosed as COPD.

Statistical analysis

Continuous variables are reported as mean ± SD and categorical variables as n (%). Due to non-normal distributions, non-parametric tests were used. Spearman's ρ assessed correlations between vitamin D or AC-VAS and continuous variables. The Mann–Whitney U and Kruskal–Wallis tests were used to compare vitamin D and AC-VAS across binary and multi-category clinical variables, respectively. Subgroup analyses by asthma phenotypes examined AC-VAS across 25(OH)D categories (<20, 20–30, >30 ng/mL) using Kruskal–Wallis tests. General linear models were used to assess crude and multivariable-adjusted associations between age, BMI, vitamin D, asthma phenotype, and asthma control (AC-VAS), with Bonferroni correction applied for multiple pairwise comparisons of asthma phenotypes.

Moderation analyses were conducted using PROCESS for SPSS (Model 1) to assess whether 25(OH)D status (<20 ng/mL vs ≥ 20 ng/mL) modified associations between

predictors and asthma control (AC-VAS). Age, asthma phenotype, and BMI were tested in separate models. Main effects, predictor × 25(OH)D interactions, and conditional effects were examined.

Results

Among 163 patients, 109(66.9%) were females and 54(33.1%) were males. The mean age was 48.24 ± 16.70 years, while the mean age at asthma diagnosis was 32.88 ± 16.71 years. The mean body mass index (BMI) was 28.26 ± 5.73 kg/m². The mean AC-VAS score was 14.58±3.86. Serum 25(OH)D levels were 18.35 ± 8.72 ng/mL for 155 participants. Regarding asthma phenotype distribution, phenotype 2 was the most prevalent (64/39.3% cases), followed by phenotype 1 (58/35.6% cases). The remaining phenotypes were less frequent. Smokers accounted for 26(16.0%) participants. Rhinosinusitis was present in 74(45.7%) patients, and nasal polyposis in 29(17.8%) patients. Skin prick testing for aeroallergens was negative in 82 (50.3%) patients, while sensitization to only indoor allergens was observed in 32 (19.6%) cases, to only outdoor allergens in 12 (7.4%) cases, and to both indoor and outdoor allergens in 37 (22.7%) cases (Table 3).

Table 3.

Baseline demographic and clinical characteristics of the study population.

Variable	Value
Age (years)	48.24 ± 16.70
Age at diagnosis (years)	32.88 ± 16.71
Body mass index (kg/m²)	28.26 ± 5.73
Serum 25(OH)D (ng/mL)	18.35 ± 8.72 †
Asthma control (AC-VAS, 0–25)	14.58 ± 3.86
Gender	
Female	109 (66.9)
Male	54 (33.1)
Asthma phenotype	
Phenotype 1	58 (35.6)
Phenotype 2	64 (39.3)
Phenotype 3	7 (4.3)
Phenotype 4	9 (5.5)
Phenotype 5	10 (6.1)
Phenotype 6	15 (9.2)
Smoking status	
Yes	26 (16.0)
No	137 (84.0)
Rhinosinusitis	
Yes	74 (45.7)
No	88 (54.3)
Nasal polyposis	
Yes	29 (17.8)
No	134 (82.2)
Skin prick test	
Negative	82 (50.3)
Indoor	32 (19.6)
Outdoor	12 (7.4)
Both	37 (22.7)

Data are presented as mean ± standard deviation or n (%), as appropriate.
† Vitamin D values were available for 155 participants.
AC-VAS: Asthma Control Visual Analogue Scale.

Spearman's rank correlation analysis demonstrated a statistically significant negative correlation between age and serum 25(OH)D levels (ρ = −0.24, P = 0.003). No significant correlation was observed between 25(OH)D levels and BMI (ρ = −0.08, P = 0.352). Comparisons of gender, asthma phenotype, smoking status, rhinosinusitis, nasal polyposis, and skin prick test categories showed no statistically significant differences in 25(OH)D levels (Table 4).

Table 4.

Associations between serum 25(OH)D levels and demographic and clinical variables.

Variables compared	Statistical test	Test statistic	P-value*
Vitamin D and age	Spearman's rank correlation	ρ = −0.24	0.003
Vitamin D and BMI	Spearman's rank correlation	ρ = −0.08	0.352
Vitamin D across sex (male vs female)	Mann–Whitney U test	Z = 0.63	0.532
Vitamin D across asthma phenotype	Kruskal–Wallis test	H = 3.07	0.690
Vitamin D across smoking status	Mann–Whitney U test	Z = 0.25	0.805
Vitamin D across rhinosinusitis	Mann–Whitney U test	Z = −0.50	0.619
Vitamin D across nasal polyposis	Mann–Whitney U test	Z = −0.70	0.483
Vitamin D across prick test categories	Kruskal–Wallis test	H = 0.21	0.976

** P-values derived from Spearman's rank correlation, Mann–Whitney U test, or Kruskal–Wallis test. A P-value of < 0.05 was considered statistically significant.*

Spearman's rank correlation analysis demonstrated a statistically significant negative correlation between AC-VAS scores and age (ρ = −0.19, P = 0.015), as well as between AC-VAS scores and BMI (ρ = −0.17, P = 0.031). No significant correlation was observed between AC-VAS scores and age at diagnosis (ρ = −0.04, P = 0.641) or serum 25(OH)D levels (ρ = 0.14, P = 0.095).

Comparisons across gender, smoking status, rhinosinusitis, nasal polyposis, and skin prick test categories showed no statistically significant differences in AC-VAS scores (all P > 0.05). In contrast, a statistically significant difference in AC-VAS scores was observed across asthma phenotypes (H = 13.11, P = 0.022). In subgroup analyses stratified by asthma phenotypes, no statistically significant differences in AC-VAS scores were observed across 25(OH)D categories in either likely T2-high or likely T2-low phenotypes (Table 5).

In crude (unadjusted) analyses, increasing age was significantly associated with lower AC-VAS scores (B = −0.042, SE = 0.018; P = 0.021). BMI also showed a significant negative association with asthma control (B = −0.110, SE = 0.052; P= 0.037). Serum 25(OH)D levels were positively associated with AC-VAS scores, although this association did not reach statistical significance (B = 0.060, SE = 0.036; P = 0.097). In the unadjusted model, asthma phenotypes showed a significant overall association with AC-VAS scores, as indicated by the global test (P = 0.026), with phenotype 6 demonstrating higher AC-VAS scores than phenotype 1.

Table 5.

Associations between asthma control (AC-VAS) and demographic and clinical variables.

Variables compared	Statistical test	Test statistic	*P*-value*
AC-VAS and age	Spearman's rank correlation	ρ = −0.19	0.015
AC-VAS and age at diagnosis	Spearman's rank correlation	ρ = −0.04	0.641
AC-VAS and BMI	Spearman's rank correlation	ρ = −0.17	0.031
AC-VAS and Vit D	Spearman's rank correlation	ρ = 0.14	0.095
AC-VAS across sex (male vs female)	Mann–Whitney U test	Z = 0.86	0.388
AC-VAS across asthma phenotype	Kruskal–Wallis test	H = 13.11	0.022
AC-VAS across smoking status	Mann–Whitney U test	Z = −0.33	0.742
AC-VAS across rhinosinusitis	Mann–Whitney U test	Z = −1.15	0.252
AC-VAS across prick test categories	Kruskal–Wallis test	H = 7.06	0.070
AC-VAS across nasal polyposis	Mann–Whitney U test	Z = −0.27	0.787
AC-VAS across Vit D categories in T_2- high asthma phenotypes	Kruskal–Wallis test	H = 1.98	0.372
AC-VAS across Vit D categories in T_2-low asthma phenotypes	Kruskal–Wallis test	H = 1.75	0.418

** P-values derived from Spearman's rank correlation, Mann–Whitney U test, or Kruskal–Wallis test. A P-value of < 0.05 was considered statistically significant.*

In the multivariable-adjusted general linear model, age remained independently and negatively associated with AC-VAS scores (B = −0.048, SE = 0.022; *P* = 0.030). Serum 25(OH)D levels (B = 0.039, SE = 0.036; *P* = 0.269) and BMI (B = −0.065, SE = 0.057; *P* = 0.253) were not significantly associated with asthma control after adjustment. Asthma phenotype remained statistically significantly associated with AC-VAS scores in the adjusted model (global test *P* = 0.031). Among the phenotype categories, phenotype 6 was independently associated with higher AC-VAS scores than phenotype 1 (B = 3.612, SE = 1.198; *P* = 0.003) (Table 6).

No statistically significant interaction effects were observed for age or asthma phenotype. A statistically significant conditional effect of BMI on AC-VAS scores was observed in participants with serum 25(OH)D levels ≥ 20 ng/mL (b = −0.22, *P* = 0.010), whereas no significant conditional effects of BMI were found in participants with 25(OH)D levels < 20 ng/mL (all *P* > 0.05). (Table 7)

Serum 25(OH)D did not show an independent association with asthma control. However, the moderation analysis indicated that the association between BMI and asthma control differed according to 25(OH)D category, with a significant conditional effect observed only at serum 25(OH)D levels ≥ 20 ng/mL (Figure 2).

Table 6.

Crude and multivariable-adjusted generalized linear model (GLM) analyses of factors associated with asthma control (AC-VAS).

Predictor	Crude B (SE)	*p*-value	Adjusted B (SE)	*P*-value
Age	-0.042 (0.018)	0.021	-0.048 (0.022)	0.030
Serum 25(OH)D	0.060 (0.036)	0.097	0.039 (0.036)	0.269
BMI	-0.110 (0.052)	0.037	-0.065 (0.057)	0.253
Asthma phenotype (global test)	—	0.026	—	0.031
Phenotype 2	0.474 (0.682)	0.488	1.097 (0.733)	0.137
Phenotype 3	-2.591 (1.505)	0.087	-0.757 (1.670)	0.651
Phenotype 4	-2.448 (1.348)	0.071	-0.766 (1.453)	0.599
Phenotype 5	-0.148 (1.288)	0.908	1.093 (1.399)	0.436
Phenotype 6	2.218 (1.090)	0.043	3.612 (1.198)	0.003
Phenotype 1	Reference	—	Reference	—

Two-tailed P-values are reported. A P-value of < 0.05 was considered statistically significant.

Table 7.

Moderation analysis of the association between selected predictors and asthma control (AC-VAS) by vitamin D category (PROCESS Model 1).

Focal predictor (X)	n	Main effect on AC-VAS	Interaction X × Vit D status	Conditional effects of X on AC-VAS
Age	155	b = −0.04 *P* = 0.030	b = 0.04 *P* = 0.266	Conditional effects not reported; no evidence of differential effects by vitamin D category
Asthma phenotype	155	b = −0.24 *P* = 0.762	b = 0.26 *P* = 0.876	Conditional effects not reported; no evidence of conditional effects
BMI	154	b = −0.10 *P* = 0.055	b = −0.19 *P* = 0.082	Vitamin D <20 ng/mL: b = −0.03, *P* = 0.673 Vitamin D ≥20ng/mL: b = −0.22, *P*= 0.010

A P-value of < 0.05 was considered statistically significant.

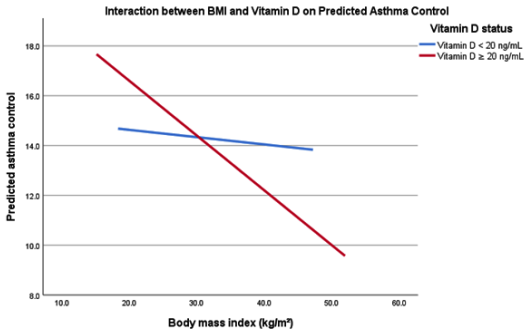

Figure 2. *Predicted AC-VAS scores across BMI levels stratified by vitamin D category.*

Discussion

In this cross-sectional study of Albanian adults with asthma, serum 25(OH)D levels were generally low, with mean concentrations in the deficient range, confirming a high prevalence of suboptimal serum 25(OH)D status in this population. This finding is consistent with reports from other European cohorts and may reflect limited sun exposure, dietary habits, or lifestyle factors.[7,8] Serum 25(OH)D levels were inversely associated with age, consistent with previous evidence that advancing age is associated with reduced vitamin D synthesis and availability.[9]

Despite widespread deficiency, serum 25(OH)D was not independently associated with reported asthma control, as assessed by the AC-VAS. The lack of a direct association persisted across correlation analyses, subgroup comparisons, and multivariable-adjusted regression models. These findings align with several randomized trials and observational studies suggesting that vitamin D may not exert a strong direct effect on symptom control, particularly when assessed cross-sectionally.[10]

In contrast, age and BMI emerged as more consistent determinants of asthma control, with older age and higher BMI associated with poorer control. These findings are clinically relevant, with BMI modifiable or addressable through targeted interventions. In adjusted models, asthma phenotype was associated with asthma control; notably, phenotype 6 was independently associated with higher AC-VAS scores than phenotype 1. Serum 25(OH)D levels did not differ significantly across phenotypes, suggesting comparable serum 25(OH)D status across clinical asthma subtypes.

An important and novel observation of this study was the moderating role of vitamin D on the relationship between BMI and asthma control. The negative association between BMI and asthma control was evident only among participants with serum 25(OH)D levels ≥ 20 ng/mL, whereas no significant association was observed in those with vitamin D deficiency. This finding suggests that serum 25(OH) D status may modify the impact of adiposity on asthma-related symptoms, potentially through immunomodulatory or metabolic pathways. Although the interaction term reached only borderline statistical significance, the conditional effects analysis supports a biologically plausible modifying role of vitamin D rather than a direct effect on disease control.

Contrary to some prior studies, serum 25(OH)D was not associated with asthma subtype, smoking status, rhinosinusitis, nasal polyposis, or allergic sensitization patterns. This may reflect population-specific factors, limited statistical power for subgroup analyses, or the multifactorial nature of asthma control, in which vitamin D plays a secondary or context-dependent role.

Overall, these findings suggest that serum 25(OH)D deficiency is highly prevalent in Albanian asthma patients but does not independently determine asthma control. Instead, vitamin D may act as a contextual modifier, influencing the relationship between metabolic factors, such as BMI, and asthma outcomes. Longitudinal studies and randomized controlled trials are needed to determine whether vitamin D supplementation improves asthma-related outcomes in selected subgroups, particularly overweight or obese patients.

Limitations

It should be noted that cross-sectional design limits causal interpretation, and vitamin D was assessed at a single time point. Residual confounding and limited power in subgroup analyses cannot be excluded.

Conclusion

Vitamin D deficiency was highly prevalent among Albanian adults with asthma but was not independently associated with asthma control. Asthma control was associated with age, body mass index, and asthma phenotype. Vitamin D did not show a direct effect but appeared to modify the association between BMI and asthma control, suggesting a context-dependent role. Further longitudinal and interventional studies are required to confirm these findings and clarify their clinical implications.

Ethical Statement

This study was approved by the Ethical Committee at the University of Medicine (Tirana) with decision no. 29, dated 29.08.2024, and informed consent was obtained from each participant.

Author Contributions

Mehmet Hoxha: Conceptualization, Methodology, Formal analysis, Investigation, Writing – original draft, Supervision.
Eralda Lekli: Methodology, Investigation, Data curation, Writing – review and editing.
Dorian Shkembi: Investigation, Data curation.
Ester Ndreu: Investigation, Data Curation.
Xhein Hajrulla: Investigation, Data curation.
Etleva Qirko: Supervision, Writing – review and editing.
Mehmet Hoxha is the primary author of this work.
All authors reviewed and approved the final manuscript.

Conflict of Interest

The authors have declared no conflict of interest.

Acknowledgments

The authors gratefully acknowledge the support of AKKSHI (National Agency for Scientific Research and Innovation) for funding this research.

Funding

This research was funded by AKKSHI (National Agency for Scientific Research and Innovation), as part of PKKZH 2024-2025 with Decision no. 6, dated 10 June 2024. The APC was funded by AKKSHI.

Data Availability Statement

The datasets generated and analyzed during the current study are available from the corresponding author upon reasonable request.

References

1. Status Asthmaticus Medication: Anticholinergics, Respiratory, Beta2 Agonists, Corticosteroids, Electrolytes, Monoclonal Antibodies, Anti-asthmatics, Xanthine Derivatives [Internet]. [cited 2026 Jan 23]. Available from: https://emedicine.medscape.com/article/2129484-medication?form=fpf
2. Salmanpour F, Kian N, Samieefar N, Khazeei Tabari MA, Rezaei N. Asthma and Vitamin D Deficiency: Occurrence, Immune Mechanisms, and New Perspectives. J Immunol Res. 2022 Jul 15;2022:6735900. doi: 10.1155/2022/6735900. PMID: 35874901; PMCID: PMC9307373.
3. Ogeyingbo OD, Ahmed R, Gyawali M, Venkatesan N, Bhandari R, Botleroo RA, Kareem R, Elshaikh AO. The Relationship Between Vitamin D and Asthma Exacerbation. Cureus. 2021 Aug 18;13(8):e17279. doi: 10.7759/cureus.17279. PMID: 34462708; PMCID: PMC8389855.
4. Wang Q, Ying Q, Zhu W, Chen J. Vitamin D and asthma occurrence in children: A systematic review and meta-analysis. J Pediatr Nurs. 2022 Jan-Feb;62:e60-e68. doi: 10.1016/j.pedn.2021.07.005. Epub 2021 Aug 6. PMID: 34366195.
5. Zhu Y, Jing D, Liang H, Li D, Chang Q, Shen M, Pan P, Liu H, Zhang Y. Vitamin D status and asthma, lung function, and hospitalization among British adults. Front Nutr. 2022 Aug 10;9:954768. doi: 10.3389/fnut.2022.954768. PMID: 36034921; PMCID: PMC9399919.
6. El Abd A, Dasari H, Dodin P, Trottier H, Ducharme FM. The effects of vitamin D supplementation on inflammatory biomarkers in patients with asthma: a systematic review and meta-analysis of randomized controlled trials. Front Immunol. 2024 Mar 13;15:1335968. doi: 10.3389/fimmu.2024.1335968. PMID: 38545098; PMCID: PMC10965564.
7. Cashman KD, Dowling KG, Škrabáková Z, Gonzalez-Gross M, Valtueña J, De Henauw S, et al. Vitamin D deficiency in Europe: pandemic? Am J Clin Nutr. 2016 Apr;103(4):1033-44. doi: 10.3945/ajcn.115.120873. Epub 2016 Feb 10. PMID: 26864360; PMCID: PMC5527850.
8. Spiro A, Buttriss JL. Vitamin D: An overview of vitamin D status and intake in Europe. Nutr Bull. 2014 Dec;39(4):322-350. doi: 10.1111/nbu.12108. PMID: 25635171; PMCID: PMC4288313.
9. Giustina A, Bouillon R, Dawson-Hughes B, Ebeling PR, Lazaretti-Castro M, Lips P, Marcocci C, Bilezikian JP. Vitamin D in the older population: a consensus statement. Endocrine. 2023 Jan;79(1):31-44. doi: 10.1007/s12020-022-03208-3. Epub 2022 Oct 26. PMID: 36287374; PMCID: PMC9607753.
10. Williamson A, Martineau AR, Sheikh A, Jolliffe D, Griffiths CJ. Vitamin D for the management of asthma. Cochrane Database Syst Rev. 2023 Feb 6;2(2):CD011511. doi: 10.1002/14651858.CD011511.pub3. PMID: 36744416; PMCID: PMC9899558.

Corresponding author:

Mehmet Hoxha, E-mail: mehmethoxha@ymail.com

International Journal of Biomedicine 16(2) (2026) 207-211
http://dx.doi.org/10.21103/Article16(2)_OA8

ORIGINAL ARTICLE

INTERNATIONAL JOURNAL OF BIOMEDICINE

Asthma-Obesity Association among under 5 Years Children

Noor A. Younes[1], Khaleel I. Alsuwayfee[2,3*]

[1]*College of Nursing, University of Mosul, Mosul Iraq*
[2]*Department of Pediatrics, College of Medicine, Ninevah University, Mosul, Iraq*
[3]*Mosul Cardiac Centre, Mosul, Iraq*

Abstract

Background: The association between asthma and obesity is well-studied in school-age and older children, but such research among preschool children is limited. The aim of this study was to measure obesity prevalence and evaluate its association with asthma among young children under 5 years.

Methods and Results: This case–control study was conducted in pediatric hospitals and pediatric wards of general hospitals in Mosul city, in northern Iraq. The study included 271 asthmatic children (with an allergic type of asthma) and 271 non-asthmatics of both sexes aged <60 months.

Body mass index (BMI) was used to classify children as underweight, normal weight, overweight, or obese, based on the percentile line on the gender-appropriate BMI/age growth chart provided by the World Health Organization. According to WHO definitions, children were divided into the following groups: BMI <3rd centile (underweight), BMI 3rd–85th centile (normal weight), BMI 85th–97th centile (overweight), BMI >97th centile (obese).

The prevalence of obesity (36.5%) was significantly higher among asthmatic children than non-asthmatics (23.2%) (P=0.000). The OR of being obese and asthmatic was 1.9 [95% CI: 1.30–2.76]. In addition, the mean BMI for cases and controls was 18.24±3.14 kg/m^2 and 17.49±2.48 kg/m^2, respectively, and, by Z-test, there was a significant difference between the groups: asthmatic patients had a higher BMI than controls (P=0.0021). Significantly more obese asthmatic children had a high frequency of severe asthmatic attacks requiring hospital admissions (>4 admissions/year) (67.7% vs. 37.8%, P=0.000), and the increase in the BMI was positively correlated with such a number (R^2=0.12, P=0.01). Asthmatic obese young children experienced poor control of their asthma symptoms when using long-term control drugs than the non-obese ones (75.8 % vs 46.5 %, P=0.000). The mean ages of onset of asthma among obese asthmatic and non-obese asthmatic patients were 7.91±7.75 and 14.61±14.41 months, respectively (P<0.0001).

Conclusion: Obesity is prevalent among asthmatic young children, and it affects the disease profile in many aspects, including the age of onset, frequency of severe attacks, and the difficulty in controlling the symptoms.(**International Journal of Biomedicine. 2026;16(2):207-211.**)

Keywords: asthma • obesity • children • case–control study

For citation: Younes NA, Alsuwayfee KI. Asthma-Obesity Association among under 5 Years Children. International Journal of Biomedicine. 2026;16(2):207-211. doi:10.21103/Article16(2)_OA8

Introduction

There is significant epidemiological and research evidence of an obesity-related asthma phenotype. Compared to children with healthy weight, children with obesity have a higher chance of developing asthma. Obesity in children has an increasing prevalence all over the world.[1,2] The asthma–obesity syndrome remains poorly understood and lacks a specific treatment strategy.[3] Obesity causes significant changes to the chest wall and lungs' mechanics, and these mechanical changes cause asthma and asthma-like symptoms such as dyspnea, wheezing, and airway hyperresponsiveness. Excess adiposity is also associated with increased production of inflammatory cytokines and immune cells, which may lead to disease.[4] A recent study reported, a prevalence of 72.9% of obesity among school-age and adolescent asthmatic children.[5]A systematic review conducted by Malden et al.[6] reported that obese children aged <10 years were at significant risk for the development of asthma with an odds ratio (OR)=1.5.

The aim of this study was to measure obesity prevalence and evaluate its association with asthma among young children under 5 years.

Materials and Methods

This case–control study was conducted in pediatric hospitals and pediatric wards of general hospitals in Mosul city, in northern Iraq, from December 1, 2022, to May 1, 2023. The study included 271 asthmatic children (with an allergic type of asthma) and 271 non-asthmatics of both sexes aged <60 months. The diagnosis of asthma was established by specialist pediatricians based on a history of asthma symptoms, a wheezy chest on examination, a history of asthma symptom recurrence, and chest X-ray findings consistent with asthma. Drugs for long-term control of symptoms, including short-acting inhaled β_2-agonists, long-acting β_2-agonists, leukotriene modifiers (montelukast), systemic steroids (prednisolone and dexamethasone), and oral theophylline were all recorded. Classification of asthma control was based on the symptoms during the day, nighttime awakenings, need for short-acting β-agonist drugs, and interference with normal child activity, as shown below.

Component of control	Well controlled	Not well controlled	Very poorly controlled
Impairment symptoms	≤ 2day/week, but less than once on each day	> days/ week or multiple times on ≤2day/week	Throughout the day
Night time awaking	≤1/month	>1/month	>1/week
Short acting B2-agonist use for symptoms	≤ 2day/week	> days/ week	Several times per day
Interference with normal activity	None	Some limitation	Extremely limited

Adapted from Kliegman RM, St Geme JW III, Blum NJ, Shah SS, Tasker RC, Wilson KM, editors. Nelson textbook of pediatrics. 20th ed. Philadelphia (PA): Elsevier; 2016. p. 1195.).[7]

Children with other diseases that mimic asthma were excluded by their doctors. The control group was age-matched to 271 healthy children attending the hospital's vaccination units who had no history of asthma symptoms. The exclusion criteria for both cases and controls were children with any disease that causes chronic respiratory complaints, children with edema due to different causes, and children with chronic use of drugs that can affect their BMI, like systemic steroids.

Written parental consent was obtained to participate in the study, and specially designed questionnaires were used to collect information and determine study parameters during a direct interview.

The sample size of 271 children with asthma was calculated according to the equation (Cochran's Formula):

$N = Z^2PQ/d^2$, where

N = sample size, Z = statistical certainty, P = probability problem under study (as a fraction of 1), Q = 1.0 – p, d = desired margin of error

For both cases and controls, body weight was measured to the nearest 0.1kg using a digital scale (Seca) with lightly dressed, barefoot subjects. Then, standing heights or lying lengths were measured with a stability scale or infantometer to the nearest 0.1cm. Physical measurements of body weight and length were used to calculate BMI (kg/m^2). BMI was used to classify children as underweight, normal weight, overweight, or obese, based on the percentile line on the gender-appropriate BMI/age growth chart provided by the World Health Organization. According to WHO definitions, children were divided into the following groups: BMI <3rd centile (underweight), BMI 3rd–85th centile (normal weight), BMI 85th–97th centile (overweight), BMI >97th centile (obese).[8]

Microsoft Excel 2020 and SPSS (Statistical Package for the Social Sciences) v. 27 were used for statistical analysis. Baseline characteristics were summarized as frequencies and percentages for categorical variables and mean±standard deviation (SD) for continuous variables. The chi-square test was used for studying associations, Fisher's exact test was an alternative to the chi-square test for small samples, a two-sample Z-test was used to compare means, Pearson's correlation coefficient was used to study correlations, crosstabs statistics in SPSS was used for calculating OR and 95% confidence interval (CI), and linear regression was used to study relationships. Statistical significance was set at a *P*-value of <0.05.

Results

In the basic demographic data table for cases and controls, there were no significant differences in gender distribution or age groups (*P*=0.343). The means of the age of both groups were also matched. The mean age of cases in months was 29.0±18.3, the mean age of controls in months was 26.0±18.3, *P*=0.057 (Table 1).

Table 1.

Demographic characteristics of cases (asthmatics) and controls (non-asthmatics).

Variable		Cases (asthmatics)	Controls (non-asthmatics)	*P*-value
Gender	Male	120 (44.3%)	131 (48.3%)	0.343
	Female	151 (55.7%)	140 (51.7%)	
	Total	271 (100%)	271 (100%)	
Age groups (months)	≤ 12	77 (28.4%)	93 (34.3%)	0.189
	13 - 24	67 (24.7%)	69 (25.5%)	
	25 - 36	36 (13.3%)	38 (14.0%)	
	37 - 48	54 (19.9%)	34 (12.5%)	
	49 - 60	37 (13.7%)	37 (13.7%)	
	Mean ±SD	29.0± 18.3	26.0±18.3	0.057

The prevalence of obesity (36.5%) was significantly higher among asthmatic children than non-asthmatics (23.2%) (*P*=0.000) (Table 2). The OR of being obese and asthmatic was 1.9 [95% CI: 1.30–2.76]. In addition, the mean BMI for cases and controls was 18.24±3.14 kg/m^2 and 17.49±2.48 kg/m^2, respectively, and, by Z-test, there was a significant difference between the groups: asthmatic patients had a higher BMI than controls (*P*=0.0021).

Table 2.

Prevalence of overweight and obesity among cases and controls.

BMI	Cases	Controls	*P*-value
Obese BMI (> 97%)	99 (36.5%)	63 (23.2%)	0.000
Overweight BMI (85% - 97%)	61 (22.5%)	50 (18.5%)	0.242
BMI (< 85%)	111 (41.0%)	158 (58.3%)	0.000
Total	271 (100%)	271 (100%)	

Significantly more obese asthmatic children had a high frequency of severe asthmatic attacks requiring hospital admissions (>4 admissions/year) (67.7% vs. 37.8%, *P*=0.000), and the increase in the BMI was positively correlated with such a number (R^2=0.12, *P*=0.01) (Table 3 and Figure 1).

Table 3.

Frequency of hospital admissions/year among obese asthmatic patients and nonobese asthmatic patients.

Number of hospital admissions per year	Obese asthmatics	None-obese asthmatic	*P*-value
1 or less	1(1%)	8 (4.7%)	0.140
2-4	31(31.3%)	99 (57.5%)	0.000
5-6	48(48.5%)	49 (28,5%)	0.001
>6	19(19.2%)	16 (9.3%)	0.019
Total	99(100%)	172(100%)	

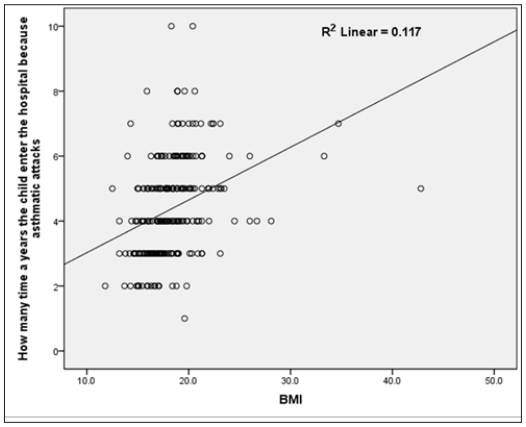

Figure 1. *Correlation between BMI and the number of yearly hospital admissions because of asthmatic attacks among asthmatic children.*

In the current study, significantly more asthmatic obese young children experienced not well control of their asthma symptoms when using long-term control drugs than the non-obese ones (75.8 % vs 46.5 %, *P*=0.000) (Table 4).

The mean ages of onset of asthma among obese asthmatic and non-obese asthmatic patients were 7.91±7.75 and 14.61±14.41 months, respectively. Obese patients had an earlier onset of their symptoms than the non-obese group (*P*<0.0001) (Figure 2).

Table 4.

Asthma control by drugs among obese and asthmatic patients and non-obese asthmatic patients.

Type of asthma control	Obese asthmatics	None-obese asthmatics	*P*-value
Well-controlled	23 (23.2%)	92 (53.5%)	0.000
Not well controlled	75(75.8%)	80 (46.5%)	0.000
Poorly controlled	1(1.0%)	0 (0%)	0.365
Total	99(100%)	172(100%)	

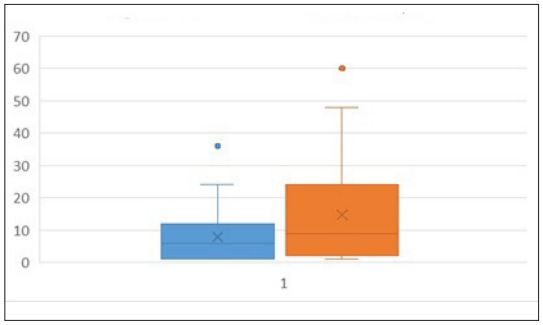

Figure 2*. Age of asthma onset (in months) among obese and non-obese asthmatic patients.*

Discussion

The worldwide prevalence of childhood obesity is about 10%, and in Iraq, this prevalence ranges from 19% to 21.1% in different cities.[9-11] In the current study, obesity prevalence was not far from this range among non-asthmatic children (23%), but a significantly higher prevalence (36.5%) was found among the asthmatic group, i.e., more than one-third of them were obese with a high OR (1.9), and such finding supports the association between these two morbidities. We think that the rather sedentary lifestyle due to the avoidance of strenuous physical activity or active play that may precipitate asthmatic attacks is the main cause of such a high prevalence of obesity among asthmatic children. Borgmeyer et al.[12] also found a high prevalence of obesity (19.6%) among the studied asthmatic children in their study, but it was less than ours, which is most likely explained by the regional variation of childhood obesity prevalence, because many studies in Iraq documented a higher prevalence of childhood obesity than the global one.[9,13-15] Although overweight was more prevalent among the asthmatic children in this study (22.5%) than in the control group (18.5%), this difference was not statistically significant, indicating the high prevalence of overweight in the pediatric population in general, and future studies on a large scale of the pediatric population may find different results. A lot of controversy exists about the association between obesity and asthma severity, expressed as the frequency of attacks and the patient's response to the controller drug therapy. Some studies support this association,[16-19] while others contradict

it [20,21] The current study found that significantly more obese asthmatic children had a higher annual frequency of severe asthmatic attacks requiring hospital admissions than the non-obese asthmatics, 67.7% vs. 37.8%, respectively (P=0.000). Moreover, the increase in BMI was positively correlated with such frequency (R^2=0.12, P=0.01).

The asthma–obesity phenotype and its effect on the response to drug treatment strategies are a matter of debate among studies. Some studies confirm this effect, while others deny it.[22-24] In this study, a significantly high percentage of obese asthmatic children had either partly controlled or poorly controlled asthma (based on their daytime and nighttime symptoms) using controller drugs than did their non-obese asthmatic peers. The other way in which obesity is likely to affect the asthma profile is the age of onset of asthma symptoms. According to this study, the asthma–obesity phenotype is associated with a significantly earlier mean age of onset of asthmatic symptoms compared to the non-obese group (7.91±7.75 and 14.61±14.41 months). A similar finding is reported by other investigators.[25]

In conclusion, obesity is prevalent among asthmatic young children, and it affects the disease profile in many aspects, including the age of onset, frequency of severe attacks, and the difficulty in controlling the symptoms.

Ethics Statement

This study was conducted in accordance with the World Medical Association Declaration of Helsinki (1975), as revised in 2013, and approved by Mosul University Collegiate Committee for Medical Research Ethics (Ethical approval number 91 dated 29/2/2022; CCMRE-NUR-22-25). Written informed consent was obtained from each patient's parent/ guardian/ relative.

Author Contributions

Noor A. Younes: Investigation, Data curation, Formal analysis, Writing – original draft, Visualization.
Khaleel I. Alsuwayfee: Conceptualization, Methodology, Supervision, Validation, Writing – review and editing.
All authors have approved the final article.

Acknowledgments

We would like to express our deep thanks to all nursing staff in our hospitals for their assistance in accomplishing this work.

Conflict of Interest

The authors have declared no conflict of interest.

References

1. Reyes-Angel J, Kaviany P, Rastogi D, Forno E. Obesity-related asthma in children and adolescents. Lancet Child Adolesc Health. 2022 Oct;6(10):713-724. doi: 10.1016/S2352-4642(22)00185-7. Epub 2022 Aug 19. PMID: 35988550; PMCID: PMC12090466.
2. Mohammed AM, Al-Rawi RA, Abdulmajeed BY, Ayoub NI. The relationship between blood pressure and body mass index among primary-school children. Med J Babylon. 2022;19(3):482-487. doi:10.4103/MJBL.MJBL_91_22.
3. Sharma V, Cowan DC. Obesity, Inflammation, and Severe Asthma: an Update. Curr Allergy Asthma Rep. 2021 Dec 18;21(12):46. doi: 10.1007/s11882-021-01024-9. PMID: 34921631; PMCID: PMC8684548.
4. Dixon AE, Peters U. The effect of obesity on lung function. Expert Rev Respir Med. 2018 Sep;12(9):755-767. doi: 10.1080/17476348.2018.1506331. Epub 2018 Aug 14. PMID: 30056777; PMCID: PMC6311385.
5. Fitzpatrick AM, Mutic AD, Mohammad AF, Stephenson ST, Grunwell JR. Obesity Is Associated with Sustained Symptomatology and Unique Inflammatory Features in Children with Asthma. J Allergy Clin Immunol Pract. 2022 Mar;10(3):815-826.e2. doi: 10.1016/j.jaip.2021.10.020. Epub 2021 Oct 22. PMID: 34688962; PMCID: PMC8917992.
6. Malden S, Gillespie J, Hughes A, Gibson AM, Farooq A, Martin A, Summerbell C, Reilly JJ. Obesity in young children and its relationship with diagnosis of asthma, vitamin D deficiency, iron deficiency, specific allergies and flat-footedness: A systematic review and meta-analysis. Obes Rev. 2021 Mar;22(3):e13129. doi: 10.1111/obr.13129. Epub 2020 Aug 18. PMID: 32808447; PMCID: PMC7611974.
7. Liu AH, Spahn JD, Sicherer SH. Childhood asthma. In: Kliegman RM, St Geme JW III, Blum NJ, Shah SS, Tasker RC, Wilson KM, editors. Nelson textbook of pediatrics. 20th ed. Philadelphia (PA): Elsevier; 2016. p. 1195.
8. Tyson N, Frank M. Childhood and adolescent obesity definitions as related to BMI, evaluation and management options. Best Pract Res Clin Obstet Gynaecol. 2018 Apr;48:158-164. doi: 10.1016/j.bpobgyn.2017.06.003. Epub 2017 Aug 12. PMID: 28838829.
9. Vats MG, Mahboub BH, Al Hariri H, Al Zaabi A, Vats D. Obesity and Sleep-Related Breathing Disorders in Middle East and UAE. Can Respir J. 2016;2016:9673054. doi: 10.1155/2016/9673054. Epub 2016 Dec 1. PMID: 28070158; PMCID: PMC5192288.
10. Contreras ZA, Chen Z, Roumeliotaki T, Annesi-Maesano I, Baïz N, von Berg A, et al. Does early onset asthma increase childhood obesity risk? A pooled analysis of 16 European cohorts. Eur Respir J. 2018 Sep 27;52(3):1800504. doi: 10.1183/13993003.00504-2018. PMID: 30209194; PMCID: PMC6443037.
11. Brüske I, Flexeder C, Heinrich J. Body mass index and the incidence of asthma in children. Curr Opin Allergy Clin Immunol. 2014 Apr;14(2):155-60. doi: 10.1097/ACI.0000000000000035. PMID: 24500295.
12. Borgmeyer A, Ercole PM, Niesen A, Strunk RC. Lack of Recognition, Diagnosis, and Treatment of Overweight/ Obesity in Children Hospitalized for Asthma. Hosp Pediatr. 2016 Nov;6(11):667-676. doi: 10.1542/hpeds.2015-0242. Epub 2016 Oct 12. PMID: 27733428.
13. Sulaiman SJ, Al-Ani MH. Prevalence of obesity and physical activity among primary school children in Erbil City/ Iraq. Mosul J Nurs. 2020;8(1):1-11.
14. Alredainy R, Lami FA. Overweight and obesity in a sample of primary school children in Baghdad. Iraqi Med J. 2020;16(1):42-48.

15. Michelson PH, Williams LW, Benjamin DK, Barnato AE. Obesity, inflammation, and asthma severity in childhood: data from the National Health and Nutrition Examination Survey 2001-2004. Ann Allergy Asthma Immunol. 2009 Nov;103(5):381-5. doi: 10.1016/S1081-1206(10)60356-0. PMID: 19927535.
16. Tai A, Volkmer R, Burton A. Association between asthma symptoms and obesity in preschool (4-5 year old) children. J Asthma. 2009 May;46(4):362-5. doi: 10.1080/02770900902759260. PMID: 19484670.
17. Carroll CL, Stoltz P, Raykov N, Smith SR, Zucker AR. Childhood overweight increases hospital admission rates for asthma. Pediatrics. 2007 Oct;120(4):734-40. doi: 10.1542/peds.2007-0409. PMID: 17908759.
18. Ginde AA, Santillan AA, Clark S, Camargo CA Jr. Body mass index and acute asthma severity among children presenting to the emergency department. Pediatr Allergy Immunol. 2010 May;21(3):480-8. doi: 10.1111/j.1399-3038.2009.00911.x. Epub 2009 Jun 22. PMID: 19548965.
19. Ross KR, Hart MA, Storfer-Isser A, Kibler AM, Johnson NL, Rosen CL, Kercsmar CM, Redline S. Obesity and obesity related co-morbidities in a referral population of children with asthma. Pediatr Pulmonol. 2009 Sep;44(9):877-84. doi: 10.1002/ppul.21065. PMID: 19639627; PMCID: PMC2940418.
20. Hom J, Morley EJ, Sasso P, Sinert R. Body mass index and pediatric asthma outcomes. Pediatr Emerg Care. 2009 Sep;25(9):569-71. doi: 10.1097/PEC.0b013e3181b4f639. PMID: 19755889.
21. Ahmadizar F, Vijverberg SJ, Arets HG, de Boer A, Lang JE, Kattan M, Palmer CN, Mukhopadhyay S, Turner S, Maitland-van der Zee AH. Childhood obesity in relation to poor asthma control and exacerbation: a meta-analysis. Eur Respir J. 2016 Oct;48(4):1063-1073. doi: 10.1183/13993003.00766-2016. Epub 2016 Sep 1. PMID: 27587561.
22. Okubo Y, Nochioka K, Hataya H, Sakakibara H, Terakawa T, Testa M. Burden of Obesity on Pediatric Inpatients with Acute Asthma Exacerbation in the United States. J Allergy Clin Immunol Pract. 2016 Nov-Dec;4(6):1227-1231. doi: 10.1016/j.jaip.2016.06.004. Epub 2016 Jun 30. PMID: 27372599.
23. Forno E, Lescher R, Strunk R, Weiss S, Fuhlbrigge A, Celedón JC; Childhood Asthma Management Program Research Group. Decreased response to inhaled steroids in overweight and obese asthmatic children. J Allergy Clin Immunol. 2011 Mar;127(3):741-9. doi: 10.1016/j.jaci.2010.12.010. PMID: 21377042; PMCID: PMC3056233.
24. Di Genova L, Penta L, Biscarini A, Di Cara G, Esposito S. Children with Obesity and Asthma: Which Are the Best Options for Their Management? Nutrients. 2018 Nov 2;10(11):1634. doi: 10.3390/nu10111634. PMID: 30400197; PMCID: PMC6267365.
25. Holguin F, Bleecker ER, Busse WW, Calhoun WJ, Castro M, Erzurum SC, Fitzpatrick AM, Gaston B, Israel E, Jarjour NN, Moore WC, Peters SP, Yonas M, Teague WG, Wenzel SE. Obesity and asthma: an association modified by age of asthma onset. J Allergy Clin Immunol. 2011 Jun;127(6):1486-93.e2. doi: 10.1016/j.jaci.2011.03.036. PMID: 21624618; PMCID: PMC3128802.

***Correspondence**: Dr. Khaleel I. Alsuwayfee. E-mail: Khaleel.mahmood@uoninevah.edu.iq*

International Journal of Biomedicine 16(2) (2026) 212-216
http://dx.doi.org/10.21103/Article16(2)_OA9

ORIGINAL ARTICLE

INTERNATIONAL JOURNAL OF BIOMEDICINE

The Role of Spectral Analysis of Cough Sounds in the Diagnostics of Pneumonia

Andrey V. Budnevsky[1], Sergey N. Avdeev[2], Evgeniy S. Ovsyannikov[1*], Avag G. Kitoyan[1], Sofia N. Feigelman[1]

[1]*Voronezh State Medical University named after N.N. Burdenko, Voronezh, Russia*
[2]*I. M. Sechenov First Moscow State Medical University (Sechenov University), Moscow, Russia*

Abstract

Background: Community-acquired pneumonia (CAP) is a global healthcare problem and one of the leading causes of death and hospitalization among respiratory diseases. Cough is the most common symptom of pneumonia. Diagnosing pneumonia using cough sounds is a useful non-invasive test that can be performed outside a hospital. The objective of this study was to conduct a spectral analysis of cough sounds in patients with pneumonia compared with the cough in patients with asthma (BA), chronic obstructive pulmonary disease (COPD), coronavirus disease 2019 (COVID-19), and an induced cough in healthy individuals, using citric acid.

Methods and Results: The study's main group consisted of 65 patients with pneumonia (81.4% men and 18.6% women; mean age of 43.5 [18.0; 70.0] years). The comparison groups consisted of patients with BA (n=38), COPD (n=35), COVID-19 (n=40), and healthy individuals (n=45). The cough sounds were recorded using the spectral tussophonobarography method based on the Fast Fourier Transform Algorithm, which provides a frequency-based distribution of sound energy. We estimated the time-frequency parameters of sounds of the entire cough episode, as well as for separated phases of the cough sound: duration (T, T1, T2, T3), the ratio of the energy of low and medium frequencies (60-600 Hz) to the energy of high frequencies (600-6000 Hz) (Q, Q1, Q2, Q3), and the frequency of maximum sound energy (Hz) (Fmax, Fmax1, Fmax2, Fmax3).

The cough parameters in the main group and the comparison groups had significant differences. In patients with pneumonia, the total cough duration (T) and T2 were significantly shorter than in all comparison groups. In contrast, T1 was significantly prolonged compared with patients with COPD, BA, COVID-19, and healthy subjects with induced cough. T3 was significantly shorter in pneumonia than in healthy individuals with experimentally induced cough. Overall, cough episodes in pneumonia were characterized by a predominance of low-frequency energy compared with BA and COVID-19. During the first cough phase, the Q coefficient was significantly higher in pneumonia than in COVID-19. In the second cough phase, energy distribution shifted toward lower frequencies compared with asthma and toward higher frequencies compared with COPD and COVID-19. In the third cough phase, pneumonia-related cough demonstrated a significantly greater proportion of high-frequency energy than induced cough in healthy subjects. The maximum frequency (Fmax) in pneumonia was significantly lower than in COVID-19 and BA. Fmax1 was significantly lower than in all comparison groups. Fmax2 was significantly lower than in BA, COPD, and COVID-19. Fmax3 was also significantly lower in pneumonia compared with COVID-19.

Conclusion: Cough in patients with pneumonia demonstrates significant differences in key frequency–time characteristics compared with cough sounds in patients with BA, COPD, and COVID-19. These findings suggest that spectral tussophonobarography may be a useful tool for differential diagnosis of pneumonia. (**International Journal of Biomedicine. 2026;16(2):212-216.**)

Keywords: pneumonia • cough • spectral analysis

For citation: Budnevsky AV, Avdeev SN, Ovsyannikov ES, Kitoyan AG, Feigelman SN. The Role of Spectral Analysis of Cough Sounds in the Diagnostics of Pneumonia. International Journal of Biomedicine. 2026;16(2):212-216. doi:10.21103/Article16(2)_OA9

Abbreviations

BA, bronchial asthma; **CAP**, community-acquired pneumonia; **COPD**, chronic obstructive pulmonary disease; **COVID-19**, coronavirus disease 2019; **STFBG**, spectral tussophonobarography.

Introduction

Community-acquired pneumonia (CAP) is an infectious lung inflammation contracted outside the hospital. CAP incidence among all adults can reach 14 cases per 1,000. Up to 50% of cases require inpatient hospitalization, and the mortality rate reaches 0.7 per 1,000 persons per year. The World Health Organization has reported that CAP accounts for 4 million deaths per year, representing 7% of total annual mortality.[1] Verification of pneumonia is based on the presence of radiologically confirmed focal pulmonary infiltration and clinical symptoms, identification of the causative pathogen, assessment of disease severity and prognosis, and detection of complications.[2] Pneumonia is a seasonal disease, with its peak incidence occurring during the autumn–winter period. The timely use of radiological diagnostic methods may be limited by heavy medical personnel workload, high demand for X-ray equipment in primary health care facilities, and limited access to appropriate diagnostic options in remote areas.

Clinically, the disease manifests with fever (77.1%), dyspnea (62.7%), chest pain/discomfort (52.5%), and increased sweating (20–50%).[3-6] One of the most common symptoms of pneumonia is a productive cough with sputum expectoration (78.1%).[4,7] Cough is among the most frequent complaints of patients seeking primary health care for respiratory diseases such as bronchial asthma (BA), chronic obstructive pulmonary disease (COPD), chronic bronchitis (CB), COVID-19, pertussis, and pneumonia.[8-11] Subjective methods of cough assessment do not allow verification of the diagnosis of pneumonia; rather, they serve as indirect measures reflecting the patient's perception of actual cough episodes rather than an objective evaluation of cough itself. Objective assessment aims to provide a quantitative and unbiased evaluation of cough as a physiological and pathological phenomenon. Various physical characteristics can be measured, including cough strength/intensity, frequency, and acoustic properties. Given that cough is a common symptom of pneumonia, its acoustic characteristics may have diagnostic value and could be considered an additional tool for early identification of disease probability.[12,13]

The objective of this study was to conduct a spectral analysis of cough sounds in patients with pneumonia compared with the cough in patients with asthma (BA), chronic obstructive pulmonary disease (COPD), coronavirus disease 2019 (COVID-19), and an induced cough in healthy individuals, using citric acid.

Materials and Methods

The study's main group consisted of 65 patients with non-severe pneumonia (81.4% men and 18.6% women; mean age of 43.5 [18.0; 70.0] years) without prior chronic respiratory diseases who were treated on an outpatient basis at Voronezh City Clinical Polyclinic №7 or hospitalized in the Pulmonology department of Voronezh City Clinical Emergency Hospital №1 from October 2024 to October 2025. The diagnosis of pneumonia was established in accordance with current clinical guidelines,[3] based on chest radiography or computed tomography (CT) findings. The first comparison group included 45 healthy individuals (78% male, 22% female; mean age of 45.3 [32.2; 53.0] years) without prior chronic respiratory diseases, in whom cough was induced by inhalation of citric acid.[9] The second comparison group consisted of 40 patients (73.68% male, 26.32% female; mean age of 43.1 [30.2; 51.0] years) diagnosed with confirmed COVID-19 (mild to moderate form). The third comparison group included 38 patients with moderate persistent BA in the phase of moderate exacerbation (82.74% male, 17.26% female; mean age of 38.3 [32.2; 48.1] years). The fourth comparison group comprised 35 patients with COPD, clinical group E, in the phase of moderate exacerbation (72.54% male, 27.46% female; mean age of 52.3 [41.2; 65.3] years). No significant differences in age or sex distribution were observed between the groups.

Spectral tussophonobarography (STFBG) was performed to assess cough sound characteristics in the study participants, allowing evaluation of cough duration and frequency distributions according to the methodology previously described.[14]

Cough sounds were recorded in all patients using a microphone. The recordings were normalized for amplitude (up to 6 dB), the sampling rate was set to 48,000 Hz, and each cough event was segmented into phases using Sound Forge 18 (MAGIX Software GmbH, Germany).

Each cough event was divided into three phases:

Phase 1 – opening of the glottis
Phase 2 – rapid air release from the lungs
Phase 3 – closing of the glottis.

Phase 3 may be absent in approximately one-third of patients.

Subsequently, spectral analysis of cough sounds was performed using the Fast Fourier Transform algorithm.

The following time–frequency parameters were evaluated:

- Total cough duration (T) and the duration of each phase separately (T1, T2, T3), ms
- The ratio of low-frequency energy and mid-frequency energy (60–600 Hz) to high-frequency energy (600–6000 Hz) for the entire cough event (Q) and for each phase separately (Q1, Q2, Q3)
- The frequency of maximum sound energy of the entire cough event (Fmax) and of each individual phase (Fmax1, Fmax2, Fmax3), Hz.

Statistical data processing was assessed using IBM SPSS Statistics 23 (SPSS: An IBM Company, USA). The sample's compliance with the Gaussian distribution was assessed using the Kolmogorov–Smirnov criterion. Numerical indicators of cough parameters are presented as a median, with the upper and lower quartiles indicated in brackets. For comparative analysis, the Kruskal-Wallis test was used. Differences were considered statistically significant at $P<0.05$.

Results

Table 1 presents the indicators of the comparative analysis of the studied cough sound parameters.

Table 1.

Spectral characteristics of the cough sounds in patients with Pneumonia, COVID-19, BA, COPD, and healthy individuals.

Parameter	Pneumonia (n=65)	Healthy individuals (n=45)	COVID-19 (n=40)	Bronchial asthma (n=38)	COPD (n=35)
T (ms)	330.0 (253.0;410.0)	390.5 (358.2;456.5)*	343.5 (280.0;400.2)	501.0 (419.2;624.5)#	452.2 (368.0;538.0)##
T1 (ms)	81.0 (58.5;102.0)	46.5 (37.7;55.2)*	45.0 (35.0;57.0)**	46.5 (37,0;58,0)#	44,9 (36,0;51,0)##
T2 (ms)	160.0 (124.0;211.5)	271.5 (202.7;321.7)*	227.0 (189.7;275.2)**	369.5 (286.0;467.7)#	311.0 (251.0;428.0)##
T3 (ms)	93.0 (88.6;41.2)	100.0 (71.0;131.0)*	82.0 (61.0;114.7)	81.0 (68.2;107.2)	71.0 (56.0;93.0)
Q	0.390 (0.302;0.673)	0.437 (0.366;0.563)	0.306 (0.223;0.448)**	0.305 (0.174;0.385)#	0.443 (0.316;0.547)
Q1	0.540 (0.354;0.811)	0.505 (0.444;0.671)	0.405 (0.262;0.578)**	0.626 (0.509;0.732)	0.505 (0.386;0.709)
Q2	0.254 (0.1835;0.447)	0.284 (0.207;0.402)	0.197 (0.197;0.289)**	0.181 (0.131;0.268)#	0.346 (0.258;476)##
Q3	0.590 (0.300;1.007)	0.970 (0.736;1.398)*	0.719 (0.478;1.108)	0.568 (0.412;1.106)	0.713 (0.464;1.026)
Fmax (HZ)	370.0 (219.0;482.0)	382.5 (258.7;490.5)	452.0 (273.7;1034.4)**	1.202.5 (357.0;1678.2)#	371.0 (328.0;453.0)
Fmax1 (HZ)	274.0 (213.0;542.0)	397.5 (258.7;565.5)*	440.0 (282.5;620.5)**	386.5 (291.2;567.0)#	337.0 (276.0;574.0)##
Fmax2 (HZ)	539.0 (331.0;1235.5)	1126.5 (226.5;1532.)	960.0 (352.0;1609.7)**	1382.5 (975.5;1832.5)#	414.0 (211.0;556.0)##
Fmax3 (HZ)	388.0 (234.5;532.0)	326.0 (218.2;433.7)	313.0 (246.0;402.2)**	358.5 (329.6;477.0)	338.5 (297.2;401.5)

T, T1, T2, and T3 - duration (ms) of the cough act as a whole, Phase 1, Phase 2, Phase 3, respectively; Q, QI, Q2, and Q3 - the ratio of the total energy of low and medium frequencies to the energy of high frequencies of the cough act as a whole, Phase 1, Phase 2, Phase 3, respectively; Fmax, Fmax1, Fmax2, Fmax3 — the frequency of maximum sound energy (Hz) of the cough act as a whole, Phase 1, Phase 2 Phase 3, respectively.

**- differences between the main group and the group of healthy individuals are significant at P<0.05; **- differences between the main group and the group of patients with COVID-19 are significant at P<0.05; #- differences between the main group and the group of patients with BA are significant at P<0.05; ##- differences between the main group and the group of patients with COPD are significant at P<0.05.*

A comparative analysis of cough sounds in patients with pneumonia and in healthy individuals with induced cough revealed statistically significant differences in cough act duration, which was shorter across all cough phases in the pneumonia group. When comparing the Q coefficient, significant differences were observed only in the third phase of cough (Q3). In pneumonia, low-frequency energy predominated. Analysis of the maximum sound energy frequency revealed significant differences in Fmax only in the first phase of cough (Fmax1), which was lower in patients with pneumonia.

Comparison between patients with pneumonia and COVID-19 showed statistically significant differences in T1 and T2 of the cough act. The duration of the first phase was shorter in the COVID-19 group, whereas the duration of the second phase was longer in the pneumonia group. When comparing the Q coefficients, significant differences were observed in the second and third cough phases (Q2 and Q3), with low-frequency energy predominating in pneumonia. Fmax showed significant differences throughout the entire cough act: Fmax, Fmax1, and Fmax2 were significantly lower in patients with pneumonia, while Fmax3 was higher.

Comparative analysis of cough sounds in patients with pneumonia and those with BA revealed significant differences in overall cough duration (T) and in the first (T1) and second (T2) phases. In pneumonia, overall T and T2 were significantly shorter, whereas T1 was significantly longer. Statistically significant differences in the Q coefficient were observed across the entire cough act and in the second phase, with low-frequency energy predominating in pneumonia. The maximum sound energy frequency (Fmax) in pneumonia was significantly lower for the entire cough act and in the first and second phases.

Comparative analysis of cough sounds in patients with pneumonia and those with COPD revealed significant differences in overall cough duration (T) and in the first (T1) and second (T2) phases. In pneumonia, overall T and T2 were shorter, whereas T1 was longer. When comparing the Q coefficient, statistically significant differences were detected only in the second phase of the cough act, with low-frequency energy predominating in COPD. Fmax showed significant differences in the first (Fmax1) and second (Fmax2) phases. Compared with COPD, the maximum sound energy frequency in pneumonia was significantly lower in the first phase and significantly higher in the second phase.

Discussion

The study results demonstrate that the time–frequency characteristics of cough sounds in pneumonia differ significantly from those in patients with COVID-19, COPD, BA, and citric acid–induced cough in healthy individuals, suggesting diagnostic and differential diagnostic value. Cough in patients with pneumonia is characterized by a shorter cough act duration and a predominance of low-frequency energy. The shift of the energy spectrum toward lower frequencies may be caused by inflammatory consolidation of lung tissue, decreased elasticity, and increased mass of the oscillating medium due to intra-alveolar exudation.

In COVID-19, the predominance of high-frequency energy may be associated with more pronounced interstitial involvement and bronchospasm,[14] whereas in patients with BA, a more uniform energy distribution may result from variability in bronchial obstruction, mucosal edema, and bronchospasm. In COPD, compared with the main group, energy distribution shifts toward lower-frequency components during the second phase of cough, which may be related to the presence of more viscous, difficult-to-expectorate sputum.

At the Department of Faculty Therapy of Voronezh State Medical University named after N.N. Burdenko, STFBG has been studied as a diagnostic method for COPD,[15] BA,[16] COVID-19,[16] and pneumonia.[17] Using STFBG, a characteristic cough sound pattern was identified in patients with COVID-19. For rapid diagnosis, a prognostic model based on a multiple regression equation was developed. In addition, the effectiveness of antitussive therapy for dry cough in COVID-19 was assessed using spectral analysis of cough sounds.[17]

In the late 1990s, researchers in the same department attempted to perform STFBG in patients with pneumonia; however, reproducible, diagnostically significant results were not obtained. This was likely due to the use of a more complex data-processing technique based on the discrete Fourier transform, which required powerful equipment that was not readily available at the time.

In recent years, there has been a growing trend toward increasing the number of studies aimed at diagnosing respiratory tract diseases using spectral analysis of cough sounds.

Porter et al.[18] developed an automated algorithm for analyzing cough sounds in various respiratory diseases, which can be integrated into smartphones that also serve as recording devices. The algorithm analyzed cough sounds in combination with five clinical symptoms, including fever, rhinorrhea, audible wheezing, hoarseness, and symptom duration. Mel-frequency cepstral coefficients (MFCCs) and non-Gaussian acoustic features were extracted from cough sounds, and a classifier was trained. Diagnostic accuracy improved when additional clinical parameters, such as respiratory rate, were included. The proposed methods enabled the diagnosis of pneumonia, with positive percent agreement of 87% and negative percent agreement of 85%.

Liao S. et al.[19] attempted to diagnose pneumonia and bronchitis in children using cough sound analysis based on CFCS. Cough sounds were recorded in 173 patients. Support vector machines (SVM) and long short-term memory (LSTM) neural networks were used to select diagnostically significant parameters and train the classifier. The sensitivity and specificity of the classifier for diagnosing pneumonia were 87.5% and 93.3%, respectively.These results suggest that the proposed CFCS-based classifier effectively diagnoses pneumonia via cough-sound analysis.

Despite the potential of these approaches, the studies have several significant limitations that hinder their practical implementation. The use of neural networks does not always allow the identification of specific parameters necessary for accurate diagnosis and differential diagnosis of diseases based on cough sounds. The need for subjective clinical assessment reduces the sensitivity of the proposed algorithms.

Our study provides new data on the potential of spectral analysis of cough sounds and its possible use as a reliable, noninvasive marker for diagnosing pneumonia. In the future, we plan to develop a prognostic model for pneumonia diagnosis based on data obtained using STFBG and to investigate its role in the dynamic assessment of the disease following treatment initiation.

Conclusion

Pneumonia is a global healthcare problem and one of the leading causes of death and hospitalization among respiratory diseases. Cough is among the most frequent complaints of patients seeking primary health care for respiratory diseases. Cough in patients with pneumonia demonstrates significant differences in key frequency–time characteristics compared with cough sounds in patients with BA, COPD, and COVID-19. These findings suggest that STFBG may be a useful tool for differential diagnosis of pneumonia.

Ethical Considerations

The study was approved by the Ethics Committee of Voronezh State Medical University named after N.N. Burdenko (Protocol #5 dated 21.10.2024). Written informed consent was obtained from all study individuals.

Author Contributions

Andrey V. Budnevsky: Conceptualization, Methodology, Formal Analysis, Writing – review & editing.
Sergey N. Avdeev: Conceptualization, Supervision, Validation, Visualization.
Evgeniy S. Ovsyannikov: Supervision, Project administration, Writing – review & editing.
Avag G. Kitoyan: Investigation, Data curation, Writing – original draft.
Sofia N. Feigelman: Investigation, Data curation, Writing – original draft.
All authors have approved the final article.

Conflict of Interest

The authors have declared no conflict of interest.

Disclaimer

Views expressed in the submitted article represent the opinions of the authors and not an official position of the universities or funder.

References

1. Tsoumani E, Carter JA, Salomonsson S, Stephens JM, Bencina G. Clinical, economic, and humanistic burden of community acquired pneumonia in Europe: a

systematic literature review. Expert Rev Vaccines. 2023 Jan-Dec;22(1):876-884. doi: 10.1080/14760584.2023.2261785. Epub 2023 Oct 13. PMID: 37823894.
2. Avdeev SN, Dekhnich AV, Zaytsev AA, et al. [Community-acquired pneumonia in adults]. Clinical Guidelines 2024 (short version). Journal of Respiratory Medicine. 2025;1(3):618. (In Russian). doi: 10.17116/respmed202510316_
3. Avdeev SN, Beloborodov VB, Belotserkovskiy BZ, et al. [Severe community-acquired pneumonia in adults. Clinical recommendations from Russian Federation of Anesthesiologists and Reanimatologists]. Russian Journal of Anesthesiology and Reanimatology. 2022;(1):6-35. (In Russian). doi: 10.17116/anaesthesiology20220116.
4. Ferreira-Coimbra J, Sarda C, Rello J. Burden of Community-Acquired Pneumonia and Unmet Clinical Needs. Adv Ther. 2020 Apr;37(4):1302-1318. doi: 10.1007/s12325-020-01248-7. Epub 2020 Feb 18. PMID: 32072494; PMCID: PMC7140754.
5. Tellapragada C, Giske CG. The Unyvero Hospital-Acquired pneumonia panel for diagnosis of secondary bacterial pneumonia in COVID-19 patients. Eur J Clin Microbiol Infect Dis. 2021 Dec;40(12):2479-2485. doi: 10.1007/s10096-021-04194-6. Epub 2021 Mar 4. Erratum in: Eur J Clin Microbiol Infect Dis. 2021 Dec;40(12):2487-2488. doi: 10.1007/s10096-021-04331-1. PMID: 33661410; PMCID: PMC7930892.
6. Fally M, Hansel J, Robey RC, Haseeb F, Kouta A, Williams T, Felton T, Mathioudakis AG. Decoding community-acquired pneumonia: a systematic review and analysis of diagnostic criteria and definitions used in clinical trials. Clin Microbiol Infect. 2025 May;31(5):724-730. doi: 10.1016/j.cmi.2024.12.028. Epub 2024 Dec 24. PMID: 39725075.
7. Self WH, Courtney DM, McNaughton CD, Wunderink RG, Kline JA. High discordance of chest x-ray and computed tomography for detection of pulmonary opacities in ED patients: implications for diagnosing pneumonia. Am J Emerg Med. 2013 Feb;31(2):401-5. doi: 10.1016/j.ajem.2012.08.041. Epub 2012 Oct 18. PMID: 23083885; PMCID: PMC3556231.
8. Chung KF, McGarvey L, Song WJ, Chang AB, Lai K, Canning BJ, Birring SS, Smith JA, Mazzone SB. Cough hypersensitivity and chronic cough. Nat Rev Dis Primers. 2022 Jun 30;8(1):45. doi: 10.1038/s41572-022-00370-w. PMID: 35773287; PMCID: PMC9244241.
9. Budnevsky AV, Ovsyannikov ES, Avdeev SN, Choporov ON, Feigelman SN, Maksimov AV. [The role of spectral analysis of cough sounds in the diagnosis of COVID-19]. Ter Arkh. 2024 Apr 16;96(3):228-232. [In Russian]. doi: 10.26442/00403660.2024.03.202636. PMID: 38713036.
10. Chung KF, McGarvey L, Song WJ, Chang AB, Lai K, Canning BJ, Birring SS, Smith JA, Mazzone SB. Cough hypersensitivity and chronic cough. Nat Rev Dis Primers. 2022 Jun 30;8(1):45. doi: 10.1038/s41572-022-00370-w. PMID: 35773287; PMCID: PMC9244241.
11. Foti Randazzese S, Toscano F, Gambadauro A, La Rocca M, Altavilla G, Carlino M, Caminiti L, Ruggeri P, Manti S. Neuromodulators in Acute and Chronic Cough in Children: An Update from the Literature. Int J Mol Sci. 2024 Oct 18;25(20):11229. doi: 10.3390/ijms252011229. PMID: 39457010; PMCID: PMC11508565.
12. Andrani F, Aiello M, Bertorelli G, Crisafulli E, Chetta A. Cough, a vital reflex. mechanisms, determinants and measurements. Acta Biomed. 2019 Jan 15;89(4):477-480. doi: 10.23750/abm.v89i4.6182. PMID: 30657115; PMCID: PMC6502102.
13. Serrurier A, Neuschaefer-Rube C, Röhrig R. Past and Trends in Cough Sound Acquisition, Automatic Detection and Automatic Classification: A Comparative Review. Sensors (Basel). 2022 Apr 10;22(8):2896. doi: 10.3390/s22082896. PMID: 35458885; PMCID: PMC9027375.
14. Patent Nº 2776535, int. Cl. A61B 5/08 (2006.01). [Method for rapid detection of Coronavirus infection COVID-19 using the method of spectral analysis of cough sounds: №2022110055: register 14.04.2022: published 21.07.2022]. Budnevsky AV, Ovsyannikov ES, Avdeev SN, Choporov ON, Maksimov AV, Kozhevnikova SA, Pertsev AV, Feigelman SN, Savushkina IA; the patent holder Voronezh State Medical University named after N.N.Burdenko
15. Ovsyannikov ES, Avdeev SN, Budnevsky AV, Drobysheva ES. [Cough diagnosis: present and future]. Tuberculosis and Lung Diseases. 2021;99(11):56-64. (In Russian). doi: 10.21292/2075-1230-2021-99-11-56-64
16. Budnevsky AV, Avdeev SN, Ovsyannikov ES, Feygelman SN, Choporov ON, Maximov AV, Pertsev AV. [Spectral analysis of cough sounds of patients with COVID-19]. Pul'monologiya. 2022;3 (6):834–841. (In Russian). doi: 10.18093/0869-0189-2022-32-6-834-841
17. Provotorov VM, Chesnokov PE, Pritzepov YuL, Semenkova GG, Kuznetzov SI, Zimemskaya EV. [The clinical evaluation of cough efficacy by means of expectoration time and tussography method in patients with nonspecific diseases of the lungs]. Pul'monologiya. 1992;(2):49-51. (In Russian)]. https://journal.pulmonology.ru/pulm/article/view/3922/3280
18. Porter P, Abeyratne U, Swarnkar V, Tan J, Ng TW, Brisbane JM, Speldewinde D, Choveaux J, Sharan R, Kosasih K, Della P. A prospective multicentre study testing the diagnostic accuracy of an automated cough sound centred analytic system for the identification of common respiratory disorders in children. Respir Res. 2019 Jun 6;20(1):81. doi: 10.1186/s12931-019-1046-6. PMID: 31167662; PMCID: PMC6551890.
19. Liao S, Song C, Wang X, Wang Y. A classification framework for identifying bronchitis and pneumonia in children based on a small-scale cough sounds dataset. PLoS One. 2022 Oct 27;17(10):e0275479. doi: 10.1371/journal.pone.0275479. PMID: 36301797; PMCID: PMC9612535.

***Corresponding author**: Prof. Evgeniy S. Ovsyannikov, PhD, DSc. Department of faculty therapy, Voronezh State Medical University named after N.N. Burdenko. Voronezh, Russia. E-mail: ovses@yandex.ru*

International Journal of Biomedicine 16(2) (2026) 217-222
http://dx.doi.org/10.21103/Article16(2)_OA10

ORIGINAL ARTICLE

INTERNATIONAL JOURNAL OF BIOMEDICINE

Serum cfDNA and TNF-α in Adult Men with Obstructive Sleep Apnea

Waheeb Alharbi[1*], Ahmad H. Mufti[2]

[1]*Department of Physiology, Faculty of Medicine, Umm Al-Qura University (UQU), Makkah 21955, Saudi Arabia*
[2]*Department of Medical Genetics, Faculty of Medicine, Umm Al-Qura University (UQU), Makkah 21955, Saudi Arabia*

Abstract

Background: Obstructive sleep apnea (OSA) is a common sleep-related chronic respiratory disorder. There are several factors for characterizing OSA in adults. Two of the potential biomarkers in OSA are cell-free DNA (cfDNA) and tumor necrosis factor-alpha (TNF-α). Some reports indicate that obesity and other variables are likely the major risk factors influencing changes in serum cfDNA and TNF-α levels. Given the controversial role of these two biomarkers, we planned to conduct the present study in male patients with mild OSA and normal body mass index (BMI).

Methods and Results: Two groups of subjects were examined. Group 1 included 195 OSA men. Group 2 included 201 men as normal controls (NC) without OSA. The participants in both groups were aged 51-60 years and had normal BMI in the range of 18.5 to 24.9 kg/m^2. Polysomnography was used to determine the apnea-hypopnea index (AHI) and assess the severity of OSA. The routine ELISA method was used to assess TNF-α and cfDNA in blood serum.

The present report found a significant increase in serum levels of cfDNA and TNF-α in OSA men with normal BMI compared to healthy control men with normal BMI. Still, we did not find a significant correlation between serum cfDNA and TNF-α in the NC and OSA groups.

Conclusion: The role of significantly increased levels of serum cfDNA and TNF-α is evident in OSA men with normal weight BMI. Though both cfDNA and TNF-α show a significant correlation with BMI in obese patients with obstructive sleep apnea, a direct association between cfDNA and TNF-α in normal-weight men with obstructive sleep apnea is not evident. Future studies examining the involvement of key pro-inflammatory and anti-inflammatory biomarkers will clarify the precise roles of serum cfDNA and TNF-α in patients with obstructive sleep apnea.(**International Journal of Biomedicine. 2026;16(2):217-222.**)

Keywords: obstructive sleep apnea • TNF-α • cfDNA • BMI • adult men

For citation: Alharbi W, Mufti AH. Serum cfDNA and TNF-α in Adult Men with Obstructive Sleep Apnea. Laboratory and Clinical Correlates of Lupus Anticoagulant Positivity in an Albanian Cohort. International Journal of Biomedicine. 2026;16(2):217-222. doi:10.21103/Article16(2)_OA10

Abbreviations

AHI, apnea-hypopnea index; **AOPPs,** advanced oxidation protein products; **BMI,** body mass index; **cfDNA,** cell-free DNA; **CPAP,** continuous positive airway pressure; **CVDs,** cardiovascular diseases; **dsDNA,** double-stranded DNA; **ELISA,** enzyme-linked immunosorbent assay; **KSA,** Kingdom of Saudi Arabia; **MetS,** metabolic syndrome; **NC,** normal control; **OSA,** obstructive sleep apnea; **OSAHS,** obstructive sleep apnea-hypopnea syndrome; **OSAS,** obstructive sleep apnea syndrome; **TNF-α,** tumor necrosis factor-alpha; **UQU,** Umm Al-Qura University.

Introduction

Obstructive sleep apnea (OSA) is a common sleep-related chronic respiratory disorder[1] that occurs due to repeated episodes of partial or complete upper airway collapse or obstruction during sleep, leading to transient asphyxia or temporary, reversible hypoxia and ischemia. It influences health and quality of life.[2] Obstructive sleep apnea is considered one

of the independent risk factors in various disorders, including cardiovascular diseases (CVDs), neurovascular disorders (e.g., stroke), daytime sleepiness, etc.[3,4]

If daytime sleepiness and daytime-related symptoms appear, the OSA is considered obstructive sleep apnea–hypopnea syndrome (OSAHS) or obstructive sleep apnea syndrome (OSAS).[3] The daytime sleepiness, awakenings with snoring, and restless sleep are the common manifestations with less common symptoms of headaches in the morning, insomnia, mood changes, increased blood pressure or heart rate, weight gain, nocturia, gastroesophageal reflux, erectile dysfunction etc.[5,6] Adolescents or adult people having OSA of long-term go into sleep for a short period if they get rest.[7] Despite the high prevalence of OSA, only about 10% are properly diagnosed.[8] Men are afflicted with OSA more frequently than women, which could be the protective effect of progesterone in women. However, postmenopausal women present a similar frequency of OSA occurrence and have a higher frequency than women in pregnancy.[9] There is a link between body mass index (BMI) and the high prevalence of OSA since an increase in body weight is associated with the development of a higher risk of OSA.[10] The OSA is managed by proper exercise (even without weight loss), weight loss, and avoiding smoking, muscle relaxants, and sedatives. Continuous positive airway pressure (CPAP) is quite effective.[11] Considering prognosis, people with OSA have an increased risk of hypertension, heart attack, congestive heart failure, depression, and diabetes, compared to those without OSA. Cardiovascular diseases and stroke associated with OSA contribute to early death in older adults.[12]

Smoking increases the risk of developing OSA.[3] Some of the medications, including sedatives, and medical conditions of asthma and allergic rhinitis, may complicate the occurrence of OSA.[13] Genetic factors and various phenotypes contribute to the development and progression of OSA.[14] Physiological changes appearing are sleep fragmentation, hypoxia, hyperoxia, and dysfunction of the autonomic nervous system that may lead to inflammatory changes and to clinical consequences.[15] Some of the physiological/metabolic consequences in adults are diabetes, hypertension, ischemic heart disease, obesity, stroke, metabolic syndrome (MetS), etc.[3,16,17]

Biomarkers comprising the genetic factors for the characterization in adults with OSA were studied.[18,19] Cell-free DNA (cfDNA) was studied as a biomarker[20] in inflammation-related disorders.[18,21-26] Several studies have shown an increase in serum/plasma cfDNA in patients with OSA.[27-29] However, no significant change in cfDNA was also investigated in OSA patients compared to controls.[26,30,31] In several studies, increased serum/plasma TNF-alpha (TNF-α) levels have been observed in patients with OSA.[28,32] No change in the levels of TNF-α in patients with OSA compared to controls was also documented, and it was revealed that there is no association of TNF-α and cfDNA in patients with OSA.[26] A report presents an association between TNF-α and pro-inflammatory cytokines, especially in autoimmune diseases,[33] though no clear evidence of a correlation between serum/ plasma TNF-α and cfDNA exists. In view of the limited and controversial information regarding the role of serum/plasma TNF-α and cfDNA, and their association in patients with OSA, we planned the present study.

Materials and Methods

The present case-control study was conducted after obtaining ethical approval (Approval No: HAPO-02-K-012-2022-01-1085) from the College of Medicine of Umm Al-Qura University (UQU), Makkah, Kingdom of Saudi Arabia (KSA). The research work was carried out from Jan 20, 2023, to Dec 20, 2025, at the UQU-associated hospitals/ medical clinics.

The male adult OSA participants were well informed about the purpose and the schedule of collecting their history and blood samples. Detailed interviews were arranged after selecting the patients/control subjects. A comprehensive medical history/physical examination of OSA in adult male patients was performed.

Two groups of subjects were examined. Group 1 included 195 OSA men. Group 2 included 201 men as normal controls (NC) without OSA. The participants in both groups were aged 51-60 years. The participants in both groups in the current study had normal BMI in the range of 18.5 to 24.9 kg/m^2. The sample size was calculated using the calculator and the sample size formula.

Symptoms, including daytime sleepiness, loud snoring, morning headaches, restless sleep, high blood pressure, and high apnea-hypopnea index (AHI) scores, were specifically documented in patients with OSA. The inclusion and exclusion criteria for the various conditions/disorders were established. Exclusion criteria were patients with CVDs, diabetes, MetS, and other serious respiratory disorders, as well as obese and overweight patients.

Polysomnography was used to determine the AHI and assess the severity of OSA. To determine AHI, the total number of apnea and hypopnea episodes/events was divided by the total sleep hours. Episodes of apnea and hypopnea were considered as such if they lasted at least 10 seconds. The OSA diagnosis in adults is defined by an AHI exceeding 5 events per hour, leading to daytime sleepiness (mild: 5-<15; moderate: 15-<30; severe: ≥30 with fatigue). The present study examined mild cases of OSA (AHI: >5–<15), as well as subjects in a control group (NC) (AHI: ≤5). Routine ELISA (Enzyme-Linked Immunosorbent Assay) method was used to assess TNF-α and cfDNA in blood serum.

The IBM SPSS Statistics (version 24.0, IBM Corp., Armonk, NY) and GraphPad Prism (version 6.0, San Diego, CA, USA) software were used for data analysis. The mean±SEM were the values for the unpaired t-test analysis for obtaining two-tailed p-values. The linear correlation was analyzed by plotting the regression lines and obtaining R2 and corresponding p-values. The *P*-value of ≤0.05 was considered the threshold level showing a significant difference.

Results

Mean age in the OSA and NC groups were 55.51±0.20 and 55.39±0.20 years, respectively (*P*=0.67). The BMI values

in the OSA and NC groups were 21.89±0.15 and 21.81±0.15 kg/m^2, respectively (P=0.69).

Serum TNF-α level in NC and OSA groups was 5.19±0.29 and 9.42±0.52 pg/mL, respectively (P<0.001) (Fig.1). Serum level of cfDNA in NC and OSA groups was 114.50±4.76 and 186.65±8.03 ng/mL, respectively (P<0.001) (Fig.2).

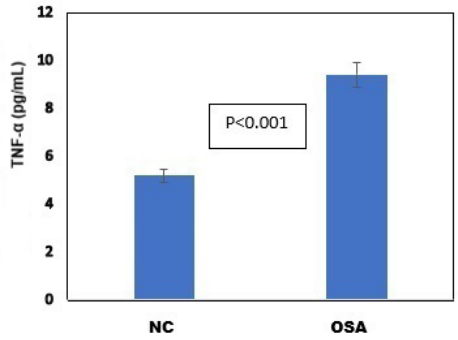

Fig.1. *Serum TNF-α in adult men with OSA and NC adult men with normal BMI.*

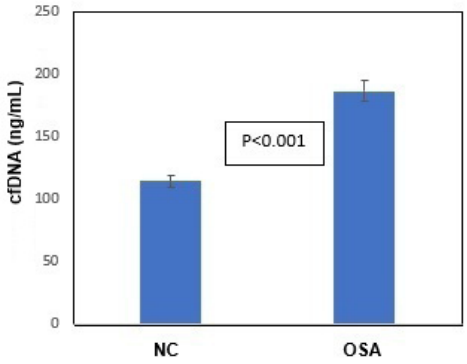

Fig.2. *Serum cfDNA in adult men with OSA and NC adult men with normal BMI.*

The NC group showed a non-significant association between BMI and serum TNF-α (R^2=0.005, P=0.30). In the OSA group, we found a significant weak positive association between BMI and TNF-α (R^2=0.033, P=0.01). The NC group showed a non-significant association between BMI and serum cfDNA (R^2=0.000, P=0.89). In the OSA group, a significant weak positive association between BMI and cfDNA (R^2=0.024, P=0.03) was found. The associations of BMI with TNF-α and cfDNA in the study groups are shown in Table 1.

Table 1.

Association of BMI with serum TNF-α and cfDNA in study groups.

Variable	Groups	Association of BMI with TNF-α and cfDNA		
		R^2	df	P-value
TNF-α	NC	0.005	199	0.30
	OSA	0.033	193	0.01
cfDNA	NC	0.000	199	0.89
	OSA	0.024	193	0.03

BMI, body mass index; TNF-α, tumor necrosis factor-alpha; cfDNA, cell-free DNA; NC, normal control; OSA, obstructive sleep apnea; R^2, coefficient of determination.

Table 2 presents the association between serum TNF-α and cfDNA. The slope, intercept, R^2, and P-value indicate that the association between TNF-α and cfDNA was not significant in both groups.

Table 2.

Association between serum TNF-α and cfDNA in study groups.

Groups	Association between serum TNF-α and cfDNA				
	Slope	Intercept	R^2	df	P-value
NC	1.25	108.03	0.006	199	0.28
OSA	0.97	105.31	0.010	193	0.16

TNF-α, tumor necrosis factor-alpha; cfDNA, cell-free DNA; NC, normal control; OSA, obstructive sleep apnea; R^2, coefficient of determination.

Discussion

Oxidative stress-related lipid and DNA oxidation have been reported in previous studies in obstructive sleep apnea. Ozben et al.[20] showed that high systemic oxidative stress in obstructive sleep apnea is associated with increased levels of advanced oxidation protein products (AOPPs). The connection between AOPPs, β-globin, and ischemia in OSA highlights a cascade of oxidative stress that leads to molecular damage, including DNA fragmentation (often assessed by cfDNA or nucleosome levels). Studies of cfDNA indicate that, while healthy individuals exhibit low levels of cfDNA in blood serum, patients with OSA demonstrate significantly elevated concentrations—often measured using the β-globin (HBB) gene as a marker.[20]

An oxidative stress biomarker, cfDNA, at high levels serves as a biomarker in several inflammation-related diseases, including autoimmune diseases, ischemic heart disease, stroke, cancer, acute coronary syndrome, and OSA.[18,21-25]

While investigating the best global tests for characterization, OSA patients showed elevated plasma cfDNA levels.[29] It was found that cfDNA, which is released in apoptosis and shows elevated levels in cardiovascular diseases, cancer, and other disorders, was significantly higher in severe OSA than in subjects with mild to moderate OSA and those without OSA.[30] Furthermore, it was revealed that OSA-related free radicals cause degradation and destruction of fragmented nucleic acid-DNA, and resultantly, high levels of cfDNA and nucleosomes are found.[36,37] Higher levels of cfDNA were obtained in OSA vs. healthy controls,[27] showing linear correlation with the OSA severity.[33] The patients with severe and moderate OSA presented higher outcomes than those with mild OSAS.[38] Furthermore, double-stranded DNA (dsDNA) and nucleosome levels were higher in OSA patients than in the control healthy subject group.[28] While studying several biomarkers of endothelial function/damage in OSA patients in baseline and after 3-month therapy of CPAP, it was revealed that circulating cfDNA increased significantly.[39]

The above-mentioned reports provide extensive evidence for the results for serum cfDNA obtained in the present study. However, OSA patients with AHI > 30 showed higher plasma DNA levels, but no significant difference was

observed between mild-to-moderate OSA patients with AHI 5-30.[30] We suggest that the study of the collective effects of 5-30 AHA shows the presentation of collective variations not explainable logically. Additionally, DNA damage and oxidative stress were not found in another study of patients with OSA.[31] In view of these findings, we suggest that the criteria, methodology, and scenario of the mentioned studies were different and that this was most likely the reason behind the non-significant change of cfDNA in OSA patients compared to their well-matched controls.

Several pro-inflammatory cytokines, including TNF-α, were also found to be increased in OSA.[28] The TNF-α postoperative levels at the third month decreased significantly compared to preoperative levels under the expansion sphincter pharyngoplasty for OSA patients, which explains the role of TNF-α in OSA patients.[32] Other studies also reveal that the adult patients with OSA showed significantly higher levels of TNF-α compared to healthy and age-matched control subjects.[40,41] This indicates a strong association between OSA and systemic inflammation.[42] This is evident from the investigation that a healthy weight loss lifestyle lowered the plasma levels of TNF-a in OSA patients.[42] These observations are in accordance with our results in the present study.

On the other hand, there are several studies showing a non-significant difference of TNF-α in OSA patients compared to controls, mainly due to obesity/ overweight status instead of apnea[41,43] The subgroup analysis showed no significant difference in plasma TNF-α levels between OSA and control adult subjects with BMI ≤ 30 kg/m².[41] No significant change in TNF-α is due to the confounding factors, mainly obesity, differences in sample size, detection methods, study design, and diurnal rhythms.[41,44,45]

Serum/plasma levels of cfDNA associate positively with pro-inflammatory cytokines, especially in autoimmune diseases.[33] Another report reveals a concomitant increase in cfDNA and TNF-α in OSA.[28] On the other hand, it is known that CPAP therapy or moderate intensity physical activity for OSA patients influences cfDNA and several inflammatory biomarkers, including TNF-α. However, short-term treatment with medium- to long-term CPAP or aerobic exercise therapy in moderate-to-severe OSA patients did not alter blood levels of cfDNA or TNF-α.[26] This report and some of the other cited reports explain that obesity and other variables are most likely the major risk factors influencing the change in serum cfDNA and TNF-α levels. Since we studied OSA patients with normal-weight BMI in the present study. The present report found a significant increase in serum levels of cfDNA and TNF-α in OSA men with normal BMI compared to healthy control men with normal BMI. Still, we did not find a significant correlation between serum cfDNA and TNF-α in the NC and OSA groups. The present study emphasizes the need for further studies to better understand the roles of relevant inflammatory markers in interpreting the net contribution of serum cfDNA and TNF-α, as well as their association with each other in OSA patients with normal-weight, overweight, and obese subjects. There are some studies that suggest limitations, corrections for comorbidities, study design, sample size, methodological limitations, diurnal rhythms, or different scenarios in patients with mild-to-moderate OSA, and therefore, it is possible that there is no significant correlation between serum/plasma levels of cfDNA and TNF-α in OSA patients.

Conclusion

The role of significantly increased levels of serum cfDNA and TNF-α is evident in OSA men with normal weight BMI. The cfDNA is a biomarker for ischemia and hypoxia. Though both cfDNA and TNF-α show a significant correlation with BMI in obese patients with obstructive sleep apnea, a direct association between cfDNA and TNF-α in normal-weight men with obstructive sleep apnea is not evident. Future studies examining the involvement of key pro-inflammatory and anti-inflammatory biomarkers will clarify the precise roles of serum cfDNA and TNF-α in patients with obstructive sleep apnea.

Ethical Considerations

The study was carried out in accordance with ethical principles of the WMA Declaration of Helsinki (1964, ed. 2013) and approved by the Ethical Committee of the Faculty of Medicine, Umm Al-Qura University (UQU); Approval Number: "HAPO-02-K-012-2022-01-1085." Written informed consent was obtained from all participants.

Author Contributions

Waheeb Alharbi: Supervision, Conceptualization, Investigation, Writing – review and editing.
Ahmad H. Mufti: Conceptualization, Investigation, Data curation. Formal analysis, Writing – original draft.

All authors have approved the final article.

Conflict of Interest

The authors have declared no conflict of interest.

Acknowledgments

The authors thank the laboratory experts and medical consultants for their invaluable support.

References

1. Heinzer R, Vat S, Marques-Vidal P, Marti-Soler H, Andries D, Tobback N, Mooser V, Preisig M, Malhotra A, Waeber G, Vollenweider P, Tafti M, Haba-Rubio J. Prevalence of sleep-disordered breathing in the general population: the HypnoLaus study. Lancet Respir Med. 2015 Apr;3(4):310-8. doi: 10.1016/S2213-2600(15)00043-0.
2. Punjabi NM, Caffo BS, Goodwin JL, Gottlieb DJ, Newman AB, O'Connor GT, Rapoport DM, Redline S, Resnick HE, Robbins JA, Shahar E, Unruh ML, Samet JM. Sleep-disordered breathing and mortality: a prospective cohort study. PLoS Med. 2009 Aug;6(8):e1000132. doi: 10.1371/journal.pmed.1000132. Epub 2009 Aug 18. PMID: 19688045; PMCID: PMC2722083.

3. Young T, Skatrud J, Peppard PE. Risk factors for obstructive sleep apnea in adults. JAMA. 2004 Apr 28;291(16):2013-6. doi: 10.1001/jama.291.16.2013. PMID: 15113821.
4. Mediano O, Cano-Pumarega I, Sánchez-de-la-Torre M, Alonso-Álvarez ML, Troncoso MF, García-Río F, Egea C; Spanish Sleep Network; Spanish Sleep Network. Upcoming Scenarios for the Comprehensive Management of Obstructive Sleep Apnea: An Overview of the Spanish Sleep Network. Arch Bronconeumol (Engl Ed). 2020 Jan;56(1):35-41. English, Spanish. doi: 10.1016/j.arbres.2019.05.017. Epub 2019 Aug 5. PMID: 31395388.
5. Li D, Kuang B, Lobbezoo F, de Vries N, Hilgevoord A, Aarab G. Sleep bruxism is highly prevalent in adults with obstructive sleep apnea: a large-scale polysomnographic study. J Clin Sleep Med. 2023 Mar 1;19(3):443-451. doi: 10.5664/jcsm.10348. PMID: 36448332; PMCID: PMC9978428.
6. Patel SR. Entering a New Era in Sleep-Apnea Treatment. N Engl J Med. 2024 Oct 3;391(13):1248-1249. doi: 10.1056/NEJMe2407117. Epub 2024 Jun 21. PMID: 38912659.
7. Lal C, Weaver TE, Bae CJ, Strohl KP. Excessive Daytime Sleepiness in Obstructive Sleep Apnea. Mechanisms and Clinical Management. Ann Am Thorac Soc. 2021 May;18(5):757-768. doi: 10.1513/AnnalsATS.202006-696FR. PMID: 33621163; PMCID: PMC8086534.
8. Chen X, Wang R, Zee P, Lutsey PL, Javaheri S, Alcántara C, Jackson CL, Williams MA, Redline S. Racial/Ethnic Differences in Sleep Disturbances: The Multi-Ethnic Study of Atherosclerosis (MESA). Sleep. 2015 Jun 1;38(6):877-88. doi: 10.5665/sleep.4732. PMID: 25409106; PMCID: PMC4434554.
9. Chinese Thoracic Society. [Expert consensus on the diagnosis and treatment of obstructive sleep apnea in women]. Zhonghua Jie He He Hu Xi Za Zhi. 2024 Jun 12;47(6):509-528. Chinese. doi: 10.3760/cma.j.cn112147-20240206-00072. PMID: 38858201.
10. Senaratna CV, Perret JL, Lodge CJ, Lowe AJ, Campbell BE, Matheson MC, Hamilton GS, Dharmage SC. Prevalence of obstructive sleep apnea in the general population: A systematic review. Sleep Med Rev. 2017 Aug;34:70-81. doi: 10.1016/j.smrv.2016.07.002. Epub 2016 Jul 18. PMID: 27568340.
11. Iftikhar IH, Kline CE, Youngstedt SD. Effects of exercise training on sleep apnea: a meta-analysis. Lung. 2014 Feb;192(1):175-84. doi: 10.1007/s00408-013-9511-3. PMID: 24077936; PMCID: PMC4216726.
12. Franklin KA, Lindberg E. Obstructive sleep apnea is a common disorder in the population-a review on the epidemiology of sleep apnea. J Thorac Dis. 2015 Aug;7(8):1311-22. doi: 10.3978/j.issn.2072-1439.2015.06.11. PMID: 26380759; PMCID: PMC4561280.
13. Lu LR, Peat JK, Sullivan CE. Snoring in preschool children: prevalence and association with nocturnal cough and asthma. Chest. 2003 Aug;124(2):587-93. doi: 10.1378/chest.124.2.587. PMID: 12907547.
14. Mukherjee S, Saxena R, Palmer LJ. The genetics of obstructive sleep apnoea. Respirology. 2018 Jan;23(1):18-27. doi: 10.1111/resp.13212. Epub 2017 Nov 7. PMID: 29113020; PMCID: PMC7308164.
15. Foldvary-Schaefer NR, Waters TE. Sleep-Disordered Breathing. Continuum (Minneap Minn). 2017 Aug;23(4, Sleep Neurology):1093-1116. doi: 10.1212/01.CON.0000522245.13784.f6. PMID: 28777178.
16. Eskandari D, Zou D, Grote L, Schneider H, Penzel T, Hedner J. Independent associations between arterial bicarbonate, apnea severity and hypertension in obstructive sleep apnea. Respir Res. 2017 Jun 28;18(1):130. doi: 10.1186/s12931-017-0607-9. PMID: 28659192; PMCID: PMC5490198.
17. Reutrakul S, Mokhlesi B. Obstructive Sleep Apnea and Diabetes: A State of the Art Review. Chest. 2017 Nov;152(5):1070-1086. doi: 10.1016/j.chest.2017.05.009. Epub 2017 May 17. PMID: 28527878; PMCID: PMC5812754.
18. Stanek A, Brożyna-Tkaczyk K, Myśliński W. Oxidative Stress Markers among Obstructive Sleep Apnea Patients. Oxid Med Cell Longev. 2021 Jul 19;2021:9681595. doi: 10.1155/2021/9681595. PMID: 34336121; PMCID: PMC8321764.
19. Zapater A, Benítez ID, Santamaria-Martos F, Pinilla L, Targa A, De Gonzalo-Calvo D, Torres G, Mínguez O, Cortijo A, Dalmases M, Barbé F, Sánchez-de-la-Torre M. Endogenous controls and microRNA profile in female patients with obstructive sleep apnea. Sci Rep. 2022 Feb 3;12(1):1916. doi: 10.1038/s41598-022-05782-y. PMID: 35115631; PMCID: PMC8813920.
20. Ozben S, Huseyinoglu N, Hanikoglu F, Guvenc TS, Yildirim BZ, Cort A, Ozdem S, Ozben T. Advanced oxidation protein products and ischaemia-modified albumin in obstructive sleep apnea. Eur J Clin Invest. 2014 Nov;44(11):1045-52. doi: 10.1111/eci.12338. Epub 2014 Oct 4. PMID: 25223839.
21. Shimony A, Zahger D, Gilutz H, Goldstein H, Orlov G, Merkin M, Shalev A, Ilia R, Douvdevani A. Cell free DNA detected by a novel method in acute ST-elevation myocardial infarction patients. Acute Card Care. 2010 Sep;12(3):109-11. doi: 10.3109/17482941.2010.513732. PMID: 20712451.
22. Tsai NW, Lin TK, Chen SD, Chang WN, Wang HC, Yang TM, Lin YJ, Jan CR, Huang CR, Liou CW, Lu CH. The value of serial plasma nuclear and mitochondrial DNA levels in patients with acute ischemic stroke. Clin Chim Acta. 2011 Feb 20;412(5-6):476-9. doi: 10.1016/j.cca.2010.11.036. Epub 2010 Dec 3. PMID: 21130757.
23. Simiakakis M, Kapsimalis F, Chaligiannis E, Loukides S, Sitaras N, Alchanatis M. Lack of effect of sleep apnea on oxidative stress in obstructive sleep apnea syndrome (OSAS) patients. PLoS One. 2012;7(6):e39172. doi: 10.1371/journal.pone.0039172. Epub 2012 Jun 25. PMID: 22761732; PMCID: PMC3382594.
24. He Y, Chen R, Wang J, Pan W, Sun Y, Han F, Wang Q, Liu C. Neurocognitive impairment is correlated with oxidative stress in patients with moderate-to-severe obstructive sleep apnea hypopnea syndrome. Respir Med. 2016 Nov;120:25-30. doi: 10.1016/j.rmed.2016.09.009. Epub 2016 Sep 9. PMID: 27817812.
25. Passali D, Corallo G, Petti A, Longini M, Passali FM, Buonocore G, Bellussi LM. A comparative study on oxidative stress role in nasal breathing impairment and obstructive sleep apnoea syndrome. Acta Otorhinolaryngol Ital. 2016 Dec;36(6):490-495. doi: 10.14639/0392-100X-1361. PMID: 28177332; PMCID: PMC5317128.
26. Borges YG, Cipriano LHC, Aires R, Zovico PVC, Campos FV, de Araújo MTM, Gouvea SA. Oxidative stress and inflammatory profiles in obstructive sleep apnea: are short-term CPAP or aerobic exercise therapies effective? Sleep

Breath. 2020 Jun;24(2):541-549. doi: 10.1007/s11325-019-01898-0. Epub 2019 Jul 16. PMID: 31313021.
27. Bauça JM, Yañez A, Fueyo L, de la Peña M, Pierola J, Sánchez-de-la-Torre A, et al.; Spanish Sleep Network. Cell Death Biomarkers and Obstructive Sleep Apnea: Implications in the Acute Coronary Syndrome. Sleep. 2017 May 1;40(5). doi: 10.1093/sleep/zsx049. PMID: 28419383.
28. Maniaci A, Iannella G, Cocuzza S, Vicini C, Magliulo G, Ferlito S, Cammaroto G, Meccariello G, De Vito A, Nicolai A, Pace A, Artico M, Taurone S. Oxidative Stress and Inflammation Biomarker Expression in Obstructive Sleep Apnea Patients. J Clin Med. 2021 Jan 13;10(2):277. doi: 10.3390/jcm10020277. PMID: 33451164; PMCID: PMC7828672.
29. Fernández-Bello I, Monzón Manzano E, García Río F, Justo Sanz R, Cubillos-Zapata C, Casitas R, et al. Procoagulant State of Sleep Apnea Depends on Systemic Inflammation and Endothelial Damage. Arch Bronconeumol. 2022 Feb;58(2):117-124. English, Spanish. doi: 10.1016/j.arbres.2020.11.017. Epub 2020 Dec 24. PMID: 33461785.
30. Shin C, Kim JK, Kim JH, Jung KH, Cho KJ, Lee CK, Lee SG. Increased cell-free DNA concentrations in patients with obstructive sleep apnea. Psychiatry Clin Neurosci. 2008 Dec;62(6):721-7. doi: 10.1111/j.1440-1819.2008.01876.x. PMID: 19068010.
31. Kang IG, Jung JH, Kim ST. The effect of obstructive sleep apnea on DNA damage and oxidative stress. Clin Exp Otorhinolaryngol. 2013 Jun;6(2):68-72. doi: 10.3342/ceo.2013.6.2.68. Epub 2013 Jun 14. PMID: 23799162; PMCID: PMC3687064.
32. Bilal N, Kurutas EB, Orhan I, Bilal B, Doganer A. Evaluation of preoperative and postoperative serum interleukin-6, interleukin-8, tumor necrosis factor α and raftlin levels in patients with obstructive sleep apnea. Sleep Breath. 2021 Jun;25(2):819-826. doi: 10.1007/s11325-020-02161-7. Epub 2020 Aug 10. Erratum in: Sleep Breath. 2021 Jun;25(2):827. doi: 10.1007/s11325-021-02317-z. PMID: 32776303.
33. Ye L, Ma GH, Chen L, Li M, Liu JL, Yang K, Li QY, Li N, Wan HY. Quantification of circulating cell-free DNA in the serum of patients with obstructive sleep apnea-hypopnea syndrome. Lung. 2010 Dec;188(6):469-74. doi: 10.1007/s00408-010-9253-4. Epub 2010 Jul 29. PMID: 20668869.
34. Kapur VK, Auckley DH, Chowdhuri S, Kuhlmann DC, Mehra R, Ramar K, Harrod CG. Clinical Practice Guideline for Diagnostic Testing for Adult Obstructive Sleep Apnea: An American Academy of Sleep Medicine Clinical Practice Guideline. J Clin Sleep Med. 2017 Mar 15;13(3):479-504. doi: 10.5664/jcsm.6506. PMID: 28162150; PMCID: PMC5337595.
35. Crook S, Sievi NA, Bloch KE, Stradling JR, Frei A, Puhan MA, Kohler M. Minimum important difference of the Epworth Sleepiness Scale in obstructive sleep apnoea: estimation from three randomised controlled trials. Thorax. 2019 Apr;74(4):390-396. doi: 10.1136/thoraxjnl-2018-211959. Epub 2018 Aug 12. PMID: 30100576.
36. Ermakov AV, Konkova MS, Kostyuk SV, Izevskaya VL, Baranova A, Veiko NN. Oxidized extracellular DNA as a stress signal in human cells. Oxid Med Cell Longev. 2013;2013:649747. doi: 10.1155/2013/649747. Epub 2013 Mar 6. PMID: 23533696; PMCID: PMC3606786.
37. Zhou L, Chen P, Peng Y, Ouyang R. Role of Oxidative Stress in the Neurocognitive Dysfunction of Obstructive Sleep Apnea Syndrome. Oxid Med Cell Longev. 2016;2016:9626831. doi: 10.1155/2016/9626831. Epub 2016 Sep 28. PMID: 27774119; PMCID: PMC5059616.
38. Tóthová L, Hodosy J, Mucska I, Celec P. Salivary markers of oxidative stress in patients with obstructive sleep apnea treated with continuous positive airway pressure. Sleep Breath. 2014 Sep;18(3):563-70. doi: 10.1007/s11325-013-0919-z. Epub 2013 Dec 10. PMID: 24323279.
39. Muñoz-Hernandez R, Vallejo-Vaz AJ, Sanchez Armengol A, Moreno-Luna R, Caballero-Eraso C, Macher HC, Villar J, Merino AM, Castell J, Capote F, Stiefel P. Obstructive sleep apnoea syndrome, endothelial function and markers of endothelialization. Changes after CPAP. PLoS One. 2015 Mar 27;10(3):e0122091. doi: 10.1371/journal.pone.0122091. PMID: 25815511; PMCID: PMC4376903.
40. Kanbay A, Kokturk O, Ciftci TU, Tavil Y, Bukan N. Comparison of serum adiponectin and tumor necrosis factor-alpha levels between patients with and without obstructive sleep apnea syndrome. Respiration. 2008;76(3):324-30. doi: 10.1159/000134010. Epub 2008 May 19. PMID: 18487876.
41. Imani MM, Sadeghi M, Khazaie H, Emami M, Sadeghi Bahmani D, Brand S. Serum and Plasma Tumor Necrosis Factor Alpha Levels in Individuals with Obstructive Sleep Apnea Syndrome: A Meta-Analysis and Meta-Regression. Life (Basel). 2020 Jun 12;10(6):87. doi: 10.3390/life10060087. PMID: 32545460; PMCID: PMC7345342.
42. Georgoulis M, Yiannakouris N, Tenta R, Kechribari I, Lamprou K, Vagiakis E, Kontogianni MD. Improvements in Plasma Tumor Necrosis Factor-Alpha Levels after a Weight-Loss Lifestyle Intervention in Patients with Obstructive Sleep Apnea. Life (Basel). 2022 Aug 17;12(8):1252. doi: 10.3390/life12081252. PMID: 36013431; PMCID: PMC9410143.
43. Archontogeorgis K, Nena E, Papanas N, Steiropoulos P. Biomarkers to improve diagnosis and monitoring of obstructive sleep apnea syndrome: current status and future perspectives. Pulm Med. 2014;2014:930535. doi: 10.1155/2014/930535. Epub 2014 Nov 27. PMID: 25538852; PMCID: PMC4265695.
44. Sarac F, Basoglu OK, Gunduz C, Bayrak H, Biray Avci C, Akcicek F. Association of osteopontin and tumor necrosis factor-α levels with insulin resistance in obese patients with obstructive sleep apnea syndrome. J Endocrinol Invest. 2011 Jul-Aug;34(7):528-33. doi: 10.3275/7287. Epub 2010 Oct 8. PMID: 20935448.
45. Cao Y, Song Y, Ning P, Zhang L, Wu S, Quan J, Li Q. Association between tumor necrosis factor alpha and obstructive sleep apnea in adults: a meta-analysis update. BMC Pulm Med. 2020 Aug 12;20(1):215. doi: 10.1186/s12890-020-01253-0. PMID: 32787816; PMCID: PMC7425010.

***Corresponding author:** Dr. Waheeb Alharbi, PhD, Associate Professor, Department of Physiology, Faculty of Medicine, Umm Al-Qura University, Makkah 21955, Saudi Arabia. Email: wdharbi@uqu.edu.sa*

International Journal of Biomedicine 16(2) (2026) 223-226
http://dx.doi.org/10.21103/Article16(2)_OA11

ORIGINAL ARTICLE

INTERNATIONAL JOURNAL OF BIOMEDICINE

Laboratory and Clinical Correlates of Lupus Anticoagulant Positivity in an Albanian Cohort

Ina Toska[1*], Ervin Rapushi[2], Rexhep Shkurti[1], Anila Mitre[3], Ervin Toçi[2]

[1]*Department of Biotechnology, Faculty of Natural Sciences, University of Tirana, Tirana, Albania*
[2]*University of Medicine, Tirana, Albania*
[3]*Department of Biology, Faculty of Natural Sciences, University of Tirana, Tirana, Albania*

Abstract

Background: Antiphospholipid syndrome (APS) is an autoimmune disease in which immune-mediated mechanisms promote a chronic prothrombotic state, leading to an increased risk for thrombotic events and obstetric complications. Particularly during their reproductive ages, females are disproportionately affected, making APS a major clinical concern in female populations. Lupus anticoagulant (LAC) is recognized as the strongest laboratory predictor for thrombosis and adverse pregnancy outcomes, among antiphospholipid antibodies. However, the clinical and laboratory correlates of LAC in women, including thrombosis, homocysteine metabolism, genetic thrombophilia, and reproductive complications, remain poorly understood.
Methods and Results: This observational study included 522 individuals with a thrombotic event or pregnancy morbidity, suspected of having APS. They were tested for LAC, homocysteine (HCY), and antiphospholipid antibodies. Subsequent analyses were conducted exclusively among female participants to provide a more clinically meaningful and statistically reliable evaluation. Association between LAC levels and APS classification, thrombotic events, homocysteine levels, the *MTHFR* gene mutations (C677T and A1298C), and other conditions of pregnancy losses were evaluated using chi-square tests, Welch two-sample t-test, and Pearson correlation as appropriate. Statistical analyses were performed using R software.
Among female participants (n=452), LAC positivity was observed in 35.2%, elevated homocysteine levels in 18.8%, and APS in 11.3%. Lupus anticoagulant levels were highly significant in participants with thrombotic events and APS classified. No significant linear correlation was observed between LAC and homocysteine levels. In contrast, significant differences in LAC levels were observed according to the *MTHFR* mutation status and history of other pregnancy losses.
Conclusion: This study highlights the central role of lupus anticoagulant as a key laboratory marker associated with thrombotic events and APS-related manifestations in women. The lack of association with homocysteine further supports the concept of independent pathogenic pathways. These findings underscore the importance of LAC assessment in the clinical evaluation and risk stratification of patients with suspected antiphospholipid syndrome.(**International Journal of Biomedicine. 2026;16(2):223-226.**)

Keywords: antiphospholipid syndrome • lupus anticoagulant • homocysteine • *MTHFR* gene

For citation: Toska I, Rapushi E, Shkurti R, Mitre A, Toçi E. Laboratory and Clinical Correlates of Lupus Anticoagulant Positivity in an Albanian Cohort. International Journal of Biomedicine. 2026;16(2):223-226. doi:10.21103/Article16(2)_OA11

Abbreviations

APS, antiphospholipid syndrome; **aCL**, anticardiolipin; **ß2-GPI**, ß2-glycoprotein I; **HCY**, homocysteine; **LAC**, lupus anticoagulant; **MTHFR**, methylenetetrahydrofolate reductase.

Introduction

Antiphospholipid syndrome (APS) is an autoimmune disease in which immune-mediated mechanisms promote a chronic prothrombotic state, leading to an increased risk for thrombotic events and obstetric complications.[1] Antiphospholipid syndrome represents one of the leading causes of arterial and venous thrombosis, as well known for its contribution to pregnancy morbidity, including recurrent pregnancy loss, placental insufficiency, and preeclampsia.

The diagnosis and risk stratification rely on the detection of antiphospholipid antibodies, including lupus anticoagulant (LAC), anti-cardiolipin (aCL), and anti-ß2-glycoprotein I (anti-ß2GPI), in combination with clinical criteria.[2] Among antiphospholipid antibodies, LAC has been shown to be the strongest laboratory predictor of thrombotic events and pregnancy morbidity.[3] Despite LAC being established as a criterion for APS diagnosis, its contribution to the broader clinical and laboratory spectrum of APS remains poorly understood. Elevated levels of homocysteine represent an independent risk factor for endothelial dysfunction and thrombosis and have been associated with adverse pregnancy outcomes. Similarly, the *MTHFR* gene mutations may alter homocysteine levels, contributing to thrombotic manifestations and pregnancy complications.[4]

However, data that integrates LAC levels with homocysteine metabolism, genetic thrombophilia, thrombotic manifestations, and pregnancy morbidity in female cohorts remains limited. Given the clinical impact of APS in women and the central role of LAC in APS-pathology, a focused evaluation of LAC-associated clinical and laboratory features in female populations is warranted.

The aim of the present study was to investigate the laboratory and clinical correlates of lupus anticoagulant in a female cohort evaluated for APS, with emphasis on thrombotic events, homocysteine levels, *MTHFR* mutations, other causes of pregnancy loss, and antiphospholipid antibodies (aCL, anti-β2GPI).

Materials and Methods

This retrospective, observational study was based on data obtained from Intermedica Laboratory in Tirana, Albania, collected between 2017 and 2025. All laboratory tests included in the analyses were performed during routine clinical care and are requested by treating clinicians. All data are analyzed in anonymized form, with no access to identify personal information. In this study, a total of 522 individuals/patients were initially included with a thrombotic event or pregnancy morbidity. Demographic characteristics, including age and sex, were recorded. Age was analyzed as a continuous variable. Because of the clinical relevance of APS in females and unequal gender distribution, analyses were restricted only to females (n = 452). All female participants were classified according to clinical history and laboratory data. They were stratified into four clinical groups: females with thrombotic events, females with pregnancy losses associated with *MTHFR* positivity, females with pregnancy losses related to APS, and females with pregnancy losses for other conditions. Thrombotic events were recorded as a binary variable (presence/absence) based on clinical history. Detailed classification into venous or arterial thrombosis was not available. The *MTHFR* mutation status was assessed as part of routine thrombophilia screening and was analyzed as a dichotomous variable (positive/negative), without distinction between polymorphism type (C677T or A1298C) or zygosity. APS status in this study reflects antiphospholipid antibody positivity rather than a confirmed APS diagnosis based on repeat testing after 12 weeks. Lupus anticoagulant was measured using the dilute Russell's viper venom time (dRVVT) assay, according to standard laboratory procedures, and expressed as ratio values. Positivity was defined according to laboratory-specific cut-off values. Anticardiolipin antibodies and anti-β2GPI (IgM/IgG) were measured using a standardized enzyme-linked immunosorbent assay (ELISA). Homocysteine levels were determined using a standardized chemiluminescent immunoassay (CLIA).

For comparative analyses, participants were grouped according to a binary classification (negative vs. positive) for each variable of interest. Statistical analyses were performed using Pearson's chi-square test for categorical variables and the Welch two-sample t-test for continuous variables. Pearson correlation analysis was applied to assess linear relationships between continuous variables. All analyses were conducted using R software (version 4.5.1).

Results

A total of 522 participants were included in the analysis (86.6% female, 13.4% male). The mean age of the study population was 36.45±11.45 years. Among female participants, the mean age was 36.15±10.73 years, ranging from 3 to 74 years. A small number of pediatric cases were included, as testing for thrombophilia and antiphospholipid antibodies was performed as part of routine clinical evaluation.

The overall prevalence of LAC, HCY, and APS positivity was 37.4%, 19.2%, and 10.7 %, respectively. LAC values showed a wide distribution within the study population (up to 111.1 dRVVT ratio), with significantly higher mean values observed among participants with thrombotic events and those classified as APS-positive. A statistically significant association was observed between gender and LAC status (P=0.0089). LAC positivity was more frequent in males than females (51.4% vs 35.2%). Male participants had nearly twofold higher odds of LAC positivity compared with females (OR=1.96, 95% CI: 1.18-3.25) (Table 1). In contrast, no statistically significant association was found between gender and HCY status (P=0.62). The prevalence of HCY positivity was comparable between males and females (21.4% vs. 18.8%). Similarly, gender was not significantly associated with APS status (P=0.30). APS positivity was observed in 11.3% of females and 7.1 % of males.

Table 1.

Overall prevalence of LAC, HCY, and APS.

Variable	Gender	Negative n (%)	Positive (%)	*P*-value	*OR (95% CI)
LAC	Female (n=452)	293 (64.8)	159 (35.2)	0.0089	1.96 (1.18-3.25)
	Male (n=70)	34 (48.6)	36 (51.4)		
HCY	Female (n=452)	367 (81.2)	85 (18.8)	0.62	1.18 (0.63-2.22)
	Male (n=70)	55 (78.6)	15 (21.4)		
APS	Female (n=452)	401(88.7)	51 (11.3)	0.30	0.77 (0.29-2.02)
	Male (n=70)	65 (92.9)	5 (7.1)		

**ORs represent the odds of positivity in males compared with females (reference category: female)*

Table 2.

Comparison of LAC levels according to clinical and laboratory characteristics in female participants (n = 452).

Variable	Negative (Mean LAC)	Positive (Mean LAC)	t (df)	*P*-value	95% CI
Thrombosis	41.11	48.92	−6.31 (99.01)	<0.001	−10.26 to −5.35
APS status	40.85	46.85	−6.93 (186.36)	<0.001	−7.71 to −4.29
MTHFR mutation	43.04	40.32	2.71 (81.41)	0.008	0.72 to 4.72
Other pregnancy losses	43.52	41.19	3.55 (444.93)	<0.001	1.04 to 3.62
aCL IgM	42.92	49.59	−1.46 (14.16)	0.166	–
aCL IgG	42.92	62.56	−1.46 (4.00)	0.219	–
Anti-β2GPI IgM	42.96	44.60	−0.85 (49.06)	0.400	–
Anti-β2GPI IgG	43.04	61.15	−1.70 (1.00)	0.338	–

Pearson correlation analysis showed no significant linear association between LAC and HCY levels (r = 0.05, *P* = 0.25). No significant correlation was observed between LAC and antiphospholipid antibodies aCL and anti-β2GPI (IgM/IgG). Given the predominance of female participants in the cohort (86.6%) and the clinical relevance of thrombotic and obstetric manifestations in women, subsequent analyses were restricted to female patients. Comparisons of LAC levels according to clinical and laboratory variables are presented in Table 2. LAC levels were higher in women who were *MTHFR* negative and in those without abortions attributable to other causes, whereas APS-positive individuals demonstrated significantly elevated LAC values. This pattern suggests a potential independent role of LAC in thrombosis and pregnancy morbidity.

Discussion

In this retrospective cross-sectional study of 522 participants, we investigated the prevalence and laboratory – clinical associations of lupus anticoagulant within an Albanian cohort, with particular emphasis on female patients. Our findings demonstrate that LAC levels are associated with thrombotic events and APS classification, while no meaningful correlation was observed with homocysteine levels. A key finding of this study is the strong association between elevated LAC levels and thrombotic events. Women with thrombosis had significantly higher mean LAC values than those without thrombosis. This observation is consistent with previous studies that have identified LAC as the strongest laboratory predictor of thrombotic risk among antiphospholipid antibodies.[2,5] Clinical and experimental evidence suggests that LAC contributes to thrombosis through endothelial activation, interference with anticoagulant pathways, and complement -mediated mechanisms.[6,7] The association observed in our cohort reinforces the clinical importance of LAC in risk stratification. Similarly, LAC levels were significantly higher in participants classified as APS- positive. This finding aligns with the established role of LAC as a laboratory criterion for APS classification. However, the magnitude of difference observed in our study suggests that LAC may reflect not only diagnostic classification but also disease activity or thrombotic burden. Importantly, APS classification in this study reflects antiphospholipid antibody positivity rather than a confirmed APS diagnosis based on repeat testing after 12 weeks, as required by classification criteria.[8] In contrast, no significant linear correlation was identified between LAC and homocysteine levels. This suggests that these factors may contribute to thrombosis through distinct and potentially independent mechanisms. Hyperhomocysteinemia is recognized as a risk factor for endothelial dysfunction and thrombosis;[9] its lack of association with LAC in our cohort indicates that it does not directly modulate the autoimmune prothrombotic state driven by antiphospholipid antibodies. This supports the concept of parallel rather than overlapping pathogenic pathways. Interestingly, LAC levels differed significantly by *MTHFR* status and a history of pregnancy losses attributed to other causes. Higher LAC levels were observed in *MTHFR*- negative individuals and in women without pregnancy losses due to other etiologies. These findings may suggest that LAC-related pathology represents a distinct autoimmune mechanism rather than a secondary effect of inherited thrombophilia. However, these observations should be interpreted cautiously, as the role of *MTHFR* polymorphisms in thrombosis and pregnancy complications remains controversial.[10,11] No statistically significant differences in LAC levels were observed according to aCL and β2GPI antibody status. This may reflect limited subgroup sizes or the known heterogeneity of antiphospholipid antibody profiles. It is well established that LAC, aCL, and anti-β2GPI antibodies may not always coexist and may exhibit different clinical associations.[12] Among these, LAC is considered the most strongly associated with thrombotic events, supporting its role as a functionally relevant marker of thrombogenic potential.[3] Notably, LAC positivity was more frequent in males compared to females, despite the predominance of females in the cohort. Although APS is more commonly reported in women, particularly with obstetric manifestations, this finding may reflect differences in referral patterns or underlying risk profiles within the studied population.

Taken together, these findings support the hypothesis that LAC may act as a primary autoimmune driver of

thrombosis and pregnancy morbidity, rather than merely reflecting secondary interactions with other risk factors such as homocysteine metabolism or inherited thrombophilia.

This study has several strengths, including a relatively large sample size, the use of both continuous and categorical analyses, and the focused evaluation of a clinically relevant female cohort. The integration of laboratory markers with clinical outcomes provides a comprehensive assessment of LAC-associated risk profiles.

Several limitations should be acknowledged. First, the APS classification in this study was based on single-time antibody positivity and did not include confirmatory testing after 12 weeks, as required by the classification criteria. Secondly, a retrospective design may lead to selection bias and limit causal inference. Third, thrombotic events were recorded as a binary variable without detailed classification into arterial and venous subtypes. Finally, subgroup analyses for certain variables were limited by small sample sizes.

In conclusion, this study highlights the central role of lupus anticoagulant as a key laboratory marker associated with thrombotic events and APS-related manifestations in women. The lack of association with homocysteine further supports the concept of independent pathogenic pathways. These findings underscore the importance of LAC assessment in the clinical evaluation and risk stratification of patients with suspected antiphospholipid syndrome.

Ethical Considerations

This retrospective observational study was conducted in accordance with the ethical principles of the World Medical Association Declaration of Helsinki (1964, revised 2013). All study data were fully anonymized prior to access and analysis, and no identifiable personal information was available to the researchers at any stage of the study. Given the retrospective design and the use of fully anonymized data, formal ethical approval and individual informed consent were not required, in accordance with applicable institutional policies and standard research practices. Institutional permission to use data was obtained from Intermedica Laboratory. An official institutional statement confirming these conditions has been provided with the manuscript submission.

Author Contributions

Ina Toska: Conceptualization, Investigation, Data curation, Writing – original draft.
Ervin Rapushi: Conceptualization, Investigation, Methodology, Writing – review and editing.
Anila Mitre: Investigation, data curation, Writing – review and editing.
Ervin Toci: Data curation, Formal analysis, Writing – original draft.
Rexhep Shkurti: Supervision, Conceptualization, Writing – review and editing.
All authors have approved the final article.

Conflict of Interest

The authors have declared no conflict of interest.

References

1. Cervera R, Piette JC, Font J, Khamashta MA, Shoenfeld Y, Camps MT, et al.; Euro-Phospholipid Project Group. Antiphospholipid syndrome: clinical and immunologic manifestations and patterns of disease expression in a cohort of 1,000 patients. Arthritis Rheum. 2002 Apr;46(4):1019-27. doi: 10.1002/art.10187. PMID: 11953980.
2. Miyakis S, Lockshin MD, Atsumi T, Branch DW, Brey RL, Cervera R, et al. International consensus statement on an update of the classification criteria for definite antiphospholipid syndrome (APS). J Thromb Haemost. 2006 Feb;4(2):295-306. doi: 10.1111/j.1538-7836.2006.01753.x. PMID: 16420554.
3. Galli M, Luciani D, Bertolini G, Barbui T. Lupus anticoagulants are stronger risk factors for thrombosis than anticardiolipin antibodies in the antiphospholipid syndrome: a systematic review of the literature. Blood. 2003 Mar 1;101(5):1827-32. doi: 10.1182/blood-2002-02-0441.
4. Den Heijer M, Lewington S, Clarke R. Homocysteine, MTHFR and risk of venous thrombosis: a meta-analysis of published epidemiological studies. J Thromb Haemost. 2005 Feb;3(2):292-9. doi: 10.1111/j.1538-7836.2005.01141.x.
5. Pengo V, Tripodi A, Reber G, Rand JH, Ortel TL, Galli M, De Groot PG; Subcommittee on Lupus Anticoagulant/ Antiphospholipid Antibody of the Scientific and Standardisation Committee of the International Society on Thrombosis and Haemostasis. Update of the guidelines for lupus anticoagulant detection. Subcommittee on Lupus Anticoagulant/ Antiphospholipid Antibody of the Scientific and Standardisation Committee of the International Society on Thrombosis and Haemostasis. J Thromb Haemost. 2009 Oct;7(10):1737-40. doi: 10.1111/j.1538-7836.2009.03555.x.
6. Meroni PL, Borghi MO, Raschi E, Tedesco F. Pathogenesis of antiphospholipid syndrome: understanding the antibodies. Nat Rev Rheumatol. 2011 Jun;7(6):330-9. doi: 10.1038/ nrrheum.2011.52.
7. Salmon JE, Girardi G. The Role of Complement in the Antiphospholipid Syndrome. KARGER eBooks. 2003 Jan 1;133–48.
8. Tektonidou MG, Andreoli L, Limper M, Amoura Z, Cervera R, Costedoat-Chalumeau N, et al. EULAR recommendations for the management of antiphospholipid syndrome in adults. Ann Rheum Dis. 2019 Oct;78(10):1296-1304. doi: 10.1136/annrheumdis-2019-215213.
9. Wald DS, Law M, Morris JK. Homocysteine and cardiovascular disease: evidence on causality from a meta-analysis. BMJ. 2002 Nov 23;325(7374):1202. doi: 10.1136/ bmj.325.7374.1202.
10. Bezemer ID, Doggen CJ, Vos HL, Rosendaal FR. No association between the common MTHFR 677C->T polymorphism and venous thrombosis: results from the MEGA study. Arch Intern Med. 2007 Mar 12;167(5):497-501. doi: 10.1001/archinte.167.5.497.
11. Hickey S, Curry C, Toriello H. ACMG Practice Guideline: lack of evidence for *MTHFR* polymorphism testing. Genet Med. 2013;15:153–156. doi:10.1038/gim.2012.165
12. de Laat HB, Derksen RH, Urbanus RT, Roest M, de Groot PG. beta2-glycoprotein I-dependent lupus anticoagulant highly correlates with thrombosis in the antiphospholipid syndrome. Blood. 2004 Dec 1;104(12):3598-602. doi: 10.1182/ blood-2004-03-1107.

***Corresponding author:** *Ina Toska, PhD(C).*

ina.toska@yahoo.com, ina_toska.fshnutdr@unitir.edu.al

International Journal of Biomedicine 16(2) (2026) 227-231
http://dx.doi.org/10.21103/Article16(2)_OA12

ORIGINAL ARTICLE

Dermatology

INTERNATIONAL JOURNAL OF BIOMEDICINE

Histopathological Examination of Seborrheic Keratosis in the Saudi Population

Mohammed Saud Alsaidan[1*], Salman Bin Dayel[1], Wafaey Badawy[2], Mariyyah Abdulrahman Alnathir[3], Norah Mohammed AlKahtani[3], Lujain Mubarak Aldossari[3], Razan Saleh Bin Hazzaa[3], Asma Muneer Alharthi[3], Ghada Lazzam Allazzam[3], Faris Majed Almusayfir[3], Raghad Shudayyid R. Almutairi[4], Ali Hassan A. Ali[5]

[1]*Internal Medicine Department, Dermatology Unit, College of Medicine, Prince Sattam bin Abdulaziz University, Al-Kharj 11942, Saudi Arabia*
[2]*Department of Pathology, Military Industries Hospital, Al-Kharj, Saudi Arabia*
[3]*College of Medicine, Prince Sattam bin Abdulaziz University, Al-Kharj 11942, Saudi Arabia*
[4]*Faculty of Medicine, Almaarefa University, Riyadh, Saudi Arabia*
[5]*Basic Medical Science Department, College of Medicine, Prince Sattam bin Abdulaziz University, Al-Kharj 11942, Saudi Arabia*

Abstract

Background: One of the most prevalent skin epidermal tumors is seborrheic keratosis (SK). But only a few extensive histopathological studies have been conducted on people with SK. This study's objective was to examine different histological cases of SK.

Methods and Results: The subjects of this retrospective study were 39 patients (28 male and 11 female), aged 50-90 and older, with clinically confirmed SK who presented to the outpatient dermatology departments of Prince Sattam bin Abdulaziz University Hospital and the Military Industries Hospital between January 2024 and June 2025. Pathology sections stained with hematoxylin and eosin were categorized as acanthotic (classic), mixed, melanoacanthoma (pigmented), or irritated based on their histological characteristics.

The highest number of SK cases (13/33.3%) in this study was identified in the age group of 60 to 69 years. The trunk (21/53.8%) was the most common biopsy site for biopsy-proven seborrheic keratosis, followed by the neck (9/23.1%), the face (4/10.2%), and the extremities (5/12.8%). The acanthotic (classic) subtype was the most common histopathological subtype (23/59.0%), followed by the mixed (9/23.1%), irritated (5/12.8%), and melanoacanthoma (pigmented) (2/5.1%) subtypes.

Conclusion: The acanthotic type of seborrheic keratosis was the most common histologic type identified, predominantly observed in patients aged 60–69 years. The trunk is a primary location for seborrheic keratosis. (**International Journal of Biomedicine. 2026;16(2):227-231.**)

Keywords: seborrheic keratosis • histopathology • subtype • Saudi population

For citation: Alsaidan MS, Bin Dayel SB, Badawy W, Alnathir MA, AlKahtani NM, Aldossari LM, Hazzaa RSB, Alharthi AM, Allazzam GL, Almusayfir FM, Almutairi RSR, Ali AHA. Histopathological Examination of Seborrheic Keratosis in the Saudi Population. International Journal of Biomedicine. 2026;16(2):227-231. doi:10.21103/Article16(2)_OA12

Introduction

The most prevalent benign, pigmented epidermal lesion in the older population is seborrheic keratosis (SK).[1] It appears as distinct, slightly elevated, brownish patches or plaques, typically on sun-exposed skin.[2] Research conducted by the US National Health and Nutrition Examination Survey estimates that 23 million Americans suffer from SK. It was initially described in 1869 as a well-defined, black, spherical, raised, adherent skin lesion that enlarges with age.[3] Clinically, these tumors appear as pigmented growths resembling papules or skin warts, with a greasy crust. Microscopically, these lesions

show hyperproliferation of basal-layer immature keratinocytes, most of which exhibit melanocytic pigmentation.[4] These benign tumors are more common in older people. Seborrheic keratosis is frequently discovered by accident. Treatment is not required because this tumor is benign. Nonetheless, the lesions are frequently removed, particularly for aesthetic reasons.[5] Sometimes it is important to differentiate SK from other skin tumors that could be benign or malignant. For example, deeply pigmented SK may be mistaken for malignant melanoma by non-dermatologist doctors or laypeople.[6] Even though SK can show in a variety of ways, the diagnosis is typically clinically simple. However, the tumor may mimic other conditions, such as lentigines, melanocytic nevi, actinic keratosis, Bowen's disease, common warts, and more serious conditions, including squamous cell and basal cell carcinomas, and even cutaneous melanomas.[7] Acanthosis, papillomatosis, hyperkeratosis, and horn pseudocysts are the histological features of SK. Seborrheic keratosis may be classified into several histological subgroups based on the relative dominance of these characteristics. The acanthotic, hyperkeratotic, and adenoid are the most significant of them.[5] The disorder's pathophysiology remains largely unknown. Although tumors can occur in relatively young patients, it is known that the occurrence of SK rises noticeably with age. It is believed that there is a genetic susceptibility to numerous SKs. It is also being discussed how UV light contributes to lesion formation.[8] Even though SK is a benign condition, there are several reasons lesions should be removed, including irritation and inflammation, exclusion of cancer (if the clinical presentation is ambiguous), and cosmetic concerns in patients with many lesions.[5] Surgical therapy, laser therapy, electrocautery, cryotherapy, and topical medication therapy, which is still under development, are among the available treatment options. Individualized treatment should be based on the patient's preferences and the clinical picture.(9) This study intended to identify the histological pattern of seborrheic keratosis in Saudi individuals.

Materials and Methods

The subjects of this retrospective study were patients with clinically confirmed SK who presented to the outpatient dermatology departments of Prince Sattam bin Abdulaziz University Hospital and the Military Industries Hospital between January 2024 and June 2025. A retrospective analysis of medical records was conducted to identify variations in age, sex, and lesion location. Pathology sections stained with hematoxylin and eosin were categorized as acanthotic (classic), mixed, melanoacanthoma (pigmented), or irritated based on their histological characteristics. However, only cases with adequate tissue samples and thorough clinical information were examined. All materials and important clinical information, such as age, sex, and clinical examination results, were sent to the histopathology section of the pathology department in 10% formalin. All tissue sections were processed according to the standard biopsy procedure for paraffin-embedded sections. After creating slices that were three to five microns thick, eosin and hematoxylin stains were applied. Two qualified pathologists examined each slide under a light microscope to ensure diagnostic consistency.

The biopsy-proven sites were divided into the following categories for convenience: face, neck, trunk, and extremities.

Statistical analysis was performed using the statistical software package SPSS version 22.0 (SPSS Inc, Armonk, NY: IBM Corp). Baseline characteristics were summarized as frequencies and percentages.

Results

All 39 of the cases (28 male and 11 female) of SK that were clinically diagnosed were later confirmed by histological examination of biopsy samples. The patients were aged 50-90 and older. The highest number of cases (13/33.3%) in this study was identified in the age group of 60 to 69 years. The next most frequent age group affected was 70 to 79 years old (Table 1). The trunk (21/53.8%) was the most common biopsy site for biopsy-proven SK, followed by the neck (9/23.1%), the face (4/10.2%), and the extremities (5/12.8%). (Table 2).

Table 1.

Lesion distribution according to histology, age, and gender (n=39)

Parameter	Category	n	Percentage
Gender	Male	28	71.8 %
	Female	11	28.2 %
Age	50-59	5	12.8 %
	60-69	13	33.3 %
	70-79	12	30.8 %
	80-89	7	17.9 %
	90 and above	2	5.1 %
Type of lesion	Acanthotic (Classic)	23	59.0 %
	Mixed (Irritated and Pigmented)	9	23.1 %
	Irritated	5	12.8 %
	Melanoacanthoma (Pigmented)	2	5.1 %

Table 2.

Location of seborrhoeic keratosis.

Location	n	Percentage
Face	4	10.2 %
Neck	9	23.1 %
Trunk	21	53.8 %
Limbs	5	12.8 %

A comprehensive analysis showed that the acanthotic (classic) subtype was the most common histopathological subtype (23/59.0%), followed by the mixed (9/23.1%), irritated (5/12.8%), and melanoacanthoma (pigmented) (2/5.1%).subtypes.

The acanthotic variety has numerous basaloid cells and pronounced acanthosis. The vertical diameter of the acanthosis can be at least 3 mm (Figure 1). Wide keratinocyte bands enlarged the epidermis. Hyperkeratosis and papillomatosis are typically mild. Horn cysts, also known as pseudocysts, are a

defining characteristic, and in certain situations, there may be several cysts (Figure 2).

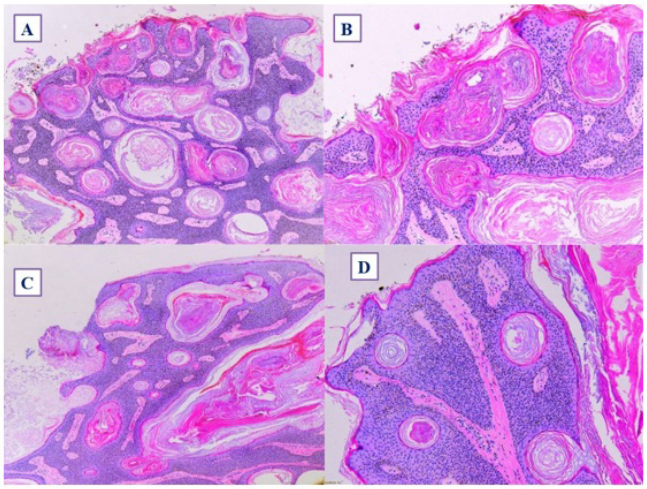

Fig. 1. *Images of the acanthotic (classic) type of seborrheic keratosis stained with H&E. There is significant thickening of the epidermis. The appearance of horny invaginations is similar to pseudohorn cysts. (A X200), (B, C, and D X400)*

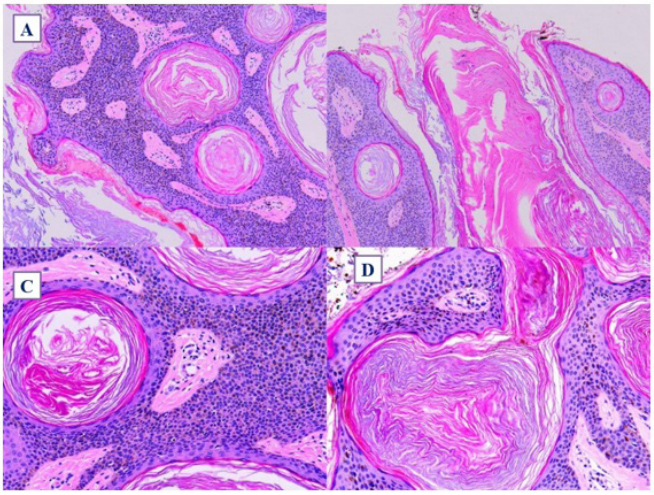

Fig. 2. *Images of the acanthotic (classic) type of seborrheic keratosis stained with H&E. There are horn pseudocysts and horn cysts. In contrast to pseudohorn cysts, which are created by keratin downgrowths from the underlying stratum corneum and are thus attached to it, horn cysts develop intraepidermally and are discharged transepidermally. A thin granular cell layer surrounds the surrounding keratinocytes in the spherical, keratin-filled center of both cysts. (A, B, C, and D X 400).*

In the mixed (irritated and pigmented) subtype, we found acantholysis, dyskeratosis, spongiosis, an inflammatory cell infiltrate with partially lichenoid appearances in the dermis (which may not be present), eosinophilic squamous epithelial cell aggregations (squamous eddies) resembling onion skin, and apoptotic basal cells. The mixed form was highly pigmented, with melanocytes proliferating (Figure 3 A,B).

Aggregated eosinophilic squamous cells were observed in the irritated type, along with acantholysis, dyskeratosis, spongiosis, and degeneration of the basal cell layer. (Figure 3 CD).

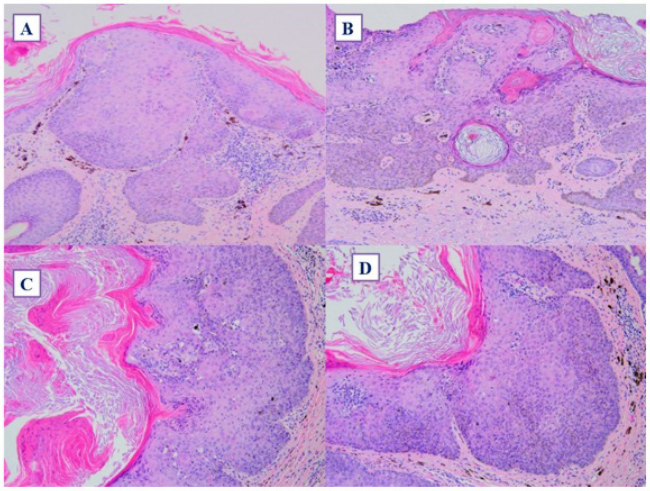

Fig. 3. *(A, B) Two images of mixed (irritated and pigmented) type of seborrheic keratosis stained with H&E. (C, D) Two images of irritated type of seborrheic keratosis stained with H&E. (A, B, C, and D X 400).*

Melanoacanthoma (pigmented), characterized by rapid, dark pigmentation and proliferation of dendritic melanocytes across an acanthotic epidermis, was detected in only two cases (Figure 4).

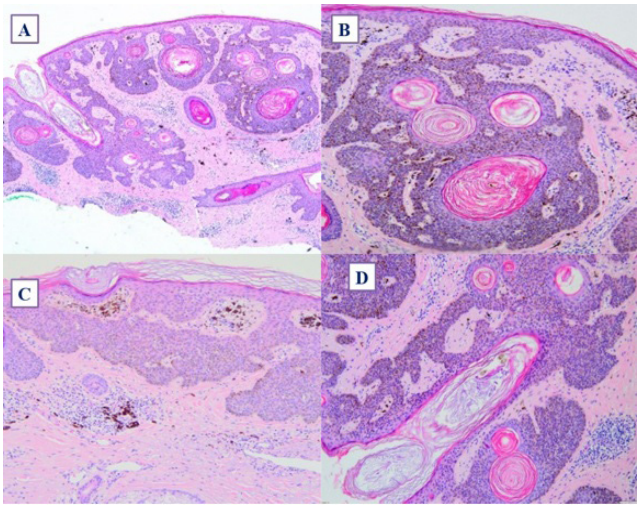

Fig. 4. *Images of melanoacanthoma (pigmented) stained with H&E. (A, B, C, and D X 400)*

Discussion

Dermatologists see seborrheic keratoses every day since they are among the most prevalent skin tumors. These distinct, round or oval growths. might be flesh-colored, light brown, or black, and they seem to be adhered to the skin. Based on clinical presentation, most seborrheic keratoses are easily diagnosed. Sometimes, distinguishing certain lesions from others, including malignant melanoma, can be challenging.[5] Acanthosis, papillomatosis, hyperkeratosis, and horn pseudocysts are the histological features of seborrheic keratosis. Seborrheic keratosis is thought to be caused by several factors, including age, genetic susceptibility, and potentially UV radiation exposure.[9] It has been documented

in younger age groups, such as teens and young adults, despite being more common in the elderly.[10]

Studies and geographical areas differ greatly in how seborrheic keratosis is classified pathologically.[11] We divided seborrheic keratosis into five histological categories based on *Andrews' Diseases of the Skin: Clinical Dermatology*: acanthotic, mixed, hyperkeratotic, clonal, irritable, and melanoacanthoma.[12] The acanthotic form was the most common, accounting for 23 cases (58.9%), in line with earlier studies and confirming the general understanding of its predominance in SK. In our study, we did not find hyperkeratotic or clonal types. The correct etiopathogenesis of this lesion remains unclear despite its high incidence. Therefore, it has been proposed that human papillomavirus (HPV), sun exposure, genetics, and chronic irritation are risk factors. Recent genetic research suggests that somatic mutations in the Fibroblast Growth Factor Receptor 3 (*FGFR3)* gene may play a significant role in the onset of SK. Multiple seborrheic keratoses appearing suddenly could be an indication of Leser-Trélat, which can be linked to an underlying cancer.[13] According to current clinical viewpoints, SK shows age-dependent trends, with incidence rates increasing progressively with age. According to Hainan Province's empirical data, the old-age population is growing faster than the working-age population, supporting the region's shift toward an aging population. One etiological factor contributing to the secular trend of rising SK incidence may be demographic aging.[11]

Aside from cosmetic correction, asymptomatic SK typically does not require treatment; it may also resolve on its own in a short time.[14] According to our research, the trunk is the anatomical area most affected by seborrheic keratosis. However, according to a prior study, the face, neck, and upper extremities were more commonly impacted than the trunk.[15] In conclusion, the acanthotic type of SK was the most common histologic type identified in this research. It usually affects older people. To rule out other premalignant or malignant conditions, a biopsy should be performed on lesions.

Ethics Approval

All steps in this study complied with the Ethics Committee of the Institutional Review Board of Prince Sattam bin Abdulaziz University (SCBR-639/2026).

Author Contributions

Mohammed Saud Alsaidan: Study design, Writing – original draft.
Salman Bin Dayel: Study design, Writing – original draft.
Wafaey Badawy: Study design, Writing – original draft.
Mariyyah Abdulrahman Alnathir: Data curation, Investigation, Writing – original draft.
Norah Mohammed Al Kahtani: Data curation, Investigation, Writing – original draft.
Lujain Mubarak Aldossari: Data curation, Investigation, Writing – original draft.
Razan Saleh Bin Hazzaa: Data curation, Investigation, Writing – original draft.
Asma Muneer Alharthi: Data curation, Investigation, Writing – original draft.
Ghada Lazzam Allazzam: Data curation, Investigation, Writing – original draft.
Faris Majed Almusayfir: Study design, Formal analysis, Writing – original draft.
Raghad Shudayyid R. Almutairi: Study design, Formal analysis, Writing – original draft.
Ali Hassan A. Ali: Conceptualization, Methodology, Writing – review and editing.
All authors have approved the final article.

Conflict of Interest

The authors have declared no conflict of interest.

Acknowledgements

The author is grateful to the Deanship of Scientific Research, Prince Sattam bin Abdulaziz University, Al-Kharj, Saudi Arabia, for its support and encouragement in conducting the research and publishing this report.

Availability of Data and Materials

The data are available upon request from the authors.

References

1. Sultana M, Mandal A, Chatterjee A, Das SK, Sinha S, Chatterjee RP. Seborrheic Keratosis Through the Lens of Histopathology: A Case Report. Cureus. 2025 Oct 30;17(10):e95780. doi: 10.7759/cureus.95780. PMID: 41328095; PMCID: PMC12664931.
2. Roh NK, Hahn HJ, Lee YW, Choe YB, Ahn KJ. Clinical and Histopathological Investigation of Seborrheic Keratosis. Ann Dermatol. 2016 Apr;28(2):152-8. doi: 10.5021/ad.2016.28.2.152. Epub 2016 Mar 31. PMID: 27081260; PMCID: PMC4828376.
3. Salah B, Mahseeri M, Al-Ali Z, Gaith A, Aldwan T, Al-Rawashdeh B. Giant perianal Seborrheic keratosis: A case report. Int J Surg Case Rep. 2018;51:296-301. doi: 10.1016/j.ijscr.2018.09.001. Epub 2018 Sep 12. PMID: 30243263; PMCID: PMC6148732.
4. Sepehri N, Babaniamansour S, Karkon-Shayan S, Majidi M, Atarodi A, Mohammadzadeh H, Talaiee M. Giant seborrheic keratosis on the right flank part: a case report. Journal of Skin and Stem Cell. 2020 Sep 30;7(3).
5. Hafner C, Vogt T. Seborrheic keratosis. J Dtsch Dermatol Ges. 2008 Aug;6(8):664-77. English, German. doi: 10.1111/j.1610-0387.2008.06788.x. PMID: 18801147.
6. Duque MI, Jordan JR, Fleischer AB Jr, Williford PM, Feldman SR, Teuschler H, Chen GJ. Frequency of seborrheic keratosis biopsies in the United States: a benchmark of skin lesion care quality and cost effectiveness. Dermatol Surg. 2003 Aug;29(8):796-801; discussion 801. doi: 10.1046/j.1524-4725.2003.29211.x. PMID: 12859377.
7. Jeong YI, Lee WJ, Bak H, Oh SH, Jung HJ, Chang SE, Choi JH. Detection of human papilloma virus DNA in

seborrheic keratosis of Korean skin. Annals of Dermatology. 2007 Sep 1;19(3):99-105.
8. Hafner C, Vogt T, Landthaler M, Müsebeck J. Somatic FGFR3 and PIK3CA mutations are present in familial seborrhoeic keratoses. Br J Dermatol. 2008 Jul;159(1):214-7. doi: 10.1111/j.1365-2133.2008.08626.x. Epub 2008 Jul 1. PMID: 18503601.
9. Barthelmann S, Butsch F, Lang BM, Stege H, Großmann B, Schepler H, Grabbe S. Seborrheic keratosis. J Dtsch Dermatol Ges. 2023 Mar;21(3):265-277. doi: 10.1111/ddg.14984. Epub 2023 Mar 9. PMID: 36892019.
10. Gorai S, Ahmad S, Raza SSM, Khan HD, Raza MA, Etaee F, Cockerell CJ, Apalla Z, Goldust M. Update of pathophysiology and treatment options of seborrheic keratosis. Dermatol Ther. 2022 Dec;35(12):e15934. doi: 10.1111/dth.15934. Epub 2022 Nov 1. PMID: 36226729.
11. Luo W, Liang Y, Yang X, Wu W, Lu J. Histopathological Subtypes and Clinical Presentation of Seborrheic Keratosis: A 15-Year Retrospective Analysis of 1,169 Cases in Hainan, China. Clin Cosmet Investig Dermatol. 2025 Mar 24;18:721-727. doi: 10.2147/CCID.S517318. PMID: 40160436; PMCID: PMC11952144.
12. Odom RB, James WD, Berger TG. Andrews' Diseases of the Skin: Clinical Dermatology. 9th ed. Harcourt Asia/WB Saunders; 2004:804–805.
13. Salah B, Mahseeri M, Al-Ali Z, Gaith A, Aldwan T, Al-Rawashdeh B. Giant perianal Seborrheic keratosis: A case report. Int J Surg Case Rep. 2018;51:296-301. doi: 10.1016/j.ijscr.2018.09.001. Epub 2018 Sep 12. PMID: 30243263; PMCID: PMC6148732.
14. Li WR, Lin L. Seborrheic keratosis in a young woman: a mimicker of keratoacanthoma. International Journal of Dermatology and Venereology. 2020 Jun 1;3(02):116-7.
15. Lee GS, Ahn KJ, Kim JM, Lee ES. A histopathologic study of the seborrheic keratosis. Korean J Dermatol 1992;30:76-80.

***Corresponding author**:

Dr. Mohammed Saud Alsaidan. E-mail: m.alsaidan@psau.edu.sa

International Journal of Biomedicine 16(2) (2026) 232-241
http://dx.doi.org/10.21103/Article16(2)_OA13

ORIGINAL ARTICLE

INTERNATIONAL JOURNAL OF BIOMEDICINE

Optical Stereometric Analysis of Milled and Not-Milled Copings for Removable Overdentures on an Experimental Partially Edentulous Mandible

Srđan D. Poštić[1*], Slobodan Dodić[1], Ivan V. Tanasić[2], Miloš Milošević[3], Stevan Avramov[4], Vladimir Biočanin[5], Ljubiša Ristić[6], Igor Đorđević[1], Aleksa Milovanović[3], Miloš Maksimović[1], Ekatarina Ž. Džigurski[7], Predrag M. Šojić[7]

[1]*Department of Prosthodontics, University School of Dental Medicine, Belgrade, Serbia*
[2]*Department for Prosthetics, The College of Health Sciences, Academy of Applied Studies Belgrade, Belgrade, Serbia*
[3]*Innovation Center of the Faculty of Mechanical Engineering, University of Belgrade, Belgrade, Serbia*
[4]*Faculty of Stomatology in Pančevo, University Business Academy in Novi Sad; Institute for Biological Research "Siniša Stanković" - National Institute of Republic of Serbia, University of Belgrade, Serbia*
[5]*Faculty of Stomatology in Pančevo, University Business Academy in Novi Sad, Serbia*
[6]*Military Medical Academy, Belgrade, Serbia*
[7]*Faculty of Dental Medicine, University of Belgrade, Belgrade, Serbia*

Abstract

Background: This study aimed to examine the effect of differential stress distributions on the occlusal surfaces of the control and experimental copings.
Methods and Results: The study used two master casts of a lower jaw with bilateral terminal edentulous seats. Their topography was identical, indicating a partially edentulous lower jaw according to Eichner's B3 (and C2) classification (i.e., Kennedy class 1). The control cast had conventional oval copings. The experimental cast had the surfaces simulating three specific milled copings covering the remaining tooth substance. Controlled loading was measured using a gnathodynamometer. Loading stages were at 400, 800, and 1000 N. Measurements of strain and displacement were provided by the Digital Image Correlation Method. The "Wilcoxon Lambda" two-sample test was used in the analysis of deformation between the control rounded and experimental milled copings under loading.
Smaller values of deformations were measured on milled copings. There were statistically significant differences in displacement between the control rounded and experimental milled copings ($Pr > |Z| = 0.001$) as well as in deformations ($Pr > |Z| = 0.0298$).
Conclusion: Experimental milled copings are less susceptible to deformation than the control rounded copings. These findings may have clinical significance for improving primary and secondary retention of overdentures on milled copings.(**International Journal of Biomedicine. 2026;16(2):232-241.**)

Keywords:copings • overdenture • shortened dental arch • digital image correlation technique • optic stereometry

For citation: Poštić SD, Dodić S, Tanasić IV, Milošević M, Avramov S, Biočanin V, Ristić L, Đorđević I, Milovanović A, Maksimović M, Džigurski EŽ, Šojić PM. Optical Stereometric Analysis of Milled and Not-Milled Copings for Removable Overdentures on an Experimental Partially Edentulous Mandible. International Journal of Biomedicine. 2026;16(2):232-241. doi:10.21103/Article16(2)_OA13

Introduction

To maintain the stability of overdentures, protective copings must be placed over the coronal part of the teeth. This component plays an important role in supporting the alveolar ridge and ensuring proper axial load distribution, thereby helping preserve the alveolar ridge level. Similarly, protective copings preserve the natural tooth roots and improve the stability

and retention of overdentures compared to conventional complete dentures.[1-3] Various types of protective copings have been presented to the public.[1-4] In clinical practice, two types of protective copings are commonly used: cast (metallic) and zirconia.[5-8] Cast copings are relatively easy to fabricate but can be associated with clinical problems such as gingival inflammation (69%) and root caries (36%).[3,5] Alternatively, cast copings have the advantage of being provided with a cast post that can be easily inserted into the upper third of the root canal filling, allowing axial load distribution in accordance with the vertical reference axis of the remaining tooth.[3,4] On the other hand, zirconia copings can be very costly and difficult to implement due to the complicated technique, but the periodontal condition around them remains healthy.[3,6] In addition, zirconia copings (the most popular ceramic option) may be susceptible to fractures due to their lower elasticity.[7,8]

Similarly, the different types of interfaces between the denture base and the copings can alter the loading and stress pattern around the abutment teeth.[6,9,10]

Conventional copings usually do not have a milled shoulder for better retention and stress distribution. In this study, a special, simpler form of casted coping was examined on the residual tooth structure in the mandible. These copings functioned both as bone retainers in the surrounding alveolar areas and as retainers for the overdenture. Because they are occlusally designed to have at least some indication of the occlusal relief of the tooth that will support the mandibular prosthesis and because they are milled along the gingival surface, these copings differ from all others previously described in the dental literature. This study was based on an initial assumption and preliminary results indicating that patients in clinical practice were satisfied with the use of these specific coping designs and claimed that they contributed to better retention of their overdenture.[4]

It is still unclear whether the pressure on the copings significantly redistributes the occlusal forces in accordance with the morphologically shaped surfaces corresponding to the occlusal topography and whether it significantly contributes to the stabilization of the prosthesis on the supporting tissues.[4,9-12] We hypothesize that the milled surfaces of the experimental copings may contribute to a better axial load distribution on the roots and that less deformation of the experimental cast copings will improve the stability of the overdentures.

The aim of this study was to examine the effect of differential stress distributions on the occlusal surfaces of the control and experimental copings on artificial casts of partially edentulous jaws.

Materials and Methods

The experiment was accomplished at the Faculty of Mechanical Engineering, University of Belgrade, Serbia. This study included two master casts of a lower jaw with bilateral terminal edentulous seats. Their topography was the same, including missing lower molars, the left lower second premolar, and the right canine and incisors, representing a partially edentulous lower jaw according to the B3 (and C2) classification of Eichner (i.e., Kennedy class 1).

The control cast was designed with conventional oval copings, which are most often used in clinical practice to preserve the remaining dental substance in the crown and to receive the base surface of the overdenture (Figure 1).

Fig. 1. *The experimental cast (on the left) and the control cast (on the right).*

The experimental cast was almost identical to the control cast, except for the surfaces simulating three specific milled copings covering the remaining tooth structure. The specific copings were shaped to exhibit morphological characteristics of teeth in the occlusal third; they showed discrete, rounded protrusions that partially resembled the cusp tips of natural teeth. In the gingival third, the copings were milled so that the perimeters of each assumed a stepped configuration (forming a ledge or "shoulder"), thereby ensuring retention and stabilization of the base of the corresponding removable prosthesis (Figure 1).

The thickness of all of the resin copings was 3 mm. For the milling of the control and experimental copings, the same armamentarium (surveying device, electrically supplied dental parallelometer with model table, Heraeus CL MF 1000, Germany) and the same procedure were used.

Master casts were fabricated on a 3D printer (Builder Extreme 3000 PRO, Brose, Germany) using a specific photopolymer resin (Photopolymer Resin, Formlabs Inc., Somerville, MA, USA). After the 3D-printed resin printing process was completed, a sufficient post-curing time of at least 60 minutes under different oxygen levels was provided to improve flexural properties and flexural modulus (subsequently, the specimens were submerged in water). The corresponding elastic properties, including the Young's modulus and Poisson ratio, were determined according to the values obtained from the previously published literature.[13,14] The casting surfaces were coated with a thin layer of white paint (Motip Spray, Germany), followed by a thin layer of high-contrast black paint; this was necessary for the correct application of the Digital Image Correlation (DIC) method.

Dots of the spray occupied distances that changed under stress and were registered by cameras.[14,15]

Precise and controlled loading was measured using a dynamometer (Siemens AG, Erlangen, Germany) (Figure 2).[14-18] Axial occlusal loads were applied centrally and vertically to the distal abutment tooth (the first lower premolar), intermediate abutment tooth (canine), and the mesial abutment tooth (the second lower incisor) (Figure 2). The direction of loadings to the second experimental cast was the same. The loading stages were 400, 800, and 1000 N.[14,18]

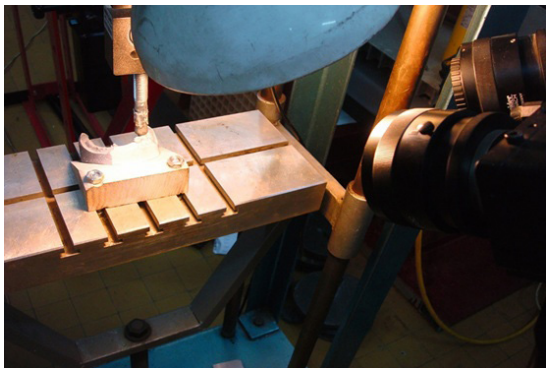

Fig. 2A. *The control cast under the load in a dynamometer.*

Fig. 2B. *Measurement of the force applied to the coping model.*

Measurements of strain and displacement were obtained using the Digital Image Correlation Method (GOM-Optical Measuring Techniques, Braunschweig, Germany). This system consists of two digital cameras and the associated software ARAMIS (Version 6.2.0; GOM-Optical Measuring Techniques). ARAMIS software, based on the principle of an objective fine-grained procedure, registered 3D changes in the shape and distribution of surface strain on statically- or dynamically loaded objects. Moreover, ARAMIS also determined the shape of the photographed object with high accuracy, its dimensions, its field of 3D motion, the vector of the distorted field, and features of the biomaterial (Figure 3).[14-17]

Mobile cameras captured the distance between the reference points at specified time intervals before the load, during the calibration phase, and during the application of the action force. Before the strains of the control and test copings were measured, a calibration procedure was carried out. To measure the 3D strains, two cameras were manually positioned and adjusted to the measurement volume of the calibration object. The strains within the selected area could be measured over a range from 0.01% to several hundred percent, and the strain measurement accuracy was up to 0.01%.[14,15]

Small and large objects, from 1.00 to 2000.00 mm, could be measured with the same sensor.[14] The software processing of the data measured enabled recording of the results and a 3D presentation (Figure 3).[14-16]

Statistical analysis: Descriptive statistics were used to visualize the results regarding the deformation and displacement of the tooth copings obtained in this experiment. The MEANS procedure from the SAS statistical package (SAS Institute [2010]) was used for the analysis. Wilcoxon lambda tests based on simple linear rank statistics were used to analyze the numerical values of the copings' deformations and displacements. The mean value was used as a measure of central tendency. To identify differences in the mean values of the parameters between the experimental and control caps, nonparametric statistical methods were employed based on the response variable (percentage of deformation and displacement).

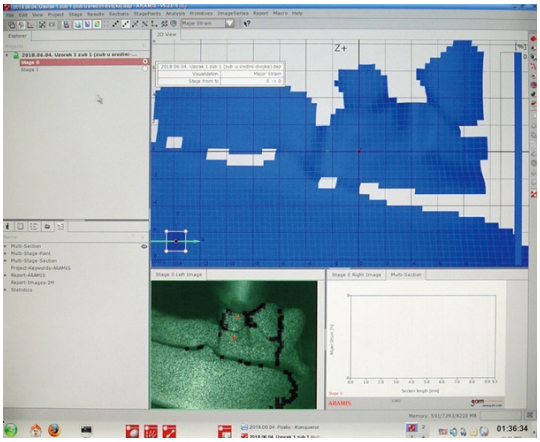

Fig. 3A. *The borders of areas of interest for the experiment.*

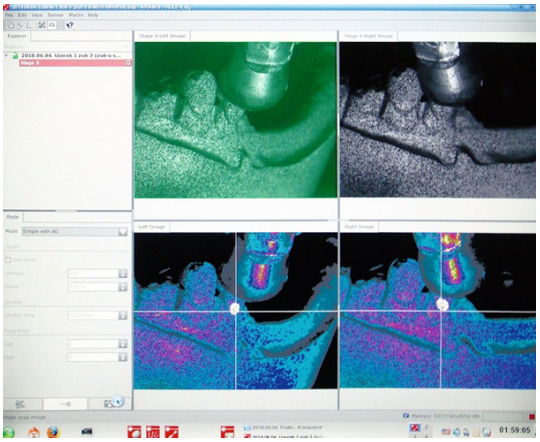

Fig.3B. *The active surface of the dynamometer, displayed on the screen during the measurement of the force directed on the coping.*

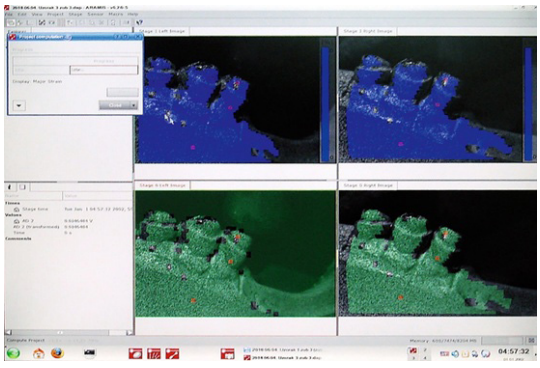

Fig.3C. *The appearance of milled coping models in computer software.*

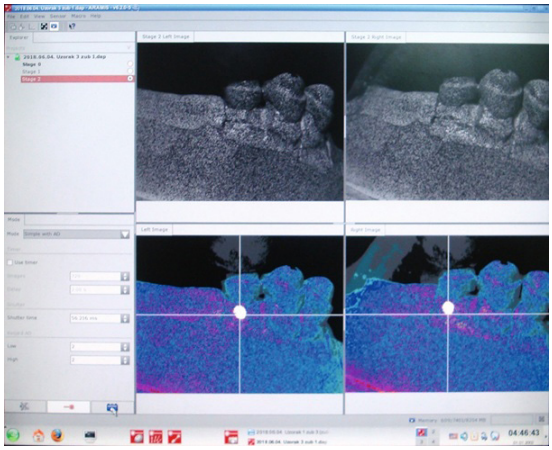

Fig. 3D. *Vector of the forces applied.*

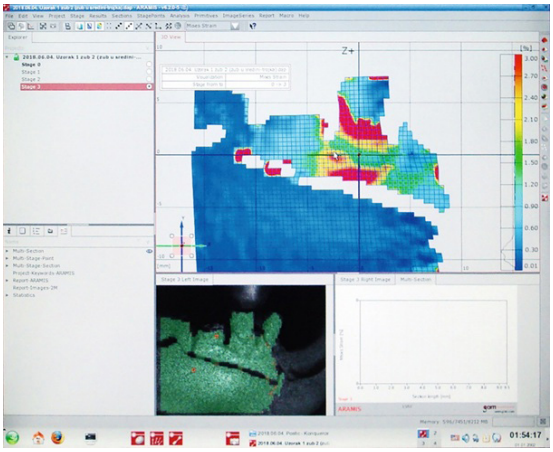

Fig. 3E. *The terminal zone of the crack (red areas).*

Results

Stress and deformation of the cast copings investigated in the present study were distributed differently. We found that the most intense deformations occurred under the actual force transmitted to the border of the coping and the immediate area of remaining tooth substance.

Significantly lower displacements were recorded in the group of teeth with experimental milled copings compared to the control group with rounded copings (Figures 4 and 5). These results were consistent across all three loading stages and across all tooth types investigated.

The deformation measures were smaller for the milled copings than for the control copings (Tables 1 and 2). There was a direct link between the percent of coping deformation and the type of coping. The type of coping was a significant determinant of the degree of tooth-coping displacement under pressure in this experiment. There were statistically significant differences in displacement between the control rounded and experimental milled copings ($Pr > |Z| = 0.001$) as well as in deformations ($Pr > |Z| = 0.0298$) (Table 3). The shape of the non-milled coping is directly responsible for the movements and cracks in the gum area.

There was significant deformation in the control rounded tooth coping when compared to the experimental milled tooth coping. These findings were observed at a pressure of 1000 N, regardless of the type of teeth evaluated (Figures 6 and 7).

A

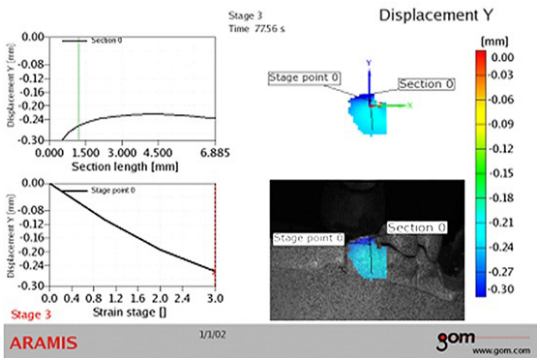

B

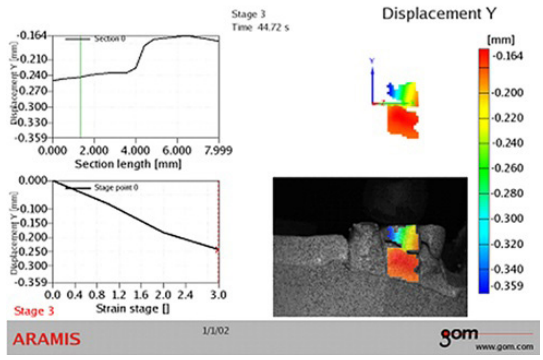

C

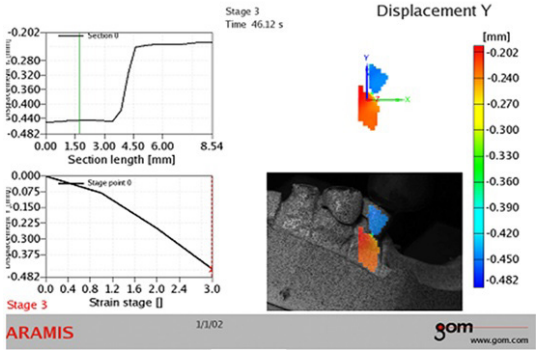

Fig. 4. *Displacement of the remaining teeth covered by the control copings. A) Displacement within the incisor with control coping under loading of 1.000 N (Final Stage 3); Upper left panel–final stage; lower left panel– initial stage; right panel– distribution of loads and stresses along and within the coping of the control incisor; B) Displacements within the control canine with coping under loading of 1.000 N (Final Stage 3); upper left panel– final stage; lower left panel– initial stage; right panel– distribution of loads and stresses along and within the coping of the control canine; C) Displacement within the coping of the premolar under loading of 1.000 N (Final Stage 3); upper left panel– final stage; lower left panel– initial stage; right panel– distribution of the loads and stresses along and within the control coping of the premolar.*

A

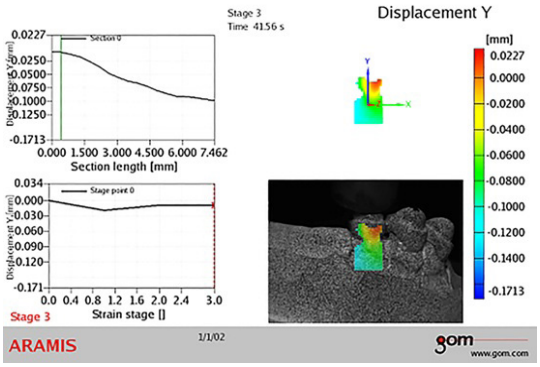

B

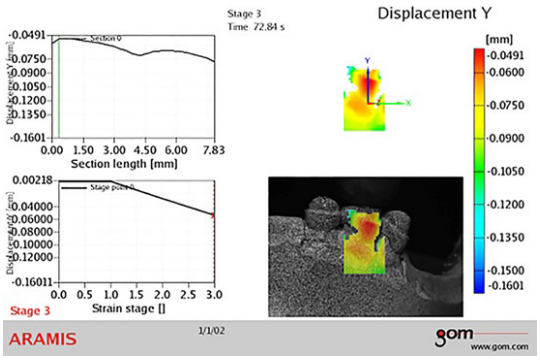

C

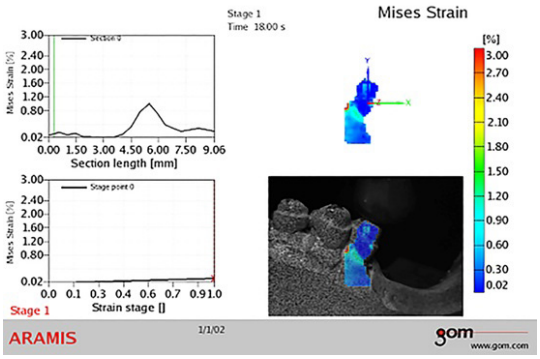

Fig. 5. *Displacement of the remaining teeth covered by the experimental copings. A) Displacement within the milled coping of the incisor under loading of 1.000 N (Final Stage 3); upper left panel– final stage; lower left panel– initial stage; right panel– distribution of loads and stresses along and within the experimental milled coping of the incisor; B) Displacement within the experimental coping of the canine under loading of 1.000 N (Final Stage 3); upper left panel– final stage; lower left panel– initial stage; right panel– distribution of loads and stresses along and within the experimental milled coping of the canine; C) Displacement within the experimental milled coping of the premolar under loading of 1.000 N (Final Stage 3); upper left panel– final stage; lower left panel– initial stage; right panel– distribution of loads and stresses along and within the experimental milled coping of the premolar.*

Table 1.

Maximum deformation of the control conventional oval copings on the incisor, canine, and premolar.

Stage	Points							
Name (Sub-project: Point-ID)	Facets XY	Actual data (mm)	Coordinate X	(Deformed) Y	Z (mm)	Coordinate X	(Undeformed) Y	Z (mm)
Incisor with conventional oval coping	0.4	+3.39	+0.57	+0.98	-1.65	+0.55	+1.24	+1.47
Canine with conventional oval coping	0.3	+0.51	+6.56	+1.86	-1.64	+6.57	+2.10	-1.39
Premolar with conventional oval coping	0.5	-0.39	+1.14	+3.29	0.99	+0.75	+3.74	+1.30

Table 2.

Maximum deformation of the experimental milled copings on the incisor, canine, and premolar.

Stage	Points							
Name (Sub-project: Point-ID)	Facets XY	Actual data (mm)	Coordinate X	(Deformed) Y	Z (mm)	Coordinate X	(Undeformed) Y	Z (mm)
Incisor with experimental milled coping	0.2	+0.12	+0.52	+3.75	-0.33	+0.53	+3.76	+0.23
Canine with experimental milled coping	0.1	+0.10	-0.12	+4.42	-1.57	-0.19	+4.47	-1.18
Premolar with experimental milled coping	0.1	+0.13	-0.61	+1.88	-2.12	-0.69	+1.87	-1.94

Table 3.

Differences in the displacement and deformation between the control rounded and experimental milled copings of the remaining tooth substances under loading.

	Displacement	Deformation
Type of coping	Mean score	
Round	5.0	10.0
Milled	13.0	5.0
Normal Approximation Z	3.2814	2.1722
Two-Sided Pr > |Z|	0.0010*	0.0298*

**Wilcoxon Two-Sample Test.*

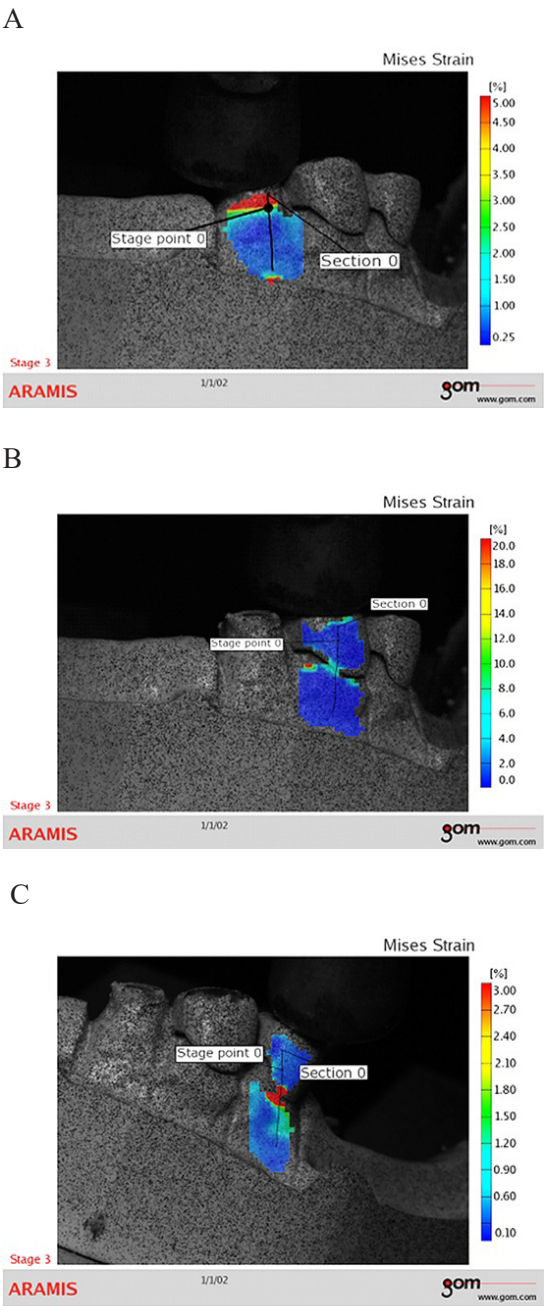

Fig. 6. *A) von Misses strain of the control coping of the incisor; B) von Mises strain of the control coping of the canine; C) von Mises strain of the control coping of the premolar.*

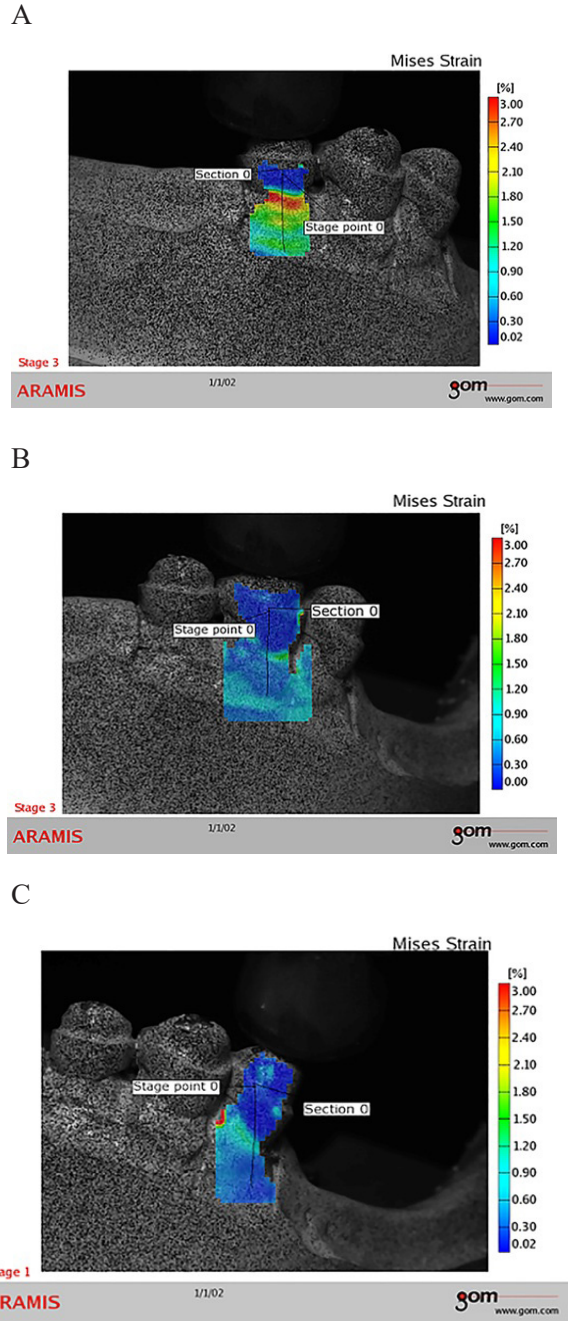

Fig. 7. *A) von Mises strain of the experimental coping of the incisor; B) von Mises strain of the experimental coping of the canine; C) von Mises strain of the experimental coping of the premolar.*

Discussion

Currently, overdentures are recommended in cases where a significant loss of the alveolar ridge is observed following multiple tooth extractions.[4,19]

Preservation of the alveolar bone and stabilization of the prosthesis can be achieved by covering the remaining teeth with copings.[3,5] Furthermore, it remains unclear why the remaining teeth in our study were present only on one side of the mandible, given the known problem that the remaining tooth structure may be exposed to an "additional load" on the edentulous side of the mandible.[4] This experiment was performed on a partially edentulous mandible of Kennedy Class 1 (i.e., Eichner's B3 [and C2] classification), as this type of partially edentulous mandible is the most common in clinical practice.[20] This type of partial edentulism is also relatively difficult to treat therapeutically.[3,4]

In this study, significantly higher deformation values were observed for the rounded control copings compared to the experimentally milled copings. The higher deformation values of the rounded copings could be explained by their spherical surface. More specifically, the axial force acting on a spherical surface consists of two components: tangential and

normal. The tangential component was the main cause of the deformation of the rounded oval control copings. However, only axial forces occurred in the milled copings, which led to significantly lower deformation. In our study, the displacement of milled copings was significantly higher than that of the rounded control copings. This result could be explained by the fact that all forces acting on milled copings were distributed axially.[4]

Researchers in dental prosthetics have long debated the issue of stability.[21] It is assumed that the morphologically developed occlusal sections of the experiment, intended only for milling copings, redirect forces precisely along the axial axis, resulting in a medically favorable load. Furthermore, it was assumed that the occlusal plateau, with the largest surface area, practically absorbs all loads (both physiological and caustic) almost completely. All other stresses that exist within an orofacial system, while the axial surfaces of custom-milled copings, with the exception of the shoulder area, would be significantly or completely relieved of tensile stresses, as found in a previous study.[20] The results of the present study did not fully confirm these assumptions; however, they demonstrated that the degree of deformation in the experimental milled copings was significantly lower.

In addition, preliminary studies on the outcomes of overdenture therapy found that both patients and the therapists evaluating success considered the prostheses resting on milled special copings of the roots of the remaining retained maxillary teeth to be quite stable.[22]

In addition, better direct and indirect stabilization of the prosthesis was achieved compared with the conventional coping shape.[4] Thus, the milled shoulder of the coping may increase the likelihood of additional retention when picking up the basal surface of the overdenture. From these findings and the loading shown (Figures 7 and 6), we cannot conclude that the milled surfaces absorb and amortize (redirect in axial and centric directions) the forces acting on the milled copings to the greatest extent. The results only show that the numerical amount of deformation in the cervical segments of the specially milled copings (Tables 1-3) was less than that of the conventional control copings.

The results of this study raise the question of whether the forces, stresses, and deformations were greatest at the top of the coping, thereby distributing the load and exerting vertical pressure on the tooth root. The present study analyzed cast copings and found that the distribution of stresses and deformations varied between them. We found that the most intense deformations occurred under the actual force transmitted to the margin of the coping and the immediate area of the remaining tooth structure. Considering that the stress was highest in the area of the element with the largest diameter, the cause of the most severe deformations at the cervical margin of the copings can be attributed to the maximum stress at this location.

Previous research on the difficulties of implementing the stereoptic (stereometric) approach has shown the usefulness of the method in some dental specialties.[24-34] With this stereo-optical method, when two cameras are installed, one can ensure that points in two images can be matched and autostereograms can be created using information about corresponding points based on the initially separated positions of the two cameras. Thus, the 3D positions of objects can be determined.[25,35,36] The stereo-optical (stereometric) method thus appears to be reliable for assessing stresses and deformations.

The resemblance between the experimental milling copings and constructs based on the ferrule effect concept lends credence to these arguments. It has already been shown that the fabrication of milled metal copings with the addition of a post emphasizes the beneficial effects of preventing the independent flexure of tooth or core/post structures.[7] Such structures are located within the supra-ferrule-margin volume of the tooth; if a force is applied to the tooth, the entire supra-ferrule-margin tooth, core, and post complex work as one unit to resist the force.[4,37]

The results of our study showed that the oval control copings were less resilient compared to the experimental milled copings. Since, to the best of our knowledge, this study represents the first investigation to employ stereoptic assessment of the shape of specialized caps, comparing the obtained results with data from other studies is extremely difficult.

This is because there is no relevant data on the effect of forces and deformations for these purposes. The results of the present study are consistent with those of other authors, who argued that metal coping has the highest degree of stress transfer to the load-bearing web. The reason for this lies in the properties of metals, which are characterized by high hardness and rigidity; these characteristics create a robust foundation for the prosthetic structure, ensure that the majority of the applied load is transmitted to the supporting teeth (abutments), and reduce the level of stress in the region of the supporting alveolar ridge.[38]

It is certain that the most desirable criterion for selecting the attachment system for overdentures is the way these attachments transfer loads to the supporting structures (Figure 8). The distribution of stress through the abutments in an arch-spanning manner and between the abutments and the posterior edentulous ridge is always favorable for the preservation of the residual ridge. To ensure the most effective distribution of stresses, the optimal solution is to design a retention system for the overdenture that maximizes load distribution between the retention element and the residual alveolar ridge.[39]

Fig. 8. *An acrylic overdenture fabricated to correspond to the copings and supporting tissues of the jaw.*

The high values of the loads (400N, 800N, and 1000N) utilized in this study are addressed in the limitations of this experimental investigation, keeping in mind that the mean occlusal loads on the premolars ranged from 39 to 66 N, and on the front teeth (apart from bruxism) from 11 to 33 N [28,40,41] with a limitation of the type of force applied and the duration of its application.

Conclusion

The results of this study underscore the need to use protective caps as extracoronal structures for teeth remaining beneath removable overdentures. Based on the results of this study, there will be an implicit demand in clinical practice to position protective copings as an extracoronal construction of remaining teeth under overdentures. Experimental milled copings are less susceptible to deformation than the control rounded copings. These findings may have clinical significance for improving primary and secondary retention of overdentures on milled copings.

Clinical Implications

There is the implicit demand in clinical practice to position protective copings as an extracoronal construction of remaining tooth substance under overdentures. Specially designed, dedicated experimental milled copings are expected to improve primary and secondary retention of overdentures. The study has a limitation because it evaluates occlusal stress distribution on master casts, which cannot replicate the functional adaptation of the periodontal ligament.

Ethics Statement

This study was conducted in laboratory conditions as an investigation on materials in in vitro conditions. No human or animal models were used.

Statement of the Authors

The materials of this study were previously published as preprints and preliminary results, and are included in the bibliography of the present manuscript as References 14,15,16 and 17.

Author Contributions

Srđan D. Poštić: Conceptualization, Methodology, Investigation, Data curation.

Slobodan Dodić: Investigation, Data curation.

Ivan V. Tanasić: Investigation, Data curation, Writing – review and editing.

Miloš Milošević: Investigation, Data curation and interpretation.

Stevan Avramov: Data curation, Formal analysis, Writing – original draft.

Vladimir Biočanin: Investigation, Writing – review and editing.

Ljubiša Ristić: Data interpretation, Writing – original draft.

Igor Đorđević: Data interpretation, Writing – original draft.

Aleksa Milovanović: Data curation, Formal analysis.

Miloš Maksimović: Investigation, Writing – review and editing.

Ekatarina Ž. Džigurski: Investigation, Data curation.

Predrag M. Šojić: Investigation, Data curation.

All authors have approved the final article.

Conflict of Interests

The authors have declared no conflict of interest.

Acknowledgments

Authors of the current study wish to express their sincere gratitude to Professor Dr. Taško Maneski, Docent Goran Mladenović, Professor Nenad R. Mitrović, employed in the Faculty of Mechanical Engineering of the University of Belgrade, Serbia, as well as to the dental labor Wisil M – Mila Simonović located in the area of New Beograd, Serbia, for their help in the realization of this experiment.

References

1. Loney RW. Removable Partial Denture Manual. Dalhousie University. 2011, pp.63-66.
2. Chen J, Ahmad R, Li W, Swain M, Li Q. Biomechanics of oral mucosa. J R Soc Interface. 2015 Aug 6;12(109):20150325. doi: 10.1098/rsif.2015.0325. PMID: 26224566; PMCID: PMC4535403.
3. Ilić D, Brković S, Poštić S. Overdenture in terms of preparation and restoration of supporting teeth: Review report. VSP 2020;77:1086-92.
4. Poštić SD. Specially designed copings for stability of overdentures. JSM Dent 2016;4:1061-5.
5. Brkovic-Popovic S, Stanisic-Sinobad D, Postic SD, Djukanovic D. Radiographic changes in alveolar bone height on overdenture abutments: a longitudinal study. Gerodontology. 2008 Jun;25(2):118-223. doi: 10.1111/j.1741-2358.2007.00182.x. PMID: 18485140.
6. Preiskel HW. Overdentures made easy: A guide to implant and root supported prostheses. Quintessence Int. Co.; London 1996, p. 21-137.
7. Sun T, Zhou S, Lai R, Liu R, Ma S, Zhou Z, Longquan S. Load-bearing capacity and the recommended thickness of dental monolithic zirconia single crowns. J Mech Behav Biomed Mater. 2014 Jul;35:93-101. doi: 10.1016/j.jmbbm.2014.03.014. Epub 2014 Apr 2. PMID: 24762856.
8. Juntavee N, Kornrum S. Effect of Marginal Designs on Fracture Strength of High Translucency Monolithic Zirconia Crowns. Int J Dent. 2020 Aug 3;2020:8875609. doi: 10.1155/2020/8875609. PMID: 32831840; PMCID: PMC7421695.
9. Chhabra A, Chhabra N, Jain A, Kabi D. Overdenture Prostheses with Metal Copings: A Retrospective Analysis of Survival and Prosthodontic Complications. J Prosthodont. 2019 Oct;28(8):876-882. doi: 10.1111/jopr.12756. Epub 2018 Feb 11. PMID: 29430787.

10. Mercouriadis-Howald A, Rollier N, Tada S, McKenna G, Igarashi K, Schimmel M. Loss of natural abutment teeth with cast copings retaining overdentures: a systematic review and meta-analysis. J Prosthodont Res. 2018 Oct;62(4):407-415. doi: 10.1016/j.jpor.2018.05.002. Epub 2018 Jun 8. PMID: 29891420.
11. The Glossary of Prosthodontic Terms: Ninth Edition. J Prosthet Dent. 2017 May;117(5S):e1-e105. doi: 10.1016/j.prosdent.2016.12.001. PMID: 28418832.
12. Zarb GA, Jacob RF, Zarb JP: Overdentures. In Zarb GA, Bolender CL, Eckert ST, et al (eds): Prosthodontic Treatment for Edentulous Patients (ed 12). St Louis, Mosby, 2004, p.160-176
13. Gul EB, Suca GÇ. Finite element stress analysis of overdentures supported by angled implants. Merit Res J Med Med Sci 2014; 2:196-206.
14. Poštić SD, Milošević M, Maneski T, Mladenović G, Brković S, Trifković B. Optical stereometric analysis of an experimental partially-edentulous mandible. Advances in Mechanical Engineering. 2022;14(6):1–9. doi: 10.1177/16878132221106648
15. Postic SD, Tihacek-Sojic Lj, Dodic S, Tanasic I, Milosevic M, Avramov S, Biocanin V, Petrovic R, Ristic Lj, Đorđević I, Milovanovic A, Maksimovic M, Dzigurski E, Sojic P. Optical stereometric analysis of milled and not-milled copings for removable overdentures on an experimental partially edentulous mandible. 2024. Preprint, doi:10.20944/preprints202409.2301.v1. Available from https://www.preprints.org/manuscript/202409.2301/v
16. Milošević, M, Poštić S, Mitrović N, Milovanović A, Travica M, Golubović Z, Mladenović G. Experimental setup development of additively manufactured mandible with teeth and compensations subjected to compressive load. 2018. Preprint. Available from https://machinery.mas.bg.ac.rs/handle/123456789/6939
17. Poštić S, Džigurski E, Mladenović G, Milovanović, A, Mitrović N, Trajković, I, Milošević, M. Compression strains and displacements of selected copings on remaining teeth for denture support. 2020. Preprint. Available from https://machinery.mas.bg.ac.rs/handle/123456789/7363
18. Windisch SI, Jung RE, Sailer I, Studer SP, Ender A, Hämmerle CH. A new optical method to evaluate three-dimensional volume changes of alveolar contours: a methodological in vitro study. Clin Oral Implants Res. 2007 Oct;18(5):545-51. doi: 10.1111/j.1600-0501.2007.01382.x. Epub 2007 Jun 21. PMID: 17590160.
19. Elawady D, Adam MA, Allam H, Mahmoud II, Alqutaibi AY, Shon AA. Single Implant-Retained Mandibular Overdentures: A Literature Review. Cureus. 2024 Jan 18;16(1):e52486. doi: 10.7759/cureus.52486. PMID: 38371006; PMCID: PMC10874113.
20. Lee DJ, Saponaro PC. Management of Edentulous Patients. Dent Clin North Am. 2019 Apr;63(2):249-261. doi: 10.1016/j.cden.2018.11.006. Epub 2019 Jan 30. PMID: 30825989.
21. Carlsson GE. Critical review of some dogmas in prosthodontics. J Prosthodont Res. 2009 Jan;53(1):3-10. doi: 10.1016/j.jpor.2008.08.003. Epub 2008 Oct 7. PMID: 19318064.
22. Ha SR, Kim SH, Han JS, Yoo SH, Jeong SC, Lee JB, Yeo IS. The influence of various core designs on stress distribution in the veneered zirconia crown: a finite element analysis study. J Adv Prosthodont. 2013 May;5(2):187-97. doi: 10.4047/jap.2013.5.2.187. PMID: 23755346; PMCID: PMC3675293.
23. Leong JZ, Beh YH, Ho TK. Tooth-Supported Overdentures Revisited. Cureus. 2024 Jan 29;16(1):e53184. doi: 10.7759/cureus.53184. PMID: 38420101; PMCID: PMC10901637.
24. Shahar R, Weiner S. Insights into whole bone and tooth function using optical metrology. J Mat Sci 2007;42:8919–33.
25. Ahn B, Kim J. Measurement and characterization of soft tissue behavior with surface deformation and force response under large deformations. Med Image Anal. 2010 Apr;14(2):138-48. doi: 10.1016/j.media.2009.10.006. Epub 2009 Nov 5. PMID: 19948423.
26. Kulchin Y, Vitrick O, Lantsov A, Vorobyev A, Moskvin Y. Measuring the deformity of dentofacial bone tissues using a speckle correlation method. Optoelectr Instrum Data Process 2008;44:264–8.
27. Durbin DM, Durbin DA. Patent US 6364660B1, https://patents.google.com/patent/US6364660B1/en
28. Kahn-Jetter Z, Chu T. Three-dimensional displacement measurements using digital image correlation and photogrammic analysis. Exp Mech 1990;30:10–6.
29. Windisch SI, Jung RE, Sailer I, Studer SP, Ender A, Hämmerle CH. A new optical method to evaluate three-dimensional volume changes of alveolar contours: a methodological in vitro study. Clin Oral Implants Res. 2007 Oct;18(5):545-51. doi: 10.1111/j.1600-0501.2007.01382.x. Epub 2007 Jun 21. PMID: 17590160.
30. Tanasic I, Milic-Lemic A, Tihacek-Sojic L, Stancic I, Mitrovic N. Analysis of the compressive strain below the removable and fixed prosthesis in the posterior mandible using a digital image correlation method. Biomech Model Mechanobiol. 2012 Jul;11(6):751-8. doi: 10.1007/s10237-011-0348-5. Epub 2011 Sep 15. PMID: 21918835.
31. Gubeljak N, Kocak M, Huther M, Valh T. Fitnet fitness-for-service fracture module SOFTWARE. FME Transactions 2008;36:39–44.
32. Lovald ST, Wagner JD, Baack B. Biomechanical optimization of bone plates used in rigid fixation of mandibular fractures. J Oral Maxillofac Surg. 2009 May;67(5):973-85. doi: 10.1016/j.joms.2008.12.032. PMID: 19375006.
33. Sedmak A, Milošević M, Mitrović N, Petrović A, Maneski T. Digital image correlation in experimental mechanical analysis. Struct Integr Life 2012;12:39-42.
34. Sojic LT, Milic Lemic A, Tanasic I, Mitrovic N, Milosevic M, Petrovic A. Compressive strains and displacement in a partially dentate lower jaw rehabilitated with two different treatment modalities. Gerodontology. 2012 Jun;29(2):e851-7. doi: 10.1111/j.1741-2358.2011.00572.x. Epub 2011 Oct 17. PMID: 22004157.
35. Yang HS, Park JM, Han JS, Lee JB, Kim SH, Yeo IS. Measuring abutment convergence angles using stereovision dental image processing system. J Adv Prosthodont. 2014 Aug;6(4):259-65. doi: 10.4047/jap.2014.6.4.259. Epub 2014 Aug 14. PMID: 25177468; PMCID: PMC4146725.
36. Bradski GR., Kaehler A., Learning open CV: computer vision

with the open CV library. Farnham: O'Reilly; 2008. p. 555.
37. Mamoun JS. On the ferrule effect and the biomechanical stability of teeth restored with cores, posts, and crowns. Eur J Dent. 2014 Apr;8(2):281-286. doi: 10.4103/1305-7456.130639. PMID: 24966784; PMCID: PMC4054064.
38. Ghorab S, Mohamed Z, Mahmoud E. Comparative stress analysis study between different coping materials in complete overdenture cases (An in-vitro study). Egypt Dent J 2024; 70(2):1683-1691.DOI:10.21608/edj.2024.263753.2897
39. Dwivedi A, Vyas R, Gupta A. Quantitative evaluation and comparison of stress transmission characteristics of bar-clip and short coping overdenture attachments under dynamic loading: a photoelastic stress analysis. J Contemp Dent Pract. 2013 Mar 1;14(2):287-92. doi: 10.5005/jp-journals-10024-1315. PMID: 23811661.
40. Ye Y, Di P, Jia S, Lin Y. [Occlusal force and its distribution in the position of maximum intercuspation in individual normal occlusion: a cross-sectional study]. Zhonghua Kou Qiang Yi Xue Za Zhi. 2015 Sep;50(9):536-9. Chinese. PMID: 26759295.
41. Hidaka O, Iwasaki M, Saito M, Morimoto T. Influence of clenching intensity on bite force balance, occlusal contact area, and average bite pressure. J Dent Res. 1999 Jul;78(7):1336-44. doi: 10.1177/00220345990780070801. PMID: 10403461.

***Corresponding author**: Dr. Srđan D. Poštić, PhD. University School of Dental Medicine in Beograd, Rankeova street 4, University of Belgrade, 11000 Belgrade, Serbia. E-mail: srdjan.postic@stomf.bg.ac.rs*

International Journal of Biomedicine 16(2) (2026) 242-247
http://dx.doi.org/10.21103/Article16(2)_OA14

ORIGINAL ARTICLE

INTERNATIONAL JOURNAL OF BIOMEDICINE

In Vitro Dentin Bond Durability of Additively Manufactured Hybrid Composite Restorations Luted with Preheated Composite: A Comparative Analysis of Fourth- and Sixth-Generation Adhesives

Timur V. Melkumyan[1,2*], Kakhramon E. Shomurodov[1], Ibrokhimjon M. Azimov[1], Zurab S. Khabadze[2], Maria K. Makeeva[2], Roman A. Meremkulov[2], Surayo Sh. Sheralieva[1], Diyorakhon A. Inoyatova[1], Shakhnoza K. Musoshaykhova[1], Nuriddin Kh. Kamilov[1], Shukhrat M. Shakirov[3], Azad A. Mukhamedov[3], Gerhard K. Seeberger[4], Bedros Y. Sakuk[5], Angela D. Dadamova[1]

[1]*Tashkent State Medical University, Tashkent, Uzbekistan*
[2]*Peoples' Friendship University of Russia (RUDN University), Moscow, Russia*
[3]*Tashkent State Technical University, Tashkent, Uzbekistan*
[4]*Order of Physicians and Dentists of the Province of Cagliari, Sardinia, Italy*
[5]*NYU College of Dentistry, USA*

Abstract

Background: The purpose of this in vitro study was to evaluate and compare the shear bond strength (SBS) and failure mode kinetics of indirect 3D-printed ceramic-reinforced hybrid composite restorations to human tooth dentin using fourth-generation etch-and-rinse and sixth-generation self-etch adhesive systems under a co-curing protocol with a preheated universal composite resin luting material.

Methods and Results: Sound human third molars (N=156) were prepared to expose flat mid-dentin surfaces. Simulated indirect restorations were additively manufactured as composite cylinders (VarseoSmile TriniQ, BEGO) using a Formlabs Form 4B 3D printer. Samples were randomly divided into two experimental groups based on the adhesive system used: Group 1 (n=78, OptiBond FL, fourth generation) and Group 2 (n=78, Clearfil SE Bond 2, sixth generation). Preheated universal composite resin (Filtek Z350, 55°C) was used for luting under a co-curing sequence. Each group was subdivided (n=39) into a baseline subgroup (immediate testing) and a thermocycling subgroup (10,000 cycles, 5°C/55°C). SBS trials were performed at a crosshead speed of 1 mm/min, and debonded surfaces were evaluated under 40× magnification to classify failure modes. Statistical analysis was performed using SciPy 1.11. For continuous data with a normal distribution, inter-group comparisons were performed using Student's t-test. Categorical variables were analyzed using the chi-square test. A P-value <0.05 was considered statistically significant.

At baseline, OptiBond FL (20.7 ± 4.6 MPa) and Clearfil SE Bond 2 (20.6 ± 4.2 MPa) demonstrated equivalent immediate bond strengths ($P > 0.05$) and identical mixed failure profiles. Thermocycling significantly degraded dentin bond integrity across all cohorts ($P=0.000$). However, post-aging evaluation revealed that Clearfil SE Bond 2 (16.8 ± 4.4 MPa) had a significantly higher remaining SBS than OptiBond FL (14.4 ± 4.7 MPa), $P = 0.023$. Microscopic analysis confirmed a complete absence of cohesive failures. Following thermal aging, the OptiBond FL interface underwent an acute intra-group shift toward true adhesive failures (84.6%), whereas Clearfil SE Bond 2 maintained high structural stability with a lower adhesive failure rate (61.5%), $P= 0.022$.

Conclusion. While both adhesive strategies exhibit equivalent immediate performance during preheated composite co-curing, the null hypothesis must be rejected after artificial aging. The sixth-generation 10-MDP-containing self-etch system provides superior hydrolytic stability and interfacial durability compared to the fourth-generation system. Clinically, a two-step self-etch protocol provides a more predictable, chemically driven interface for the long-term cementation of contemporary additively manufactured restorations**.** (**International Journal of Biomedicine. 2026;16(2):242-247.**)

Keywords: 3D-printed composite • preheated resin composite • 10-MDP • shear bond strength • failure mode

For citation: Melkumyan TV, Shomurodov KE, Azimov IM, Khabadze ZS, Makeeva MK, Meremkulov RA, Sheralieva SSh, Inoyatova DA, Musoshaykhova ShK, Kamilov NKh, Shakirov ShM, Mukhamedov AA, Seeberger GK, Sakuk BY, Dadamova AD. In Vitro Dentin Bond Durability of Additively Manufactured Hybrid Composite Restorations Luted with Preheated Composite: A Comparative Analysis of Fourth- and Sixth-Generation Adhesives.International Journal of Biomedicine. 2026;16(2):242-247. doi:10.21103/Article16(2)_OA14

Introduction

The clinical demand for durable indirect adhesive restorations has led to a paradigm shift from traditional dual-cure resin cements toward preheated universal composite resins for luting procedures. Dual-cure cements, while chemically versatile, frequently exhibit lower filler volume fractions, accelerated chemical degradation, and discoloration over time. Using a highly filled, preheated universal composite resin addresses these drawbacks by significantly reducing structural viscosity to achieve an optimal, micro-thin luting layer while enhancing physical properties and marginal sealing.[1-3]

Crucial to the long-term success of this approach is the integrity of the dentin-adhesive hybrid layer, which must withstand the sudden thermal energy and unique polymerization kinetics of the co-curing technique. Co-curing means that the unpolymerized adhesive layer and the overlying preheated luting composite are light-activated simultaneously. It streamlines clinical protocols but presents a challenging biomechanical scenario.[4,5]

The choice of dental adhesive strategy remains highly debated. Fourth-generation etch-and-rinse systems involve separate phosphoric acid etching, a hydrophilic primer, and a hydrophobic bonding resin layer, which acts as a robust mechanical buffer against immediate composite shrinkage forces. In turn, two-step sixth-generation self-etching adhesive systems eliminate the separate rinsing step by using a self-etching primer followed by an adhesive layer. This simplifies clinical placement and minimizes technique sensitivity, though their acidic monomers remain prone to phase separation and subsequent water treeing when subjected to rapid polymerization heat.[6,7]

To mitigate the rapid volumetric shrinkage associated with preheated universal composites, using prefabricated indirect restorations is a promising approach, as it drastically reduces the overall volume of unpolymerized resin within the tooth cavity. Historically, the fabrication of indirect restorations has evolved from traditional laboratory manual layering to subtractive CAD/CAM milling and, more recently, to additive manufacturing. Contemporary 3D-printed ceramic-reinforced hybrid composite resins (such as VarseoSmile Crown plus, BEGO) represent a breakthrough in this evolutionary trajectory, offering high-precision definitive restorations via vat polymerization.[8] These additively manufactured materials provide notable clinical benefits, including excellent dimensional adaptation, simplified chairside workflows, minimized material waste, and an antagonist-friendly mechanical buffering effect.[9] Consequently, they offer a highly promising future in restorative dentistry as a sustainable, cost-effective alternative to permanent single-unit restorations and conservative indirect treatments.[10] However, achieving predictable adhesive cementation for these contemporary printed restorations remains a highly challenging aspect of the clinical procedure.

Although several studies have evaluated the shear bond strength (SBS) of conventional polymer cements, limited data exist on how the distinct chemistries of fourth- and sixth-generation adhesive systems perform under rapid, high-temperature co-curing when a preheated composite serves as the luting material for indirect restorations.[11-13]

Therefore, the purpose of this in vitro study was to evaluate and compare the shear bond strength of indirect-printed composite restorations to human tooth dentin using fourth- and sixth-generation adhesive systems during co-curing with a preheated universal composite. The null hypothesis tested was that there is no statistically significant difference in SBS to dentin between the two adhesive generations when utilized in a preheated composite luting protocol.

Materials and Methods

Sound human third molars extracted for orthodontic reasons were selected and stored in a 0.1% thymol solution. Sample preparation required that the roots of the teeth be removed and the crowns be sliced mesiodistally into two halves. The obtained tooth slabs were embedded in self-curing acrylic resin blocks. The buccal and lingual enamel was removed using a low-speed diamond saw under constant water cooling to expose a flat, uniform mid-dentin surface. The dentin surfaces were polished with 600-grit silicon carbide paper for 60 seconds to create a standardized smear layer.

Simulated indirect restorations were additively manufactured in the shape of cylinders utilizing a ceramic-reinforced hybrid composite resin (VarseoSmile TriniQ, BEGO, Bremen, Germany). The specimens were printed using a Low Force Stereolithography (LFS) 3D printer (Formlabs Form 4B, Formlabs, Somerville, MA, USA) utilizing a flexible build platform (Build Platform Flex) at a standardized layer thickness of 50 µm. Following completion of the print cycle, the cylinders were automatically washed in high-purity isopropyl alcohol (99%) (IPA) using an automated washing unit (Form Wash, Formlabs) for 3 minutes, rinsed with fresh IPA, and thoroughly air-dried. Final post-curing was performed in a validated UV light-curing chamber (Form Cure, Formlabs) in accordance with the manufacturer's instructions for use to ensure complete monomer conversion. The finalized composite cylinders presented a height of 2.4 ± 0.1 mm and a diameter of 2.36 ± 0.02 mm. Immediately prior to adhesive application and luting, the bonding butt surfaces of the cylinders were airborne-particle abraded (sandblasted) with 27µm Al_2O_3 particles at a pressure of 2.0 bar, rinsed with water, and air-dried.

A total of 156 dentin samples were randomly allocated into two experimental groups based on the adhesive system used. In Group 1 (n=78), a fourth-generation etch-and-rinse adhesive (OptiBond FL [OFL], Kerr Corp., Orange, CA, USA) was applied. In Group 2 (n=78), a sixth-generation two-step self-etch system (Clearfil SE Bond 2 [CSEB2], Kuraray Noritake Dental, Tokyo, Japan) was utilized.

To eliminate solvent-trap-induced micro-voids, all applied adhesives were thoroughly air-dried with a gentle, continuous air stream until a completely still, glossy film

was achieved. The clean, sandblasted butt surfaces of the prefabricated composite cylinders were coated with their respective adhesive bonding resins and then thoroughly air-dried in the same manner. The adhesive layers on both the dentin and the composite columns remained unpolymerized prior to the luting stage.

For luting, a highly filled universal resin composite (Filtek Z350, 3M ESPE, St. Paul, MN, USA) was utilized as the material of choice. It was preheated incrementally on a commercial heating panel up to 55 ± 3°C. The temperature of the heated composite was verified using a thermal imaging camera (UNI-T UTi260A, Uni-Trend Technology, China). A precise amount of the preheated composite was placed directly onto the adhesive-coated butt surface of the composite cylinder. To avoid rapid heat dissipation, the cylinders were immediately transferred to a bonding clamp holding the fixed tooth sample and driven into a plastic mold to a predetermined depth. This controlled insertion guaranteed a standardized uniform luting composite thickness. Constant seating pressure on the cylinders was maintained with a 1-mm-thick transparent plastic shield and the light-emitting tip of a Valo X light-curing unit (Ultradent Products Inc., South Jordan, UT, USA), which was kept in tight contact with the shield during photoactivation.

Each main adhesive group was further subdivided into two equal subgroups (n=39) based on the artificial aging parameter. In the baseline subgroup, SBS testing was conducted immediately without preliminary artificial aging. In the thermocycling subgroup, all samples underwent 10,000 thermal cycles in alternating water baths at 5°C and 55°C. The dwell time in each bath was 10 seconds, and the transfer time between baths was 5 seconds. SBS trials were performed using an Ultra Test Machine (Ultradent Products Inc., South Jordan, UT, USA). The load was applied at a constant crosshead speed of 1 mm/min until failure occurred. The maximum peak values were recorded in pounds and converted into megapascals (MPa).

Following shear testing, the debonded dentin surfaces were examined under a stereomicroscope at 40× magnification. To simplify the assessment and maximize practical relevance for clinicians and scientists, failure modes were classified into three distinct categories based on the percentage of adhesive remnants left on the substrate surface: Type I (Adhesive), characterized by less than 25% substrate coverage; Type II (Mixed), presenting between 25% and 75% substrate coverage; and Type III (Cohesive), demonstrating greater than 75% substrate coverage. This standardized thresholding eliminated ambiguous boundary definitions between mixed and pure failure types.

Statistical analysis was performed using SciPy 1.11. Baseline characteristics were summarized as frequencies and percentages for categorical variables and as mean ± standard deviation (SD) for continuous variables. For continuous data with a normal distribution, inter-group comparisons were performed using Student's t-test. Categorical variables were analyzed using the chi-square test. A P-value <0.05 was considered statistically significant.

Results

Shear bond strength (SBS) analysis (Table 1) revealed comparable baseline performance for OptiBond FL (20.7 ± 4.6 MPa) and Clearfil SE Bond 2 (20.6 ± 4.2 MPa), showing no statistically significant differences between the two adhesive strategies immediately after luting (P = 0.920). However, artificial thermal aging via thermocycling significantly degraded the integrity of the dentin bond in both primary experimental groups (P = 0.000). In the post-aging scenario, Clearfil SE Bond 2 (16.8 ± 4.4 MPa) performed significantly better than OptiBond FL (14.4 ± 4.7 MPa), indicating greater resistance to hydrolytic breakdown (P = 0.023).

Table 1.

Shear bond strength values (MPa) and statistical comparisons between experimental groups under immediate and aged conditions.

Adhesive group	Baseline subgroup (n=39)	Thermocycle subgroup (n=39)	P-value (aging effect)
Group 1 (OFL)	20.7 ± 4.6	14.4 ± 4.7	0.000
Group 2 (CSEB2)	20.6 ± 4.2	16.8 ± 4.4	0.000
P-value (adhesive effect)	0.920	0.023	

Visual analysis of the debonded surfaces revealed no cohesive failures across all treatment modalities. Because this failure mode did not occur, it was excluded from further description and statistical analysis. The distribution of debonding patterns was presented in Table 2 as adhesive and mixed failure modes, which together accounted for 100% of the evaluated samples.

At baseline, no statistically significant differences in the distribution of failure modes were detected between the OFL and CSEB2 groups (P > 0.05). Both systems demonstrated a balanced mix of pure adhesive and mixed failures. However, artificial aging induced a highly significant divergence between the two adhesive strategies.

Following 10,000 thermal cycles, a significant intragroup shift occurred in the OFL group (P = 0.013): the proportion of cases with purely adhesive failure rose sharply to 84.6%. Conversely, the CSEB2 group remained remarkably stable, with no significant structural shift after aging (P = 0.366), maintaining a high proportion of mixed failures (38.5%). Thus, following thermal aging, the interface in the OptiBond FL group demonstrated a high rate of adhesive failures (84.6%), whereas Clearfil SE Bond 2 maintained high structural stability with a lower frequency of adhesive failures (61.5%); P = 0.022.

Consequently, the post-aging comparison between the two primary adhesive systems revealed a highly significant difference, objectively confirming the superior structural durability of the CSEB2 interface over long-term thermal stress.

Table 2.

Distribution of failure modes and statistical significance among experimental groups.

Primary adhesive group	Subgroup (n=39)	Adhesive failure n (%)	Mixed failure n (%)	Inter-Failure mode significance (*P*-value)
Group 1 (OFL)	Baseline subgroup	23(59.0)	16 (41.0)	0.114
	Thermocycling subgroup	33 (84.6)	6 (15.4)	0.000
	Intra-Failure mode significance (*P*-value)	0.013	0.013	
Group 2 (CSEB2)	Baseline subgroup	20 (51.3%)	19 (48.7%)	0.820
	Thermocycling subgroup	24 (61.5%)	15 (38.5%)	0.043
	Intra-Failure mode significance (*P*-value)	0.366	0.366	

Discussion

Modern minimally invasive dentistry dictates a paradigm shift toward maximum tooth preservation, utilizing biomimetic materials to recreate the natural dentin-enamel junction. In indirect restorative approaches, the creation of a durable multi-layered interface relies on interfacial co-polymerization between distinct resin components.[5] Consequently, evaluating both macroscopic bond-strength parameters and microscopic failure kinetics is paramount for understanding the clinical longevity of these hybrid complexes.

In the present study, the baseline SBS testing demonstrated comparable immediate bonding efficacy between the fourth-generation etch-and-rinse (OFL) and sixth-generation self-etch (CSEB2) groups ($P > 0.05$). This initial equivalence was supported by statistically similar failure profiles, which exhibited a predominance of Type II interfacial failures localized strictly at the dentin-adhesive boundary. This baseline phenomenon is driven by a stark biomechanical mismatch: the highly resilient, 3D-printed composite cylinders possess a significantly lower elastic modulus (4 GPa) than the rigid, highly filled universal luting composite (Filtek Z350 XT, 14 GPa).[2,8] Under monotonic loading, the compliant printed substrate acts as an elastic buffer, undergoing micro-deformation and transferring destructive kinetic energy downward, where it concentrates on the rigid dentin floor.[14]

This mechanical stress concentration is further exacerbated by thermal and optical attenuation kinetics during the immediate curing phase. When the preheated (55°C) Filtek Z350 is applied, its initial contact with the room-temperature Bego cylinder surface is highly effective due to the shared resin-to-resin chemical affinity. However, immediate contact with the underlying dentin substrate results in rapid thermal dissipation within the tooth mass.[11] This localized cooling abruptly spikes the luting composite's viscosity, micro-mechanically compromising its adaptation to the unpolymerized adhesive film at the dentin floor.[3,12] Furthermore, during photoactivation, the curing light intensity attenuates exponentially as it propagates through the 2.4-mm-high printed cylinder and the intervening luting matrix.[15] The resulting reduction in total radiant exposure at the deepest interface yields a lower degree of conversion, establishing the under-polymerized dentin floor as the primary locus for structural cleavage under peak baseline loads, thereby explaining why both groups performed identically prior to aging.

Following 10,000 thermal cycles, a distinct divergence in bond durability emerged, with CSEB2 exhibiting significantly greater resistance to hydrolytic degradation than OFL. This long-term stability is fundamentally rooted in the chemical interaction of the 10-MDP monomer within CSEB2.[1,6] While water is mandatory for self-etch ionization, this bonding occurs dynamically during the active 20-second scrubbing phase. Subsequent air-drying stabilizes these self-assembled, water-insoluble 10-MDP–Ca nanolayers by eliminating volatile solvents without disrupting the newly formed ionic chemical anchor.[16] Additionally, the localized heat from the preheated luting composite acts as a thermodynamic catalyst, increasing molecular mobility and consolidating this interface prior to vitrification.[2]

This pre-established chemical foundation fundamentally dictates how the aging networks tolerate polymerization contraction stress. In the OFL group, which lacks primary chemical stabilization and relies solely on a micromechanical hybrid layer,[14] severe polymerization contraction forces easily rupture the vulnerable dentin interface over time.[17] This acute internal strain manifests after thermocycling as a statistically significant shift in failure kinetics, culminating in a predominant distribution of true adhesive failures (84.6%).

Conversely, the pre-formed 10-MDP–Ca ionic bonds in the CSEB2 group serve as robust structural anchors that buffer polymerization stress and resist hydrolytic cleavage. According to Yoshida et al.,[18] this mechanism may well explain the high clinical longevity of adhesive bonds produced by 10-MDP-based adhesives.This superior durability highlights the critical role of the hydrophilic dihydrogen phosphate functional group within the 10-MDP monomer.[6,7] By creating a stable chemical link rather than a purely mechanical one, this interaction opens

highly promising avenues for biomimetic tooth restoration, successfully absorbing functional stresses while preserving the structural integrity of the treated dentin substrate.

Conclusion

Within the limitations of this in vitro laboratory study, it can be concluded that while both adhesive generations exhibit equivalent immediate bonding performance when using a co-curing technique with preheated universal composite, the null hypothesis must be rejected after thermocycling. Artificial thermal stress significantly compromises the long-term dentin bond integrity of both strategies; however, the sixth-generation 10-MDP-containing self-etch system (Clearfil SE Bond 2) demonstrates significantly superior hydrolytic stability and interfacial durability compared to the fourth-generation etch-and-rinse system (OptiBond FL).

Clinically, the use of a two-step self-etch protocol provides a more predictable, chemically driven interface for the cementation of contemporary 3D-printed ceramic-reinforced hybrid composite restorations, offering promising prospects for the longevity of biomimetic indirect treatments.

Ethical Statement

The study was approved by the Ethics Committee of the Institute of Medicine RUDN (Protocol Number: 29, dated 06.20.2024). Written informed consent was obtained from all participants prior to the processing of their teeth.

Author Contributions

Timur Melkumyan: Conceptualization, Methodology, Formal analysis, Writing – review and editing.

Kakhramon Shomurodov: Supervision, Methodology.

Ibrokhimjon M. Azimov: Investigation, Data curation.

Zurab Khabadze: Data interpretation, Writing – review and editing.

Maria Makeeva: Data interpretation, Writing – original draft.

Roman A. Meremkulov: Data interpretation, Writing – original draft.

Surayo Sh. Sheralieva: Investigation, Data curation.

Diyorakhon A. Inoyatova: Investigation, Data curation.

Shakhnoza K. Musoshaykhova: Investigation, Data curation.

Nuriddin Kamilov: Investigation, Writing – original draft.

Shukhrat Shakirov: Investigation, Writing – original draft.

Azad Mukhamedov: Investigation, Data curation.

Gerhard K. Seeberger: Data interpretation, Writing - review and editing.

Bedros Y. Sakuk - Data interpretation, Writing - review and editing.

Angela Dadamova: Data interpretation, Writing – review and editing.

All authors have approved the final article.

Conflict of Interests

The authors have declared no conflict of interest.

References

1. Van Meerbeek B, Yoshihara K, Yoshida Y, Mine A, De Munck J, Van Landuyt KL. Mechanisms of resin-dentin bonding and main reasons for bond degradation. Jpn Dent Sci Rev. 2020;56(1):208-215.
2. Melkumyan TV, Sheralieva SSh, Mendosa EJu, Khabadze ZS, Makeeva MK, Kamilov NKh, et al. Effect of Preheating on Mechanical Properties of Different Commercially Available Dental Resin Composites. International Journal of Biomedicine. 2023;13(4):317-322. doi: 10.21103/Article13(4)_OA14
3. Souza JPDV, Piacenza LT, Mazaro JVQ, Moreno ALM, Moreno NVA, Dos Santos DM, Goiato MC. Do preheated composite resins provide better cementation results for indirect restorations? A Systematic Review. J Clin Exp Dent. 2025 Jan 1;17(1):e11-e17. doi: 10.4317/jced.62356. PMID: 39958251; PMCID: PMC11829726.
4. Vukelja J, Klarić Sever E, Sever I, Jukić Krmek S, Tarle Z. Effect of Conventional Adhesive Application or Co-Curing Technique on Dentin Bond Strength. Materials. 2021;14(24):7664.
5. Breschi L, Maravic T, Comba A, Mazzitelli C, Burgess JO, Ferracane JL, et al. Simultaneous polymerization of adhesive-composite interfaces: Polymerization kinetics and stress development. Dent Mater. 2021;37(6):912-922.
6. Van Landuyt KL, Snauwaert J, De Munck J, Peumans M, Yoshida Y, Poitevin A, Coutinho E, Suzuki K, Lambrechts P, Van Meerbeek B. Systematic review of the chemical composition of contemporary dental adhesives. Biomaterials. 2007 Sep;28(26):3757-85. doi: 10.1016/j.biomaterials.2007.04.044. Epub 2007 May 7. PMID: 17543382.
7. Melkumyan TV, Khabadze ZS, Makeeva MK, Dashtieva MU, Badalov FV, Musashaykhova SK, Hamidov HI, Suleymanov SX, Kulagina NA, Chuan DHK, Seeberger GK, Sakuk BY, Rau JY, Kamilov NKh, Dadamova AD. Enhancing Dentin Bonding of Fifth-Generation Adhesive Through Experimental 10-MDP Primer: A Pilot Study on Human Teeth. International Journal of Biomedicine. 2026;16(1):101-106. doi:10.21103/Article16(1)_OA14
8. Grzebieluch W, Kowalewski P, Grygier D, Jachimowicz M, Wolfart S, Bürgers R. Mechanical Properties of Additive-Manufactured Composite Resins Used for Definitive Restorations: A Scoping Review. Materials. 2024;17(16):3948.
9. Son CN, Kim JE, Kim JH. Evaluation of Shear Bond Strength in the Repair of Additively and Subtractively Manufactured Resin Composites. Polymers. 2025;17(13):1842.
10. Kariper E, Cilingir A. Bond strength of different resin-based cements to 3D-printed permanent restorations. Am J Dent. 2025 Feb;38(1):39-45. PMID: 40000006.
11. Takahashi R, Nikaido T, Ariyoshi M, Foxton RM, Tagami J. Effect of thermal preconditioning on the polymerisation performance of light-cured resin composites. Dent Mater J. 2019;38(4):584-591.

12. D'Amario M, Vassilli M, Marini R, Capogreco M, Baldi M. Influence of preheated composite resins on the margin quality of indirect restorations: a review of current evidence. Eur J Oral Sci. 2023;131(2): e12914.
13. Melkumyan TV, Kakhkharova D, Masouleh S, et al. Comparative Analysis of in vitro Performance of Total-Etch and Self-Etch Adhesives. International Journal of Biomedicine. 2016;6(4):283-286. doi: 10.21103/Article6(4)_OA7
14. Pashley DH, Tay FR, Breschi L, Tjäderhane L, Carvalho RM, Carrilho M, Tezvergil-Mutluay A. State of the art etch-and-rinse adhesives. Dent Mater. 2011 Jan;27(1):1-16. doi: 10.1016/j.dental.2010.10.016. Epub 2010 Nov 27. PMID: 21112620; PMCID: PMC3857593.
15. Price RB, Ferracane JL, Shortall AC. Light-Curing Units: A Review of What We Need to Know. J Dent Res. 2015 Sep;94(9):1179-86. doi: 10.1177/0022034515594786. Epub 2015 Jul 8. PMID: 26156516.
16. Yoshihara K, Yoshida Y, Hayakawa S, Nagaoka N, Torii Y, Osaka A, Suzuki K, Minagi S, Van Meerbeek B, Van Landuyt KL. Self-etch monomer-calcium salt deposition on dentin. J Dent Res. 2011 May;90(5):602-6. doi: 10.1177/0022034510397197. Epub 2011 Feb 18. PMID: 21335540.
17. Tay FR, Pashley DH. Have dentin adhesives become too hydrophilic? J Can Dent Assoc. 2003 Dec;69(11):726-31. PMID: 14653938.
18. Yoshida Y, Yoshihara K, Nagaoka N, Hayakawa S, Torii Y, Ogawa T, Osaka A, Meerbeek BV. Self-assembled Nano-layering at the Adhesive interface. J Dent Res. 2012 Apr;91(4):376-81. doi: 10.1177/0022034512437375. Epub 2012 Feb 1. PMID: 22302145.

Corresponding author:

Prof. Timur V. Melkumyan, PhD, DSc. Tashkent State Dental Institute, Tashkent, Uzbekistan. Peoples' Friendship University of Russia (RUDN University), Moscow, Russia. E-mail: t.dadamov@gmail.com

International Journal of Biomedicine 16(2) (2026) 248-252
http://dx.doi.org/10.21103/Article16(2)_OA15

ORIGINAL ARTICLE

INTERNATIONAL JOURNAL OF BIOMEDICINE

The Effect of Treating Acrylic Resin Denture Base Material with Processed Mushroom Microparticle Solution on the Engineering and Biomaterial Properties

Zahraa Saad A. Karkosh[1*], Omer Abdul Jabbar Abdul Qader[2], Abeer A. Yahya[1], Alyaa Saad Abed[3]

[1]*College of Dentistry, Ibn Sina University of Medical and Pharmaceutical Science, Baghdad, Iraq*
[2]*Al-Mashreq University, Baghdad, Iraq*
[3]*College of Biotechnology, Al Qasim Green University, Babylon 51013, Iraq*

Abstract

Background: Different types of material have been used for many years as a denture base material, but heat-cure acrylic denture base material is still the most popular for making removable prostheses due to its many advantages, including good strength, stability, aesthetic low water sorption; however, this material also has many drawbacks, including mechanical and hygienic weaknesses, as it is porous and can trap food and microorganisms. The aim of this study was to measure the effect on biomaterial properties of adding a processed mushroom microparticle (PMM) solution to methyl methacrylate (MMA), the monomer of polymethyl methacrylate (PMMA), including transverse and impact strength, water sorption, and its effect on specific types of microorganisms.

Methods and Results: The edible mushroom type *Agaricus bisporus* (white button mushroom) was used as a microparticle solution to be mixed with MMA to test its antibacterial, antifungal effects, and its effect on the PMMA mechanical properties. According to the test type, 120 samples were prepared; 10 samples were used for each test and each group.

Bacterial strains (*Staphylococcus aureus* and *Klebsiella* spp.) and *Candida albicans* were used in this study to investigate antibacterial and antifungal activity. A scanning electron microscope (SEM) was used to confirm the size of processed micro particles. Fourier transform infrared spectroscopy (FTIR) was used to identify organic, inorganic, and polymeric materials.

PMM was tested against *Staphylococcus aureus*, *Klebsiella* spp., and *Candida albicans*, and the results showed no effect on the bacteria; it inhibited only *Candida albicans*, with an inhibition zone diameter of 10mm. The results for MMA alone showed no effect on *Staphylococcus aureus* and *Candida albicans*, but it did affect only *Klebsiella* spp. However, after mixing MMA with 10% PMM, the natural extract showed a synergistic effect against *Staphylococcus aureus*, *Klebsiella* spp., and *Candida albicans*, with inhibition zones of 7 mm, 8 mm, and 9 mm, respectively. The inhibition zone diameters of acrylic discs containing PMM were 19 mm, 21 mm, and 16 mm for *Staphylococcus aureus*, *Klebsiella* spp., and *Candida albicans,* respectively, whereas the MMA group showed no effect. There was a highly significant increase in transverse and impact strengths for the processed group, compared to the MMA group, and a highly significant reduction in water sorption for the processed group, compared to the MMA group.

Conclusion: The addition of PMM to the MMA monomer and subsequent mixing with PMMA powder yielded noticeable results from both mechanical and biological perspectives.(**International Journal of Biomedicine. 2026;16(2):248-252.**)

Keywords: acrylic denture material • antifungal agents • mechanical phenomena

For citation: Karkosh ZSA, Qader OAJA, Yahya AA, Abed AS. The Effect of Treating Acrylic Resin Denture Base Material with Processed Mushroom Microparticle Solution on the Engineering and Biomaterial Properties. International Journal of Biomedicine. 2026;16(2):248-252. doi:10.21103/Article16(2)_OA15

Abbreviations

AFM, atomic force microscopy; **FTIR**, Fourier transform infrared spectroscopy; **PMMA**, polymethyl methacrylate; **PMM**, processed mushroom microparticle; **SEM**, scanning electron microscopy.

Introduction

Different types of material have been used for many years as a denture base material, but heat-cure acrylic denture base material is still the most popular for making removable prostheses due to its many advantages, including good strength, stability, aesthetic low water sorption; however, this material also has many drawbacks, including mechanical and hygienic weaknesses, as it is porous and can trap food and microorganisms.[1] Therefore, many attempts have been made over the years to improve the mechanical properties of polymethyl methacrylate (PMMA). These methods included adding fiber and graft copolymerization, and using natural extracts, all considered promising approaches to improve the material's properties.[2-4] Also, these additions or alterations to PMMA to improve its mechanical properties need to be safe and maintain biocompatibility.[5]

Edible mushrooms show no harmful or toxic effects.[6] Mushrooms contain amino acids, protein, fiber, and erythritol, a widely recognized, non-cariogenic sweetener that does not contribute to tooth decay and, unlike sugar, is not metabolized by oral cariogenic bacteria such as *Streptococcus mutans* and *Streptococcus sobrinus*.[7] Furthermore, studies indicate that erythritol actively inhibits the growth, adherence, and biofilm formation of *Streptococcus mutans* and *Streptococcus sobrinus*.

Based on previous studies that used edible mushroom type *Lentinula edodes* (shiitake mushroom), it was found to have an antiplaque effect as it reduces *Streptococcus mutans* growth through inhibiting DNA production, in addition to the same effect on streptococcal species.[8,9,10]

The aim of this study was to measure the effect on biomaterial properties of adding a processed mushroom microparticle (PMM) solution to methyl methacrylate (MMA), the monomer of PMMA, including transverse and impact strength, water sorption, and its effect on specific types of microorganisms.

Methods

In this study, the edible mushroom type *Agaricus bisporus* (white button mushroom) was used as a microparticle solution to be mixed with MMA to test its antibacterial, antifungal effects, and its effect on the PMMA mechanical properties.

In the processed group, MMA was mixed with 10% PMM and heat-cure acrylic powder of PMMA (Pyrax, India), according to the manufacturer's instructions. The 10% PMM concentration was selected based on a pilot study in which 3 PMM concentrations (5%, 10%, and 15%) were added to MMA to assess their effects on *Staphylococcus aureus, Klebsiella* spp., and *Candida albicans*. The ingredients were mixed by slowly adding PMM to MMA to ensure complete coverage at a temperature below 50°C, thereby preventing structural damage.

Preparation of Processed Mushroom Microparticle Solution

The mushroom powder was prepared by drying mushrooms for 3 weeks, then smashing them with a silver-crest grinding degree of 30-300 at a rotating speed of 28,000 r/min for 5 min per round, 3 times. After each smashing process, the powder was sifted through a 38-micrometer-pore sieve. The final powder was converted into a microparticle solution by a physical method (top-down): 2g of mushroom powder was added to 100ml of distilled water in a magnetic stirrer at 50°C for 10 hours, then the solution was filtered 4 times using filter paper. Next, the solution was precipitated at 50 µL/min using a stirrer at 60°C to produce tin films for testing[11] (Figure 1). A scanning electron microscope (SEM) was used to confirm the size of processed micro particles. The particle size was between 1-2 µm, according to the SEM test.

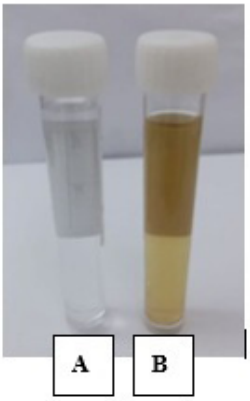

Fig. 1. *A represents distilled water, B represents PMM.*

Antibacterial Activity

Bacterial strains (*Staphylococcus aureus* and *Klebsiella* spp.) and *Candida albicans* were used in this study to investigate antibacterial and antifungal activity. The cork borer method was used to make the agar well in the plates.[12] Incubation durations for *Staphylococcus aureus* were 18 and 24 hours, while for *Candida albicans*, it was 24-72 hours. Then the inhibition zone was calculated in mm.[13] The bacterial and Candida sources were obtained from Medical City, a teaching hospital in Baghdad. The measurement method was used in an in vitro study and did not involve human subjects or animals.

Preparation of Samples

According to the test type, 120 samples were prepared; 10 samples were used for each test and each group (Figure 2). The rectangular-shaped samples were prepared for each of the flexural tests with dimensions based on ANSI/ADA No.12; for the impact test, the dimensions of the samples were 60 mm ×12 mm × 3 mm; for the water sorption test circle samples with dimensions 50 mm × 0.5 mm were prepared according to ADA No.12.[14] For water sorption, the measuring method involved the equation (M2-M1 mg/surface area cm^2) by immersing the samples in distilled water for one week. Samples were measured with a sensitive electronic balance with precision 0.00001g. The dimensions of the bacterial inhibition zone were 10 mm × 2 mm. Flexural tests were performed on a universal testing machine; impact tests were performed using the Izod impact test.

Fourier transform infrared spectroscopy (FTIR) was used to identify organic, inorganic, and polymeric materials.

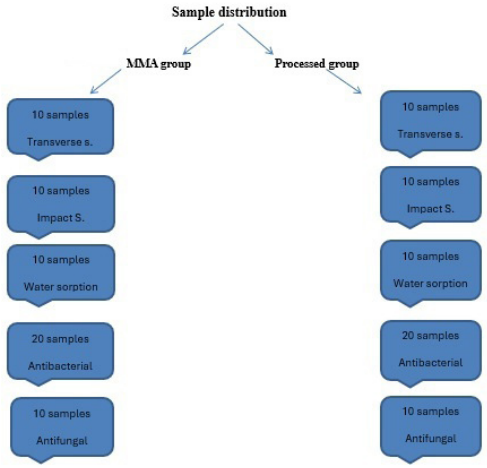

Fig. 2. *Sample numbers and distribution for each test and group.*

Statistical analysis was performed using SPSS version 24.0 (IBM Corp., Armonk, NY). For the descriptive analysis, results are presented as mean (M) ± standard deviation (SD). For normally distributed data, inter-group comparisons were performed using Student's t-test. A probability value of $P < 0.05$ was considered statistically significant.

Results

The results of scanning electron microscopy (SEM) and atomic force microscopy (AFM) indicated that the PMM particles had reached the microscale, as the material contained fibers that could not be further reduced, and that the particle surfaces were smooth (Figure 3).

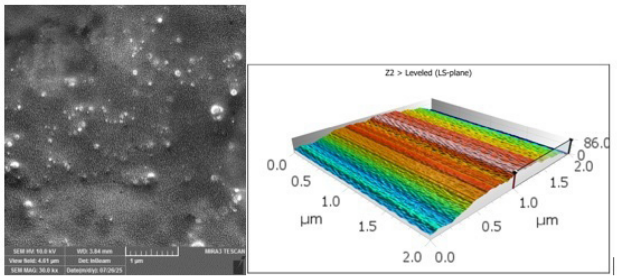

Fig. 3. *The results of SEM and AFM.*

The results of FTIR for both control and processed groups showed that the changes that occurred in the processed group involved a shortage at peak 2924 cm^{-1} and 2854 cm^{-1} that refer to C-H alkane, and this could be explained as the PMM was added in a small amount (10%) as an additive that made the changes in the chemical formula of the new group unremarkable (Figure 4).

PMM was tested against *Staphylococcus aureus*, *Klebsiella* spp., and *Candida albicans*, and the results showed no effect on the bacteria; it inhibited only *Candida albicans*, with an inhibition zone diameter of 10 mm. The results for MMA alone showed no effect on *Staphylococcus aureus* and *Candida albicans*, but it did affect only *Klebsiella* spp. However, after mixing MMA with 10% PMM, the natural extract showed a synergistic effect against *Staphylococcus aureus*, *Klebsiella* spp., and *Candida albicans,* with inhibition zones of 7 mm, 8 mm, and 9 mm, respectively. The inhibition zone diameters of acrylic discs containing PMM were 19mm, 21mm, and 16mm for *Staphylococcus aureus*, *Klebsiella* spp., and *Candida albicans*, respectively, whereas the MMA group showed no effect (Figure 5).

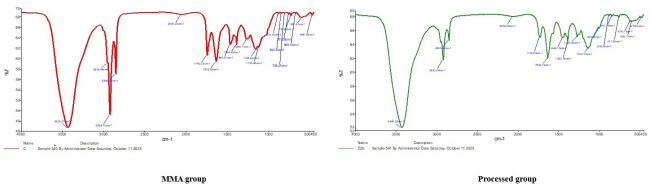

Fig. 4. *FTIR for the MMA and processed groups.*

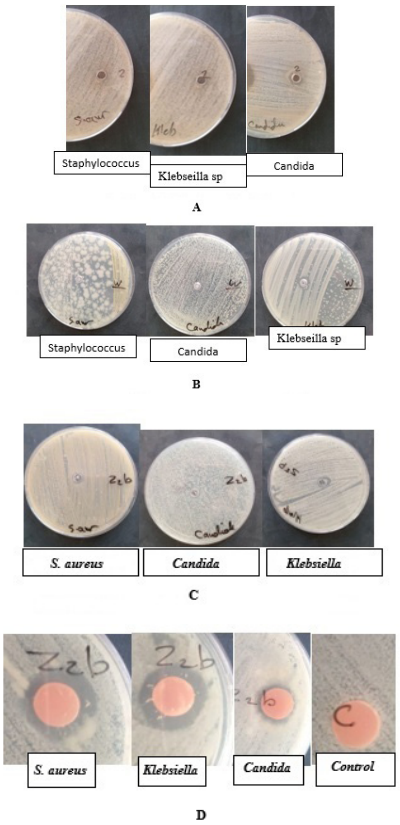

Figure 5.

A*. Effects of PMM on Staphylococcus aureus, Klebsiella spp., and Candida.*

B*. Effects of MMA on Staphylococcus aureus, Klebsiella spp., and Candida.*

C*. Effects of PMM and MMA on Staphylococcus aureus, Klebsiella spp., and Candida.*

D*. Diameter of inhibition zone.*

Statistical analysis showed a highly significant increase in transverse and impact strengths for the processed group, compared to the MMA group (Tables 1 and 2), and a highly

significant reduction in water sorption for the processed group, compared to the MMA group (Table 3).

Table 1.

Descriptive and statistical test of transverse strength (MPa) between groups.

	MMA group	Processed group	*P*-value
Minimum	45.000	70.000	0.004
Maximum	70.000	93.000	
Mean	60.800	75.100	
±SD	9.693	9.562	

Table 2.

Descriptive and statistical test of impact strength (J/m²) between groups.

	MMA group	Processed group	*P*-value
Minimum	0.400	0.400	0.002
Maximum	0.450	0.550	
Mean	0.430	0.490	
±SD	0.026	0.046	

Table 3.

Descriptive and statistical test of water sorption (µg/mm³) between groups.

	MMA group	Processed group	*P*-value
Minimum	20	20	0.026
Maximum	80	40	
Mean	52	30	
±SD	8	3	

Discussion

A synergistic inhibition effect of MMA with 10% PMM on the growth of *Staphylococcus aureus*, *Klebsiella* spp., and *Candida albicans* was probably due to the homogenous mixing and dissolving process of PMM in MMA.

As for mechanical properties, transverse and impact strength were significantly higher in the processed group than in the MMA group. This is probably due to PMM acting as a filler to fill the spaces left after MMA evaporation and may also be attributed to homogeneous distribution between PMM and MMA. Both PMM and PMMA are considered organic materials.[15] Our study aligns with principles used to improve PMMA's mechanical properties by altering its chemistry or adding fillers.[16,17] The results also coincide with those reported by Fahimeh et al.,[18] who improved some mechanical properties of PMMA by adding nanosilver.

The water sorption is considered an important mechanical property in PMMA as it could affect the quality of denture materials, which are affected by the nature of the water environment, the polymer molecular composition, and the additives present in the mixture. The results of this study for water sorption showed a significantly reduced effect for the processed group, compared to the MMA group. This was probably due to a reduced number of microscopic pores and homogenous mixing between PMM and PMMA.[19-22]

In conclusion, the addition of PMM to the MMA monomer and subsequent mixing with PMMA powder yielded noticeable results from both mechanical and biological perspectives.

Author Contributions

Zahraa Saad A. Karkosh: Conceptualization, Investigation, Data analysis/interpretation, Writing – review and editing.
Omer Abdul Jabbar Abdul Qader: Data curation, Data analysis, Writing – original draft.
Abeer A. Yahya: Investigation, Data curation, Sample preparation.
Alyaa Saad Abed: Investigation, Formal analysis, Writing – original draft.
All authors have approved the final article.

Conflict of Interest

The authors have declared no conflict of interest.

References

1. Salih SI, Braihi AZJ, Sadeq HM. The Fracture Toughness of Heat Cured Acrylic- Natural Rubber/Silicone Rubber Blend Reinforced with Pomegranate Peels Powder. JUBES. 2019;27:4:175-184.
2. Carlos NB, Harrison A. The effect of untreated UHMWPE beads on some properties of acrylic resin denture base material. J Dent. 1997 Jan;25(1):59-64. doi: 10.1016/0300-5712(95)00121-2. PMID: 9080742.
3. Lagashetty A, Venkataraman A. Polymer Nanocomposites. Resonance. July 2005;10(6):49-60
4. Pauli MC, Kanemaru MYS, Vieira-Junior WF, Lima DANL, Bicas JL, Leonardi GR. Current status of whitening agents and enzymes in dentistry. Braz J Pharm Sci. 2022;58:e19501
5. Saraf S, Mishra SK, Agrawal B. Effect of beverages, denture cleanser and chlorhexidine gluconate on surface roughness of flexible denture base material: an in vitro study. Eur Oral Res. 2024 May 5;58(2):76-82. doi: 10.26650/eor.20231177548. PMID: 39011171; PMCID: PMC11246716.
6. Heleno SA, Barros L, Martins A, Queiroz MJ, Santos-Buelga C, Ferreira IC. Phenolic, polysaccharidic, and lipidic fractions of mushrooms from northeastern Portugal: chemical compounds with antioxidant properties. J Agric Food Chem. 2012 May 9;60(18):4634-40. doi: 10.1021/jf300739m. Epub 2012 Apr 27. PMID: 22515547.
7. Shadia AA. EDIBLE MUSHROOMS: A GREEN BIOTECHNOLOGY AND GREAT NUTRITIONAL VALUE FOR IMPROVING HUMAN HEALTH. EPH - International Journal of Science And Engineering. 2015;1(3):9-18. doi: 10.53555/eijse.v1i3.67.

8. Thaper S, Lakshmi T. Effects of mushroom on dental caries. J Adv Pharm Edu Res 2017;7(3):197-199.
9. Daglia M, Papetti A, Mascherpa D, Grisoli P, Giusto G, Lingström P, Pratten J, Signoretto C, Spratt DA, Wilson M, Zaura E, Gazzani G. Plant and fungal food components with potential activity on the development of microbial oral diseases. J Biomed Biotechnol. 2011;2011:274578. doi: 10.1155/2011/274578. Epub 2011 Oct 17. PMID: 22013381; PMCID: PMC3196265.
10. Lindequist U, Niedermeyer TH, Jülich WD. The pharmacological potential of mushrooms. Evid Based Complement Alternat Med. 2005 Sep;2(3):285-99. doi: 10.1093/ecam/neh107. PMID: 16136207; PMCID: PMC1193547.
11. Ahmed HH, Ali AM, Abed AN. Biosynthesis and characterization of (Co3O4) for solar cell applications via N-Sativa extract. Global Journal of Engineering and Technology Advances. 2023;14(03):033–041.
12. Jahangirian H, Haron J, Ismail MHS, Moghaddam RR, Hejri LA, Abdollahi Y, et al. Well diffusion method for evaluation of antibacterial activity of copper phenyl fatty hydroxamate synthesized from canola and palm kernel oils. Digest Journal of Nanomaterials and Biostructures. 2013;8(3):1263-1270.
13. Karkosh ZSA. Effect of different modified heat cure acrylic denture base material on adherence of Candida albicans and on some of mechanical properties. Doctoral dissertation, University of Baghdad; 2017.
14. AMERICAN NATIONAL STANDARD/AMERICAN DENTAL ASSOCIATION SPECIFICATION NO. 12 FOR DENTURE BASE POLYMERS. ANSI/ADA Specification No. 12 – 2002
15. Alves MJ, Ferreira IC, Dias J, Teixeira V, Martins A, Pintado M. A review on antifungal activity of mushroom (basidiomycetes) extracts and isolated compounds. Curr Top Med Chem. 2013;13(21):2648-59. doi: 10.2174/15680266113136660191. PMID: 24083794.
16. Marei MK, El-Sabrooty A, Ragab AY, El-Osairy MA. A study of some physical and mechanical properties of metal filled acrylic resin. Saudi Dental Journal. 1994;6:69–77.
17. Jagger DC, Harrison A, Jandt KD. The reinforcement of dentures. J Oral Rehabil. 1999 Mar;26(3):185-94. doi: 10.1046/j.1365-2842.1999.00375.x. PMID: 10194725.
18. Hamedi-Rad F, Ghaffari T, Rezaii F, Ramazani A. Effect of nanosilver on thermal and mechanical properties of acrylic base complete dentures. J Dent (Tehran). 2014 Sep;11(5):495-505. Epub 2014 Sep 30. PMID: 25628675; PMCID: PMC4290768.
19. Hamza M, Alsolam M, Oudah AM, Alhadi AAB, Alarjan A. Appraise the Different Types of Polymer Used in Denture Base Through their Physical Property (Water Sorption). EIMJ. 2020; 25(6):1-16 .
20. Abdul-Baqi HJ, Safi IN, Nima Ahmad A, Fatalla AA. Investigating Tensile Bonding and Other Properties of Yttrium Oxide Nanoparticles Impregnated Heat-Cured Soft-Denture Lining Composite *In Vitro*. J Int Soc Prev Community Dent. 2022 Jan 29;12(1):93-99. doi: 10.4103/jispcd.JISPCD_274_21. PMID: 35281690; PMCID: PMC8896588.
21. Bacali C, Constantiniuc M, Moldovan M, Nastase V, Badea M, Constantin A. Reinforcement of PMMA Denture Base Resins: From Macro to Nano Scale. Int J Med Dent. 2019 b; 23 (3): 374-378.
22. Laura MO, Paulina ROJ, Jizhel BCM, Alvaro GP. Sorption and Solubility of Acrylic Resin Self polimer by 3 Process Tech-niques in Orthodontics. Dent Pract. 2019; 2(1): 001-005.

***Corresponding author:** Zahraa Saad A. Karkosh. E-mail: zahraasaad282@yahoo.com*

International Journal of Biomedicine 16(2) (2026) 253-258
http://dx.doi.org/10.21103/Article16(2)_OA16

ORIGINAL ARTICLE

INTERNATIONAL JOURNAL OF BIOMEDICINE

Bleeding on Probing Associated with Two Different Bonded Fixed Retainers: A 12-Month Evaluation

Jeta Kiseri Kubati[1*], Diona Panxhaj[1], Gabriela Kjurchieva Cuckova[2], Luis Pablo Cruz-Hervert[3]

[1]*Orthodontic Department, Dental Faculty, UBT Kolegji, Prishtina, Kosovo*
[2]*Orthodontic Department, Ss. Cyril and Methodius University in Skopje Faculty of Dentistry, Skopje, North Macedonia.*
[3]*Faculty of Dentistry, National Autonomous University of Mexico, Mexico City, Mexico*

Abstract

Background: Orthodontic retention is critical to preserving treatment results and preventing relapses. Fixed retainers, while effective, have been associated with plaque accumulation and gingival inflammation. This study assessed bleeding on probing (BOP) in patients using different retainer designs. The aim is to compare the periodontal impact—specifically bleeding on probing—of two different designs of fixed retainers bonded to the mandibular anterior teeth over 12 months.
Methods and Results: Sixty patients (age 16–25) completing orthodontic treatment were randomly assigned to receive either a flat (FR) or round (RR) NiTi retainer. BOP was assessed at 3, 6, 9, and 12 months using a standardized periodontal probe. Data were analyzed using SPSS 22.0 with Chi-square and Mann–Whitney U tests, considering $P<0.05$ as significant.
At 3 months, the FR group showed significantly lower BOP than the RR group ($P = 0.024$). Differences at 6 and 9 months were not statistically significant. At 12 months, BOP was again significantly higher in the RR group ($P = 0.001$). Intra-group changes over time were not significant for either group. The FR group consistently presented lower BOP means at all time points.
Conclusion: Flat fixed retainers resulted in significantly lower BOP at early and late follow-up, suggesting a potentially more favorable periodontal response. Long-term monitoring and individualized hygiene reinforcement remain essential in retainer management.(**International Journal of Biomedicine. 2026;16(2):253-258.**)

Keywords: orthodontic retention • bonded fixed retainers • bleeding on probing • periodontal response

For citation: Kubati JK, Panxhaj D, Cuckova GK, Cruz-Hervert LP. Bleeding on Probing Associated with Two Different Bonded Fixed Retainers: A 12-Month Evaluation. International Journal of Biomedicine. 2026;16(2):253-258. doi:10.21103/Article16(2)_OA16

Introduction

Orthodontic retention is a key part of modern care and is planned for nearly every patient, regardless of age, malocclusion, or appliance. This is because relapse is likely without retention, and long-term aesthetic and functional stability is increasingly emphasized.[1,2] Many orthodontists recommend lifelong retention to maintain treatment results, since teeth may relapse due to occlusal forces, soft-tissue pressures, and ongoing craniofacial growth.[3] Retention is typically provided with bonded lingual fixed retainers or removable vacuum-formed retainers, often worn canine-to-canine in either arch, with selection tailored to the treatment plan, malocclusion, age, and other factors.[4] Fixed retainers differ in design and materials, ranging from stainless steel and nickel-titanium to newer CAD/CAM-milled and fiber-reinforced composites.[5] Despite these advancements, all types share a common limitation: they lie against the tooth surface and may disrupt proper oral hygiene practices. This physical presence often promotes plaque and calculus accumulation in the retainer region, which may compromise periodontal health over time and eventually provoke bleeding on probing (BOP) during the retention phase.[6]

There is ongoing debate about the long-term effects of fixed retainers on oral hygiene and periodontal outcomes. While some studies show increased plaque retention and gingival inflammation, others report no significant periodontal damage, even with prolonged use.[7,8] For example, Levin et al. observed higher rates of plaque accumulation, gingival recession, and BOP in patients with fixed retainers.[9] Conversely, Rody et

al.[10] and Booth et al.[11] reported no significant periodontal impact after years of fixed retention.

Given this conflicting evidence, our study aimed to compare periodontal outcomes, specifically BOP, between two different designs of bonded fixed retainers.

The objective was to investigate whether the design and dimension of these retainers affect BOP of lingual surfaces of the lower incisor region in the mandible, after orthodontic treatment during the first years of retention. Our null hypothesis was that all fixed retainers provoke similar periodontal responses after long-term use. Our working hypothesis is that the flat prefabricated NiTi retainer has a more favorable impact on periodontal health than the round multistranded NiTi retainer.

Material and Methods

This study received ethical approval from the Ethical Committee of the Kosova Dental Chamber (Approval No. 04/L-150-23-12/2021). Throughout the process, we adhered to the ethical principles outlined in the Declaration of Helsinki to ensure the study was conducted with respect and integrity.

Study Design and Participants

A total of 60 subjects (aged 16–25 years), who had recently completed fixed orthodontic treatment at the UBT College Dental Faculty, Orthodontic Department (Kosovo), were enrolled at the start of their retention phase. All participants signed an informed consent form. In individuals younger than 18, written informed consent to participate was obtained from their parents or legal guardians. Participants were randomly allocated into two groups, each receiving a different type of fixed retainer bonded to the lingual surfaces of the six lower anterior teeth (canine to canine) (Figure 1):

- Group 1 (n=30) received a flat, prefabricated nickel-titanium retainer (FR) (0.010″×0.029″, four-strand twist) manufactured by FORESTADENT, Germany.
- Group 2 (n=30) received a multistranded round nickel-titanium retainer (RR) (ø0.44mm/17″), manufactured by DENTAURUM, Germany.

(a) (b)

Fig. 1. *(a) FR- Flat retainer; (b) RR- Round retainer.*

All retainers were bonded by the same experienced orthodontist, using a standardized protocol.

Inclusion criteria: Patients completing full fixed appliance treatment with no mandibular extractions during treatment or the 12-month follow-up; intact lower anterior segment (no caries/restorations/crowns/bridges); no parafunctional habits or occlusal interferences; no IPR or supracrestal fiberotomy; and no syndromic conditions. Exclusion criteria: Missed follow-up visits, prosthetic treatment during the study period, smoking, or functional habits (e.g., bruxism or tongue thrust).

Procedure and Clinical Assessment

All bonding procedures followed a uniform protocol, including tooth cleaning, etching, and adhesive application over retainer wire. The primary outcome was BOP, evaluated in the intercanine region (from tooth 33 to 43) at 3, 6, 9, and 12 months. At each follow-up appointment, patients were reminded and encouraged to maintain proper oral hygiene. BOP was assessed using a periodontal probe (NC 15, HuFriedy), and the number of teeth with BOP among the six lower anterior teeth was recorded. Bleeding on probing was visually assessed as the proportion of sites that were bleeding 30 s after 6 sites per tooth were probed[12] (Figure 2).

Fig. 2. *Measurement of BOP indices after (a) 3months, (b) 6 months, (c) 9 months, and (d) 12 months of observation period with bonded flat retainer.*

Statistical Analysis: All data collected in the study were analyzed using SPSS software, version 22.0 for Windows, and the findings were presented in tables and graphs. Categorical variables (such as yes/no responses) were summarized using frequencies and percentages, while numerical data (e.g., age or clinical measurements) were described using means, medians, ranges (minimum and maximum values), and standard deviations to indicate variability. Prior to conducting group comparisons, the Shapiro–Wilk test was used to assess whether the numerical data followed a normal distribution. For statistical analysis, the Chi-square test was applied to

examine associations between categorical variables, and odds ratios (OR) were calculated to estimate the likelihood of outcomes between groups. Differences in proportions were assessed using a test for proportion differences. For numerical variables that did not meet the assumption of normality, the Mann–Whitney U test was used. All tests were two-sided, and results were considered statistically significant if $P<0.05$.

Results

Gender Distribution

In the FR (flat retainer) group, 11 participants were male (36.7%), and 19 were female (63.3%), resulting in a male-to-female ratio of 0.58:1. In the RR (round retainer) group, 7 participants were male (23.3%), and 23 were female (76.7%), with a male-to-female ratio of 0.30:1. Chi-square test results showed no significant association between gender and group allocation ($\chi^2 = 1.269$; df = 1; $P = 0.259$) (Table 1)

Table 1.

Analysis of study groups by gender.

Gender	Groups		Statistics*
	FR	RR	
Total (n=60)			
Male	11 (36.7%)	7 (23.3%)	$\chi^2 = 1.269$ df = 1 $P = 0.259$
Female	19 (63.3%)	23 (76.7%)	
Difference test:	$P = 0.0410$	$P = 0.0001$	
*Mann-Whitney U Test			

Bleeding on probing was assessed on the six lower anterior teeth (intercanine region). For each participant, the number of teeth showing bleeding during probing was recorded. The presence of bleeding was analyzed at each of the four follow-up visits for both groups (FR and RR).

Data Distribution and Statistical Approach

The distribution of BOP values at all four time points did not follow a normal distribution, as confirmed by the Shapiro-Wilk test:

- 3 months: W = 0.9088, $P = 0.0003$
- 6 months: W = 0.9278, $P = 0.0016$
- 9 months: W = 0.9048, $P = 0.0002$
- 12 months: W = 0.8902, $P = 0.0001$

As a result, non-parametric statistical tests were applied for both intra-group (within FR or RR groups over time) and inter-group (FR vs. RR at each time point) analyses of BOP (Graph 1).

Intragroup Comparison of BOP

In the FR group, the lowest BOP was observed at 3 months (mean: 3.20±1.58; median: 3.00). A slight increase was noted at 6 and 9 months, with a median of 4.00 at both time points. By 12 months, BOP slightly decreased again (mean: 3.37±1.21). No significant difference was observed across time points (Friedman Test, $\chi^2 = 0.622$, $P = 0.891$).

In the RR group, BOP values were fairly stable during the first three time points, with a median of 4.00. At 12 months, BOP increased noticeably (mean: 4.53±1.33; median: 5.00). The increase was borderline non-significant across time points (Friedman Test, $\chi^2 = 7.758$, $P = 0.051$). (Table 2 and Graph 2).

Intergroup Comparison of BOP

Intergroup comparisons were made at each of the four follow-up time points (Table 3, Graph 3). At 3 months, BOP was significantly higher in the RR group than the FR group ($P = 0.024$). At 6 and 9 months, no statistically significant differences were observed. At 12 months, BOP was again significantly higher in the RR group ($P = 0.001$), indicating a possible long-term periodontal impact of the round retainer.

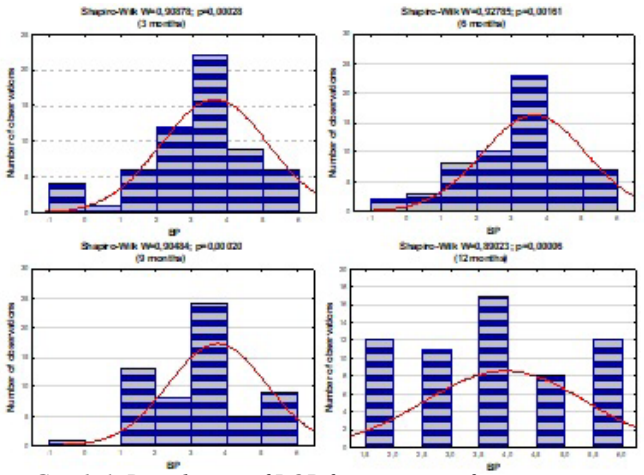

Graph 1. *Distribution of BOP frequencies at four time points.*

Table 2.

Intragroup comparison of BOP at four time points.

Intragroup comparison	Bleeding on probing - BOP					Statistics*
	n	Mean± SD	(Min/ Max)	Median (IQR)	Mean Rank	
FR						
3 months	30	3.20±1.58	0.00/6.00	3.00 (2.00-4.00)	2.42	χ^2=0.622 df=3 P=0.891
6 months	30	3.40±1.73	0.00/6.00	4.00 (2.00-4.25)	2.58	
9 months	30	3.47±1.36	0.00/6.00	4.00 (2.00-4.00)	2.58	
12 months	30	3.37±1.21	2.00/6.00	3.00 (2.00-4.00)	2.42	
RR						
3 months	30	4.07±1.31	0.00/6.00	4.00 (3.75-5.00)	2.50	χ^2=7.758 df=3 P=0.0.51
6 months	30	3.87±1.13	2.00/6.00	4.00 (3.00-4.25)	2.27	
9 months	30	4.03±1.38	2.00/6.00	4.00 (3.00-5.00)	2.40	
12 months	30	4.53±1.33	2.00/6.00	5.00 (4.00-6.00)	2.93	
*Friedman Test; IQR - Interquartile Range.						

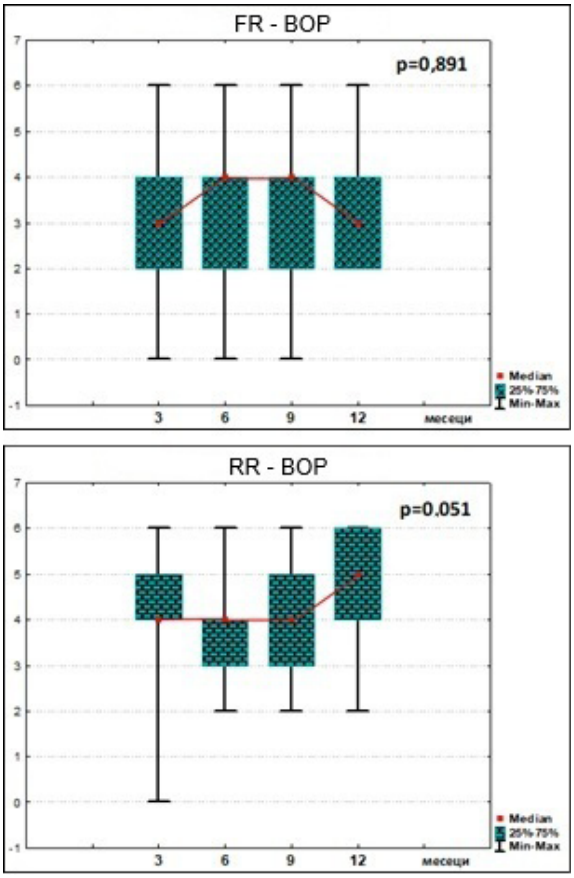

Graph 2. *Intragroup comparison of BOP at four time points (FR and RR groups)*

Table 3.

Intergroup comparison of BOP at four time points.

Intergroup comparison	Bleeding on probing (BOP)						
	n	Mean± SD	Min/ Max	IQR			Statistics*
				Q1	Q2	Q3h	
3 months							
FR	30	3.20±1.58	0.00/6.00	2.00	3.00	4.00	Z=-2.262 *P*=0.024
RR	30	4.07±1.31	0.00/6.00	3.75	4.00	5.00	
6 months							
FR	30	3.40±1.73	0.00/6.00	2.00	4.00	4.25	Z=-0.997 *P*=0.375
RR	30	3.87±1.13	2.00/6.00	3.00	4.00	4.25	
9 months							
FR	30	3.47±1.36	0.00/6.00	2.00	4.00	4.00	Z=-1.478 *P*=0.179
RR	30	4.03±1.38	2.00/6.00	3.00	4.00	5.00	
12 months							
FR	30	3.37±1.21	2.00/6.00	2.00	3.00	4.00	Z=-3.238 *P*=0.001
RR	30	4.53±1.33	2.00/6.00	4.00	5.00	6.00	

Mann-Whitney U Test; IQR - Interquartile Range; Q2- Median.

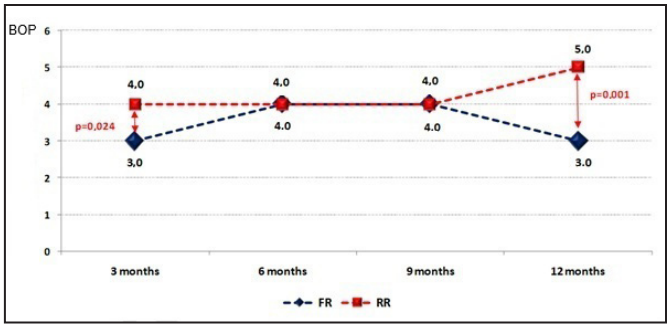

Graph 3. *Comparison of the BOP median value by study groups at four time points.*

Discussion

This study aimed to examine how two types of bonded fixed nickel-titanium orthodontic retainers—flat and round—affect bleeding on probing over a 12-month period. The first hypothesis, that both retainer types induce a periodontal response, can be accepted. The second hypothesis—that flat retainers lead to a milder periodontal response than round ones—can only be partially supported. Our findings demonstrated significantly higher BOP in the RR group compared to the flat retainer (FR) group at 3 months (P = 0.024) and again at 12 months (P = 0.001). No statistically significant differences were observed at 6 and 9 months. These results align with previous research by Levin et al. (9), who found higher BOP in patients with bonded retainers than in those without, although they did not differentiate between types of retainers. Levin et al. (9) also noted that participants' younger age might mask stronger differences observed in older populations. Hence, placing bonded retainers as far from the gingival margin as possible is advised to reduce plaque retention and bleeding risk.

In our study, BOP was recorded as a "yes" or "no" response, regardless of bleeding severity or speed following probing. While this binary system allowed for standardized data collection, it did not account for differences in bleeding intensity or onset. Future studies should consider using a graded scale (e.g., mild, moderate, severe) to capture the variability in clinical presentation. Our findings are consistent with Knaup et al.,[13] who observed higher BOP, plaque index (PI), and gingival index (GI) in patients with 0.0175-in round retainers than in those with digitally printed flat retainers—similar to the FR used in our study. Storey et al.[14] also reported increased periodontal indices, including BOP, with 0.0195-in round stainless steel retainers at 1-year follow-up. These findings support the notion that wire type and thickness can influence periodontal health, even when the design is the only difference. However, Buzzatta et al.[15] emphasized that existing studies comparing flat and round retainers are limited by small sample sizes, short follow-ups, and variability in wire type and bonding method. In contrast, other studies found no significant differences in periodontal health between flat and multistranded wires, which may reflect inconsistencies in study design, patient behavior, or measurement tools.[16,17]

Although many studies assess periodontal health in patients with bonded retainers, very few specifically evaluate retainer designs that allow or obstruct interproximal flossing. This is an important gap, as numerous studies have reported that bonded fixed retainers may contribute to increased plaque and calculus accumulation and gingival inflammation. Conversely, several studies have not found any negative impact on periodontal parameters. Factors such as periodontal phenotype, brushing habits, oral hygiene motivation, and toothbrush type all play critical roles. For instance, Corbett et al.[18] found no clinical difference in gingival health between flat and round retainers over a 2–4 year period. The authors speculated that the lack of difference may be due to patients being better educated about the potential oral hygiene challenges associated with retainers, thus improving compliance—especially in the mandibular arch. Similarly, J. Artun[7] found no negative effects of bonded retainers on teeth or surrounding hard/soft tissues, even after up to 8 years of wear. Nevertheless, it is widely acknowledged that fixed retainers complicate daily hygiene routines. Therefore, patients must be thoroughly instructed in proper retainer care, including the use of interdental cleaning devices.[19]

The patient's motivation is a crucial factor in maintaining hygiene while using bonded retainers. Improper bonding (e.g., on every anterior tooth) can impede toothbrush access, reduce the effectiveness of flossing, and ultimately lower compliance and oral health.[20,21]

Limitations

This study has several limitations, including a relatively small sample size, a 12-month follow-up period, and a monocentric design, which may limit the generalizability of the findings. Additionally, variations in individual oral hygiene practices and the absence of long-term assessments beyond one year may have influenced the observed periodontal outcomes.

However, close monitoring protocols are essential for patients with bonded fixed retainers. Periodontal parameters tended to rise in both groups during the 12-month observation period, underscoring the need for regular follow-ups and reinforced oral hygiene instruction.

AI Statement

The authors acknowledge OpenAI ChatGPT for providing proofreading support during the writing process.

Author Contributions

Jeta Kiseri Kubati: Investigation, Methodology, Data curation, Writing – original draft.
Diona Panxhaj: Methodology, Data analysis/Interpretation
Gabriela Kjurciceva Cuckova: Methodology, Writing – original draft
Luis Pablo Cruz-Hervert: Supervision, Data interpretation, Formal analysis, Writing – review and editing.

All authors have approved the final article.

Competing Interests

The authors have declared no conflict of interest.

References

1. Pratt MC, Kluemper GT, Hartsfield JK Jr, Fardo D, Nash DA. Evaluation of retention protocols among members of the American Association of Orthodontists in the United States. Am J Orthod Dentofacial Orthop. 2011 Oct;140(4):520-6. doi: 10.1016/j.ajodo.2010.10.023. PMID: 21967939; PMCID: PMC5161457.
2. Lai CS, Grossen JM, Renkema AM, Bronkhorst E, Fudalej PS, Katsaros C. Orthodontic retention procedures in Switzerland. Swiss Dent J. 2014;124(6):655-61. doi: 10.61872/sdj-2014-06-01. PMID: 24943474.
3. Bearn DR. Bonded orthodontic retainers: a review. Am J Orthod Dentofacial Orthop. 1995 Aug;108(2):207-13. doi: 10.1016/s0889-5406(95)70085-4. PMID: 7625397.
4. Kubati JK, Dzipunova B, Zigante M, Kantor S, Dzipunova M, Spalj S. Retention practices of orthodontists in the Western Balkans. Int J Biomed. 2025;15(3):552-8. doi:10.21103/Article15(3)_OA16.
5. Roser CJ, Bauer C, Hodecker L, Zenthöfer A, Lux CJ, Rues S. Comparison of six different CAD/CAM retainers vs. the stainless steel twistflex retainer: an in vitro investigation of survival rate and stability. J Orofac Orthop. 2025 Mar;86(2):119-128. doi: 10.1007/s00056-023-00486-y. Epub 2023 Jun 28. PMID: 37378840; PMCID: PMC11861246.
6. Pandis N, Vlahopoulos K, Madianos P, Eliades T. Long-term periodontal status of patients with mandibular lingual fixed retention. Eur J Orthod. 2007 Oct;29(5):471-6. doi: 10.1093/ejo/cjm042. PMID: 17974536.
7. Artun J. Caries and periodontal reactions associated with long-term use of different types of bonded lingual retainers. Am J Orthod. 1984 Aug;86(2):112-8. doi: 10.1016/0002-9416(84)90302-6. PMID: 6380296.
8. Kubati JK, Sllamniku Z, Sllamniku A, Kiseri B. Variations of the plaque index in four timelines during 12 months in patients with two models of fixed retainers after orthodontic treatment is finished. Int J Biomed. 2024;14(1):148-52. doi:10.21103/Article14(1)_OA23.
9. Levin L, Samorodnitzky-Naveh GR, Machtei EE. The association of orthodontic treatment and fixed retainers with gingival health. J Periodontol. 2008 Nov;79(11):2087-92. doi: 10.1902/jop.2008.080128. PMID: 18980517.
10. Rody WJ Jr, Akhlaghi H, Akyalcin S, Wiltshire WA, Wijegunasinghe M, Filho GN. Impact of orthodontic retainers on periodontal health status assessed by biomarkers in gingival crevicular fluid. Angle Orthod. 2011 Nov;81(6):1083-9. doi: 10.2319/011011-15.1. Epub 2011 Jun 9. PMID: 21657829; PMCID: PMC8903857.
11. Booth FA, Edelman JM, Proffit WR. Twenty-year follow-up of patients with permanently bonded mandibular canine-to-canine retainers. Am J Orthod Dentofacial Orthop. 2008 Jan;133(1):70-6. doi: 10.1016/j.ajodo.2006.10.023. PMID: 18174074.
12. Petsos H, Ramich T, Nickles K, Dannewitz B, Pfeifer L, Zuhr O, Eickholz P. Tooth loss in periodontally compromised

patients: Retrospective long-term results 10 years after active periodontal therapy - tooth-related outcomes. J Periodontol. 2021 Dec;92(12):1761-1775. doi: 10.1002/JPER.21-0056. Epub 2021 May 6. PMID: 33748997.
13. Knaup I, Wagner Y, Wego J, Fritz U, Jäger A, Wolf M. Potential impact of lingual retainers on oral health: comparison between conventional twistflex retainers and CAD/CAM fabricated nitinol retainers : A clinical in vitro and in vivo investigation. J Orofac Orthop. 2019 Mar;80(2):88-96. English. doi: 10.1007/s00056-019-00169-7. Epub 2019 Feb 18. PMID: 30778609.
14. Storey M, Forde K, Littlewood SJ, Scott P, Luther F, Kang J. Bonded versus vacuum-formed retainers: a randomized controlled trial. Part 2: periodontal health outcomes after 12 months. Eur J Orthod. 2018 Jul 27;40(4):399-408. doi: 10.1093/ejo/cjx059. PMID: 29059293.
15. Buzatta LN, Shimizu RH, Shimizu IA, Pachêco-Pereira C, Flores-Mir C, Taba M Jr, Porporatti AL, De Luca Canto G. Gingival condition associated with two types of orthodontic fixed retainers: a meta-analysis. Eur J Orthod. 2017 Aug 1;39(4):446-452. doi: 10.1093/ejo/cjw057. PMID: 27629261.
16. Torkan S, Oshagh M, Khojastepour L, Shahidi S, Heidari S. Clinical and radiographic comparison of the effects of two types of fixed retainers on periodontium - a randomized clinical trial. Prog Orthod. 2014 Aug 27;15(1):47. doi: 10.1186/s40510-014-0047-8. PMID: 25162332; PMCID: PMC4145221.
17. Gökçe B, Kaya B. Periodontal effects and survival rates of different mandibular retainers: comparison of bonding technique and wire thickness. Eur J Orthod. 2019 Nov 15;41(6):591-600. doi: 10.1093/ejo/cjz060. PMID: 31365926.
18. Corbett AI, Leggitt VL, Angelov N, Olson G, Caruso JM. Periodontal health of anterior teeth with two types of fixed retainers. Angle Orthod. 2015 Jul;85(4):699-705. doi: 10.2319/060314-398.1. Epub 2014 Oct 7. PMID: 25289654; PMCID: PMC8611743.
19. Sambunjak D, Nickerson JW, Poklepovic T, Johnson TM, Imai P, Tugwell P, Worthington HV. Flossing for the management of periodontal diseases and dental caries in adults. Cochrane Database Syst Rev. 2011 Dec 7;(12):CD008829. doi: 10.1002/14651858.CD008829.pub2. Update in: Cochrane Database Syst Rev. 2019 Apr 23;4:CD008829. doi: 10.1002/14651858.CD008829.pub3. PMID: 22161438.
20. Berchier CE, Slot DE, Haps S, Van der Weijden GA. The efficacy of dental floss in addition to a toothbrush on plaque and parameters of gingival inflammation: a systematic review. Int J Dent Hyg. 2008 Nov;6(4):265-79. doi: 10.1111/j.1601-5037.2008.00336.x. PMID: 19138178.
21. Zotti F, Dalessandri D, Salgarello S, Piancino M, Bonetti S, Visconti L, Paganelli C. Usefulness of an app in improving oral hygiene compliance in adolescent orthodontic patients. Angle Orthod. 2016 Jan;86(1):101-7. doi: 10.2319/010915-19.1. Epub 2015 Mar 23. PMID: 25799001; PMCID: PMC8603968.

***Corresponding author:** Jeta Kiseri Kubati. E-mail: jeta.kubati@ubt-uni.net.*

International Journal of Biomedicine 16(2) (2026) 259-265
http://dx.doi.org/10.21103/Article16(2)_OA17

ORIGINAL ARTICLE

INTERNATIONAL JOURNAL OF BIOMEDICINE

Efficacy of Root Canal Chemomechanical Debridement in Patient Pain Perception: From Preoperative Baseline to 48-Hour Follow-Up

Mohammed S. Alzahrani*

Restorative Dental Sciences Department, College of Dentistry, Al-Baha University

Abstract

Background: The primary aim of this study was to evaluate the efficacy of root canal chemomechanical debridement in reducing patient pain from preoperative baseline to 48 hours post-treatment and to identify clinical or demographic predictors of postoperative discomfort.

Materials and Methods: In this prospective clinical study, 92 patients requiring non-surgical root canal treatment were enrolled. Canals were prepared using the ProTaper Gold rotary system and 5.25% sodium hypochlorite irrigation. Patients were randomly assigned to receive either calcium hydroxide intracanal medicament or no medicament. Pain intensity was recorded preoperatively, and at 24 and 48 hours using a 4-point visual analog scale (VAS). Data were analyzed using Spearman's rank correlation, Chi-square, and Wilcoxon signed-rank tests ($P < 0.05$).

A highly significant reduction in pain was observed at both 24 and 48 hours ($P < 0.0001$). Preoperative pain severity showed a strong negative correlation with the magnitude of pain reduction at 48 hours ($\rho = -0.8709$, $P < 0.0001$). Demographic factors (age, gender), tooth type, pulpal/periapical diagnosis, and the use of calcium hydroxide did not significantly influence postoperative pain levels ($P > 0.05$).

Conclusion: Chemomechanical debridement is highly effective for immediate pain resolution, particularly in patients with high baseline symptoms. Postoperative pain is independent of anatomical location or the use of interim medications.(**International Journal of Biomedicine. 2026;16(2):259-265.**)

Keywords: endodontics • postoperative pain • chemomechanical debridement • calcium hydroxide

For citation: Alzahrani MS. Efficacy of Root Canal Chemomechanical Debridement in Patient Pain Perception: From Preoperative Baseline to 48-Hour Follow-Up. International Journal of Biomedicine. 2026;16(2):259-265. doi:10.21103/Article16(2)_OA17

Introduction

The biological rationale for pain resolution in endodontics rests on the effective reduction of the intracanal microbial load and the removal of inflamed or necrotic pulp tissue, which are the main causes of pulpal and periapical pain. In cases of inflamed pulp and/or periapical tissues, the pulp and periapical tissues are characterized by a significant elevation of inflammatory mediators.[1,2] It is often hypothesized that these patients are more prone to sustained postoperative discomfort due to the "central sensitization" of periapical tissues.[3] However, research into whether these preoperative diagnoses act as definitive predictors of postoperative pain remains inconclusive, as clinical outcomes often vary regardless of the initial pulpal state.[4] Root canal treatment (RCT) is a highly predictable procedure aimed at eliminating microbial infection within the root canal system and preventing apical periodontitis.[5] Despite its high success rate (often exceeding 90%), postoperative pain remains a significant concern for both patients and clinicians. Postoperative pain following root canal treatment is a frequent occurrence, with reported prevalence exceeding 50% in many studies, and is largely influenced by factors including the patient's preoperative pain condition, the periapical diagnosis, and the treatment protocol employed.[6,7] The primary causes of this flare-up pain are thought to be the extrusion of infected debris into the periapical tissues and chemical irritation from irrigants or physical pressure.[8,9]

Endodontic treatment may be completed in either a single visit or multiple visits. Multiple-visit endodontic therapy offers several advantages, including enhanced control of infection using intracanal medicaments, improved management of

***Corresponding author**: Mohammed Sarhan Alzahrani. E-mail: m.sarhan@bu.edu.sa*

persistent exudation or symptoms, and the opportunity to monitor healing and patient response between appointments. Yet, the correlation of the incidence of postoperative pain in cases treated with single or multiple visits is inconclusive in many studies.[10,11]

The choice of instrumentation plays a pivotal role in managing these inflammatory responses. The ProTaper Gold rotary system utilizes advanced metallurgy that provides high flexibility and cyclic fatigue resistance, enabling a more centered preparation and more efficient debris removal.[12,13] This is critical because the extrusion of infected debris into the periapical space is one of the triggers for postoperative flare-ups. By combining this mechanical efficiency with the robust proteolytic and antimicrobial properties of 5.25% Sodium Hypochlorite, clinicians can achieve a level of disinfection that significantly shifts the patient's experience toward recovery.[14]

Furthermore, the management of the root canal space between appointments often involves the use of intracanal medicaments. Calcium hydroxide ($Ca(OH)_2$) is widely utilized for its high pH, which aids in neutralizing bacterial by-products and potentially dampening the inflammatory cascade.[15] Despite its theoretical benefits, statistical evidence regarding its ability to reduce immediate postoperative pain compared to empty canals is often inconsistent, suggesting that the quality of the initial biomechanical debridement may be the more significant factor in pain perception.[16]

A unique aspect of this study is the isolation of the biomechanical preparation phase, as no root canal obturation was performed. This allows for an assessment of the "cleaning and shaping" efficacy independent of potential pressure or chemical irritation caused by sealer and gutta-percha placement. The present study was therefore designed to evaluate the short-term effect of Chemomechanical Debridement of the root canal on postoperative pain levels at 24 and 48 hours, and to assess potential correlations between pain changes and procedure, patient- or tooth-specific variables.

Materials and Methods

A random sampling method was employed to select participants from the pool of patients referred to the Endodontic Department at Al-Baha Dental Center. All prospective participants were thoroughly informed about the study's aims, design, and procedures. Written informed consent was obtained from every patient prior to their enrollment in the study. Only adult patients aged 18 years or older who were referred for non-surgical root canal treatment and met the diagnostic criteria for non-surgical root canal treatment were included in this study.

To ensure a homogeneous study group and minimize confounding variables, the following cases were excluded: medically compromised patients, teeth with non-healing prior root canal treatment, teeth with procedural mishaps (e.g., perforations, instrument separation), teeth with an open apex, pregnant patients, teeth exhibiting severe periodontitis, teeth with complex root canal anatomy and teeth with calcified root canals.

The primary outcome variable, pain, was assessed preoperatively and at defined postoperative time points (24 and 48 hours) following completion of root canal biomechanical preparation.

Pain intensity was assessed using a four-point visual pain scale. A score of 1 indicated the absence of pain. A score of 2 represented mild pain, defined as tolerable discomfort that typically does not require analgesic medication. A score of 3 denoted moderate pain, characterized by discomfort generally relieved with analgesics. A score of 4 corresponded to severe pain, defined as intense discomfort that is not adequately controlled by analgesic therapy.

A single examiner performed the clinical follow-up to ensure consistency in the assessment and categorization of post-treatment pain and swelling at the 24-hour and 48-hour checkpoints.

A standardized case record form was employed to systematically collect relevant information for each participant, including demographic characteristics (age and gender), clinical variables (tooth category—anterior, upper premolar, upper molar, lower premolar, or lower molar—pulpal and periradicular diagnoses, and the presence and intensity of preoperative pain), as well as the treatment variable concerning the use or non-use of calcium hydroxide as an intracanal medicament.

The root canal treatment (RCT) procedure was performed under strict aseptic conditions, in accordance with the established standard of care. The tooth and surrounding tissues were thoroughly anesthetized via infiltration and/or nerve block using Xylocaine 2% with Epinephrine 1:100,000. Complete rubber dam isolation was achieved to maintain an aseptic field, prevent microbial contamination from saliva, and protect the patient from irritating irrigating solutions. A standard endodontic access cavity was prepared to allow straight-line access to all root canal orifices. The working length (WL) of each canal was precisely determined using a DentaPort ZX electronic apex locator (MORITA). This measurement was confirmed with a verifying intra-oral periapical radiograph to ensure accuracy. The root canals were prepared (Cleaning and Shaping) using the ProTaper Gold rotary file system according to the manufacturer's instructions in a crown-down technique. During the entire shaping process and as a final rinse, the canals were copiously irrigated with 5.25% Sodium Hypochlorite solution to dissolve organic tissue and disinfect the canal system. Following mechanical preparation and final irrigation, the canals were dried using sterile paper points. Based on the study protocol, the prepared canals were managed in one of two ways:

Intracanal Medication Group: A non-setting calcium hydroxide paste was placed into the canal as an antimicrobial intracanal medicament.

Control Group: The canals were left dry and empty. The canal orifices were covered with a small cotton pellet. A layer of Cavit was then placed over the cotton pellet to provide a secure coronal temporary seal. The occlusion of the treated tooth was checked, and any necessary occlusal adjustments were performed to eliminate premature contacts and reduce biting forces on the temporarily restored tooth, thereby

minimizing postoperative discomfort. For pain management, the patients were instructed to take 400 mg of Ibuprofen if needed.

The post-operative pain intensity was assessed using the visual analog scale (VAS) at 24 and 48 hours after treatment.

Statistical Analysis: All collected data were compiled and analyzed using SPSS Statistics, Version 22.0 (IBM Corp., Armonk, New York, USA). Ordinal statistical methods (Spearman's rank correlation [ρ] and chi-square analysis) were used to evaluate the presence and strength of associations between categorical variables. A *P*-value of ≤ 0.05 was considered statistically significant.

Results

The study population (92 patients) demonstrated profound pain resolution across both postoperative assessment periods, revealing the substantial therapeutic efficacy of endodontic treatment. Preoperatively, the cohort presented with a heavily symptomatic distribution: 43 patients (46.7%) experienced severe pain, representing nearly half of all cases. This high baseline symptomatology reflects the nature of endodontic referrals, where patients typically seek treatment due to symptomatic pulpal pathology requiring urgent intervention.

Table 1 illustrates the relationship between demographic and clinical factors and the intensity of postoperative pain at the 24-hour mark. Neither gender ($P = 0.931$) nor age ($P = 0.121$) showed a significant association with postoperative pain. Notably, all cases of severe pain (n=6) were reported by patients under the age of 40, though this did not reach statistical significance. Tooth category ($P = 0.397$), pulpal diagnosis ($P = 0.282$), and periapical diagnosis ($P = 0.451$) did not significantly influence pain levels. Lower molars and premolars accounted for the highest frequency of severe pain (n=5). There was no significant correlation between preoperative pain levels and 24-hour postoperative pain ($P = 0.314$). Furthermore, the use of calcium hydroxide as an intracanal medicament did not significantly affect pain outcomes ($P = 0.700$), with similar "no pain" rates reported in both the $Ca(OH)_2$ group (52.2%) and the group without it (58.3%).

Table 1.

Relationship between demographic and clinical factors and 24-hour postoperative pain level. after treatment.

		n	Postoperative pain			*P*-value	Spearman's ρ
			Mild	Mod	Sev		
Gender	Male	24	13	4	3	0.931	
	Female	27	12	6	3		
Age	<40 years	26	12	6	6	0.121	
	>40 years	25	13	4	0		
Tooth category	Anterior	7	5	3	0	0.397	
	Upper premolars	13	4	2	1		
	Upper molars	13	6	4	0		
	Lower premolars	6	2	0	2		
	Lower molars	12	8	1	3		
Preoperative pain	No	13	7	4	1	0.314	-0.8341
	Mild	7	3	3	0		
	Moderate	4	5	0	2		
	Severe	27	10	3	3		
Pulp diagnosis	SIP	23	7	4	0	0.282	
	AIP	3	2	0	0		
	N	4	3	0	2		
	PI	21	13	6	4		
Periapical diagnosis	NP	12	3	3	1	0.451	
	SAP	28	12	3	4		
	AAP	6	4	2	0		
	AAA	4	3	0	1		
	CAA	1	3	2	0		
$Ca(OH)_2$	Used	23	13	4	4	0.700	
	Not used	28	12	6	2		

P- value derived from Pearson's chi-square test; Mod, moderate; Sev, severe; SIP, symptomatic irreversible pulpitis; AIP, asymptomatic irreversible pulpitis; N, necrosis; PI, previously initiated; NP, normal periapical tissues; SAP, symptomatic apical periodontitis; AAP, asymptomatic apical periodontitis; AAA, acute apical abscess; CAA, chronic apical abscess.

Table 2.

Relationship between demographic and clinical factors and 48-hour postoperative pain level. after treatment.

		Postoperative pain				*P*-value	Spearman's ρ
		n	Mild	Mod	Sev		
Gender	Male	29	7	7	1	0.929	
	Female	32	8	6	2		
Age	<40 years	31	7	9	3	0.227	
	>40 years	30	8	4	0		
Tooth category	Anterior	11	3	1	0	0.806	
	Upper premolars	15	3	1	1		
	Upper molars	15	3	5	0		
	Lower premolars	6	2	2	0		
	Lower molars	14	4	4	2		
Preoperative pain	No	16	5	3	1	0.098	-0.8709
	Mild	8	2	3	0		
	Moderate	3	5	2	1		
	Severe	34	3	5	1		
Pulp diagnosis	SIP	27	4	3	0	0.368	
	AIP	3	2	0	0		
	N	6	1	1	1		
	PI	25	8	9	2		
Periapical diagnosis	NP	13	4	1	1	0.611	
	SAP	33	6	7	1		
	AAP	6	3	3	0		
	AAA	6	1	0	1		
	CAA	3	1	2	0		
$Ca(OH)_2$	Used	31	7	4	2	0.538	
	Not used	30	8	9	1		

P- value derived from Pearson's chi-square test; Mod, moderate; Sev, severe; SIP, symptomatic irreversible pulpitis; AIP, asymptomatic irreversible pulpitis; N, necrosis; PI, previously initiated; NP, normal periapical tissues; SAP, symptomatic apical periodontitis; AAP, asymptomatic apical periodontitis; AAA, acute apical abscess; CAA, chronic apical abscess.

Table 2 summarizes the relationship between various demographic and clinical factors and the intensity of postoperative pain recorded 48 hours after treatment. Consistent with the 24-hour data, none of the variables examined reached statistical significance ($P<0.05$), indicating that none of these factors were significant predictors of pain intensity at the 48-hour mark. No significant association was found between gender (P = 0.929) or age (P = 0.227) and postoperative pain.

Similar to the 24-hour findings, all reported cases of severe pain (n=3) occurred in patients under the age of 40. Tooth category (P = 0.806), pulpal diagnosis (P = 0.368), and periapical diagnosis (P = 0.611) showed no statistically significant impact on pain levels. Lower molars remained the category with the highest frequency of moderate-to-severe pain. Preoperative pain levels did not significantly influence 48-hour postoperative outcomes (P = 0.098). Notably, the majority of patients presented with severe preoperative pain (34 out of 43) reported "No pain" by the 48-hour mark. The use of $Ca(OH)_2$ did not result in a significant difference in pain outcomes compared with cases without it (P = 0.538). Both groups showed similar rates of being pain-free at 48 hours (70.4% in the "Used" group vs 62.5% in the "Not used" group).

To analyze the change in pain from the preoperative state to the postoperative intervals (24 and 48 hours), a Wilcoxon signed-rank test was used. This test is appropriate for comparing paired ordinal data (e.g., pain levels) within the same group of patients at different times.

Analysis of pain progression over time revealed highly significant clinical improvement following treatment (Table 3 and Figure 1). When comparing preoperative baseline levels to the 24-hour mark, 56 patients experienced improved (lower) pain levels (P < 0.0001). This trend of resolution persisted through the 48-hour mark, with 58 patients reporting improved pain scores compared with their preoperative state (P < 0.0001). While most of the cohort showed immediate relief, a small subset of patients experienced either the same level of discomfort or a temporary worsening of symptoms at 24 hours (19 and 17 patients, respectively) and 48 hours (21 and 13 patients, respectively).

The graphs in Figure 2 illustrate a strong negative correlation between initial pain levels and the degree of pain change after treatment. Spearman's rank correlation revealed ρ = -0.8341 at 24 hours and ρ = -0.8709 at 48 hours (both P < 0.0001), indicating that patients with higher preoperative pain experienced the greatest reductions in symptoms following the procedure.

Table 3.

Comparison of pain level transitions from preoperative baseline to 24 and 48 hours post-treatment.

Time Comparison	Improved (Lower pain)	Same pain	Worsened (Higher pain)	*P*-value
Pre-op vs. 24 hours	56	19	17	<0.0001
Pre-op vs. 48 hours	58	21	13	<0.0001

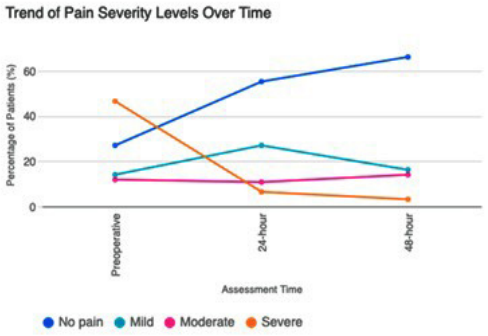

Figure 1. *This line graph illustrates the percentage of patients experiencing various pain intensities (No pain, Mild, Moderate, Severe) across three assessment intervals: Preoperative, 24-hour, and 48-hour postoperative. A significant upward trend is observed in the "No pain" category, while "Severe" pain shows a sharp decline following treatment, confirming the procedure's overall clinical efficacy (P < 0.0001).*

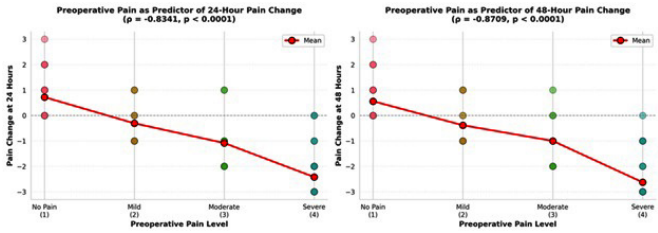

Figure 2. *Scatter plots with mean regression lines showing the relationship between baseline pain severity and subsequent pain level changes.*

Discussion

The primary objective of this study was to determine the patients' pain perception before and after biomechanical preparation of the root canal system. The results demonstrated a clear, clinically significant trend toward overall pain reduction in the sample studied (n=92). At 24 hours, 55.4% of patients reported an improvement in pain, and this figure rose to 63.04% at 48 hours, with a mean pain change of -1.25 on the scale. Furthermore, the most the most clinically important finding of this study is the strong negative correlation between preoperative pain severity and the magnitude of pain reduction following treatment. At 24-hour post-treatment, this correlation reached ρ = -0.8341 (P < 0.0001) and strengthened further to ρ = -0.8709 (P < 0.0001) at 48 hours. These are extraordinarily strong correlations in biomedical research, indicating a robust and highly statistically significant relationship. The negative direction means that patients presenting with the highest preoperative pain experienced the greatest absolute reduction in pain following treatment—a counterintuitive but clinically profound finding. This overall positive outcome aligns with the established efficacy of standard root canal procedures, which, through mechanical debridement and disinfection, successfully remove the primary cause of inflammation—the microbial load and high levels of endotoxins, thereby

relieving pressure and chemical irritation.[17] This finding has profound implications for patient counseling and expectations management. A patient presenting severe pulpal pain should be informed that endodontic treatment will likely provide substantial and rapid pain relief, with the expectation of achieving no pain or minimal discomfort within 24-48 hours. Conversely, a patient requiring elective endodontic treatment despite minimal or no symptoms should be counseled that the procedure itself may produce postoperative discomfort, even though no preoperative pain existed. The extraordinary strength of this correlation (ρ = -0.87) makes it one of the most predictive relationships in the entire dataset, far outweighing the weak associations observed with anatomical or demographic variables.

Pulpal diagnosis showed no correlation with postoperative pain outcomes, as previously reported by Harrison et al.[18] Yet this finding contrasts sharply with the previous study by Segura-Egea et al.,[19] which identified pulpal diagnosis as a significant predictor. Furthermore, these results challenge the hypothesis that patients diagnosed with symptomatic irreversible pulpitis exhibit an increased propensity for prolonged postoperative pain. Conventional theories suggest that such cases involve an elevated release of inflammatory mediators and neuropeptides—specifically Substance P and Calcitonin Gene-Related Peptide—into the periapical tissues, potentially leading to persistent discomfort despite comprehensive chemomechanical debridement. This suggests that other factors—potentially including operator technique, individual inflammatory response capacity, and psychological pain perception—are more influential than the pulpal diagnosis category.

Periapical diagnosis, representing the extent or severity of apical pathology visible radiographically, showed no significant correlation with postoperative pain at either assessment time point. These results indicate that the radiographic appearance of periapical pathology—traditionally considered indicative of the chronicity and severity of apical inflammation—does not meaningfully predict the acute postoperative pain response.[20] This finding suggests a dissociation between the chronic periapical inflammatory burden and the acute inflammatory response generated by endodontic instrumentation. A patient with extensive apical lesions may experience minimal postoperative pain, while a patient with minimal periapical findings might experience substantial discomfort. This emphasizes that postoperative pain is driven by acute procedural inflammation rather than by the pre-existing chronic pathological burden.

Demographic characteristics of the patient population demonstrated complete independence from postoperative pain outcomes. Whether a patient was in their twenties or their seventies, endodontic postoperative pain was equally likely or unlikely. Similarly, patient sex showed no significant association with postoperative pain levels. This finding supports the principle of sex-neutral clinical care for endodontic treatment and suggests that clinical decision-making regarding pain management should not be predicated on patient sex. This finding contrasts with some clinical assumptions about sex and age-related pain sensitivity and suggests that biological age does not fundamentally alter the postoperative pain response to endodontic treatment.2[1]While preoperative pain severity is an extraordinary predictor of pain reduction (as discussed previously), it surprisingly does not predict the absolute magnitude of postoperative pain itself. Spearman's ρ between preoperative and postoperative pain levels were -0.8341 at 24 hours and -0.8709 at 48 hours (both $P < 0.0001$), indicating that patients with higher preoperative pain experienced the greatest reductions in symptoms following the procedure. This apparent paradox reveals important information about the distribution of outcomes..

The explanation lies in the ceiling and floor effects of the ordinal scale. Patients who present with severe preoperative pain (category 4) experience large reductions but often end at no pain (category 1), while patients who present with no preoperative pain (category 1) experience small increases and may remain at mild pain (category 2). The absolute postoperative pain values thus converge toward the middle-to-lower range regardless of starting point. A patient with severe preoperative pain and another with mild preoperative pain may both achieve no pain by 24 hours, resulting in identical postoperative values despite markedly different pain trajectories. This demonstrates why examining pain change rather than absolute postoperative pain is more informative for understanding treatment effects—the clinical reality is that endodontic treatment benefits patients across the spectrum of preoperative severity, but with different magnitudes of change.

Despite widespread clinical use of calcium hydroxide as an interim dressing between appointments, the analysis revealed no significant correlation between dressing application and postoperative pain levels. These findings suggest that calcium hydroxide dressing does not substantially mitigate postoperative pain in this patient population. This suggests that while the entire treatment protocol effectively reduces pain, the specific use of $CaOH_2$ as the medicament may not be the overriding factor influencing immediate pain relief compared to other variables. This is consistent with studies suggesting that the major decrease in pain after the first visit is attributable to thorough instrumentation and irrigation, which drastically reduce intracanal pressure and endotoxin levels, rather than the subsequent action of the medicament over the short 48-hour period.[20] While the most dramatic pain changes occur in this window, the full antimicrobial and tissue-healing benefits of $CaOH_2$ may require a longer duration,[22] especially in promoting the healing of periapical lesions.

The anatomical location or number of the treated tooth demonstrated no significant correlation with postoperative pain levels. This finding contradicts potential clinical assumptions that anterior teeth might experience different postoperative pain than posterior teeth, or that teeth in different positions might have varying pain propensities due to biomechanical or vascular differences.[23] The null finding regarding tooth position emphasizes that postoperative pain is determined by patient and procedure factors rather than anatomical location. Whether treatment involved an anterior

incisor or a posterior molar, postoperative pain patterns were statistically indistinguishable. This suggests that clinicians can apply consistent pain management protocols across all tooth positions without the need for location-specific modifications based solely on anatomical considerations.

A limitation of this study is the short, 48-hour follow-up period. Future research should utilize a randomized controlled design with a standardized placebo group and extend the observation period.

Conclusion

Root canal chemomechanical debridement provides statistically significant pain reduction within 24 to 48 hours. The procedure is most effective for patients presenting with severe preoperative pain. Clinical variables, including tooth location and intracanal medicaments, do not significantly influence short-term pain perception.

Ethics Statement

This study adhered to the ethical guidelines established by the Declaration of Helsinki and was formally approved by the Research and Ethics Committee of Al-Baha University under the reference number [74110179].

Author Contribution Statement

Mohammed S. Alzahrani confirms sole responsibility for all aspects of the research.

Conflicts of Interest

The author has declared no conflict of interest.

References

1. Hirsch V, Wolgin M, Mitronin AV, Kielbassa AM. Inflammatory cytokines in normal and irreversibly inflamed pulps: A systematic review. Arch Oral Biol. 2017 Oct;82:38-46. doi: 10.1016/j.archoralbio.2017.05.008. Epub 2017 Jun 1. PMID: 28600966.
2. Galler KM, Weber M, Korkmaz Y, Widbiller M, Feuerer M. Inflammatory Response Mechanisms of the Dentine-Pulp Complex and the Periapical Tissues. Int J Mol Sci. 2021 Feb 2;22(3):1480. doi: 10.3390/ijms22031480. PMID: 33540711; PMCID: PMC7867227.
3. Owatz CB, Khan AA, Schindler WG, Schwartz SA, Keiser K, Hargreaves KM. The incidence of mechanical allodynia in patients with irreversible pulpitis. J Endod. 2007 May;33(5):552-6. doi: 10.1016/j.joen.2007.01.023. Epub 2007 Mar 6. PMID: 17437870.
4. Ng YL, Mann V, Gulabivala K. A prospective study of the factors affecting outcomes of nonsurgical root canal treatment: part 1: periapical health. Int Endod J. 2011 Jul;44(7):583-609. doi: 10.1111/j.1365-2591.2011.01872.x. Epub 2011 Mar 2. PMID: 21366626.
5. Sjögren U, Figdor D, Persson S, Sundqvist G. Influence of infection at the time of root filling on the outcome of endodontic treatment of teeth with apical periodontitis. Int Endod J. 1997 Sep;30(5):297-306. doi: 10.1046/j.1365-2591.1997.00092.x. Erratum in: Int Endod J 1998 Mar;31(2):148. PMID: 9477818.
6. Glennon JP, Ng YL, Setchell DJ, Gulabivala K. Prevalence of and factors affecting postpreparation pain in patients undergoing two-visit root canal treatment. Int Endod J. 2004 Jan;37(1):29-37. doi: 10.1111/j.1365-2591.2004.00748.x. PMID: 14718054.
7. Oliveira PS, Ferreira MC, Paula NGN, Loguercio AD, Grazziotin-Soares R, da Silva GR, da Mata HCS, Bauer J, Carvalho CN. Postoperative Pain Following Root Canal Instrumentation Using ProTaper Next or Reciproc in Asymptomatic Molars: A Randomized Controlled Single-Blind Clinical Trial. J Clin Med. 2022 Jul 1;11(13):3816. doi: 10.3390/jcm11133816. PMID: 35807101; PMCID: PMC9267392.
8. Nair PN. Pathogenesis of apical periodontitis and the causes of endodontic failures. Crit Rev Oral Biol Med. 2004 Nov 1;15(6):348-81. doi: 10.1177/154411130401500604. PMID: 15574679.
9. Siqueira JF Jr. Microbial causes of endodontic flare-ups. Int Endod J. 2003 Jul;36(7):453-63. doi: 10.1046/j.1365-2591.2003.00671.x. PMID: 12823700.
10. Chaitanya M, Bhawalkar A, Bagchi A, Divyatammana, Shetty A, Chohan H, Mustafa M. Comparative Analysis of Post-operative Pain Relief and Healing Outcomes between Single-Visit and Multiple-Visit Root Canal Therapy: A Tertiary Care Study. J Pharm Bioallied Sci. 2024 Jul;16(Suppl 3):S2388-S2390. doi: 10.4103/jpbs.jpbs_281_24. Epub 2024 Jun 7. PMID: 39346224; PMCID: PMC11426698.
11. Mirza MB, Cherukuri P, Mathew T, Bagewadi N, Krishna VV, Chohan H, Thakkar R. Evaluation of Post-Operative Pain and Healing in Single-Visit versus Multiple-Visit Root Canal Therapy. J Pharm Bioallied Sci. 2024 Jul;16(Suppl 3):S2381-S2384. doi: 10.4103/jpbs.jpbs_278_24. Epub 2024 Jul 31. PMID: 39346385; PMCID: PMC11426807.
12. Uygun AD, Kol E, Topcu MK, Seckin F, Ersoy I, Tanriver M. Variations in cyclic fatigue resistance among ProTaper Gold, ProTaper Next and ProTaper Universal instruments at different levels. Int Endod J. 2016 May;49(5):494-9. doi: 10.1111/iej.12471. Epub 2015 Jun 5. PMID: 26011308.
13. Alhayki MM, Eid B, Elemam R, Elsewify T. Evaluation of Apically Extruded Debris During Root Canal Preparation Using ProTaper Ultimate and ProTaper Gold: An Ex Vivo Study. Eur Endod J. 2025 Jan;10(1):41-46. doi: 10.14744/eej.2024.43650. PMID: 40145483; PMCID: PMC11971712.
14. Usta SN, Solana C, Ruiz-Linares M, Baca P, Ferrer-Luque CM, Cabeo M, Arias-Moliz MT. Effectiveness of conservative instrumentation in root canal disinfection. Clin Oral Investig. 2023 Jun;27(6):3181-3188. doi: 10.1007/s00784-023-04929-z. Epub 2023 Mar 3. PMID: 36867258; PMCID: PMC10264279.
15. Mohammadi Z, Dummer PM. Properties and applications of calcium hydroxide in endodontics and dental traumatology. Int Endod J. 2011 Aug;44(8):697-730. doi: 10.1111/j.1365-2591.2011.01886.x. Epub 2011 May 2. PMID: 21535021.
16. Ahmad MZ, Sadaf D, Merdad KA, Almohaimeed

A, Onakpoya IJ. Calcium hydroxide as an intracanal medication for postoperative pain during primary root canal therapy: A systematic review and meta-analysis with trial sequential analysis of randomised controlled trials. J Evid Based Dent Pract. 2022 Mar;22(1):101680. doi: 10.1016/j.jebdp.2021.101680. Epub 2021 Dec 3. PMID: 35219466.

17. Vianna ME, Horz HP, Conrads G, Zaia AA, Souza-Filho FJ, Gomes BP. Effect of root canal procedures on endotoxins and endodontic pathogens. Oral Microbiol Immunol. 2007 Dec;22(6):411-8. doi: 10.1111/j.1399-302X.2007.00379.x. PMID: 17949345.

18. Harrison JW, Gaumgartner JC, Svec TA. Incidence of pain associated with clinical factors during and after root canal therapy. Part 1. Interappointment pain. J Endod. 1983 Sep;9(9):384-7. doi: 10.1016/s0099-2399(83)80190-3. PMID: 6579198.

19. Segura-Egea JJ, Cisneros-Cabello R, Llamas-Carreras JM, Velasco-Ortega E. Pain associated with root canal treatment. Int Endod J. 2009 Jul;42(7):614-20. doi: 10.1111/j.1365-2591.2009.01562.x. Epub 2009 May 8. PMID: 19467050.

20. Walton RE. Interappointment flare-ups: incidence, related factors, prevention, and management. Endod Topics. 2002;3(1):67–76. doi:10.1034/j.1601-1546.2002.30107.x

21. Nair M, Rahul J, Devadathan A, Mathew J. Incidence of Endodontic Flare-ups and Its Related Factors: A Retrospective Study. J Int Soc Prev Community Dent. 2017 Jul-Aug;7(4):175-179. doi: 10.4103/jispcd.JISPCD_61_17. Epub 2017 Jul 31. PMID: 28852632; PMCID: PMC5558250.

22. Estrela C, Pimenta FC, Ito IY, Bammann LL. Antimicrobial evaluation of calcium hydroxide in infected dentinal tubules. J Endod. 1999 Jun;25(6):416-8. doi: 10.1016/S0099-2399(99)80269-6. PMID: 10530241.

23. Shresha R , Shrestha D , Kayastha R . Post-Operative Pain and Associated Factors in Patients Undergoing Single Visit Root Canal Treatment on Teeth with Vital Pulp. Kathmandu Univ Med J (KUMJ). 2018 Apr-Jun;16(62):220-223. PMID: 30636751.

International Journal of Biomedicine 16(2) (2026) 266-269
http://dx.doi.org/10.21103/Article16(2)_CR1

CASE REPORT

INTERNATIONAL JOURNAL OF BIOMEDICINE

Giant Cell Arteritis Case with Low Inflammatory Markers: A Case Report

Abdulrahman Ali M. Khormi[1*]

[1]*Department of Internal medicine, College of Medicine, Prince Sattam bin Abdulaziz University, Al-Kharj, KSA*

Abstract

Giant cell arteritis (GCA), or temporal arteritis, is a common disease of senior age. GCA requires an early diagnosis to avoid serious disability and morbidity in the elderly population. Laboratory findings include elevated ESR and C-reactive protein. However, ESR may be normal in some biopsy-proven cases of GCA. Herein, we report the case of a 57-year-old woman with diabetes mellitus and hypertension who presented with a two-month history of progressive, painless visual loss in the right eye, associated with headache, shoulder girdle pain, and mild morning stiffness. Ophthalmologic evaluation raised concern for arteritic anterior ischemic optic neuropathy (AAION). Despite strong clinical suspicion, laboratory investigations revealed normal ESR and CRP levels prior to glucocorticoid exposure. Temporal artery ultrasound demonstrated subtle wall thickening with a perivascular halo sign involving the right temporal artery, consistent with temporal arteritis. The patient declined a temporal artery biopsy. Empirical high-dose oral glucocorticoid therapy was initiated due to the imminent risk of permanent visual loss, resulting in significant clinical improvement of vision. Given concerns regarding long-term steroid toxicity, particularly poor glycemic control, steroid-sparing therapy with tocilizumab was considered.

This case highlights that GCA may present with normal inflammatory markers and emphasizes the importance of maintaining a high index of clinical suspicion. Normal ESR and CRP values should not delay treatment in patients with compatible clinical and imaging findings, as prompt intervention is critical to prevent irreversible complications.(**International Journal of Biomedicine. 2026;16(2):266-269.**)

Keywords: giant cell arteritis • temporal arteritis • inflammatory markers • diagnosis • vasculitis

For citation: Khormi AAM. Giant Cell Arteritis Case with Low Inflammatory Markers: A Case Report. International Journal of Biomedicine. 2026;16(2):266-269. doi:10.21103/Article16(2)_CR1

Abbreviations

AAION, arteritic anterior ischemic optic neuropathy; **CRP**, C-reactive protein; **ESR**, erythrocyte sedimentation rate; **GCA**, giant cell arteritis; **PMR**, polymyalgia rheumatica; **TAB**, temporal artery biopsy.

Introduction

Temporal arteritis, or giant cell arteritis (GCA), is the most common vasculitis in older adults. The prevalence of the disease is around 0.2% in patients over the age of 50. It is an important cause of morbidity. Irreversible visual loss is the most feared complication of GCA, affecting approximately 20% of cases. The clinical presentation is diverse, and the signs and symptoms are typically caused by ischemia in the territory of the superficial temporal artery (STA) or any of its branches. GCA's neurological manifestations include neuropathies, strokes, and neuro-rheumatological manifestations such as hearing loss and vertigo. Abnormal laboratory findings, such as elevated ESR and C-reactive protein, are quite common. Nonetheless, inflammatory markers may be normal in some biopsy-proven cases of GCA.[1-5]

Polymyalgia rheumatica (PMR) is another rheumatological disease marked by joint arthralgias, morning stiffness, elevated ESR, and a dramatic response to low-dose steroids. These two conditions are associated. PMR affects approximately 60% of GCA cases.[1,6]

***Corresponding author:** Dr. Abdulrahman Ali M Khormi. E-mail: isameldin2015@gmail.com*

Herein, we describe one case of GCA with positive clinical and radiological findings but normal inflammatory markers.

Case Presentation

A 57-year-old woman with diabetes and hypertension takes oral medications but does not adhere to the treatment regimen.She presented with a two-month history of gradual but progressive painless loss of vision in her right eye associated with pain in the shoulder joints and headache. She had mild early morning stiffness with an undocumented fever but no associated weight loss. She was seen by her ophthalmologist, who noted pallor and swelling of the optic nerves, and expressed concern for arteritic anterior ischemic optic neuropathy (AAION) associated with temporal arteritis.

The patient's visual acuity was counting fingers (CF). She was referred to neurology and rheumatology clinics, and after careful clinical evaluation, giant cell arteritis was suspected, and Laboratory tests were sent. Additionally, a vascular ultrasound was ordered to evaluate the temporal artery. The possibility of polymyalgia rheumatica (PMR) was also considered. Meanwhile, oral prednisolone at a dose of 40 mg was initiated because of high clinical suspicion and the risk to her vision. Interestingly, laboratory results showed normal ESR and CRP levels despite the patient not having started any steroid or immunosuppressive treatment yet. That raised a concern about the accuracy of the diagnosis, and the patient was sent back to the ophthalmologist to assess for other diagnoses like glaucoma and diabetic neuropathy. The right temporal artery ultrasound performed by an experienced radiologist showed subtle wall thickening with a mild perivascular halo sign at the distal aspect of the right temporal artery. The lumen appears narrowed but patent. Peak systolic velocity was 28 cm/second. The temporal artery diameter measures 1.9 mm, and the wall thickness measures 0.7 mm. Features are suggestive of right temporal arteritis (Figure 1).

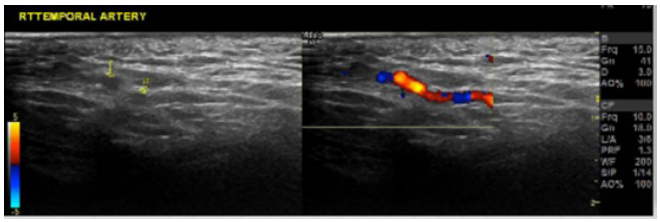

Figure 1. *Color Doppler (right panel). Color flow is present within the lumen, confirming the structure is an artery. The lumen appears narrowed but patent, which is typical in GCA. Flow may look irregular due to luminal compression by the inflamed wall. Halo sign is the circumferential, homogeneous hypoechoic (dark) thickening of the arterial wall. This image shows a right temporal artery ultrasound with a positive halo sign, consistent with active giant cell arteritis (temporal arteritis).*

The patient declined to undergo a temporal artery biopsy (TAB). Diagnosis of GCA was very likely, and the decision was made to continue oral steroids with careful, slow tapering. The patient responded to oral steroids, and her vision improved after a few weeks. Follow-up ophthalmology examination showed visual acuity 20/200. She was given a follow-up appointment. Other alternative treatments, like tocilizumab, were considered to avoid unwanted long-term steroid side effects like high blood sugar readings. The patient was referred to another hospital, where she is eligible for biologic treatment, and further follow-up will be more convenient for her.

Discussion

Giant cell arteritis, also known as temporal arteritis, is the most common vasculitis in older adults, and its incidence increases proportionally with age. The 2022 American College of Rheumatology (ACR)/European Alliance of Associations for Rheumatology (EULAR) classification criteria for Giant Cell Arteritis (GCA) require patients to be at least 50 years old at the time of diagnosis as an absolute requirement. The criteria is based on scoring system items and weights were as follows: positive temporal artery biopsy or temporal artery halo sign on ultrasound (+5); erythrocyte sedimentation rate ≥50 mm/hour or C reactive protein ≥10 mg/L (+3); sudden visual loss (+3); morning stiffness in shoulders or neck, jaw or tongue claudication, new temporal headache, scalp tenderness, temporal artery abnormality on vascular examination, bilateral axillary involvement on imaging and fluorodeoxyglucose positron emission tomography (FDG-PET))activity throughout the aorta (+2 each).

A patient could be classified as a GCA case if the cumulative score is ≥6 points. Complications of this illness include AAION, ischemic damage to the visual axis, and stroke. Aortic dissection and aneurysms might require emergency interventions.[1,7] The exact etiology of the disease is unknown, but multiple genetic and environmental factors are associated with the disease. Inflammation of medium- and large-sized arteries arising from the aortic arch is the primary pathogenic characteristic of GCA. Both innate and adaptive immune system cells are important in the pathophysiology of GCA because they contribute to the formation of granulomas that may include giant cells, a hallmark of the disease. Activation of vascular dendritic cells and T lymphocytes plays an essential role in disease pathogenesis. A positive biopsy gives the doctor the confidence to carry on with the aggressive steroid therapy that is necessary in this case. Histopathological sampling and study must be done diligently. A positive TAB is the gold standard for diagnosing GCA, but its sensitivity ranges from ~70% to >90%. A negative biopsy does not rule out GCA, as false-negative results of TAB may occur due to Skip lesions. GCA typically responds to steroids at a daily dose of 40-60 mg, and treatment should begin as soon as the diagnosis is suspected. There is no justification for delaying treatment pending biopsy because histopathology shows no significant change within the first two weeks of steroid administration. Tocilizumab demonstrated clinical efficacy as a glucocorticoid-sparing medication and was helpful for patients prone to developing complications from glucocorticoids. Other options are methotrexate and abatacept.[1,7-9]

Giant cell arteritis with a normal ESR and/or normal CRP level is rare but has been described in many cases of

this disease (Table 1). A study by Kermani et al. included 764 patients (65% women) who underwent TAB. Biopsy was consistent with GCA in 177 patients (23%). Seven patients (4%) with a positive TAB for GCA had a normal ESR and CRP at diagnosis. It showed that the sensitivity of CRP is 86.9% and of ESR is 84.1%. Compared with GCA patients with elevated markers of inflammation, a greater proportion of these patients had polymyalgia rheumatica symptoms, whereas constitutional symptoms, anemia, and thrombocytosis, are less often. Neither the ESR nor the CRP is a specific biomarker for GCA, and they might be normal in GCA. Normal values do not exclude the diagnosis in an appropriate clinical setting, nor do marked elevations certify that a diagnosis of GCA is correct.[10-12]

Recent work in Egyptian cohorts underscores the spectrum of GCA and its overlap with polymyalgia rheumatica, including the utility of imaging in early detection and monitoring of disease activity in diverse clinical settings. Routine screening and comprehensive assessment are recommended to reduce the risk of delayed diagnosis and complications.[13,14]

Table 1 compares three similar cases with low ESR and CRP values and presents the results of the present case in comparison with them.[15-17]

Table 1.

Three GCA cases with low ESR and CRP values.

Case	Age/Sex	ESR / CRP	Key Features	Reference
Case 1	75/Female	Normal ESR & CRP	Occult GCA, cranial symptoms, biopsy-proven	Poole et al., Eye (Lond). 2003 [15]
Case 2	72/Female	Normal ESR & CRP	Biopsy- and ultrasound-proven GCA, AION	Martins et al., Clin Rheumatol. 2020 [16]
Case 3	68/Male	ESR 15mm/hr, near-normal CRP	Atypical presentation, biopsy-proven GCA	Singh R et al. BMJ Case Rep. 2018 [17]
Current case	60/female	Normal ESR &CRP	Positive halo sign on temporal artery ultrasound	Present case

Conclusion

Giant cell arteritis must be diagnosed early to prevent serious disability and morbidity in the elderly population. While TAB remains the gold standard for diagnosing GCA, it is an invasive procedure with associated risks and limited reliability due to sampling variability. Normal ESR and CRP values should not delay treatment in patients with compatible clinical and imaging findings, as prompt intervention is critical to prevent irreversible complications.

Author Contribution Statement

Abdulrahman Ali M. Khormi confirms sole responsibility for all aspects of the research.

Conflict of Interest

The author declares that he has no known competing interests.

Acknowledgements

The author is grateful to the Deanship of Scientific Research, Prince Sattam bin Abdulaziz University, Al-Kharj, Saudi Arabia, for its support and encouragement in conducting the research and publishing this report.

References

1. Laldinpuii J, Sanchetee P, Borah AL, Ghose M, Borah NC. Giant cell arteritis (temporal arteritis): A report of four cases from north east India. Ann Indian Acad Neurol. 2008 Jul;11(3):185-9. doi: 10.4103/0972-2327.42940. PMID: 19893667; PMCID: PMC2771971.
2. Lawrence RC, Helmick CG, Arnett FC, Deyo RA, Felson DT, Giannini EH, et al. Estimates of the prevalence of arthritis and selected musculoskeletal disorders in the United States. Arthritis Rheum. 1998 May;41(5):778-99. doi: 10.1002/1529-0131(199805)41:5<778::AID-ART4>3.0.CO;2-V. PMID: 9588729.
3. Salvarani C, Gabriel SE, O'Fallon WM, Hunder GG. The incidence of giant cell arteritis in Olmsted County, Minnesota: apparent fluctuations in a cyclic pattern. Ann Intern Med. 1995 Aug 1;123(3):192-4. doi: 10.7326/0003-4819-123-3-199508010-00006. PMID: 7598301.
4. Mesquita-Filho PM, Manzato LB, Varela DL, Rodrigues R , Padua WL, et al. Giant Cell Arteritis – A Case Report., Revista Brasileira de Análises Clínicas. 2022;54(3). DOI: 10.21877/2448-3877.202200047
5. Aiello PD, Trautmann JC, McPhee TJ, Kunselman AR, Hunder GG. Visual prognosis in giant cell arteritis. Ophthalmology. 1993 Apr;100(4):550-5. doi: 10.1016/s0161-6420(93)31608-8. PMID: 8479714.
6. Salvarani C, Cantini F, Boiardi L, Hunder GG. Polymyalgia rheumatica and giant-cell arteritis. N Engl J Med. 2002 Jul 25;347(4):261-71. doi: 10.1056/NEJMra011913. PMID: 12140303.
7. Ponte C, Grayson PC, Robson JC, Suppiah R, Gribbons KB, Judge A, et al.; DCVAS Study Group. 2022 American College of Rheumatology/EULAR classification criteria for giant cell arteritis. Ann Rheum Dis. 2022 Dec;81(12):1647-1653. doi: 10.1136/ard-2022-223480. Epub 2022 Nov 9. Erratum in: Ann Rheum Dis. 2023 Feb;82(2):e52. doi: 10.1136/annrheumdis-2022-223480corr1. PMID: 36351706.
8. Achkar AA, Lie JT, Hunder GG, O'Fallon WM, Gabriel SE. How does previous corticosteroid treatment affect the biopsy findings in giant cell (temporal) arteritis? Ann Intern Med. 1994 Jun 15;120(12):987-92. doi: 10.7326/0003-4819-120-12-199406150-00003. PMID: 8185147.
9. Dejaco C, Duftner C, Buttgereit F, Matteson EL, Dasgupta B. The spectrum of giant cell arteritis and polymyalgia rheumatica: revisiting the concept of the disease. Rheumatology (Oxford). 2017 Apr 1;56(4):506-515. doi: 10.1093/rheumatology/kew273. PMID: 27481272.
10. Martínez-Taboada VM, Blanco R, Armona J, Uriarte E,

Figueroa M, Gonzalez-Gay MA, Rodriguez-Valverde V. Giant cell arteritis with an erythrocyte sedimentation rate lower than 50. Clin Rheumatol. 2000;19(1):73-5. doi: 10.1007/s100670050017. PMID: 10752506.
11. Crain MA, Lakhani DA, Winkler L, Adelanwa A, Kim C. Giant cell arteritis: A case report and review of literature. Radiol Case Rep. 2021 Oct 2;16(12):3734-3738. doi: 10.1016/j.radcr.2021.08.072. PMID: 34630809; PMCID: PMC8493503.
12. Kermani TA, Schmidt J, Crowson CS, Ytterberg SR, Hunder GG, Matteson EL, Warrington KJ. Utility of erythrocyte sedimentation rate and C-reactive protein for the diagnosis of giant cell arteritis. Semin Arthritis Rheum. 2012 Jun;41(6):866-71. doi: 10.1016/j.semarthrit.2011.10.005. Epub 2011 Nov 25. PMID: 22119103; PMCID: PMC3307891.
13. El Miedany Y, El Gaafary M, Toth M, et al. The spectrum of giant cell arteritis and polymyalgia rheumatica: a longitudinal prospective study to assess for subclinical giant cell arteritis in new onset polymyalgia rheumatica. Egypt Rheumatol Rehabil. 2025;52:7. doi:10.1186/s43166-025-00307-7
14. El Miedany Y, El Gaafary M, Toth M, et al. Step forward towards treat-to-target management of giant cell arteritis: patients stratification aiming to targeted remission – updated guidelines. Egypt Rheumatol Rehabil. 2024;51:5. doi:10.1186/s43166-024-00237-w
15. Poole TR, Graham EM, Lucas SB. Giant cell arteritis with a normal ESR and CRP. Eye (Lond). 2003 Jan;17(1):92-3. doi: 10.1038/sj.eye.6700240. PMID: 12579178.
16. Martins P, Teixeira V, Teixeira FJ, Canastro M, Palha A, Fonseca JE, Ponte C. Giant cell arteritis with normal inflammatory markers: case report and review of the literature. Clin Rheumatol. 2020 Oct;39(10):3115-3125. doi: 10.1007/s10067-020-05116-1. Epub 2020 May 29. PMID: 32472460.
17. Singh R, Sahbudin I, Filer A. New headaches with normal inflammatory markers: an early atypical presentation of giant cell arteritis. BMJ Case Rep. 2018 Jun 27;2018:bcr2017223240. doi: 10.1136/bcr-2017-223240. PMID: 29950495; PMCID: PMC6040475.

International Journal of Biomedicine 16(2) (2026) 270-273
http://dx.doi.org/10.21103/Article16(2)_CR2

CASE REPORT

INTERNATIONAL JOURNAL OF BIOMEDICINE

Carotid Web in Elderly Patient with Recurrent Ischemic Stroke: A Case Report

Adel Alzahrani[1*], Faisal Alghamdi[1], Meshari Alzahrani[1], Jumanah Ardawi[1], Fatima Altalhi[1], Mahammad Bokhary[1], Mohammad Shebly[1]

[1]*Department of Radiology and Medical Imaging, King Abdullah Medical City, Makkah, Saudi Arabia*

Abstract

Background: A carotid web is a focal, shelf-like fibroelastic intimal protrusion in the proximal internal carotid artery, regarded as a variant of intimal fibromuscular dysplasia. It disrupts normal laminar flow, creating areas of stasis that predispose to thrombus formation and distal embolization, and is increasingly recognised as a cause of cryptogenic ischemic stroke, particularly in young and middle-aged adults without conventional vascular risk factors.

Case Presentation: A 61-year-old male with multiple vascular risk factors and a history of right-sided ischemic stroke who presented with recurrent transient left-sided weakness. CT angiography was limited by motion artefact, preventing accurate assessment. Subsequent duplex ultrasound revealed a characteristic echogenic shelf-like projection at the posterior wall of the right carotid bulb consistent with a carotid web. In view of recurrent ischemic symptoms, the patient underwent successful carotid artery stenting with restoration of normal flow dynamics.

Conclusion: This case emphasises the importance of multimodality vascular imaging and heightened clinical suspicion for carotid web in patients presenting with recurrent embolic events and minimal atherosclerosis. Early recognition and definitive intervention are essential to prevent recurrent cerebrovascular episodes.(**International Journal of Biomedicine. 2026;16(2):270-273.**)

Keywords: carotid web • embolic stroke • carotid artery stenting • duplex ultrasound • CT angiography • fibromuscular dysplasia

For citation: Alzahrani A, Alghamdi F, Alzahrani M, Ardawi J, Altalhi F, Bokhary M, Shebly M. Carotid Web in Elderly Patient with Recurrent Ischemic Stroke: A Case Report. International Journal of Biomedicine. 2026;16(2):270-273. doi:10.21103/Article16(2)_CR2

Introduction

Carotid web is a rare, focal intimal variant of fibromuscular dysplasia (FMD) that predominantly involves the proximal internal carotid artery at the carotid bulb. Morphologically, it is characterized by a thin, shelf-like membranous projection that extends into the arterial lumen. Histopathologically, carotid webs are characterized as a distinct, non-atherosclerotic vascular pathology consisting of focal fibroelastic thickening of the arterial intima. Although uncommon, carotid webs are increasingly recognized as an etiology of cryptogenic and recurrent embolic ischemic strokes, particularly in younger adults and in patients lacking conventional cardiovascular risk factors.[1,2]

***Corresponding author:** Adel Alzahrani. E-mail: adel.alzahrani14@alumni.imperial.ac.uk*

The pathophysiological mechanism underlying stroke in carotid webs is primarily artery-to-artery thromboembolism. The protruding intimal shelf alters normal laminar flow, generating localized regions of flow separation, low shear stress, and blood stasis, which predispose to thrombus formation on the web surface. Embolization of these thrombi can result in distal cerebral ischemia, often leading to recurrent strokes in the ipsilateral vascular territory. Unlike atherosclerotic stenosis, carotid webs frequently cause ischemic events without significant luminal narrowing, highlighting the importance of flow dynamics rather than occlusion per se in their clinical significance.[3]

Despite growing awareness, carotid web remains underdiagnosed, partly because of its subtle radiologic appearance and potential to be misinterpreted as a noncalcified atherosclerotic plaque, intimal dissection, or intraluminal thrombus. The development and widespread use of high-resolution imaging modalities, including computed tomography

angiography (CTA), magnetic resonance angiography (MRA), and duplex ultrasonography, have significantly improved the detection and characterization of these lesions.[4] CTA, in particular, provides excellent spatial resolution and allows visualization of the thin, membranous shelf that defines the web, while duplex ultrasonography can detect hemodynamic disturbances and intimal protrusions.

Management of carotid web remains controversial, with options ranging from antiplatelet therapy for secondary stroke prevention to surgical or endovascular interventions. Carotid endarterectomy (CEA) and carotid artery stenting (CAS) have been reported as effective strategies, particularly in patients with recurrent ischemic events despite medical therapy. Long-term outcomes remain under investigation, and consensus guidelines for management are lacking due to the rarity of the condition and the limited number of available studies.[5,6]

Herein, we report a case of a 61-year-old man with recurrent ischemic events attributable to a carotid web, successfully treated with CAS. We also provide a comprehensive review of current evidence regarding pathophysiology, diagnostic evaluation, and therapeutic strategies for this underrecognized but clinically significant vascular abnormality.

Case Presentation

A 61-year-old male with a medical history of diabetes mellitus, hypertension, ischemic heart disease, and prior percutaneous coronary intervention presented for evaluation of suspected carotid artery stenosis. He had a previous right-sided ischemic stroke resulting in residual right hemiparesis. Two months before presentation, he experienced an episode of left-sided weakness and slurred speech that improved with medical therapy and physiotherapy. Recurrent symptoms prompted further vascular assessment.

Vital Signs and Laboratory Investigations

On admission, vital signs were stable (HR - 90 bpm, BP - 114/54 mmHg, RR - 16). Laboratory values, including liver enzymes, renal parameters, albumin, and coagulation profile, were within normal limits (Table 1). ECG demonstrated a sinus rhythm.

Table 1.

Basic laboratory parameters

Parameter	Result	Reference Range	Interpretation
ALT	8 U/L	0–55 U/L	Normal
AST	17 U/L	8–48 U/L	Normal
Albumin	4.3 g/dL	3.2–4.6 g/dL	Normal
BUN	16 mg/dL	8–24 mg/dL	Normal
BNP	15.6 pg/mL	0–380 pg/mL	Normal

CT Angiography

CTA of the neck was performed, but the CTA exam was substantially degraded by motion artefact, limiting diagnostic clarity (Figure 1). Chronic occlusion of the right MCA distal M1 segment with collateral formation was observed. Irregularities in the left MCA and bilateral PCAs were noted, but suspected luminal narrowing at the distal right common carotid artery could not be conclusively assessed.

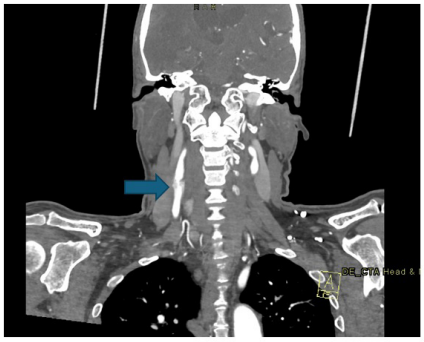

Figure 1. *CT angiography of the neck showing a motion-degraded image with suspected luminal narrowing at the origin of the right distal common carotid artery (arrow).*

Carotid Duplex Ultrasound

Duplex ultrasound demonstrated a thin, echogenic, shelf-like intraluminal projection arising from the posterior wall of the right carotid bulb and extending into the internal carotid artery, producing local turbulence on color Doppler imaging (Figure 2). These findings were characteristic of a carotid web.

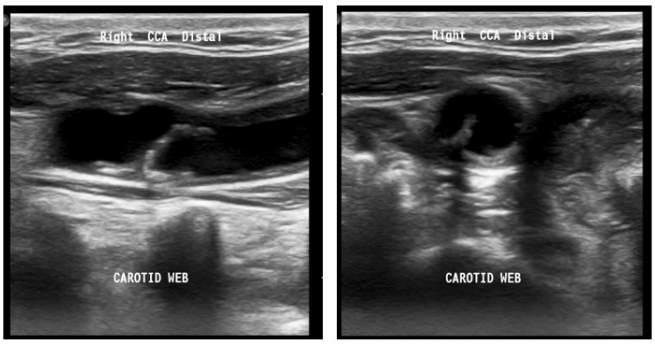

Figure 2. *Longitudinal (left) and transverse (right) distal common carotid ultrasound showing a shelf-like intraluminal projection at the posterior wall of the carotid bulb (arrow), consistent with carotid web.*

Intervention

Given the patient's recurrent ischemic episodes and supportive imaging, a multidisciplinary team recommended carotid artery stenting. The procedure was performed under local anesthesia, resulting in complete stent expansion and restoration of laminar flow. He experienced no postoperative complications and was discharged on dual antiplatelet therapy with scheduled follow-up imaging.

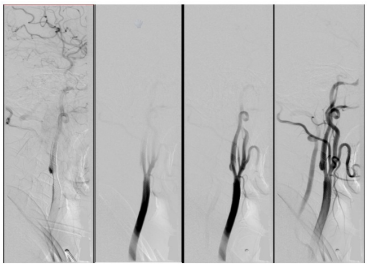

Figure 3. *Digital subtraction angiography (DSA) during carotid stenting demonstrates complete stent expansion, accompanied by restoration of laminar flow in the right internal carotid artery.*

Discussion

This case highlights several clinically important points. First, the carotid web should be actively considered in patients with recurrent embolic stroke, especially when traditional risk factors or high-grade stenosis are absent. Secondly, CTA remains the most powerful non-invasive tool, but its diagnostic accuracy depends on image quality, whilst Duplex ultrasound plays a critical complementary role, particularly when CTA findings are limited. Furthermore, early definitive intervention is essential, as reliance on medical therapy alone exposes patients to substantial risk of stroke recurrence. Lastly, CAS represents safe, durable, and effective treatment, particularly for older patients or those with complex anatomies.

Carotid web is an intimal variant of fibromuscular dysplasia increasingly recognized as an important but frequently underdiagnosed cause of recurrent embolic stroke.[1-3,7,13,14] Although historically described in young female patients without traditional vascular risk factors, emerging data suggest the condition spans a wider age range and may be encountered in individuals with vascular comorbidities, as seen in this case.[9] This growing awareness underscores the need for heightened diagnostic vigilance, particularly in patients with recurrent ischemic events despite minimal atherosclerotic burden.

Histopathologically, the carotid web represents focal intimal fibroplasia, distinct from the medial fibroplasia typical of systemic FMD.[7] The shelf-like protrusion arising from the posterior wall of the carotid bulb creates a region of geometric stenosis without the plaque features associated with atherosclerosis. High-resolution imaging and computational fluid dynamics analyses reveal that this structural anomaly produces disturbed laminar flow, with a characteristic vortex and zone of recirculation distal to the web.[8] This area of low shear stress is highly thrombogenic, predisposing to fibrin-rich mural thrombus formation and subsequent artery-to-artery embolization. Importantly, this mechanism explains why many patients with carotid web suffer recurrent strokes despite the absence of high-grade stenosis or plaque vulnerability factors.

Accurate diagnosis remains challenging because carotid webs can mimic atherosclerotic plaque, dissection flaps, intraluminal thrombus, or even imaging artefacts.[3,10,12] CTA is generally considered the preferred initial modality due to its high spatial resolution and ability to visualize thin intraluminal projections.[4,11] However, motion artefacts, suboptimal arterial opacification, or inadequate multiplanar reconstruction can obscure the lesion, as demonstrated in this case.

Duplex ultrasound, although operator-dependent, can provide valuable supportive evidence by demonstrating the echogenic intraluminal projection and associated turbulent flow patterns.[11] The sensitivity of duplex imaging is enhanced when combined with color Doppler and angle-adjusted spectral analysis. Digital subtraction angiography remains the definitive modality, offering superior spatial and temporal resolution and enabling dynamic assessment of flow patterns necessary for procedural planning.[6,15]

Given the complementary strengths of each modality, a multimodal imaging approach is often required to increase diagnostic confidence and avoid misclassification.

Although medical therapy with antiplatelet or anticoagulation agents appears reasonable in theory, multiple retrospective cohorts show that recurrent ischemic events remain common when carotid webs are managed conservatively.[2,14] This supports the concept that the lesion's embolic potential is primarily driven by abnormal flow dynamics rather than platelet activation alone.

Definitive mechanical exclusion of the web via carotid endarterectomy (CEA) or carotid artery stenting (CAS) has been associated with excellent clinical outcomes, low complication rates, and near-elimination of recurrence risk.[5,16-19] CAS, as demonstrated in this case, is minimally invasive, avoids cranial nerve injury risk associated with CEA, and reliably restores laminar flow across the affected segment. Long-term follow-up studies demonstrate durable patency, low restenosis risk, and sustained absence of recurrent stroke after stenting for carotid web.[15,18]

Conclusion

Carotid web is an important but frequently under-recognized cause of recurrent embolic ischemic stroke. Its subtle imaging characteristics and tendency to mimic other vascular pathologies contribute to diagnostic difficulty. This case illustrates the value of duplex ultrasound when CTA is inconclusive and supports carotid artery stenting as an effective and durable treatment option. Early identification and intervention are essential for preventing recurrent cerebrovascular events and improving long-term neurologic outcomes.

Author Contributions

Adel Alzahrani: Supervision, Writing – review and editing.
Faisal Alghamdi: Data interpretation, Writing – original draft.
Meshari Alzahrani: Data curation, Writing – original draft.
Jumana Aradhawi: Writing – original draft.
Fatima Altalhi: Resources, Writing – original draft.
Mohammad Bokhari: Data curation, Writing – original draft.
Mohammad Shably: Data analysis, Writing – original draft.
All authors have approved the final article.

Conflicts of Interest

The authors have declared no conflict of interest.

References

1. Choi PM, Singh D, Trivedi A, Qazi E, George D, Wong J, Demchuk AM, Goyal M, Hill MD, Menon BK. Carotid Webs and Recurrent Ischemic Strokes in the Era of CT Angiography. AJNR Am J Neuroradiol. 2015 Nov;36(11):2134-9. doi: 10.3174/ajnr.A4431. Epub 2015 Jul 30. PMID: 26228877; PMCID: PMC7964886.
2. Haussen DC, Grossberg JA, Bouslama M, Pradilla G, Belagaje S, Bianchi N, Allen JW, Frankel M, Nogueira RG. Carotid Web (Intimal Fibromuscular Dysplasia) Has High Stroke Recurrence Risk and Is Amenable to Stenting.

Stroke. 2017 Nov;48(11):3134-3137. doi: 10.1161/STROKEAHA.117.019020. Epub 2017 Oct 10. PMID: 29018133.
3. Coutinho JM, Derkatch S, Potvin AR, Tomlinson G, Casaubon LK, Silver FL, Mandell DM. Carotid artery web and ischemic stroke: A case-control study. Neurology. 2017 Jan 3;88(1):65-69. doi: 10.1212/WNL.0000000000003464. Epub 2016 Nov 18. Erratum in: Neurology. 2017 Aug 1;89(5):521. doi: 10.1212/WNL.0000000000004167. PMID: 27864523; PMCID: PMC5200857.
4. Kim SJ, Nogueira RG, Haussen DC. Current Understanding and Gaps in Research of Carotid Webs in Ischemic Strokes: A Review. JAMA Neurol. 2019 Mar 1;76(3):355-361. doi: 10.1001/jamaneurol.2018.3366. PMID: 30398546.
5. Zhang AJ, Dhruv P, Choi P, Bakker C, Koffel J, Anderson D, Kim J, Jagadeesan B, Menon BK, Streib C. A Systematic Literature Review of Patients With Carotid Web and Acute Ischemic Stroke. Stroke. 2018 Dec;49(12):2872-2876. doi: 10.1161/STROKEAHA.118.021907. PMID: 30571430.
6. Pasarikovski CR, Lynch J, Corrin M, Ku JC, Kumar A, Pereira VM, Krings T, da Costa L, Black SE, Agid R, Yang VX. Carotid stenting for symptomatic carotid artery web: Multicenter experience. Interv Neuroradiol. 2024 Jan 17:15910199231226293. doi: 10.1177/15910199231226293. Epub ahead of print. PMID: 38233047; PMCID: PMC11569737.
7. Chen H, Colasurdo M, Costa M, Nossek E, Kan P. Carotid webs: a review of pathophysiology, diagnostic findings, and treatment options. J Neurointerv Surg. 2024 Nov 22;16(12):1294-1298. doi: 10.1136/jnis-2023-021243.
8. Compagne KCJ, Dilba K, Postema EJ, van Es ACGM, Emmer BJ, Majoie CBLM, van Zwam WH, Dippel DWJ, Wentzel JJ, van der Lugt A, Gijsen FJH; MR CLEAN investigators. Flow Patterns in Carotid Webs: A Patient-Based Computational Fluid Dynamics Study. AJNR Am J Neuroradiol. 2019 Apr;40(4):703-708. doi: 10.3174/ajnr.A6012. Epub 2019 Mar 14. PMID: 30872422.
9. Landzberg D, Nogueira RG, Al-Bayati AR, Kim SJ, Bouslama M, Pisani L, da Camara CP, Frankel M, Nahab FB, Bianchi N, Haussen DC. Baseline Characteristics of Patients with Symptomatic Carotid Webs: A Matched Case Control Study. J Stroke Cerebrovasc Dis. 2021 Aug;30(8):105823. doi: 10.1016/j.jstrokecerebrovasdis.2021.105823. Epub 2021 May 23. PMID: 34034127.
10. Guillon B, Lévy C, Bousser MG. Internal carotid artery dissection: an update. J Neurol Sci. 1998 Jan 8;153(2):146-58. doi: 10.1016/s0022-510x(97)00287-6. PMID: 9511874.
11. Liang S, Qin P, Xie L, Niu S, Luo J, Chen F, Chen X, Zhang J, Wang G. The carotid web: Current research status and imaging features. Front Neurosci. 2023 Feb 13;17:1104212. doi: 10.3389/fnins.2023.1104212. PMID: 36860618; PMCID: PMC9968728.
12. Coutinho JM, Derkatch S, Potvin AR, Tomlinson G, Casaubon LK, Silver FL, Mandell DM. Carotid artery web and ischemic stroke: A case-control study. Neurology. 2017 Jan 3;88(1):65-69. doi: 10.1212/WNL.0000000000003464. Epub 2016 Nov 18. Erratum in: Neurology. 2017 Aug 1;89(5):521. doi: 10.1212/WNL.0000000000004167. PMID: 27864523; PMCID: PMC5200857.
13. Joux J, Boulanger M, Jeannin S, Chausson N, Hennequin JL, Molinié V, Smadja D, Touzé E, Olindo S. Association Between Carotid Bulb Diaphragm and Ischemic Stroke in Young Afro-Caribbean Patients: A Population-Based Case-Control Study. Stroke. 2016 Oct;47(10):2641-4. doi: 10.1161/STROKEAHA.116.013918. Epub 2016 Sep 13. PMID: 27625379.
14. Sajedi PI, Gonzalez JN, Cronin CA, Kouo T, Steven A, Zhuo J, Thompson O, Castellani R, Kittner SJ, Gandhi D, Raghavan P. Carotid Bulb Webs as a Cause of "Cryptogenic" Ischemic Stroke. AJNR Am J Neuroradiol. 2017 Jul;38(7):1399-1404. doi: 10.3174/ajnr.A5208. Epub 2017 May 11. PMID: 28495950; PMCID: PMC7959897.
15. Bounajem MT, Liang A, Trang A, El Baba B, Bielinski TM, Sangwon K, Zhang Y, Wiggan D, Grin E, Gajjar A, Pasarikovski CR, Yang VX, Agid R, Levitt M, Anderson M, Meyer RM, Cherian J, Howard B, Hendrix P, Abecassis IJ, Srinivasan V, El Naamani K, Gooch MR, Nossek E, Grandhi R. Outcomes after carotid revascularization for symptomatic carotid artery web: A multi-institutional cohort study. Interv Neuroradiol. 2025 Aug 8:15910199251365529. doi: 10.1177/15910199251365529. Epub ahead of print. PMID: 40776764; PMCID: PMC12334411.
16. Wojcik K, Milburn J, Vidal G, Tarsia J, Steven A. Survey of Current Management Practices for Carotid Webs. Ochsner J. 2019 Winter;19(4):296-302. doi: 10.31486/toj.18.0114. PMID: 31903051; PMCID: PMC6928665.
17. DaCosta M, Tadi P, Surowiec SM. Carotid Endarterectomy. 2023 Jul 24. In: StatPearls [Internet]. Treasure Island (FL): StatPearls Publishing; 2026 Jan–. PMID: 29261917.
18. Kumar R, Chadha D, Chaddha A, Chauhan R, Singh N, Kamal P, Mishra A, Kaur N. The Safety and Long-Term Efficacy of Carotid Artery Stenting: An All-Comers Registry. Cureus. 2022 Nov 30;14(11):e32060. doi: 10.7759/cureus.32060. PMID: 36600837; PMCID: PMC9800945.
19. Trystuła M, Tomaszewski T, Pąchalska M. Health-related quality of life in ischaemic stroke survivors after carotid endarterectomy (CEA) and carotid artery stenting (CAS): confounder-controlled analysis. Postepy Kardiol Interwencyjnej. 2019;15(2):226-233. doi: 10.5114/aic.2019.84441. Epub 2019 Apr 13. PMID: 31497056.

International Journal of Biomedicine 16(2) (2026) 274-277
http://dx.doi.org/10.21103/Article16(2)_CR3

CASE REPORT

INTERNATIONAL JOURNAL OF BIOMEDICINE

From Asymptomatic Carrier to Severe Epileptic Encephalopathy: First Albanian Pediatric Case of Early-Onset *KCNT1*-Related Epilepsy

Aferdita Tako[1], Rovena Aliaj[2*], Elizana Petrela[3], Aida Bushati[1], Armand Shehu[1], Xhentila Doka[1], Sindi Dizdari[2], Paskal Cullufi[4]

[1]*Department of Neuropediatrics, University Hospital Center "Mother Teresa", Tirana, Albania*
[2]*Pediatric Residency Program, Department of Pediatrics, University Hospital Center "Mother Teresa", Tirana, Albania*
[3]*Department of Statistics, University Hospital Center "Mother Teresa", Tirana, Albania*
[4]*Department of Pediatric Gastroenterology and Hepatology, University Hospital Center "Mother Teresa", Tirana, Albania*

Abstract

We report a pediatric case of genetically confirmed *KCNT1*-related epilepsy presenting with early-onset nocturnal frontal lobe seizures, multiple seizure types, and progressive psychomotor regression. Seizures were refractory to multiple anti-seizure medications. Trio exome sequencing identified a heterozygous *KCNT1* c.2882G>A (p.Arg961His) variant inherited from an asymptomatic father, consistent with autosomal dominant epilepsy with incomplete penetrance. This case highlights the phenotypic variability of *KCNT1*-related disorders and underscores the diagnostic, therapeutic, and genetic counseling challenges in early-onset developmental and epileptic encephalopathies.(**International Journal of Biomedicine. 2026;16(2):274-277.**)

Keywords: epileptic encephalopathy • pediatrics • KCNT1 • gene mutation

For citation: Tako A, Aliaj R, Petrela E, Bushati A, Shehu A, Doka X, Dizdari S, Cullufi P. From Asymptomatic Carrier to Severe Epileptic Encephalopathy: First Albanian Pediatric Case of Early-Onset *KCNT1*-Related Epilepsy. International Journal of Biomedicine. 2026;16(2):274-277. doi:10.21103/Article16(2)_CR3

Introduction

Pathogenic variants in *KCNT1*, which encodes a sodium-activated potassium channel (Slack channel), cause a group of rare developmental and epileptic encephalopathies (DEE) characterized by neuronal hyperexcitability due to gain-of-function channel dysfunction.[1,2] *KCNT1*-related epilepsies include early infantile epileptic encephalopathy type 14 (EIEE14; OMIM 614959) and autosomal dominant nocturnal frontal lobe epilepsy (ADNFLE5), representing a clinical continuum ranging from severe infantile-onset encephalopathy to later-onset focal epilepsy with preserved cognition.[3,4]

KCNT1-related disorders are rare, accounting for a small proportion of genetic epileptic encephalopathies, but are increasingly recognized with the widespread use of next-generation sequencing.[5] Most affected individuals present in infancy, typically within the first year of life, with frequent nocturnal seizures, autonomic manifestations, multiple seizure types, and early pharmacoresistance.[1,6] Neurodevelopmental delay or regression is common, particularly in early-onset forms, often leading to severe motor impairment, intellectual disability, and loss of previously acquired milestones.[2,7]

To date, numerous *KCNT1* variants, predominantly missense changes, have been identified, most of which result in channel gain-of-function.[1,8] These variants exhibit marked phenotypic heterogeneity, even within the same family, with reported outcomes ranging from asymptomatic carriers to profound developmental epileptic encephalopathy.[3,9]

***Corresponding author**: Rovena Aliaj, MD. E-mail: raliaj@hotmail.com*

Incomplete penetrance and variable expressivity pose significant diagnostic and genetic counseling challenges, particularly in autosomal dominant cases inherited from clinically unaffected parents.[4,9]

Given the overlap of clinical features with other epileptic encephalopathies and the frequent resistance to conventional anti-seizure medications, early molecular diagnosis is critical for accurate classification, prognostic assessment, and therapeutic decision-making.[5,10] Here, we report a pediatric case from Albania with severe early-onset *KCNT1*-related epilepsy and psychomotor regression, highlighting the genotype–phenotype correlation and the clinical implications of inherited *KCNT1* variants with reduced penetrance.

Case Presentation

A male child was born at 37 weeks' gestation following an uneventful pregnancy, with a birth weight of 2550 g and Apgar scores of 8 and 9 at 1 and 5 minutes, respectively. Early postnatal development was unremarkable until 7 months of age.

At 7 months, nocturnal episodes characterized by choking and vomiting shortly after sleep onset were observed, followed by seizures with chewing automatisms occurring predominantly during sleep. Seizure frequency rapidly increased, prompting hospital admission for afebrile convulsive episodes. Initial treatment with phenobarbital showed limited efficacy. Subsequently, complex focal seizures with left-sided hemiconvulsions, secondary generalization, and autonomic features (choking, chewing automatisms) were noted, often during sleep.

Laboratory investigations revealed a mild left shift in leukocyte distribution with normal biochemical parameters. Cerebrospinal fluid analysis was unremarkable. Cranial ultrasonography and computed tomography showed no structural abnormalities. Electroencephalography demonstrated fast beta activity in the frontotemporal regions with right temporal delta waves. Cardiac evaluation and abdominal ultrasonography excluded associated systemic pathology.

Despite sequential trials of multiple anti-seizure medications, including valproate, carbamazepine, levetiracetam, topiramate, vigabatrin, clonazepam, clobazam, lamotrigine, and adrenocorticotropic hormone, seizures remained refractory. Only clonazepam provided partial and transient improvement. Seizure frequency eventually increased to 20–25 episodes per day. Evaluation at a tertiary epilepsy center, "Bambino Gesù Children's Hospital" in Rome, documented infantile spasms, leading to the addition of vigabatrin.

Neurodevelopmental regression became evident after 12 months of age. At 2 years, the child exhibited profound psychomotor impairment, including axial hypotonia with peripheral hypertonia, tetraplegia, absence of speech, poor visual tracking, feeding difficulties, and global developmental regression. Ongoing management includes polytherapy with anti-seizure medications, physiotherapy, and developmental support.

Family history revealed no reported epilepsy. However, both the father and the paternal grandmother suffered from migraine, suggesting a possible underlying familial channelopathy-related neurological vulnerability. Given the early onset, pharmacoresistance, nocturnal seizure predominance, and developmental regression, a genetic etiology was strongly suspected.

Trio exome sequencing (CentoXome® Trio, Centogene, 2021) identified a heterozygous missense variant in *KCNT1* (NM_020822.2 (*KCNT1*):c.2882G>A; p.Arg961His), classified as likely pathogenic. The variant was inherited from the father, who remains clinically unaffected, while the mother tested negative. This finding established the diagnosis of autosomal dominant *KCNT1*-related epilepsy with incomplete penetrance, accounting for the severe infantile epileptic encephalopathy observed in the proband and the absence of epilepsy in the carrier parent.

Discussion

This case illustrates a severe phenotype within the spectrum of *KCNT1*-related epilepsies, characterized by early-onset, predominantly nocturnal seizures, multiple seizure types, profound pharmacoresistance, and rapid neurodevelopmental regression. Such a clinical course is consistent with previously described *KCNT1*-associated developmental and epileptic encephalopathies (DEE), in which seizure onset typically occurs within the first year of life and is frequently resistant to conventional anti-seizure medications.[1–3]

The proband demonstrated several hallmark features of *KCNT1*-related disease, including autonomic nocturnal seizures with hypermotor manifestations, evolution to infantile spasms, and progressive loss of acquired developmental milestones. These clinical characteristics support the growing view that early infantile epileptic encephalopathy type 14 (EIEE14) and autosomal dominant nocturnal frontal lobe epilepsy (ADNFLE5) represent a phenotypic continuum rather than distinct nosological entities.[2,4] The coexistence of focal seizures, spasms, and generalized seizure types in this patient further reflects the broad epileptic spectrum associated with *KCNT1* dysfunction.

Trio exome sequencing identified a heterozygous *KCNT1* c.2882G>A (p.Arg961His) variant inherited from an asymptomatic father, highlighting reduced penetrance and marked intrafamilial phenotypic variability. Incomplete penetrance has been repeatedly reported in autosomal dominant *KCNT1*-related epilepsies and poses significant challenges for clinical interpretation and genetic counselling.[6,9] The absence of epilepsy in the carrier parent underscores that severe epileptic encephalopathy can arise in offspring despite minimal or absent manifestations in transmitting relatives, emphasizing the limited predictive value of family history alone.

Functionally, most pathogenic *KCNT1* variants are gain-of-function missense mutations that increase potassium channel activity, leading to neuronal hyperexcitability and network instability.[1,8] Experimental studies have demonstrated that such mutations alter channel gating properties, resulting in excessive potassium currents and paradoxical enhancement of epileptogenic activity.[8] This molecular mechanism provides a plausible

explanation for the early onset, nocturnal predominance, and marked drug resistance observed in affected individuals.

Therapeutically, *KCNT1*-related epilepsies remain a major clinical challenge. Conventional anti-seizure medications are frequently ineffective, as observed in the present case, where extensive polytherapy yielded only transient or partial benefit. In recent years, quinidine, a partial blocker of *KCNT1* channels, has been investigated as a targeted treatment based on its ability to counteract gain-of-function channel activity.[11,12] However, reported clinical responses have been highly variable, with some patients showing seizure reduction and others deriving minimal benefit or experiencing dose-limiting adverse effects, particularly cardiac toxicity. [12,13] These findings highlight the need for careful patient selection, close monitoring, and further studies to define the role of precision therapies in *KCNT1*-associated epilepsy.

Beyond seizure control, neurodevelopmental outcome remains poor in severe early-onset forms, even when partial seizure reduction is achieved. Early and sustained epileptic activity, combined with intrinsic channel dysfunction, likely contributes to irreversible neurodevelopmental impairment. [3,7] This underscores the importance of early genetic diagnosis, not only to guide treatment decisions but also to provide realistic prognostic counseling and to initiate timely supportive and rehabilitative interventions.

Overall, this case expands the clinical spectrum of *KCNT1*-related epilepsy by documenting a severe early-onset phenotype with paternal inheritance and incomplete penetrance in an Albanian child. It reinforces the critical role of molecular diagnostics in refractory infantile epilepsies and highlights the complex interplay between genotype, penetrance, and clinical severity in *KCNT1*-associated disorders.

Conclusions

This report presents the first documented case from Albania of *KCNT1*-related early-onset developmental and epileptic encephalopathy with autosomal dominant inheritance and incomplete penetrance. The patient's severe and rapidly progressive clinical course highlights the broad phenotypic spectrum associated with *KCNT1* variants, ranging from asymptomatic carriers to profound epileptic encephalopathy within the same family.

This case underscores the critical role of early and comprehensive genetic testing in infants with refractory epilepsy, particularly when clinical features include nocturnal seizures, autonomic manifestations, and early neurodevelopmental regression. Establishing a molecular diagnosis is essential not only for accurate disease classification but also for prognostic assessment, informed genetic counseling, and appropriate family risk evaluation.

Furthermore, early identification of *KCNT1*-related epilepsy may facilitate timely consideration of precision-based therapeutic strategies and the initiation of multidisciplinary supportive care aimed at optimizing neurodevelopmental outcomes. Collectively, these findings emphasize the importance of integrating genetic diagnostics into routine clinical practice for severe early-onset epilepsies.

Sources of Funding

This study did not receive any specific grant from funding agencies in the public, commercial, or not-for-profit sectors.

Author Contributions

Aida Bushati: Clinical evaluation, Data curation, Writing – original draft.
Armand Shehu: Clinical evaluation, Data curation, Writing – original draft.
Xhentila Doka: Clinical evaluation, Data curation, Writing – original draft.
Paskal Cullufi: Investigation, Clinical evaluation, Writing – review and editing.
Rovena Aliaj: Conceptualization, Investigation, Data curation, Writing – original draft.
Sindi Dizdari: Investigation, Data curation, Clinical evaluation
Elizana Petrela: Data interpretation, Formal analysis, Writing – review and editing.
Aferdita Tako: Supervision, Conceptualization, Writing – review and editing.
All authors have approved the final article.

Conflict of Interest

The authors have declared no conflict of interest.

Acknowledgments

The authors would like to thank the medical and nursing staff of the University Hospital Center "Mother Teresa", Tirana, Albania, for their contribution to the clinical care of the patient.

Disclaimers

The views expressed in this article are those of the authors and do not necessarily reflect the official position of the affiliated institution or any funding body.

References

1. Barcia G, Fleming MR, Deligniere A, Gazula VR, Brown MR, Langouet M, Chen H, Kronengold J, Abhyankar A, Cilio R, Nitschke P, Kaminska A, Boddaert N, Casanova JL, Desguerre I, Munnich A, Dulac O, Kaczmarek LK, Colleaux L, Nabbout R. De novo gain-of-function KCNT1 channel mutations cause malignant migrating partial seizures of infancy. Nat Genet. 2012 Nov;44(11):1255-9. doi: 10.1038/ng.2441. Epub 2012 Oct 21. PMID: 23086397; PMCID: PMC3687547.
2. Milligan CJ, Li M, Gazina EV, et al. KCNT1 gain-of-function mutations produce epileptic encephalopathy. Nat Commun. 2014;5:4971.
3. Heron SE, Smith KR, Bahlo M, Nobili L, Kahana E, Licchetta L, Oliver KL, Mazarib A, Afawi Z, Korczyn A, Plazzi G, Petrou S, Berkovic SF, Scheffer IE, Dibbens LM. Missense mutations in the sodium-gated potassium channel gene KCNT1 cause severe autosomal dominant nocturnal frontal lobe epilepsy. Nat Genet. 2012 Nov;44(11):1188-90.

doi: 10.1038/ng.2440. Epub 2012 Oct 21. PMID: 23086396.
4. Ishii A, Shioda M, Okumura A, et al. KCNT1 mutations in epilepsy: genotype–phenotype correlations. Epilepsia. 2013;54(6):1081–1089.
5. Myers KA, Scheffer IE, Berkovic SF. Genetic epileptic encephalopathies: recent advances and future directions. Curr Opin Neurol. 2017;30(2):164–171.
6. Lim CX, Ricos MG, Dibbens LM, et al. KCNT1 mutations in refractory epilepsy: clinical and functional characterization. Epilepsia. 2016;57(2):e37–e41.
7. McTague A, Howell KB, Cross JH, Kurian MA, Scheffer IE. The genetic landscape of the epileptic encephalopathies of infancy and childhood. Lancet Neurol. 2016 Mar;15(3):304-16. doi: 10.1016/S1474-4422(15)00250-1. Epub 2015 Nov 17. PMID: 26597089.
8. Tang QY, Zhang Z, Xia XM, Lingle CJ. KCNT1 mutations associated with epilepsy increase channel activity by altering gating properties. J Neurosci. 2016;36(14):3867–3876.
9. Møller RS, Larsen LH, Johannesen KM, et al. Incomplete penetrance of KCNT1 mutations in autosomal dominant focal epilepsies. Eur J Hum Genet. 2015;23(7):1025–1030.
10. Wirrell EC, Shellhaas RA, Joshi C, et al. How should children with epilepsy be evaluated and treated in the era of precision medicine? Epilepsy Curr. 2020;20(4):197–203.
11. Bearden D, Strong A, Ehnot J, DiGiovine M, Dlugos D, Goldberg EM. Targeted treatment of migrating partial seizures of infancy with quinidine. Ann Neurol. 2014 Sep;76(3):457-61. doi: 10.1002/ana.24229. Epub 2014 Jul 26. PMID: 25042079.
12. Mullen SA, Carney PW, Roten A, Ching M, Lightfoot PA, Churilov L, Nair U, Li M, Berkovic SF, Petrou S, Scheffer IE. Precision therapy for epilepsy due to KCNT1 mutations: A randomized trial of oral quinidine. Neurology. 2018 Jan 2;90(1):e67-e72. doi: 10.1212/WNL.0000000000004769. Epub 2017 Dec 1. PMID: 29196578.
13. Abdelnour E, Gallentine W, McDonald M, et al. Clinical experience with quinidine in KCNT1-related epilepsy. Epilepsia. 2018;59(3):e50–e56.

International Journal of Biomedicine 16(2) (2026) 278-280
http://dx.doi.org/10.21103/Article16(2)_CR4

CASE REPORT

INTERNATIONAL JOURNAL OF BIOMEDICINE

Central Giant Cell Granuloma of the Mandible in an Elderly Patient: A Diagnostic Challenge

Samah O. Mohager[1*], Asim Saleem Almaaytah[2], Wafaey Badawy[3]

[1]*Department of Basic Medical Sciences, College of Medicine, Prince Sattam Bin Abdulaziz University, Al-Kharj, Saudi Arabia*
[2]*Department of Maxillofacial Surgery, Al-Kharj Industry Military Hospital, Al-Kharj, Saudi Arabia*
[3]*Department of Histopathology, Armed Forces Hospital, Al-Kharj. Saudi Arabia*

Abstract

Background: Central giant cell granuloma (CGCG) is a rare benign osteolytic lesion of the jaws, predominantly affecting young females. Occurrence in elderly patients is uncommon and may pose diagnostic challenges due to overlap with other giant cell lesions, particularly brown tumor of hyperparathyroidism.
Case Presentation: We report a case of a 63-year-old woman with type 1 diabetes mellitus who presented with a well-circumscribed radiolucent lesion in the left anterior mandible associated with tooth mobility. Surgical excision and curettage were performed. Histopathological examination revealed features consistent with a giant cell lesion. Comprehensive biochemical evaluation excluded hyperparathyroidism, confirming the diagnosis of non-aggressive CGCG. The postoperative course was uneventful, and follow-up imaging demonstrated satisfactory bone regeneration.
Conclusion: This case highlights the rare occurrence of CGCG in an elderly patient and emphasizes the importance of correlating clinical, radiologic, histopathologic, and biochemical findings to establish an accurate diagnosis. Conservative surgical management can achieve favorable outcomes in non-aggressive lesions. (**International Journal of Biomedicine. 2026;16(2):278-280.**)

Keywords: central giant cell granuloma • mandible • brown tumor • hyperparathyroidism

For citation: Mohager SO, Almaaytah AS, Badawy W. Central Giant Cell Granuloma of the Mandible in an Elderly Patient: A Diagnostic Challenge. International Journal of Biomedicine. 2026;16(2):278-280. doi:10.21103/Article16(2)_CR4

Introduction

Central giant cell granuloma (CGCG) is a benign jaw lytic lesion that is classified into two subtypes: non-aggressive and aggressive.[1] It tends to occur in females below 30 years[2] and has a prevalence of approximately 0.0001%. The exact etiopathogenesis of this condition is not well understood; nevertheless, certain elements like intraosseous hemorrhage, inflammation, local trauma, and genetic abnormalities are thought to play roles. CGCG of the jaw is characterized by somatic mutations in *KRAS*, *FGFR1*, and *TRPV4*.[3] These mutations occur in stromal mononuclear cells, not the giant cells. Unlike giant cell tumors of bone, CGCG lacks *H3F3A* mutations.

The term "giant cell reparative granuloma" was introduced by Henry L. Jaffe in 1953 to describe a non-neoplastic, reactive lesion of the jaw resulting from intraosseous hemorrhage and trauma.[4] The condition affects the upper and lower jaws with a predilection to the region anterior to the first premolar. Clinically, it starts as an asymptomatic lesion that may later manifest symptoms.[5] Symptomatic cases show pain and paresthesia.[1] This case is reported because central giant cell granuloma rarely presents in elderly patients and closely mimics brown tumor of hyperparathyroidism, posing a significant diagnostic challenge. The case underscores the necessity of biochemical exclusion of hyperparathyroidism and demonstrates that conservative surgical management can achieve satisfactory outcomes in non-aggressive lesions in this age group. The case is reported in accordance with CARE guidelines.

Case Presentation

A 63-year-old woman with a known history of type 1 diabetes mellitus presented with a swelling in the left mandibular region, localized to the area of the lower left

canine. Clinical examination revealed a well-defined, dome-shaped 2 cm swelling associated with a mobile tooth (tooth number 33) along the superior border of the mandibular alveolar ridge. Laboratory investigations showed a glycated hemoglobin (HbA1c) level of 7.56%, with no other abnormal findings.

Panoramic dental radiography demonstrated a well-circumscribed radiolucent 0.7 × 1.5 × 2 cm lesion with expansion of the superior mandibular cortex, along with generalized alveolar bone loss consistent with chronic periodontitis. Periapical radiography of the involved tooth revealed a corresponding radiolucent lesion (Figure 1). Aspiration of the swelling was performed and was negative for malignant cells.

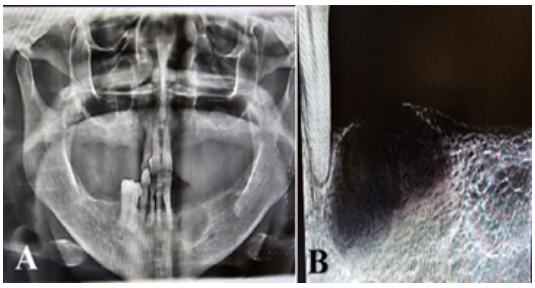

***Figure 1**. A: Panoramic X-ray; B: Periapical X-ray*

The procedure was carried out under local anesthesia using an inferior alveolar nerve block on the left side, supplemented by local infiltration of 2% lidocaine with 1:100,000 epinephrine. A mucoperiosteal flap was elevated, followed by the extraction of tooth number 33, the excision of the lesion, and the curettage of the affected area. The left mental nerve was carefully preserved. Hemostasis was achieved, and the surgical site was closed with interrupted sutures. The postoperative course was uneventful, with no reported complications.

The excised specimen was submitted for histopathological examination. Microscopic evaluation revealed an unencapsulated lesion composed of abundant fibroblasts and unevenly distributed multinucleated giant cells, with focal clustering. Areas of hemorrhage and hemosiderin deposition were also identified (Figure 2). Based on these findings, the differential diagnosis included a brown tumor related to hyperparathyroidism and central giant cell granuloma of the mandible.

Subsequent laboratory investigations were performed to exclude hyperparathyroidism, the principal mimicker. Serum calcium, phosphorus, alkaline phosphatase, and parathyroid hormone levels were all within normal limits, thereby ruling out a brown tumor.

Clinical follow-up in the outpatient setting showed satisfactory and uncomplicated healing. A periapical radiograph obtained three months postoperatively demonstrated new bone formation and a reduction in radiolucency at the surgical site (Figure 3). The patient was subsequently referred to the prosthodontics department for rehabilitation of the missing teeth.

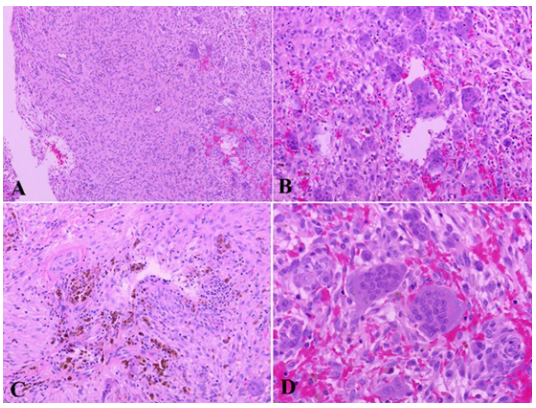

***Figure 2.** The histomorphology of the resected swelling.*

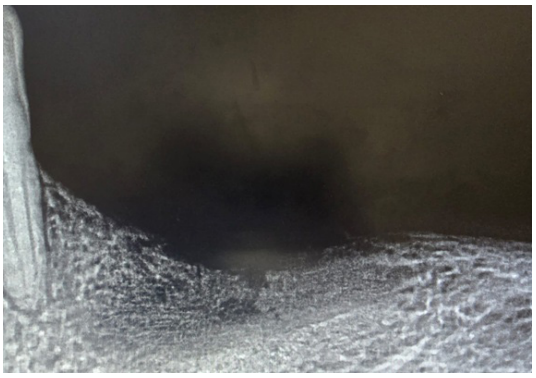

***Figure 3.** Follow-up periapical X-ray.*

Discussion

Central giant cell granuloma is a rare condition of the maxillofacial bones, with four-fifths of cases occurring in females under 20 years of age.[6] It is rarely reported after age 50.[7] The occurrence of this lesion in an older patient, as in the present case, is therefore unusual and expands the reported age spectrum of CGCG.

Central giant cell granuloma can be classified into aggressive and non-aggressive types based on lesion nature and clinical presentation. The non-aggressive type is symptomless, slowly growing, and small, causing neither root resorption nor cortical perforation. This is in contradistinction to the aggressive type, the size of which can reach more than 5 cm with possible postoperative recurrence.[1] The lesion in the current case was non-aggressive, asymptomatic, and small.

Micromorphologically, as per WHO, CGCG is composed of cellular fibrous tissue that contains multiple foci of hemorrhage, aggregations of multinucleated giant cells, and occasionally trabeculae of woven bone.[2] The present case was consistent histologically with both CGCG and brown tumor. This case underscores the importance of a systematic diagnostic approach, as a brown tumor was a strong differential diagnosis and required exclusion through comprehensive metabolic and hormonal evaluation.

Radiologically, CGCG appears as a sharply delineated radiolucent lesion extending often between the displaced

tooth roots.[8] In the current case, the lesion presented as a well-circumscribed radiolucency with cortical expansion, findings that can also mimic odontogenic cysts, benign tumors, or even malignant processes.[9] The association with tooth mobility and generalized periodontal bone loss further complicates the clinical picture and highlights the potential for CGCG to be overlooked or misdiagnosed in patients with coexisting periodontal disease.

Another noteworthy aspect of this case is the patient's history of type 1 diabetes mellitus. Although no direct causal relationship has been established between diabetes and CGCG, metabolic disorders can influence bone turnover, healing capacity, and surgical outcomes.[10] Reporting such cases contributes to the growing body of literature examining potential associations between systemic diseases and maxillofacial bone lesions, even when a definitive link cannot yet be established.

Management of CGCG depends on the lesion behavior. Treatment modalities include surgical excision or resection with continuity defects, cryotherapy, enucleation, and aggressive local curettage, either alone or combined with chemical cauterization.[6] From a therapeutic standpoint, the lesion was successfully treated by conservative surgical excision and curettage with preservation of the mental nerve and an uneventful postoperative course. This approach was favored due to the lesion's non-aggressive features, including small size, well-defined margins, and absence of cortical perforation or neurologic symptoms, as well as its anterior mandibular location. The patient's advanced age and comorbid diabetes further supported a tissue-preserving strategy. Follow-up imaging demonstrated satisfactory bone regeneration with decreasing radiolucency, confirming conservative surgery as an effective management option for non-aggressive CGCG, particularly in older patients, where more aggressive interventions may increase morbidity.

Conclusion

Central giant cell granuloma may rarely present in elderly patients and can mimic other giant cell lesions of the jaw, particularly brown tumor of hyperparathyroidism. Accurate diagnosis requires careful integration of clinical, radiologic, histopathologic, and biochemical findings. Conservative surgical management remains an effective treatment option for non-aggressive lesions, with satisfactory healing and bone regeneration.

Author Contributions

Samah O. Mohager: Data curation, Investigation, Writing – original draft.

Asim Saleem Almaaytah: Data curation, Investigation, Writing – original draft.

Wafaey Badawey: Conceptualization, Writing – review and editing.

All authors have approved the final article.

Conflicts of Interest

The authors have declared no conflict of interest.

References

1. Chi Y, Qin Z, Bai J, Yan J, Xu Z, Yang S, Li B. Update on the nature of central giant cell granuloma of the jaw with a focus on the aggressive subtype. Pathology. 2025 Jun;57(4):461-469. doi: 10.1016/j.pathol.2024.10.010.
2. Mohan RP, Verma S, Agarwal N, Singh U. Central giant cell granuloma: a case report. BMJ Case Rep. 2013 Jul 22;2013:bcr2013009903. doi: 10.1136/bcr-2013-009903.
3. Gomes CC, Diniz MG, Bastos VC, Bernardes VF, Gomez RS. Making sense of giant cell lesions of the jaws (GCLJ): lessons learned from next-generation sequencing. J Pathol. 2020 Feb;250(2):126-133. doi: 10.1002/path.5365.
4. JAFFE HL. Giant-cell reparative granuloma, traumatic bone cyst, and fibrous (fibro-oseous) dysplasia of the jawbones. Oral Surg Oral Med Oral Pathol. 1953 Jan;6(1):159-75. doi: 10.1016/0030-4220(53)90151-0.
5. Ramesh V. "Central giant cell granuloma" - An update. J Oral Maxillofac Pathol. 2020 Sep-Dec;24(3):413-415. doi: 10.4103/jomfp.jomfp_487_20.
6. Jeyaraj P. Management of Central Giant Cell Granulomas of the Jaws: An Unusual Case Report with Critical Appraisal of Existing Literature. Ann Maxillofac Surg. 2019 Jan-Jun;9(1):37-47. doi: 10.4103/ams.ams_232_18.
7. Gupta S, Narwal A, Kamboj M, Devi A, Hooda A. Giant Cell Granulomas of Jaws: a Clinicopathologic Study. J Oral Maxillofac Res. 2019 Jun 30;10(2):e5. doi: 10.5037/jomr.2019.10205.
8. Singh G, Kumar S, Kumar A. Central Giant Cell Granuloma of Maxilla: A Case Report. The Traumaxilla. 2023;5:38–41. doi:10.1177/26323273231224986
9. Kumar J, Vanagundi R, Manchanda A, Mohanty S, Meher R. Radiolucent Jaw Lesions: Imaging Approach. Indian J Radiol Imaging. 2021 Jan;31(1):224-236. doi: 10.1055/s-0041-1729769.
10. Jiao H, Xiao E, Graves DT. Diabetes and Its Effect on Bone and Fracture Healing. Curr Osteoporos Rep. 2015 Oct;13(5):327-35. doi: 10.1007/s11914-015-0286-8.

***Corresponding author**: Samah O. Mohager, MD. E-mail: samahmohager@gmail.com*

International Journal of Biomedicine 16(2) (2026) 281-283
http://dx.doi.org/10.21103/Article16(2)_BC

BRIEF COMMUNICATION

INTERNATIONAL JOURNAL OF BIOMEDICINE

Circulating and Urinary Creatine Levels in the All of Us Research Program

David Nedeljkovic[1], Sergej M. Ostojic[1,2,3*]

[1]*Applied Bioenergetics Lab, Medical Polyclinic Fizikus, Belgrade, Serbia*
[2]*Faculty of Health Sciences, University of Pécs, Pécs, Hungary*
[3]*Department of Nutritional Sciences, Texas Tech University, Lubbock, TX*

Abstract

Creatine is central to human bioenergetics, yet circulating creatine remains largely uncharacterized in population settings. Using data from the All of Us Research Program, we examined serum/plasma and urinary creatine in a demographically diverse U.S. cohort. We identified 246 adults with 1,576 serum or plasma creatine measurements and harmonized values across assay formats. Participant-level mean serum creatine was right-skewed in the full cohort but clustered tightly after exclusion of individuals with kidney disease. In adults without renal pathology (n=139), circulating creatine occupied a narrow physiological range (mean 0.94 mg/dL; median 0.90 mg/dL; interquartile range 0.76-1.10 mg/dL), indicating strong homeostatic regulation. In contrast, urinary creatine, assessed in 2,044 participants, displayed wide interindividual variability with a long upper tail. These findings establish the first population-scale reference framework for creatine in blood and urine and define ~ 1mg/dL as a pragmatic physiological anchor for circulating creatine in adults without kidney disease.(**International Journal of Biomedicine. 2026;16(2):281-283.**)

Keywords: creatine • bioenergetics • population • kidney disease

For citation: Nedeljkovic D, Ostojic SM. Circulating and Urinary Creatine Levels in the All of Us Research Program. International Journal of Biomedicine. 2026;16(2):281-283. doi:10.21103/Article16(2)_BC

Introduction

Creatine is a central component of human bioenergetics, functioning as a rapidly mobilizable phosphate buffer that stabilizes ATP availability in tissues with high, fluctuating energy demands,[1] including skeletal muscle, brain, myocardium, and immune cells. Through the phosphocreatine-creatine kinase system, creatine supports energy transfer, contributes to redox balance, and participates in osmotic and signaling processes.[2] In humans, creatine homeostasis reflects the interplay between endogenous synthesis and dietary intake from animal-source foods, positioning creatine at the intersection of metabolism and nutrition.

Despite this central role, circulating creatine remains remarkably understudied. In routine clinical practice, creatinine is ubiquitously measured as a marker of renal function, yet serum or plasma creatine itself is rarely assessed and is not part of standard chemistry panels. Measurement is typically confined to specialized contexts,[3] such as the evaluation of rare inborn errors of creatine metabolism or selected neuromuscular disorders. Consequently, population-based reference data for circulating creatine are lacking. Existing knowledge derives largely from small experimental cohorts or athletic populations. One of the few population-oriented reports from a French adult cohort suggested relatively low, tightly distributed circulating creatine concentrations[4] but was limited in size and demographic scope. Whether such narrow distributions generalize to diverse real-world populations remains unknown. As a result, even basic descriptors, such as typical concentration, interindividual variability, and physiological range of serum creatine in community-dwelling adults, remain undefined.

This gap has important implications. Circulating creatine integrates endogenous synthesis, dietary exposure, tissue uptake, and renal handling, and may therefore reflect systemic bioenergetic status. Without normative data, it is difficult to contextualize individual values or relate circulating creatine to diet, age, sex, metabolic health, or disease risk. The

***Corresponding author:** Prof. Sergej M. Ostojic, MD, PhD, FACP. E-mail addresses: sergej.ostojic@chess.edu.rs and sergej.ostojic@etk.pte.hu*

absence of reference distributions also constrains translational work on supplementation and fortification strategies, as well as on the emerging concept of creatine as a conditionally essential nutrient across the life course. Large-scale population resources now make it feasible to address this deficiency. The All of Us Research Program provides harmonized electronic health record data and laboratory measurements from a large, demographically diverse cohort of U.S. adults (https://allofus.nih.gov/), enabling empirical characterization of circulating metabolites under real-world clinical conditions. Importantly, this setting allows separation of physiological variability from pathological influences,[5] particularly renal disease, which profoundly affects creatine handling and may dominate the upper tail of observed distributions.

Methods

Using All of Us data, we identified 246 adults with serum or plasma creatine measurements, contributing 1,576 tests. Creatine was captured using LOINC-derived OMOP concepts for mass- and molar-based serum/plasma assays. Units were overwhelmingly recorded as milligrams per deciliter, with a small number labeled as micromoles per liter; a subset lacked standardized unit metadata. Given the dominance of a single assay stream and the consistency of observed value ranges, unmapped numeric values were conservatively harmonized to mg/dL, yielding standardized creatine concentrations for 1,574 of 1,576 records and retaining all participants. To avoid over-weighting individuals with frequent clinical testing and to approximate each participant's typical creatine exposure, creatine was summarized at the participant level as the mean of all available values.

Results

In the full cohort, participant-level mean creatine was right-skewed (mean 2.28 mg/dL; median 1.09 mg/dL; range 0.19-22.2 mg/dL). Trimming extreme values using a ±3SD criterion identified four outliers (1.6%). The outlier-trimmed distribution remained right-skewed but more compact (mean 2.08 mg/dL; median 1.05 mg/dL). A more restrictive ±2SD sensitivity filter further reduced the mean (1.46 mg/dL) while leaving the median (~1.0 mg/dL) and interquartile range essentially unchanged, demonstrating that the central tendency is stable and that the mean is highly sensitive to a small right tail. Renal pathology emerged as the dominant determinant of this tail. After exclusion of all participants with any recorded diagnosis of chronic kidney disease, renal failure, end-stage renal disease, or dialysis, 139 individuals remained (52% female). The mean age was 50.5±14.8 years, with a median of 49.1 years (interquartile range 41.0-62.0; range 21.2-95.8 years). In this kidney disease-free subcohort, circulating creatine clustered tightly around ~1mg/dL (mean 0.94 mg/dL; median 0.90 mg/dL; interquartile range 0.76-1.10 mg/dL; range 0.19-2.80 mg/dL). Both the mean and dispersion were markedly attenuated relative to the unfiltered cohort, indicating that impaired renal handling is a major contributor to elevated values in the population. In adults without diagnosed kidney disease, circulating creatine occupies a narrow and apparently conserved physiological window.

Urinary creatine exhibited a contrasting profile. We identified 3,939 urinary creatine tests from 2,100 individuals. The vast majority represented spot urine creatine concentrations, predominantly in mg/dL; a minority corresponded to 24-hour excretion formats and were excluded from concentration-based analyses. After harmonization, 3,850 tests from 2,044 participants were retained. Across all tests, urinary creatine showed a broad, right-skewed distribution (mean 92 mg/dL; median 71 mg/dL; range 2-595 mg/dL). Participants contributed a median of one test, indicating that the population profile is not driven by frequent testers. Aggregation at the participant level yielded a similar distribution. Application of a ±3SD criterion identified 32 extreme values (1.6% of individuals). Exclusion of these outliers yielded a physiologically coherent reference distribution in 2,012 participants, with a mean urinary creatine concentration of 86.2±58.0 mg/dL (median 72.9 mg/dL, interquartile range 41.8-115.7 mg/dL; range 2.2-295.1 mg/dL), revealing substantial biological dispersion and a long upper tail even after removal of extremes, consistent with wide interindividual variability in creatine handling under everyday conditions.

Figure 1 illustrates the population distributions of creatine concentrations, showing serum/plasma creatine in adults without kidney disease and spot urinary creatine after outlier trimming.

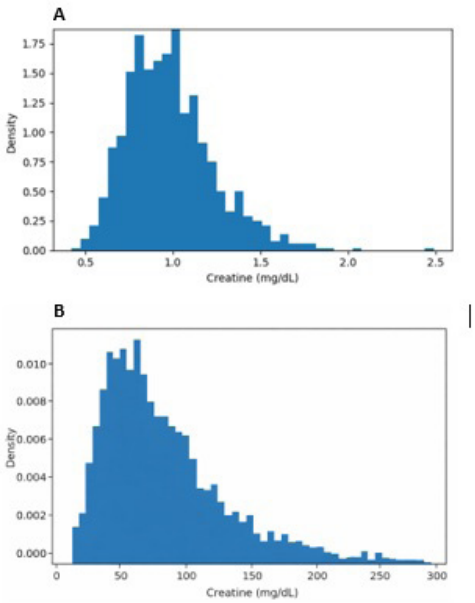

Figure 1. *Population distributions of circulating and urinary creatine. Panel A shows the distribution of participant-level mean serum/plasma creatine in adults without diagnosed kidney disease, demonstrating tight clustering around ~ 1 mg/dL and a narrow interquartile range. Panel B depicts spot urinary creatine concentration after exclusion of 24-h formats and ±3SD outliers, revealing a broad, right-skewed distribution. These distributions contrast the narrow physiological range of circulating creatine with the wide biological dispersion of urinary creatine under real-world conditions.*

Discussion

Together, these findings provide the first population-scale reference framework for creatine in human circulation and urine. The tight clustering of serum/plasma creatine around ~1mg/dL in adults without kidney disease suggests a narrow physiological range, consistent with tight homeostatic regulation across synthesis, intake, tissue uptake, and renal clearance.[3] In contrast, urinary creatine displays wide interindividual variability, likely reflecting differences in muscle mass, dietary exposure, endogenous synthesis, and renal handling under real-world conditions. Several limitations warrant consideration. All of Us laboratory data originate from routine clinical care and are not standardized for research purposes; assay platforms and calibration vary across sites. Unit metadata were incomplete for a subset of records, requiring conservative harmonization assumptions. Kidney disease was identified through diagnostic coding and may not capture subclinical impairment. Finally, the cohort reflects individuals engaged with the healthcare system and may not represent the healthiest segment of the population.

Despite these constraints, this analysis establishes the first empirical population anchors for creatine in adults. The observation that circulating creatine in individuals without kidney disease clusters tightly around ~1mg/dL defines a pragmatic physiological reference point. These data allow individual values to be interpreted in a biologically meaningful context and provide a foundation for translational studies linking creatine biology to diet, aging, metabolic health, and functional outcomes. In this light, circulating creatine may be viewed not merely as a biochemical curiosity, but as a systemic indicator of human bioenergetic status.

Ethics Statement

This research was conducted using data from the All of Us Research Program, obtained via the All of Us Researcher Workbench. The program operates under a central Institutional Review Board (IRB) protocol reviewed and approved by the Advarra IRB (IRB# IRB00009605), in accordance with the U.S. Department of Health and Human Services regulations for the protection of human subjects (45 CFR 46). The All of Us IRB provides single IRB oversight for all research activities involving program data. This study met the criteria for exempt human subjects' research as defined by the Common Rule and did not require additional IRB review at the authors' home institution. All data were de-identified and analyzed in compliance with the program's Data Use Agreement and ethical standards.

Funding

No external funding was received for this work.

Data Availability Statement

The datasets supporting the conclusions of this study are publicly available and can be accessed through the All of Us Research Program via a secure, cloud-based Researcher Workbench at https://www.researchallofus.org/. The authors do not own the data. For further information, please contact the corresponding author.

AI Statement

During the preparation of this manuscript, the authors used ChatGPT (OpenAI) for language editing, figure formatting, and grammatical refinement. All AI-assisted content was reviewed, verified, and revised by the authors, who take full responsibility for the accuracy, integrity, and final content of the manuscript.

Author Contributions

David Nedeljkovic: Investigation, Data curation, Formal analysis, Writing – original draft.
Sergej M. Ostojic (SMO): Supervision, Conceptualization, Writing – review and editing.

SMO serves on scientific advisory boards related to creatine. SMO is an inventor on creatine-related intellectual property and has received research funding on creatine from public agencies and industry partners. SMO co-founded a venture developing creatine-enriched food products

Acknowledgement

Sergej M. Ostojic expresses gratitude to Solvej Balle for her transformative initiatives.

Conflict of Interest

The authors have declared no conflict of interest.

References

1. Wallimann T, Tokarska-Schlattner M, Schlattner U. The creatine kinase system and pleiotropic effects of creatine. Amino Acids. 2011 May;40(5):1271-96. doi: 10.1007/s00726-011-0877-3. Epub 2011 Mar 30. PMID: 21448658; PMCID: PMC3080659.
2. Ribeiro F, Forbes SC, Candow DG, Perim P, Lira FS, Lancha AH Jr, Rosa Neto JC. Creatine supplementation and muscle-brain axis: a new possible mechanism? Front Nutr. 2025 Jul 23;12:1579204. doi: 10.3389/fnut.2025.1579204. PMID: 40771202; PMCID: PMC12325066.
3. Nedeljkovic DD, Ostojic SM. Biomarkers of Creatine Metabolism in Humans: From Plasma to Saliva and Beyond. Clin Bioenerg. 2025; 1(1):2. doi: 10.3390/clinbioenerg1010002.
4. Joncquel-Chevalier Curt M, Cheillan D, Briand G, Salomons GS, Mention-Mulliez K, Dobbelaere D, et al. Creatine and guanidinoacetate reference values in a French population. Mol Genet Metab. 2013 Nov;110(3):263-7. doi: 10.1016/j.ymgme.2013.09.005. Epub 2013 Sep 16. PMID: 24090707.
5. Wyss M, Kaddurah-Daouk R. Creatine and creatinine metabolism. Physiol Rev. 2000 Jul;80(3):1107-213. doi: 10.1152/physrev.2000.80.3.1107. PMID: 10893433.

IJBM

INTERNATIONAL JOURNAL OF BIOMEDICINE

Instructions for Authors

International Journal of Biomedicine (IJBM) publishes peer-reviewed articles on the topics of basic, applied, and translational research on biology and medicine. International Journal of Biomedicine welcomes submissions of the following types of paper: Original Articles, Reviews, Viewpoints, Case Reports, and Brief Communications.

All research studies involving animals must have been conducted following animal welfare guidelines such as *the National Institutes of Health (NIH) Guide for the Care and Use of Laboratory Animals*, or equivalent documents. Studies involving human subjects or tissues must adhere to the *Declaration of Helsinki and Title 45, US Code of Federal Regulations, Part 46, Protection of Human Subjects*, and must have received approval of the appropriate institutional committee charged with oversight of human studies. Informed consent must be obtained.

Pre-submissions

Authors are welcome to send an abstract or draft manuscript to obtain a view from the Editor about the suitability of their paper. Our Editors will do a quick review of your paper and advise if they believe it is appropriate for submission to our journal. It will not be a full review of your manuscript.

Manuscript Submission

Manuscript submissions should conform to the guidelines set forth in the Recommendations for the Conduct, Reporting, Editing and Publication of Scholarly Work in Medical Journals (ICMJE Recommendations), available from www.ICMJE.org.

Original works will be accepted with the understanding that they are contributed solely to the Journal, are not under review by another publication, and have not previously been published except in abstract form.

All manuscripts must be submitted through the International Journal of Biomedicine`s online submission system (www.ijbm.org/submission.php). Manuscripts must be typed, double-spaced using a 14-point font, including references, figure legends, and tables. Leave 1-inch margins on all sides. Assemble the manuscript in this order: Title Page, Abstract, Keywords, Text (Introduction, Methods, Results, and Discussion), Acknowledgments, Sources of Funding, Disclosures, References, Tables, Figures, and Figure Legends. References, Figures, and Tables should be cited in numerical order according to first mention in the text.

The preferred order for uploading files is as follows: Cover letter, Full Manuscript PDF (PDF containing all parts of the manuscript including references, legends, figures and tables), Manuscript Text File (MS Word), Figures (each figure and its corresponding legend should be presented together), and Tables. Files should be labeled with appropriate and descriptive file names (e.g., SmithText.doc, Fig1.eps, Table3.doc). Text, Tables, and Figures should be uploaded as separate files. (Multiple figure files can be compressed into a Zip file and uploaded in one step; the system will then unpack the files and prompt the naming of each figure. See www.WinZip.com for a free trial.)

Authors who are unable to provide an electronic version or have other circumstances that prevent online submission must contact the Editorial Office prior to submission to discuss alternate options (editor@ijbm.org).

Cover Letter

The cover letter should be saved as a separate file for upload. In it, the authors should (1) state that the manuscript, or parts of it, have not been and will not be submitted elsewhere for publication; (2) state that all authors have read and approved the manuscript; and (3) disclose any financial or other relations that could lead to a conflict of interest. If a potential conflict exists, its nature should be stated for each author. When there is a stated potential conflict of interest a footnote will be added indicating the author's equity interest in or other affiliation with the identified commercial firms.

The corresponding author should be specified in the cover letter. All editorial communications will be sent to this author. A short paragraph telling the editors why the authors think their paper merits publication priority may be included in the cover letter.

Types of articles

Original articles

Original articles present the results of original research. These manuscripts should present well-rounded studies reporting innovative advances that further knowledge about a topic of importance to the fields of biology or medicine. These can be submitted as either a full-length article (no more than 6,000 words, 4 figures, 4 tables) or a Short Communication (no more than 2,500 words, 2 figures, 2 tables). An original

article may be Randomized Control Trial, Controlled Clinical Trial, Experiment, Survey, and Case-control or Cohort study.

Case Reports

Case reports describe an unusual disease presentation, a new treatment, a new diagnostic method, or a difficult diagnosis. The authors must make it clear what the case adds to the field of medicine and include an up-to-date review of all prior cases. These articles should be no more than 5,000 words with no more than 6 figures and 3 tables. Case Reports should consist of the following headings: Abstract (no more than 100 words), Introduction, Case Presentation, Discussion, and Conclusions. The number of authors for a clinical case description must not exceed seven. Those who contributed to the patient's care but did not contribute directly to the intellectual work of the manuscript should be listed in the acknowledgments section.

Reviews

Reviews analyze the current state of understanding on a particular subject of research in biology or medicine, the limitations of current knowledge, future directions to be pursued in research, and the overall importance of the topic. Reviews could be non-systematic (narrative) or systematic. Reviews can be submitted as a Mini-Review (no more than 2,500 words, 3 figures, and 1 table) or a long review (no more than 6,000 words, 6 figures, and 3 tables). Reviews should contain four sections: Abstract, Introduction, Topics (with headings and subheadings, and Conclusions and Outlook.

Viewpoints

Viewpoint articles include academic papers, which address any important topic in biomedicine from a personal perspective than standard academic writing. Maximum length is 1,200 words, ≤70 references, and 1 small table or figure.

Short Communications

Short communications are concise scientific papers (typically 1,500–2,500 words) that present novel, preliminary, or urgent findings without the length or depth of a full research article. Main body of text, excluding tables (<2), figures (<2), and references (<15), not to exceed 1,000 words. Short Communications should contain Abstract, Introduction, Materials and Methods, Results, and Conclusion.

Research Reporting Guidelines

Authors are encouraged to adhere to recognized research reporting guidelines for study types:

• Randomized trials: CONSORT (https://www.equator-network.org/reporting-guidelines/consort/)

• Observational studies: STROBE (https://www.equator-network.org/reporting-guidelines/strobe/)

• Systematic reviews: PRISMA (https://www.equator-network.org/reporting-guidelines/prisma/)

• Case reports: CARE (https://www.equator-network.org/reporting-guidelines/care/)

• Qualitative research: SRQR (https://www.equator-network.org/reporting-guidelines/srqr/)

• Diagnostic / prognostic studies: STARD (https://www.equator-network.org/reporting-guidelines/stard/)

• Animal pre-clinical studies: ARRIVE (https://www.equator-network.org/reporting-guidelines/improving-bioscience-research-reporting-the-arrive-guidelines-for-reporting-animal-research/)

• Study protocols: SPIRIT (https://www.equator-network.org/reporting-guidelines/spirit-2013-statement-defining-standard-protocol-items-for-clinical-trials/)

Genetic Nomenclature and Sequence Data

DNA sequence variants should be described in the text and tables according to HGVS (Human Genome Variation Society) nomenclature (varnomen.hgvs.org). DNA-level changes must be specified relative to a specific reference sequence, such as NCBI RefSeq or a Locus Reference Genomic (LRG) record. Tabular listings of the described sequence variants must include columns for DNA, RNA, and protein, and clearly indicate whether the changes were determined experimentally or predicted exclusively theoretically.

Nucleotide sequence data can be submitted to any of the three major collaborative databases:

• DNA Data Bank of Japan (DDBJ): http://www.ddbj.nig.ac.jp

• European Nucleotide Archive (ENA): ebi.ac.uk/ena

• GenBank: https://www.ncbi.nlm.nih.gov/genbank/

Manuscript Preparation

Title Page

The first page of the manuscript (title page) should include (1) a full title of the article, (2) a short title of less than 60 characters with spaces, (3) the authors' names, academic degrees, and affiliations, (4) the total word count of the manuscript (including Abstract, Text, References, Tables, Figure Legends), (5) the number of figures and tables, and (6) the name, email address, and complete address of corresponding author.

Disclaimers. An example of a disclaimer is an author's statement that the views expressed in the submitted article are his or her own and not an official position of the institution or funder.

Abstract

The article should include a brief abstract of no more than 200 words. Limit use of acronyms and abbreviations. Define at first use with acronym or abbreviation in parentheses. The abstract should be structured with the following headings: Background, Methods and Results, and Conclusions. The Background section should describe the rationale for the study. Methods and Results should briefly describe the methods and present the significant results. Conclusions should succinctly state the interpretation of the data. Authors should supply a list of up to four key words not appearing in the title, which will be used for indexing. The key words should be listed immediately after the Abstract. Use terms from the Medical Subject Headings (MeSH) list of Index Medicus when possible.

Main text in the IMRaD format

Introduction should describe the purpose of the study and its relation to previous work in the field; it should not include an extensive literature review.

Methods should be concise but sufficiently detailed to permit repetition by other investigators. Previously published methods and modifications should be cited by reference. A subsection on statistics should be included in the Methods section.

Results should present positive and relevant negative findings of the study, supported when necessary by reference to Tables and Figures.

Discussion should interpret the results of the study, with emphasis on their relation to the original hypotheses and to previous studies. The importance of the study and its limitations should also be discussed.

The IMRaD format does not include a separate Conclusion section. The conclusion is built into the Discussion. More information on the structure and content of these sections can be found in the Recommendations for the Conduct, Reporting, Editing and Publication of Scholarly Work in Medical Journals (ICMJE Recommendations), available from www.ICMJE.org.

Author Contributions, Acknowledgments, Sources of Funding, and Disclosures

CRediT (Contributor Roles Taxonomy) author statement should be provided during the submission process**.**

Acknowledgments : All contributors who do not meet the criteria for authorship should be listed in an acknowledgments section. Examples of those who might be acknowledged include a person who provided purely technical help, writing assistance, or a department chairperson who provided only general support. Authors should declare whether they had assistance with study design, data collection, data analysis, or manuscript preparation. If such assistance was available, the authors should disclose the identity of the individuals who provided this assistance and the entity that supported it in the published article.

Sources of Funding: All sources of financial support for the study should be cited on the title page, including federal or state agencies, nonprofit organizations, and pharmaceutical or other commercial sources.

Disclosure and conflicts of interest: All authors must disclose any financial or other relations that could lead to a conflict of interest. If a potential conflict exists, its nature should be stated for each author. All sources of financial support for the study should be cited, including federal or state agencies, nonprofit organizations, and pharmaceutical or other commercial sources. Please use ICMJE Form for Disclosure of Potential Conflicts of Interest (http://www.icmje.org/conflicts-of-interest/).

References

References should follow the standards summarized in the NLM's International Committee of Medical Journal Editors (ICMJE) Recommendations for the Conduct, Reporting, Editing and Publication of Scholarly Work in Medical Journals: Sample References webpage (www.nlm.nih.gov/bsd/uniform_requirements.html) and detailed in the NLM's Citing Medicine, available from www.ncbi.nlm.nih.gov/books/NBK7256/. MEDLINE abbreviations for journal titles (www.ncbi.nlm.nih.gov/nlmcatalog/journals) should be used.

References should be presented in the Vancouver style. The first six authors should be listed in each reference citation (if there are more than six authors, "et al" should be used following the sixth). Periods are not used in authors' initials or journal abbreviations. Examples of journal reference style:

Journal Article: Serruys PW, Ormiston J, van Geuns RJ, de Bruyne B, Dudek D, Christiansen E, et al. A Polylactide Bioresorbable Scaffold Eluting Everolimus for Treatment of Coronary Stenosis: 5-Year Follow-Up. J Am Coll Cardiol. 2016;67(7):766-76. doi: 10.1016/j.jacc.2015.11.060.

Book: Murray PR, Rosenthal KS, Kobayashi GS, Pfaller MA. *Medical Microbiology*. 4th ed. St. Louis: Mosby; 2002.

Chapter in Edited Book: Meltzer PS, Kallioniemi A, Trent JM. Chromosome alterations in human solid tumors. In: Vogelstein B, Kinzler KW, editors. *The Genetic Basis of Human Cancer*. New York: McGraw-Hill; 2002:93–113.

References should be numbered consecutively in the order in which they are first mentioned in the text. Identify references in text, tables, and legends by Arabic numerals in parentheses and listed at the end of the article in citation order.

Tables

Tables should be comprehensible without reference to the text and should not be repetitive of descriptions in the text. Every table should consist of two or more columns; tables with only one column will be treated as lists and incorporated into the text. All tables must be cited in the text and numbered in order of appearance. Tables should include a short title. Place explanatory matter in footnotes, not in the heading. Explain all nonstandard abbreviations in footnotes, and use symbols to explain information if needed. Each table submitted should be double-spaced, each on its own page. Each table should be saved as its own file as a Word Document. Explanatory matter and source notations for borrowed tables should be placed in the table footnote.

Figures and Legends

All illustrations (line drawings and photographs) are classified as figures. All figures should be cited in the text and numbered in order of appearance. Figures should be provided in .tiff, .jpeg or .eps formats. Color images must be at least 300 dpi. Gray scale images should be at least 300 dpi. Line art (black and white or color) and combinations of gray scale images and line art should be at least 1,000 dpi. The optimal size of lettering is 12 points. Symbols should be of a similar size. Figures should be sized to fit within the column (86 mm) or the full text width (180 mm). Line figures must be sharp, black and white graphs or diagrams, drawn professionally or with a computer graphics package. Legends should be supplied for each figure and should be brief and not repetitive of the text. Any source notation for borrowed figures should appear at the end of the legend. Figures should be uploaded as individual files.

Units of Measurement

Measurements of length, height, weight, and volume should be reported in metric units (meter, kilogram, or liter) or their decimal multiples. Temperatures should be in degrees Celsius. Blood pressures should be in millimeters of mercury. All measurements must be given in SI or SI-derived units. Drug concentrations may be reported in either SI or mass units, but the alternative should be provided in parentheses where appropriate

Style and Language

The journal accepts manuscripts written in English. Spelling should be US English only. The language of the manuscript must meet the requirements of academic

publishing. Reviewers may advise rejection of a manuscript compromised by grammatical errors. Non-native speakers of English may choose to use a copyediting service.

Abbreviations and Symbols

Use only standard abbreviations; use of nonstandard abbreviations can be confusing to readers. Avoid abbreviations in the title of the manuscript. The spelled-out abbreviation followed by the abbreviation in parenthesis should be used on first mention unless the abbreviation is a standard unit of measurement.

Drugs should be referred to by their generic names. If proprietary drugs have been used in the study, refer to these by their generic name, mentioning the proprietary name, and the name and location of the manufacturer, in parentheses.

Permissions

To use tables or figures borrowed from another source, permission must be obtained from the copyright holder, usually the publisher. Authors are responsible for applying for permission for both print and electronic rights for all borrowed materials and are responsible for paying any fees related to the applications of these permissions. This is necessary even if you are an author of the borrowed material. It is essential to begin the process of obtaining permission early, as a delay may require removing the copyrighted material from the article. The source of a borrowed table should be noted in a footnote and of a borrowed figure in the legend. It is essential to use the exact wording required by the copyright holder. A copy of the letter granting permission, identified by table or figure number, should be sent along with the manuscript. A permission request form is provided for the authors use in requesting permission from copyright holders.

Journal Policy on Affiliation with Sanctioned Institutions

At IJBM, we uphold the highest standards of academic integrity and compliance with international laws and regulations. To ensure the ethical and legal standing of all submitted research papers, authors are required to adhere to the following policy regarding affiliation with sanctioned institutions:

1. Declaration of Non-Affiliation: Authors must provide a clear and unambiguous statement confirming their non-affiliation with any institution, organization, or individual subject to sanctions imposed by international sanctions, laws, or regulations. This declaration should be included in the cover letter accompanying their manuscript submission.

2. Sanctioned Entities: Sanctioned entities include those listed on sanctions lists maintained by international authorities, such as the United Nations, the United States Department of the Treasury's Office of Foreign Assets Control (OFAC), the European Union, or any other relevant governing body.

3. Independence and Ethical Research: Authors should affirm that their research is conducted independently and ethically, without receiving any funding, resources, or support from sanctioned sources in connection with the submitted research.

4. Disclosure of Conflicts of Interest: Authors must disclose any potential conflicts of interest that may compromise the ethical and legal standing of their submission. This includes any financial interests or affiliations that could be perceived as influencing the research.

5. Consequences of Non-Compliance: Failure to adhere to this policy, misrepresentation of affiliations, or non-disclosure of conflicts of interest may result in the rejection of the submitted manuscript or further investigation into the matter.

Authors submitting their research papers to IJBM are responsible for ensuring their compliance with this policy. We reserve the right to verify the accuracy of the provided information and take appropriate action in cases of non-compliance.

Page Proofs

Page proofs are sent from the Publisher electronically and must be returned within 72 hours to avoid delay of publication. Generally, peer review is completed within 11-12 weeks, and the editor’s decision is made within 7-14 days of this. A timeline from submission to publication is an average of 14 weeks.

It is important to note that when citing an article from IJBM, the correct citation format is **International Journal of Biomedicine.**